Thèse

Pour obtenir le grade de

DOCTEUR

de l'Université Louis Pasteur de Strasbourg

Spécialité: **CHIMIE**

Présentée par

Magno AGOSTINHO

Nouveaux ligands de type N,O et P,N et leurs applications en Chimie de Coordination et Catalyse Homogène.

Soutenue le 25 Novembre 2006 devant la commission d'examen:

Pr. B. MILANI	Professeur à l'Università di Trieste (Italie) *Rapporteur Externe*
Pr. R. GUILARD	Professeur à l'Université de Bourgogne, Dijon *Rapporteur Externe*
Pr. R. WELTER	Professeur à l'Université Louis Pasteur, Strasbourg. *Examinateur*
Pr. M. CHETCUTI	Professeur à l'ECPM, Strasbourg *Rapporteur Interne*
Dr. P. BRAUNSTEIN	Directeur de recherche CNRS à l'Université Louis Pasteur, Strasbourg. *Directeur de Thèse*
Pr. T. AVILÉS	Professeur à la Nouvelle Université de Lisbonne (Portugal) *Membre Invité*
Pr. S. KOBAYASHI	Professeur à l'Université de Tokyo (Japon) *Membre Invité*

Remerciements

Ce travail a été effectué au Laboratoire de Chimie de Coordination, UMR 7177 du CNRS, de l'Université Louis Pasteur de Strasbourg.

Je tiens à remercier le Dr. Pierre Braunstein, Directeur de Recherche au CNRS, pour m'avoir accueilli au sein de son laboratoire, pour avoir encadré ce travail, et pour la confiance qu'il m'a accordée. J'ai particulièrement apprécié son enthousiasme, sa disponibilité pour répondre à mes questions, nos discussions constructives et ses conseils très utiles.

J'exprime ma gratitude aux membres du jury, Mesdames Milani et Avilés, Messieurs Welter, Chetcuti, Guilard et Kobayashi, qui me font l'honneur de juger cette thèse.

Mes remerciements vont aussi à tous ceux qui ont contribué à ce travail: Andrei Banu, Richard Welter, Xavier Morise, Qing-Zheng Yang, Anthony Kermagoret, Olivier Siri, Luc Brissieux, Vitor Rosa, Teresa Avilés et Jonathan Kirsch.

Je tiens aussi à remercier André DeCian et Richard Welter pour la détermination des structures, Anne Degrémont pour la synthèse des précurseurs métalliques et Marc Mermillon-Fournier pour son aide avec les problèmes techniques.

Un grand merci aux membres du Laboratoire de Chimie de Coordination: Nicola, Assia, Guislaine, Jing, Nicolas, Luc, Abdelatif, Adel, Jean-philippe, Coco, Aude, Pierre, Roberto, Mireia, Anthony, Sarah, Yang, Günter, Sabrina, Farba, Bipro, Matthieu, Lisa, Nadia, Patty, Jonathan, Falk, Suyun et Christophe. Merci aux membre permanents du LCC: Anne, Jacky, Xavier, Olivier, Robi, Marc, Catherine et Soumia. Merci aussi aux voisins d'étage (et collègues de foot): Alex, Alexsandro, Nico, Jérôme et les autres.

Merci à mes amis, non chimistes, de Strasbourg: Vincent, Patrick, Julien, Pauline, Zeinab, Lucille et Julie.

Finalmente agradeço a toda a minha família, em especial aos meus pais, pelo seu apoio incondicional.

Merci à Pamela, tu vas me manquer…

Este trabalho é dedicado a um grande homem,

Daniel Maria

28/02/1925 – 10/08/1998

“O Saber não ocupa lugar…”

SOMMAIRE/CONTENTS

Fifth Framework Programme
Research Training Network
2002 - 2006

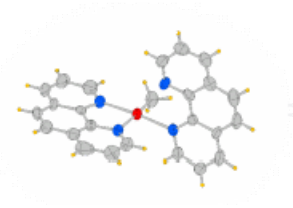

Présentation du Réseau Palladium

ATOM-ECONOMIC SYNTHESIS USING PALLADIUM THE CHAMELEON CATALYST

Cette thèse a été financée par le Réseau Européen "Palladium" (contrat N° HPRN- CT- 2002-00196), dans le domaine de la Catalyse Homogène et Chimie Organométallique, appartenant au "Fifth Framework Programme" de la Communauté Européenne pour la Recherche et Développement Technologique.

Ce Réseau consiste en une collaboration entre septe laboratoires de différents pays européens, avec l'objectif de développer des nouveaux catalyseurs basés sur des complexes de palladium. Les septe équipes de chercheurs appartenant au réseau sont les suivantes:

- Prof. Giovanni Mestroni et Dr. Barbara Milani
  Dipartimento di Scienze Chimiche, Università di Trieste (Italie)
- Prof. Dr. Kees Elsevier
  Institute of Molecular Chemistry, Universiteit van Amsterdam (Pays Bas)
- Prof. Dr. Piet van Leeuwen
  Laboratory of Inorganic Chemistry and Catalysis, Eindhoven University of Technology (Pays Bas)
- Dr. Andrea Meli
  Istituto di Chimica dei Composti Organometallici, Consiglio Nazionale delle Ricerche, Firenze (Italie)
- Dr. Pierre Braunstein
  Laboratoire de Chimie de Coordination, Universitè Luis Pasteur Strasbourg I (France)
- Prof. Dr. Carmen Claver
  Department de Quimica Fisica i Inorganica, Universitat Rovira I Virgili, Tarragona (Espagne)
- Prof. Giambattista Consiglio
  Laboratorium für Technische Chemie, ETH-Hönggerberg, Zürich (Suisse)

Composition du document et organisation de la bibliographie

Ce document se divise en 5 sections principales: une Introduction Générale, 3 chapitres et une Conclusion Générale.

L'Introduction Générale est rédigée en français et dispose en sa fin de sa propre bibliographie.

Les chapitres I, II et III sont rédigés en anglais:

> Le chapitre I a été publié dans le journal *Organometallics,* il dispose en sa fin de sa propre bibliographie;
>
> Le chapitre II est divisé en partie A et partie B, la partie A a été publiée dans le journal *Acta Crystallographica Section C: Crystal Structure Communications*, chaque partie dispose en sa fin de sa propre bibliographie;
>
> Le chapitre III est divisé en partie A et partie B, la partie A a été acceptée, sous réserve de modifications mineurs, pour publication dans le journal *Chemical Communications*, chaque partie dispose en sa fin de sa propre bibliographie.

La Conclusion Générale est rédigée en français.

Introduction Générale

pour les références, voir page 14

Introduction Générale

En raison du développement constant des méthodologies de synthèse en chimie organique, de la découverte de nouveaux outils plus efficaces, et de l'augmentation continue de l'utilisation (catalytique) des métaux, le développement de ligands est devenu une composante très importante de la chimie de synthèse.

La nécessité d'induire de nouvelles propriétés chimiques ou physiques dans des complexes métalliques a soulevé un intérêt croissant pour les ligands hybrides (ligands bi- ou multidentes possédant des fonctions coordinantes chimiquement très différentes, par exemple du type 'dur' (oxygène ou azote) et 'mou' (phosphore). L'importance des phosphines fonctionnelles en chimie de coordination et en catalyse repose essentiellement sur leurs propriétés stéréoélectroniques particulières qui permettent de 'contrôler' la sphère de coordination du centre métallique auquel elles sont liées en apportant une certaine labilité d'au moins une des liaisons entre la partie donneur faible du ligand et le métal.[1] Cette labilité permet de rendre accessible a une molécule externe un site de coordination.

Oligomérisation de l'éthylène

La synthèse sélective d'α-oléfines linéaires comportant de 4 à 20 atomes de carbone (notés C_4-C_{20}) est d'un grand intérêt pour des laboratoires de recherche publiques et privés et ce à une échelle mondiale. Ceci provient de l'augmentation des besoins, notamment comme comonomères avec l'éthylène (C_4-C_8, pour former du polyéthylène linéaire de basse densité),[2] pour la synthèse de poly-α-oléfines et lubrifiants synthétiques (C_{10}), comme additifs pour la production de polyéthylène haute densité et la production de plastifiants (C_6-C_{10}) et de surfactants (C_{12}-C_{20}).[3-5] La consommation annuelle de polyoléfines est proche de 10^8 tonnes, et la demande en α-oléfines linéaires augmente plus rapidement pour les fractions C_4-C_8 que pour les C_{10+}. Selon une estimation de la compagnie Nexant ChemSystems, la demande globale de butenes, hexenes, et octenes va croître de 6,2%, 7,9%, et 5,4%, respectivement, et cela annuellement jusqu'à 2010.[6] La demande en décènes va croître de 3,2% et l'on estime que la demande pour les fractions C_{12}-C_{14} et C_{16}-C_{18} va croître respectivement de 4,8% et 3,4%.[6] Il est donc très important de pouvoir former sélectivement des α-oléfines de courte chaîne à partir de l'éthylène, circonvenant les distributions typiques de Schulz-Flory[7] observées pour l'oligomérisation de l'éthylène.

pour les références, voir page 14

La production d'α-oléfines, par oligomérisation de l'éthylène, a été initialement réalisée par le procédé stochiométrique Alfen,[4,8] dans lequel la croissance de la chaîne oléfinique qui s'effectue sur l'aluminium est suivie de la libération du produit dans un réacteur séparé et à haute température. Cependant, en raison de la nécessité d'utiliser de grandes quantités d'alkylaluminiums, le procédé n'a pas été viable économiquement. Gulf (maintenant Chevron Phillips) a développé un procédé catalytique en une étape,[9] dans lequel les deux réactions se déroulent simultanément dans le même réacteur. Le procédé Ethyl (maintenant BP Amoco) consiste en une combinaison de réactions de croissance de chaîne de façon catalytique et stochiométrique.[4,5] Contrastant avec le procédé SHOP (Shell Higher Olefin Process) développé par Shell et basé sur des complexes organométalliques de nickel,[4,5,10] d'autres systèmes pour l'oligomérisation ou polymérisation nécessitent d'un métal de transition associé à un co-catalyseur.[11-16]

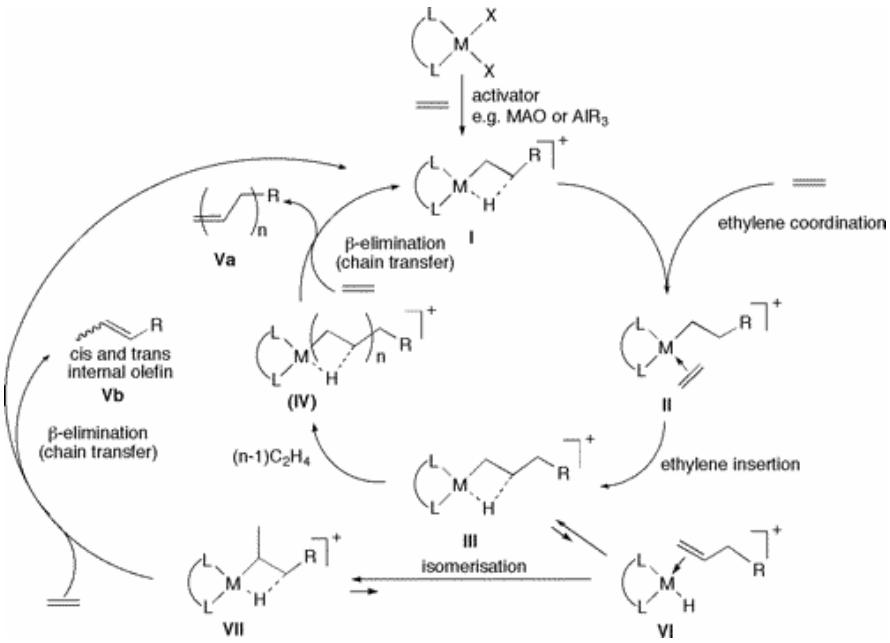

Schéma 1
Oligomérisation et polymérisation catalytique de l'éthylène.[17]

En dépit de la différence dans la distribution des produits, les deux réactions (oligomérisation et polymérisation) suivent en gros la même voie. Elles peuvent être représentées sous le même mécanisme général, avec des étapes élémentaires communes (Schéma 1).[17] Dans un premier temps, une espèce coordinativement insaturée est engendrée. Cette espèce est stabilisée après insertion d'éthylène par une interaction β-agostique **I**.[18,19] L'éthylène coordiné dans le complexe **II** s'insère dans la liaison M−alkyl pour former **III**. Finalement, après (*n*-1) insertions amenant à **IV**, le produit est éliminé (molécule **Va**). Le mécanisme exact qui régit le transfert de chaîne/élimination β-H, amenant à la libération de l'oléfine n'est pas encore complètement établi, et attire une attention considérable.[20-23] Pour des valeurs de *n* comprises

pour les références, voir page 14

entre 1 et 10, les produits formés sont des oligomères, et pour des valeurs de *n* plus élevées, on obtient des polymères (Schéma 1). Les espèces **VI** et **VII** peuvent isomériser les oléfines terminales amenant à des oléfines internes **Vb**. La voie réactionnelle avec la séquence **II**-**IV** dépend fortement de la concentration en éthylène, en effet son augmentation entraîne aussi l'augmentation du taux de transfert de chaîne, relativement à l'isomerisation.[13,24]

Parallèlement au mécanisme décrit ci-dessus, nommé polymérisation dégénérée, un autre mécanisme réactionnel peut être décrit pour des systèmes qui produisent exclusivement un seul groupe d'oléfines comme par exemple le 1-butène ou le 1-hexène.[25-28]

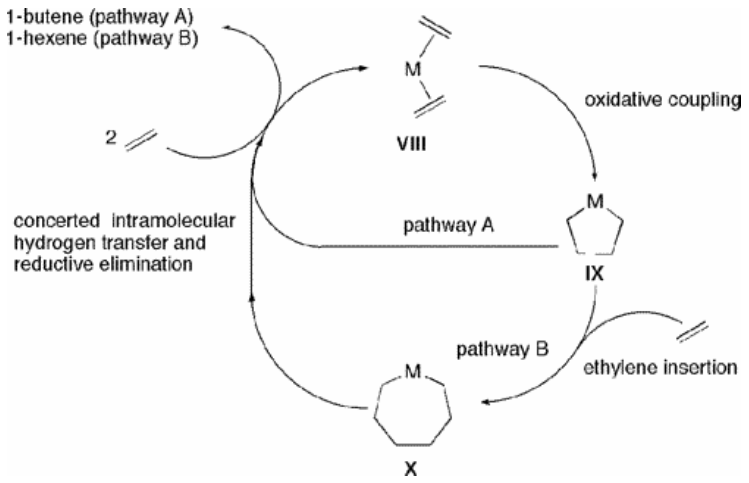

Schéma 2
Oligomérisation de l'éthylène avec des intermédiaires métallacycliques.[17]

Dans une première étape, deux molécules d'éthylène coordinées au centre métallique **VIII** réagissent par couplage oxydant pour former un métallacyclopentane **IX**. Dans le procédé Alphabutol® basé sur le titane, on observe un transfert intramoléculaire d'hydrogène et une élimination réductrice, libérant à ce stade du 1-butène (route A du Schema 2).[25] L'insertion d'une troisième molécule d'éthylène mène à un métallacycloheptane **X** qui libère le 1-hexene par élimination réductrice. Ce mécanisme opère lorsque le métal est le chrome, dans le procédé Phillips (ligand pyrrolide), le procédé SASOL (ligands S,N,S), et le système BP (ligands P,N,P) (route B du Schéma 2).

Des nombreux catalyseurs de Ni^{II} ont tendance à favoriser la terminaison de chaîne par rapport à la propagation, ce qui explique leur utilisation dans des nombreux procédés de dimérisation d'α-oléfines.[29-31] Une autre caractéristique des catalyseurs à base de nickel dans la réaction d'oligomérisation d'α-oléfines est leur tendance à produire des oléfines internes.[11,30] Néanmoins, les propriétés catalytiques des complexes de Ni^{II} peuvent être modifiées et améliorées en utilisant des ligands appropriés, ce qui accentue l'importance de la chimie de coordination en catalyse homogène.

pour les références, voir page 14

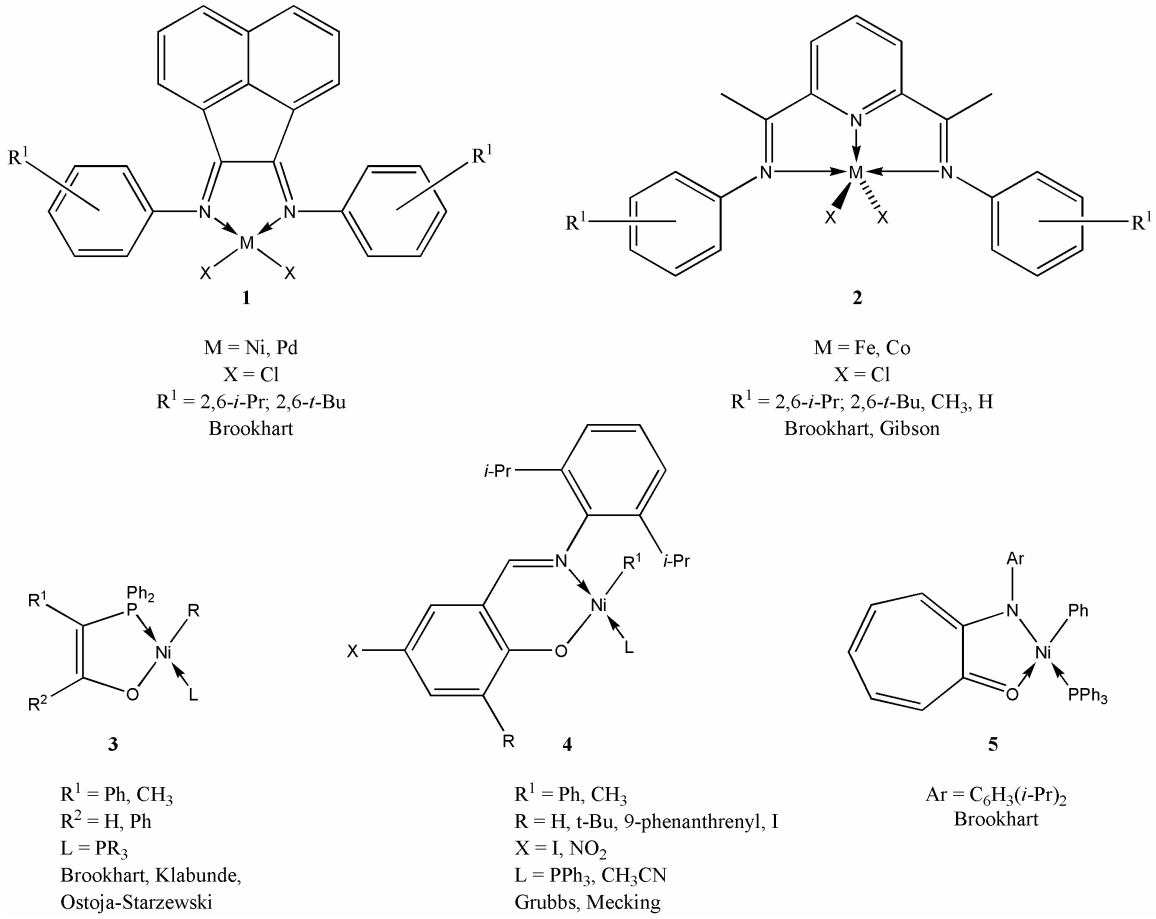

Schéma 3
Complexes pour l'oligomérisation catalytique de l'éthylène.

Les systèmes du type DAD (diazadiene) **1** développés par Brookhart[12,13,19,32,33] forment une classe de catalyseurs parmi les plus versatiles car ils peuvent servir en oligomérisation ou en polymérisation selon les propriétés stériques du ligand (Schéma 3).
Les groupes de Gibson[12,15] et de Brookhart[13] ont utilisé des complexes bisiminopyridine de Fe^{II} et Co^{II} de type **2** pour la polymérisation et l'oligomérisation de l'éthylène.

Un système possédant une activité remarquable en oligomérisation d'éthylène, qui permet de former des α-oléfines linéaires sélectivement, est le procédé SHOP (Shell Higher Olefin Process). Keim et ses collaborateurs ont utilisé le système $Ni(P,O)(PR_3)R'$ (**3**) en polymérisation[34,35] et oligomérisation[10] de l'éthylène. Klabunde *et al.* ont montré que l'abstraction du ligand PR_3 mène à des catalyseurs de polymérisation.[36,37] L'intérêt porté aux catalyseurs du type SHOP a récemment mené à des modifications intéressantes sur les substituents R^1 et R^2.[38-43] Une extension des catalyseurs type-P,O (**3**) est à l'origine des systèmes N,O neutres **4**[44,45] et **5**[46] pour la polymérisation. Mecking et ses collaborateurs ont utilisé les catalyseurs de Grubbs de type **4** en polymérisation d'éthylène en émulsion dans l'eau.[47,48]

pour les références, voir page 14

Malgré ces développements importants, les systèmes décrits produisent soit des oligomères avec une distribution large de type Schultz-Flory soit des polymères. De ce fait, des catalyseurs basés sur des métaux de transition capables de produire une distribution de produits plus étroite constituent un objectif de grande importance car très peu d'exemples sont connus dans la littérature.[26-28,49-51]

Notre laboratoire à démontré que des complexes portant des ligands N,O (avec des fonctions pyridine et oxazoline), activés par MAO ou $AlEtCl_2$ sont très efficaces et ont une sélectivité élevée pour les fraction C_4 et C_6.[52] Nous avons aussi publié la synthèse d'une série de complexes, avec différents métaux, stabilisés par des ligands zwittérioniques N,O benzoquinonemonoimine, N-substitués et possédant 6π + 6π électrons (systèmes potentiellement antiaromatiques) **5**. Le complexe **6** est actif en catalyse d'oligomérisation d'éthylène et, activé par $AlEtCl_2$, favorise la dimérisation et la trimérisation.

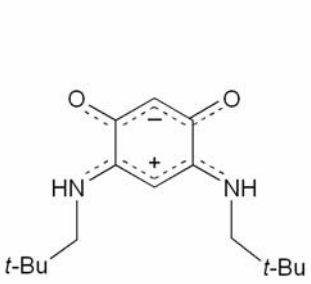

5

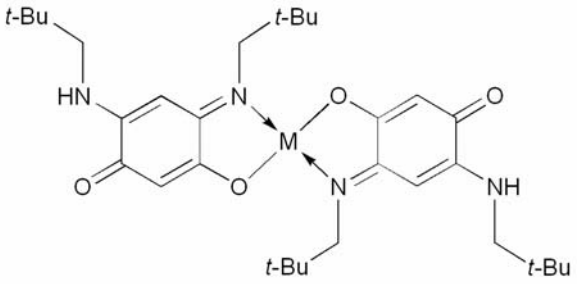

6 M = Ni
7 M = Zn
8 M = Cu

Il nous a donc paru intéressant d'évaluer des complexes de type **6** avec différents substituents sur le fragment benzoquinonemonoimine. Les nouveaux ligands **9-12** ont été préparés grâce à une nouvelle procédure, très efficace, basée sur les premières réactions de transamination en chimie des quinones.[53,54] Les complexes octaédriques **13-16** obtenus par complexation avec $Ni(acac)_2$ dans un ratio de 2:1, et le complexe **17** obtenu par réaction de **9** avec $NiCl_2 \cdot 6H_2O$ dans un ratio de 1:1 ont été synthétises, caractérisés et évalués en oligomérisation de l'éthylène.

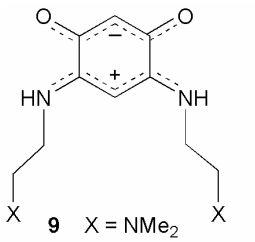

9 X = NMe_2
10 X = NHEt
11 X = OMe

12 X = 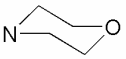

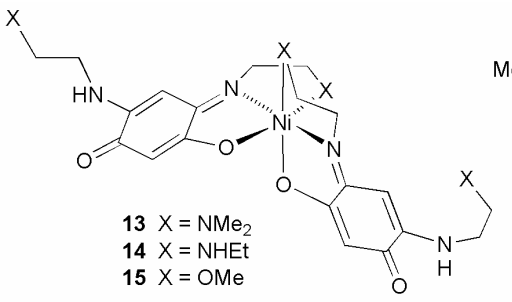

13 X = NMe_2
14 X = NHEt
15 X = OMe

16 X = 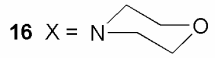

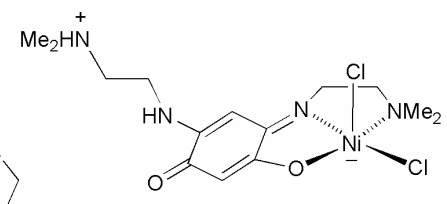

17

pour les références, voir page 14

Copolymérisation d'oléfines avec le monoxyde de carbone

La copolymérisation alternée d'oléfines avec le monoxyde de carbone (eq. 1) a suscité beaucoup d'intérêt de la part des laboratoires de recherche académiques et industriels au cours des dernières années.[12,13,55-66] L'intérêt soulevé par ces polymères, particulièrement par le copolymère éthylène/CO (température de fusion, T_m = 257 ºC),[67] est dû à leurs propriétés très intéressantes et à la facilité d'accès et le faible coût des matières premières. De plus, la présence de fonctions carbonyles tout au long de la chaîne permet d'envisager d'éventuelles modifications ultérieures du polymère par voie chimique.[68-73]

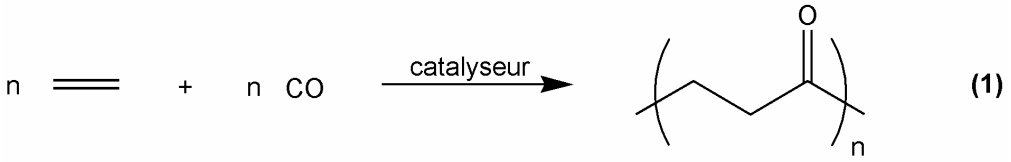

Historiquement, Walter Reppe fut le premier à obtenir, vers la fin des années 40, des copolymères d'éthylène/CO grâce à un catalyseur de nickel.[74] Puis, en 1967, le premier catalyseur à base de palladium fut découvert par Gough.[75] Cependant les conditions réactionnelles nécessaires étaient relativement drastiques et les rendements en copolymères faibles. Il fallut attendre le début des années 1980 pour que Sen décrive des systèmes à base de palladium capables de conduire à la formation de polycétones dans des conditions douces.[76] En revanche, les rendements et vitesses de réactions restent faibles.

Ces 25 dernières années ont vu l'émergence d'un grand nombre de travaux et une classe de catalyseurs très efficaces a pu être développée grâce à l'utilisation de ligands bidentes. Actuellement la plupart des systèmes actifs sont du type **A** ou **B**.

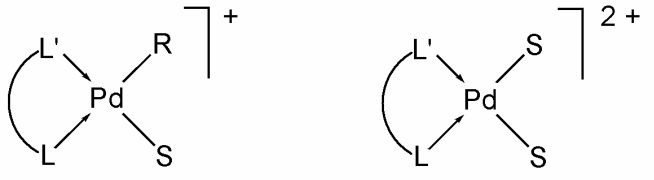

A **B**

De nombreux travaux on été réalisés avec des ligands bidentes symétriques (L = L') incluant des études catalytiques (avec des ligands P-P[67,77-88] et N-N[89-97]) et des études mécanistiques sur l'insertion de CO et/ou oléfines (avec des ligands P-P[98-112] et N-N[113-120]). Des ligands non symétriques ont aussi été utilisés dans des études catalytiques et/ou d'insertion de CO et/ou oléfines (avec des ligands P-P',[121-127] N-N',[128-134] N-O,[135-138] P-O[139, 140] et P-N[141-153]). Des études théoriques importantes on aussi été réalisées sur des copolymères CO/oléfine,[154,155] ainsi que des études cinétiques.[107,110,119]

pour les références, voir page 14

Le mécanisme réactionnel généralement admis pour la formation des polycétones est basé sur une alternance d'insertion de CO dans la liaison Pd-alkyle suivie de celle de l'oléfine dans une liaison Pd-acyle. Les composés du type **A** possèdent une liaison Pd-C préformée dans laquelle l'insertion aura lieu, dans le cas des composés de type **B**, la réaction avec du méthanol, souvent utilisé comme solvant, conduit *in situ* à la formation d'espèces Pd-H et/ou PdC(O)OMe dans lesquelles l'insertion a lieu. D'autre part, ces catalyseurs comportent, selon le cas, un ou deux ligands labiles (S est généralement une molécule de solvant comme Et_2O, MeCN ou un contre ion peux ou non coordinant, comme le CF_3SO_3) permettant de libérer un site pour la coordination des substrats (CO ou oléfines).

Dans la plupart des composés décrits, l'atome donneur du ligand qui est positionné en *trans* de la liaison Pd-C (L') appartient aux éléments principaux (N, P, O, …). Celui-ci joue un rôle fondamental dans la réaction catalytique de formation des polycétones, notamment de par l'influence *trans* qu'il exerce sur la liaison dans laquelle l'insertion a lieu.

En effet, bien que l'importance des complexes du palladium stabilisés par des ligands phosphorés en copolymérisation catalytique des oléfines avec le CO soit établie, peu d'exemples de produits d'insertion obtenus avec ces complexes ont été caractérisés structuralement. L'un d'entre-eux provient de notre laboratoire qui a publié en 2000 la caractérisation structurale d'un métallacycle (**20**) résultant de l'insertion consécutive de CO et d'éthylène dans la liaison Pd-Me d'un complexe stabilisé par un ligand acétamide $Ph_2PNHC(O)CH_3$ (**18**).[140]

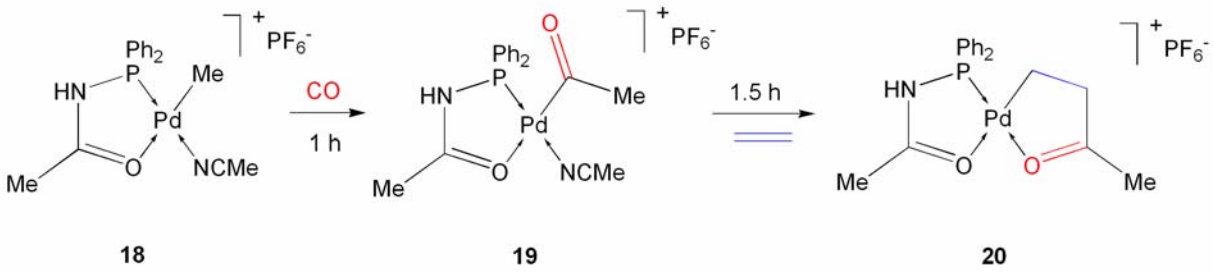

18 **19** **20**

Aussi nous a-t-il paru intéressant, dans le cadre des travaux menés au laboratoire sur l'oligomérisation de l'éthylène avec des ligands P-N, d'étudier ces systèmes en copolymérisation d'oléfines avec le monoxyde de carbonne. Pour cela, nous avons mis au point les méthodologies de synthèse permettant la préparation avec de bons rendements des nouveaux ligands de type phosphine, phosphinite et phosphonite.

pour les références, voir page 14

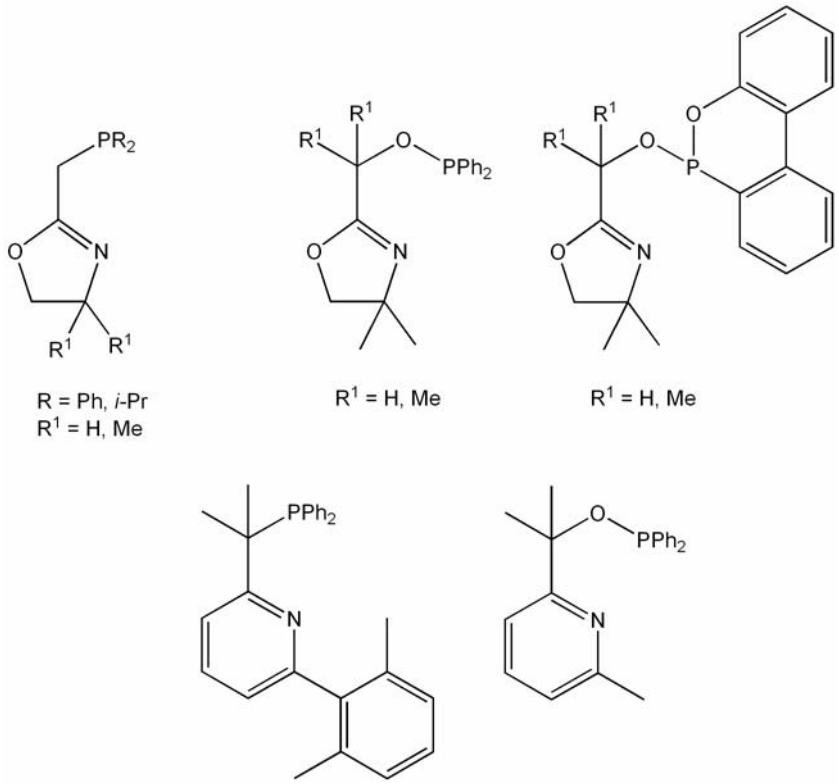

Ces ligands ont été utilisés pour synthétiser des complexes neutres de palladium de type [PdClMe(P,N)], à partir desquels on a pu préparer, par abstraction de chlorure avec $AgCF_3SO_3$, leurs analogues cationiques de type $[Pd(CF_3SO_3)Me(P,N)]$, connus pour être des systèmes plus réactifs.

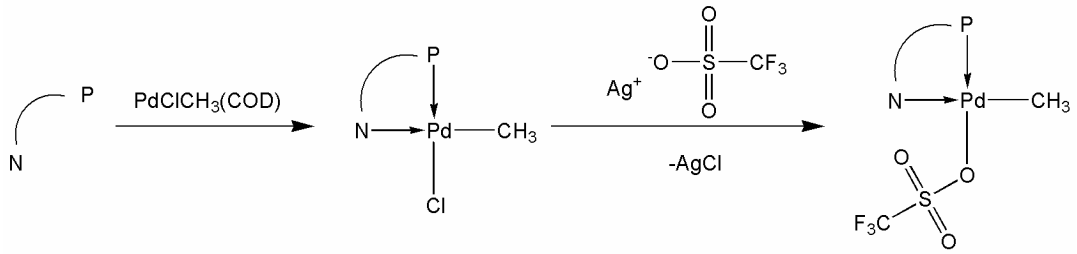

Nous nous sommes ensuite intéressés à l'étude des réactions d'insertion de monoxyde de carbone et d'éthylène ou d'acrylate de méthyle dans la liaison Pd-Me de ces complexes. Dans certains cas, nous avons réussi à isoler et caractériser les produits résultant de la première insertion de CO et d'éthylène ou d'acrylate de méthyle dans la liaison Pd-Me, et dans certains cas leur détermination structurale à été réalisée par diffraction de rayons X.

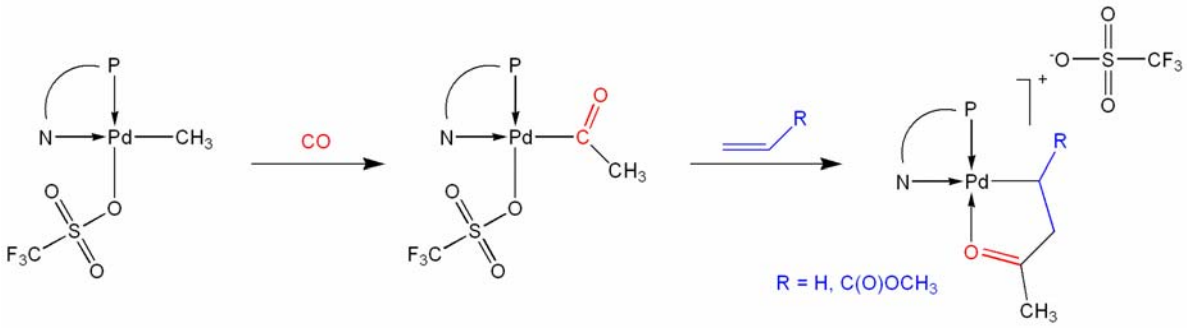

pour les références, voir page 14

Références

1. P. Braunstein and F. Naud, *Angew. Chem. Int. Ed.*, 2001, **40**, 680-699.
2. D. E. James, in *Encyclopedia of Polymer Science and Engineering*, eds. H. F. Mark, N. M. Bikales, C. G. Overberger and G. Menges, Wiley-Interscience, New York, Editon edn., 1985, vol. 6, pp. 429-454.
3. A. Tullo, *Chem. Eng. News*, 2000, **78**, 35-46.
4. D. Vogt, in *Applied Homogeneous Catalysis with Organometallic Compounds*, eds. B. Cornils and W. A. Hermann, Wiley-VCH, New York, Editon edn., 1996, vol. 1, pp. 245-258.
5. G. R. Lappin and J. D. Sauer, *Alphaolefins Applications Handbook*, Marcel Decker Inc., Berkeley, 1989.
6. A. Tullo, *Chem. Eng. News*, 2005, **83**, 30-33.
7. B. Cornils, W. A. Herrmann, R. Schlögl and C.-H. Wong, in *Catalysis from A to Z, A concise Encyclopedia*, Wiley-VCH, Weinheim, Editon edn., 2000, p. 513.
8. K. Ziegler, *Brennst.-Chem.*, 1952, **35**, 193.
9. B. Cornils, W. A. Herrmann, R. Schlögl and C.-H. Wong, in *Catalysis from A to Z, A concise Encyclopedia*, Wiley-VCH, Weinheim, Editon edn., 2000, pp. 243-244.
10. W. Keim, *Angew. Chem., Int. Ed.*, 1990, **29**, 235-244.
11. J. Skupinska, *Chem. Rev.*, 1991, **91**, 613-648.
12. G. J. P. Britovsek, V. C. Gibson and D. F. Wass, *Angew. Chem., Int. Ed.*, 1999, **38**, 428-447.
13. S. D. Ittel, L. K. Johnson and M. Brookhart, *Chem. Rev.*, 2000, **100**, 1169-1203.
14. S. Mecking, *Angew. Chem., Int. Ed.*, 2001, **40**, 534-540.
15. V. C. Gibson and S. K. Spitzmesser, *Chem. Rev.*, 2003, **103**, 283-315.
16. G. Wilke, B. Bogdanovic, P. Hardt, P. Heimbach, W. Keim, M. Kröner, O. Oberkirch, K. Tanaka, E. Steinbrücke, D. Walter and H. Zimmermann, *Angew. Chem., Int. Ed.*, 1966, **5**, 151-164.
17. F. Speiser, P. Braunstein and L. Saussine, *Acc. Chem. Res.*, 2005, **38**, 784-793.
18. S. A. Svejda, L. K. Johnson and M. Brookhart, *J. Am. Chem. Soc.*, 1999, **121**, 10634-10635.
19. L. K. Johnson, C. M. Killian and M. Brookhart, *J. Am. Chem. Soc.*, 1995, **117**, 6414-6415.
20. L. Deng, T. K. Woo, L. Cavallo, P. M. Margl and T. Ziegler, *J. Am. Chem. Soc.*, 1997, **119**, 6177-6186.
21. D. G. Musaev, R. D. J. Froese, M. Svensson and K. Morokuma, *J. Am. Chem. Soc.*, 1997, **119**, 367-374.
22. P. E. M. Siegbahn, S. Stromberg and K. Zetterberg, *Organometallics*, 1996, **15**, 5542.
23. S. Strömberg, K. Zetterberg and P. E. M. Siegbahn, *J. Chem. Soc., Dalton Trans.*, 1997, 4147-4152.
24. S. A. Svejda and M. Brookhart, *Organometallics*, 1999, **18**, 65-74.
25. A. Bré, Y. Chauvin and D. Commereuc, *New J. Chem.*, 1986, **10**, 535-537.
26. P. W. Jolly, *Acc. Chem. Res.*, 1996, **29**, 544-551.
27. R. Emmerich, O. Heinemann, P. W. Jolly, C. Krüger and G. P. J. Verhovnik, *Organometallics*, 1997, **16**, 1511-1513.
28. P. J. W. Deckers, B. Hessen and J. H. Teuben, *Angew. Chem. Int. Ed.*, 2001, **40**, 2516-2519.
29. K. Ziegler, H. G. Gellert, E. Holzkamp and G. Wilke, *Brennst.-Chem.*, 1954, **35**, 321.
30. K. Fischer, K. Jonas, P. Misbach, R. Stabba and G. Wilke, *Angew. Chem. Int. Ed.*, 1973, **12**, 943-953.

31. Y. Chauvin and H. Olivier, in *Applied Homogeneous Catalysis with Organometallic Compounds*, eds. B. Cornils and W. A. Hermann, VCH: New York, Weinheim, Editon edn., 1996, vol. 1, pp. 258-268.
32. C. M. Killian, D. J. Tempel, L. K. Johnson and M. Brookhart, *J. Am. Chem. Soc.*, 1996, **118**, 11664-11665.
33. C. M. Killian, L. K. Johnson and M. Brookhart, *Organometallics*, 1997, **16**, 2005-2007.
34. R. Bauer, H. Chung, K. W. Barnett, P. W. Glockner and W. Keim, *Shell Oil Company*, 1972, US 3 686 159.
35. J. Heinicke, M. Koesling, R. Brull, W. Keim and H. Pritzkow, *Eur. J. Inorg. Chem.*, 2000, 299-305.
36. U. Klabunde and S. D. Ittel, *J. Mol. Catal. A: Chem.*, 1987, **41**, 123-134.
37. U. Klabunde, R. Mühlhaupt, T. Herskowitz, A. H. Janowicz, J. Calabrese and S. D. Ittel, *J. Polym. Sci., Part A: Polym. Chem.*, 1987, **25**, 1989-2003.
38. P. Braunstein, Y. Chauvin, S. Mercier, L. Saussine, A. De Cian and J. Fischer, *J. Chem. Soc., Chem. Commun.*, 1994, 2203-2204.
39. A. Tomov, R. Spitz and T. Saudemont, *Elf Atochem S.A.*, 1999, FR 2 790 978.
40. Z. J. A. Komon, X. Bu and G. C. Bazan, *J. Am. Chem. Soc.*, 2000, **122**, 12379-12380.
41. V. C. Gibson, A. Tomov, A. J. P. White and D. J. Williams, *Chem. Commun.*, 2001, 719-720.
42. R. Soula, J. P. Broyer, M. F. Llauro, A. Tomov, R. Spitz, J. Claverie, X. Drujon, J. Malinge and T. Saudemont, *Macromolecules*, 2001, **8**, 2438-2442.
43. P. Kuhn, D. Semeril, C. Jeunesse, D. Matt, M. Neuburger and A. Mota, *Chem. Eur. J.*, 2006, **12**, 5210-5219.
44. T. R. Younkin, E. F. Connor, J. I. Henderson, S. K. Friedrich, R. H. Grubbs and D. A. Bansleben, *Science*, 2000, **287**, 460-462.
45. C. Wang, S. Friedrich, T. R. Younkin, R. T. Li, R. H. Grubbs, D. A. Bansleben and M. W. Day, *Organometallics*, 1998, **17**, 3149-3151.
46. F. A. Hicks and M. Brookhart, *Organometallics*, 2001, **20**, 3217-3219.
47. F. M. Bauers and S. Mecking, *Macromolecules*, 2001, **34**, 1165-1171.
48. F. M. Bauers and S. Mecking, *Angew. Chem. Int. Ed.*, 2001, **40**, 3020-3021.
49. A. Bollmann, K. Blann, J. T. Dixon, F. M. Hess, E. Killian, H. Maumela, D. S. McGuinness, D. H. Morgan, A. Neveling, S. Otto, M. Overett, A. M. Z. Slawin, P. Wasserscheid and S. Kuhlmann, *J. Am. Chem. Soc.*, 2004, **126**, 14712-14713.
50. W. K. Reagan and B. K. Conroy, 1991, CA 2020509 AA (to Phillips Petroleum Company).
51. W. K. Reagan and M. P. McDaniel, 1995, US 5 382 738 A (to Phillips Petroleum Company).
52. F. Speiser, P. Braunstein and L. Saussine, *Inorg. Chem.*, 2004, **43**, 4234-4240.
53. Q.-Z. Yang, O. Siri and P. Braunstein, *Chem.Commun.*, 2005, 2660-2662.
54. Q.-Z. Yang, O. Siri and P. Braunstein, *Chem. Eur. J.*, 2005, **11**, 7237-7246.
55. A. Sen, *Acc. Chem. Res.*, 1993, **26**, 303-310.
56. K. J. Cavell, *Coord. Chem. Rev.*, 1996, **155**, 209-243.
57. E. Drent and P. H. M. Budzelaar, *Chem. Rev.*, 1996, **96**, 663-681.
58. A. Sommazzi and F. Garbassi, *Progr. Polym. Sci.*, 1997, **22**, 1547-1605.
59. K. Nozaki and T. Hiyama, *J. Organomet. Chem.*, 1999, **576**, 248-253.
60. G. P. Belov, *Russ. Chem. Bull., Int. Ed.*, 2002, **51**, 1605-1615.
61. C. Bianchini and A. Meli, *Coord. Chem. Rev.*, 2002, **225**, 35-66.
62. E. Drent, J. A. M. van Broekhoven and P. H. M. Budzelaar, in *Applied Homogeneous Catalysis with Organometallic Compounds (2nd Edition)*, eds. B. Cornils and W. A. Herrmann, Wiley-VCH, Weinheim, Editon edn., 2002, vol. 1, pp. 344-361.
63. R. A. M. Robertson and D. J. Cole-Hamilton, *Coord. Chem. Rev.*, 2002, **225**, 67-90.
64. C. Bianchini, A. Meli and W. Oberhauser, *Dalton Trans.*, 2003, 2627-2635.

65. G. Consiglio, in *Late Transition Metal Polymerization Catalysis*, eds. B. Rieger, L. S. Baugh, S. Kacker and S. Striegler, Wiley-InterScience, Editon edn., 2003, pp. 279-305.
66. J. Durand and B. Milani, *Coord. Chem. Rev.*, 2006, **250**, 542-560.
67. E. Drent, J. A. M. Van Broekhoven and M. J. Doyle, *J. Organomet. Chem.*, 1991, **417**, 235-251.
68. A. Sen, *Adv. Polym. Sci.*, 1986, **73-74**, 125-144.
69. Z. Jiang, S. Sanganeria and A. Sen, *J. Polym. Sci., Part A: Polym. Chem.*, 1994, **32**, 841-847.
70. M. J. Green, A. R. Lucy, S.-Y. Lu and R. M. Paton, *J. Chem. Soc., Chem. Commun.*, 1994, 2063-2064.
71. M. D. E. Forbes, S. R. Ruberu, D. Nachtigallova, K. D. Jordan and J. C. Barborak, *J. Am. Chem. Soc.*, 1995, **117**, 3946-3951.
72. A. Gray, *Chem. Br.*, 1998, **34**, 44-45.
73. N. Kosaka, T. Oda, T. Hiyama and K. Nozaki, *Macromolecules*, 2004, **37**, 3159-3164.
74. *Us Pat.*, 2577208, 1951.
75. *Gb Pat.*, 1081304, 1967.
76. A. Sen and T. W. Lai, *J. Am. Chem. Soc.*, 1982, **104**, 3520-3522.
77. Z. Jiang and A. Sen, *J. Am. Chem. Soc.*, 1995, **117**, 4455-4467.
78. A. S. Abu-Surrah, R. Wursche, B. Rieger, G. Eckert and W. Pechhold, *Macromolecules*, 1996, **29**, 4806-4807.
79. S. Kacker, Z. Jiang and A. Sen, *Macromolecules*, 1996, **29**, 5852-5858.
80. A. L. Safir and B. M. Novak, *J. Am. Chem. Soc.*, 1998, **120**, 643-650.
81. S. Doherty, G. R. Eastham, R. P. Tooze, T. H. Scanlan, D. Williams, M. R. J. Elsegood and W. Clegg, *Organometallics*, 1999, **18**, 3558-3560.
82. C. Bianchini, H. M. Lee, A. Meli, W. Oberhauser, F. Vizza, P. Bruggeller, R. Haid and C. Langes, *Chem. Comm.*, 2000, 777-778.
83. J. Schwarz, E. Herdtweck, W. A. Herrmann and M. G. Gardiner, *Organometallics*, 2000, **19**, 3154-3160.
84. G. Verspui, F. Schanssema and R. A. Sheldon, *Angew. Chem., Int. Ed.*, 2000, **39**, 804-806.
85. C. Bianchini, H. M. Lee, A. Meli, W. Oberhauser, M. Peruzzini and F. Vizza, *Organometallics*, 2002, **21**, 16-33.
86. C. Bianchini, A. Meli, G. Mueller, W. Oberhauser and E. Passaglia, *Organometallics*, 2002, **21**, 4965-4977.
87. M. Caporali, C. Mueller, B. B. P. Staal, D. M. Tooke, A. L. Spek and P. W. N. M. van Leeuwen, *Chem. Commun.*, 2005, 3478-3480.
88. C. Bianchini, P. Brueggeller, C. Claver, G. Czermak, A. Dumfort, A. Meli, W. Oberhauser and E. J. Garcia Suarez, *Dalton Trans.*, 2006, 2964-2973.
89. M. Brookhart, F. C. Rix, J. M. DeSimone and J. C. Barborak, *J. Am. Chem. Soc.*, 1992, **114**, 5894-5895.
90. A. Sen and Z. Jiang, *Macromolecules*, 1993, **26**, 911-915.
91. Z. Jiang, S. E. Adams and A. Sen, *Macromolecules*, 1994, **27**, 2694-2700.
92. B. Milani, E. Alessio, G. Mestroni, E. Zangrando, L. Randaccio and G. Consiglio, *J. Chem. Soc., Dalton Trans.*, 1996, 1021-1029.
93. A. C. Gottfried and M. Brookhart, *Macromolecules*, 2003, **36**, 3085-3100.
94. B. Milani, A. Scarel, E. Zangrando, G. Mestroni, C. Carfagna and B. Binotti, *Inorg. Chim. Acta*, 2003, **350**, 592-602.
95. A. Scarel, J. Durand, D. Franchi, E. Zangrando, G. Mestroni, B. Milani, S. Gladiali, C. Carfagna, B. Binotti, S. Bronco and T. Gragnoli, *J. Organomet. Chem.*, 2005, **690**, 2106-2120.
96. D. Sirbu, G. Consiglio, B. Milani, P. G. A. Kumar, P. S. Pregosin and S. Gischig, *J. Organomet. Chem.*, 2005, **690**, 2254-2262.

97. J. Durand, A. Scarel, B. Milani, R. Seraglia, S. Gladiali, C. Carfagna and B. Binotti, *Helv. Chim. Acta*, 2006, **89**, 1752-1771.
98. F. Ozawa, T. Hayashi, H. Koide and A. Yamamoto, *J. Chem. Soc., Chem. Commun.*, 1991, 1469-1470.
99. A. Batistini and G. Consiglio, *Organometallics*, 1992, **11**, 1766-1769.
100. G. P. C. M. Dekker, C. J. Elsevier, K. Vrieze and P. W. N. M. van Leeuwen, *Organometallics*, 1992, **11**, 1598-1603.
101. G. P. C. M. Dekker, C. J. Elsevier, K. Vrieze, P. W. N. M. van Leeuwen and C. F. Roobeek, *J. Organomet. Chem.*, 1992, **430**, 357-372.
102. I. Toth and C. J. Elsevier, *J. Am. Chem. Soc.*, 1993, **115**, 10388-10389.
103. S. Kacker and A. Sen, *J. Am. Chem. Soc.*, 1997, **119**, 10028-10033.
104. M. A. Zuideveld, P. C. J. Kamer, P. W. N. M. van Leeuwen, P. A. A. Klusener, H. A. Stil and C. F. Roobeek, *J. Am. Chem. Soc.*, 1998, **120**, 7977-7978.
105. F. J. Parlevliet, M. A. Zuideveld, C. Kiener, H. Kooijman, A. L. Spek, P. C. J. Kamer and P. W. N. M. van Leeuwen, *Organometallics*, 1999, **18**, 3394-3405.
106. G. K. Barlow, J. D. Boyle, N. A. Cooley, T. Ghaffar and D. F. Wass, *Organometallics*, 2000, **19**, 1470-1476.
107. C. S. Shultz, J. Ledford, J. M. DeSimone and M. Brookhart, *J. Am. Chem. Soc.*, 2000, **122**, 6351-6356.
108. J. Ledford, C. S. Shultz, D. P. Gates, P. S. White, J. M. DeSimone and M. Brookhart, *Organometallics*, 2001, **20**, 5266-5276.
109. C. Bianchini, A. Meli, W. Oberhauser, P. W. N. M. van Leeuwen, M. A. Zuideveld, Z. Freixa, P. C. J. Kamer, A. L. Spek, O. V. Gusev and A. M. Kal'sin, *Organometallics*, 2003, **22**, 2409-2421.
110. P. W. N. M. van Leeuwen, M. A. Zuideveld, B. H. G. Swennenhuis, Z. Freixa, P. C. J. Kamer, K. Goubitz, J. Fraanje, M. Lutz and A. L. Spek, *J. Am. Chem. Soc.*, 2003, **125**, 5523-5539.
111. J. Liu, B. T. Heaton, J. A. Iggo and R. Whyman, *Angew. Chem., Int. Ed.*, 2004, **43**, 90-94.
112. J. Liu, B. T. Heaton, J. A. Iggo, R. Whyman, J. F. Bickley and A. Steiner, *Chem. Eur. J.*, 2006, **12**, 4417-4430.
113. R. van Asselt, E. E. C. G. Gielens, R. E. Rulke and C. J. Elsevier, *J. Chem. Soc., Chem. Commun.*, 1993, 1203-1205.
114. R. van Asselt, E. E. C. G. Gielens, R. E. Rulke, K. Vrieze and C. J. Elsevier, *J. Am. Chem. Soc.*, 1994, **116**, 977-985.
115. F. C. Rix and M. Brookhart, *J. Am. Chem. Soc.*, 1995, **117**, 1137-1138.
116. B. A. Markies, D. Kruis, M. H. P. Rietveld, K. A. N. Verkerk, J. Boersma, H. Kooijman, M. T. Lakin, A. L. Spek and G. van Koten, *J. Am. Chem. Soc.*, 1995, **117**, 5263-5274.
117. J. G. P. Delis, P. W. N. M. van Leeuwen, K. Vrieze, N. Veldman, A. L. Spek, J. Fraanje and K. Goubitz, *J. Organomet. Chem.*, 1996, **514**, 125-136.
118. F. C. Rix, M. Brookhart and P. S. White, *J. Am. Chem. Soc.*, 1996, **118**, 4746-4764.
119. J. H. Groen, J. G. P. Delis, P. W. N. M. van Leeuwen and K. Vrieze, *Organometallics*, 1997, **16**, 68-77.
120. C. Carfagna, M. Formica, G. Gatti, A. Musco and A. Pierleoni, *Chem. Commun.*, 1998, 1113-1114.
121. P. W. N. M. van Leeuwen, C. F. Roobeek and H. van der Heijden, *J. Am. Chem. Soc.*, 1994, **116**, 12117-12118.
122. W. Keim and H. Maas, *J. Organomet. Chem.*, 1996, **514**, 271-276.
123. K. Nozaki, N. Sato, Y. Tonomura, M. Yasutomi, H. Takaya, T. Hiyama, T. Matsubara and N. Koga, *J. Am. Chem. Soc.*, 1997, **119**, 12779-12795.
124. C. Gambs, S. Chaloupka, G. Consiglio and A. Togni, *Angew. Chem., Int. Ed.*, 2000, **39**, 2486-2488.

125. K. Nozaki, T. Hiyama, S. Kacker and I. T. Horvath, *Organometallics*, 2000, **19**, 2031-2035.
126. K. Nozaki, H. Komaki, Y. Kawashima, T. Hiyama and T. Matsubara, *J. Am. Chem. Soc.*, 2001, **123**, 534-544.
127. J. A. Iggo, Y. Kawashima, J. Liu, T. Hiyama and K. Nozaki, *Organometallics*, 2003, **22**, 5418-5422.
128. J. G. P. Delis, M. Rep, R. E. Rülke, P. W. N. M. van Leeuwen, K. Vrieze, J. Fraanje and K. Goubitz, *Inorg. Chim. Acta*, 1996, **250**, 87-103.
129. R. E. Rülke, J. G. P. Delis, A. M. Groot, C. J. Elsevier, P. W. N. M. van Leeuwen, K. Vrieze, K. Goubitz and H. Schenk, *J. Organomet. Chem.*, 1996, **508**, 109-120.
130. J. H. Groen, M. J. M. Vlaar, P. W. N. M. van Leeuwen, K. Vrieze, H. Kooijman and A. L. Spek, *J. Organomet. Chem.*, 1998, **551**, 67-79.
131. S. P. Meneghetti, P. J. Lutz and J. Kress, *Organometallics*, 1999, **18**, 2734-2737.
132. B. Milani, A. Scarel, G. Mestroni, S. Gladiali, R. Taras, C. Carfagna and L. Mosca, *Organometallics*, 2002, **21**, 1323-1325.
133. A. Scarel, B. Milani, E. Zangrando, M. Stener, S. Furlan, G. Fronzoni, G. Mestroni, S. Gladiali, C. Carfagna and L. Mosca, *Organometallics*, 2004, **23**, 5593-5605.
134. A. Bastero, A. Ruiz, C. Claver, A. Bella, B. Milani, B. Moreno-Lara, F. A. Jalon and B. R. Manzano, *Adv. Synth. Catal.*, 2005, **347**, 839-846.
135. K. Frankcombe, K. Cavell, R. Knott and B. Yates, *Chem. Commun.*, 1996, 781-782.
136. M. J. Green, G. J. P. Britovsek, K. J. Cavell, B. W. Skelton and A. H. White, *Chem. Commun.*, 1996, 1563-1564.
137. J. L. Hoare, K. J. Cavell, R. Hecker, B. W. Skelton and A. H. White, *J. Chem. Soc., Dalton Trans.*, 1996, 2197-2205.
138. M. J. Green, G. J. P. Britovsek, K. J. Cavell, F. Gerhards, B. F. Yates, K. Frankcombe, B. W. Skelton and A. H. White, *J. Chem. Soc., Dalton Trans.*, 1998, 1137-1144.
139. G. J. P. Britovsek, W. Keim, S. Mecking, D. Sainz and T. Wagner, *J. Chem. Soc., Chem. Commun.*, 1993, 1632-1634.
140. P. Braunstein, C. Frison and X. Morise, *Angew. Chem., Int. Ed.*, 2000, **39**, 2867-2870.
141. G. P. C. M. Dekker, A. Buijs, C. J. Elsevier, K. Vrieze, P. W. N. M. van Leeuwen, W. J. J. Smeets, A. L. Spek, Y. F. Wang and C. H. Stam, *Organometallics*, 1992, **11**, 1937-1948.
142. M. Sperrle, A. Aeby, G. Consiglio and A. Pfaltz, *Helv. Chim. Acta*, 1996, **79**, 1387-1392.
143. A. Aeby, F. Bangerter and G. Consiglio, *Helv. Chim. Acta*, 1998, **81**, 764-769.
144. A. Aeby and G. Consiglio, *Helv. Chim. Acta*, 1998, **81**, 35-39.
145. A. Aeby, A. Gsponer and G. Consiglio, *J. Am. Chem. Soc.*, 1998, **120**, 11000-11001.
146. G. A. Luinstra and P. H. P. Brinkmann, *Organometallics*, 1998, **17**, 5160-5165.
147. E. K. van den Beuken, W. J. J. Smeets, A. L. Spek and B. I. Feringa, *Chem. Commun.*, 1998, 223-224.
148. A. Aeby and G. Consiglio, *J. Chem. Soc., Dalton Trans.*, 1999, 655-656.
149. P. H. P. Brinkmann and G. A. Luinstra, *J. Organomet. Chem.*, 1999, **572**, 193-205.
150. P. Braunstein, M. D. Fryzuk, M. L. Dall, F. Naud, S. J. Rettig and F. Speiser, *J. Chem. Soc., Dalton Trans.*, 2000, 1067-1074.
151. K. R. Reddy, K. Surekha, G.-H. Lee, S.-M. Peng, J.-T. Chen and S.-T. Liu, *Organometallics*, 2001, **20**, 1292-1299.
152. M. Sauthier, F. Leca, L. Toupet and R. Réau, *Organometallics*, 2002, **21**, 1591-1602.
153. A. D. Burrows, M. F. Mahon and M. Varrone, *Dalton Trans.*, 2003, 4718-4730.
154. M. Svensson, T. Matsubara and K. Morokuma, *Organometallics*, 1996, **15**, 5568-5576.
155. P. Margl and T. Ziegler, *Organometallics*, 1996, **15**, 5519-5523.

Chapitre I

Complexes de Nickel, application en catalyse d'oligomerization de l'éthylène

Résumé du Chapitre I

Les dérivés zwitterioniques *N,N*'-dialkyl-2-amino-5-alcoholate-1,4-benzoquinonemonoiminium $[C_6H_2(=NHCH_2CH_2X)_2(=O)_2]$ (X = NMe_2, **9**; X = NHEt, **10**; X = OMe, **11**), préparés auparavant à partir de 4,6-diaminorésorcinol par une réaction de transamination, et **12** (X = $N(CH_2CH_2)_2O$) se comportent comme des ligands tridentés vis-à-vis du $[Ni(acac)_2]$ pour former les complexes octaédriques correspondants ayant deux ligands par centre de Ni(II) $[Ni\{C_6H_2(=NCH_2CH_2X)O(=O)(NHCH_2CH_2X)\}_2]$ (**13-16**). Par contre ligand **9** réagit avec $NiCl_2{\cdot}6H_2O$ par une réaction tandem pour former l'organométallate $[NiCl_2\{C_6H_2(=NCH_2CH_2NMe_2)O(=O)(NHCH_2CH_2NHMe_2)\}]$ (**17**). Les paramètres de liaison des complexes **13**$\cdot H_2O\cdot CH_2Cl_2$ et **17**, déterminés par diffraction des rayons X, et la conformation des ligands autour du centre de nickel ainsi que les arrangements supramoléculaires sont analysés et comparés à ceux des analogues de Zn(II) reportés auparavant. Les complexes **13-17** ont été testés pour l'oligomérisation catalytique de l'éthylène avec MAO ou $AlEtCl_2$ comme cocatalyseur. Le complexe **17** fut le plus actif, avec des fréquences de rotation (TOF, *turnover frequency*) jusqu'à 20 300 and 48 200 mol de C_2H_4/((mol de Ni) h), en présence de 400 équiv de MAO et 10 équiv de $AlEtCl_2$, respectivement. Les sélectivités pour les dimères d'éthylène sont légèrement supérieures en utilisant le MAO: 94% (**14** en présence de 100 équiv de MAO) et 90% (**14** en présence de 6 équiv de $AlEtCl_2$). Les sélectivités pour le 1-butène dans la fraction C_4 sont beaucoup plus élevées quand MAO est utilisé comme cocatalyseur, avec des valeurs jusqu'à 68% (**15** en présence de 100 équiv de MAO). Le fait que **17**, qui contient seulement un ligand tridente par centre nickel, mène à des activités plus élevées que **13-16** souligne l'importance de l'accessibilité du centre métallique dans le procédé catalytique.

Ce chapitre fait l'objet d'une publication dont la référence est donnée ci-dessous. Ma contribution à cette publication porte sur la préparation du manuscrit et la réalisation des tests catalytiques, en collaboration avec Anthony Kermagoret.

Nickel Complexes with Functional Zwitterionic *N,O*-Benzoquinonemonoimine-Tpe Ligands: Synthese, Structures and Catalytic Oligomerization of Ethylene.

Qing-Zheng Yang, Anthony Kermagoret, Magno Agostinho, Olivier Siri and Pierre Braunstein.*

Organometallics **In Press**, Web Release Date: October 4, **2006**

Laboratoire de Chimie de Coordination, UMR 7177 CNRS, Institut de Chimie, Université Louis Pasteur, 4 rue Blaise Pascal, F-67070 Strasbourg Cédex, France

pour les références, voir page 39

Abstract of Chapter I

The zwitterionic *N,N*'-dialkyl-2-amino-5-alcoholate-1,4-benzoquinonemonoiminium derivatives $[C_6H_2(^{--}NHCH_2CH_2X)_2(^{--}O)_2]$ (X = NMe_2, **9**; X = NHEt, **10**; X = OMe, **11**), previously prepared from 4,6-diaminoresorcinol by a transamination reaction, and **12** (X = $N(CH_2CH_2)_2O$) behave as tridentate ligands when reacted with $[Ni(acac)_2]$ to form the corresponding octahedral Ni(II) 2:1 complexes $[Ni\{C_6H_2(=NCH_2CH_2X)O(=O)(NHCH_2CH_2X)\}_2]$ (**13-16**), respectively. In contrast, ligand **9** reacted with $NiCl_2{\cdot}6H_2O$ in a tandemlike manner to afford the stabilized Ni(II) zwitterionic organometalate 1:1 complex $[NiCl_2\{C_6H_2(=NCH_2CH_2NMe_2)O(=O)(NHCH_2CH_2NHMe_2)\}]$ (**17**). The bonding parameters of complexes **13**$\cdot H_2O\cdot CH_2Cl_2$ and **17**, determined by X-ray diffraction, and the conformation of the ligands around the nickel center as well as the supramolecular arrangements are discussed and compared with those of their previously reported Zn(II) analogues. Complexes **13-17** were tested in catalytic ethylene oligomerization with MAO and $AlEtCl_2$ as cocatalysts. Complex **17** yielded the highest turnover frequencies, with values up to 20 300 and 48 200 mol of C_2H_4/((mol of Ni) h), in the presence of 400 equiv of MAO and 10 equiv of $AlEtCl_2$, respectively. Selectivities for ethylene dimers were slightly higher when using MAO: 94% (**14** in the presence of 100 equiv of MAO) and 90% (**14** in the presence of 6 equiv of $AlEtCl_2$). The selectivities for 1-butene within the C_4 fraction were much higher when using MAO as cocatalyst, with values up to 68% (**15** in the presence of 100 equiv of MAO). The fact that **17**, which contains only one tridentate ligand per nickel center, leads to higher activities than **13-16** underlines the importance of the metal center accessibility in the catalytic process.

This chapter has been published. My contribution to this publication, whose reference is given below, is the preparation of the manuscript and the catalytic studies, in collaboration with Anthony Kermagoret.

Nickel Complexes with Functional Zwitterionic *N,O*-Benzoquinonemonoimine-Tpe Ligands: Synthese, Structures and Catalytic Oligomerization of Ethylene.

Qing-Zheng Yang, Anthony Kermagoret, Magno Agostinho, Olivier Siri and Pierre Braunstein.*

Organometallics **In Press**, Web Release Date: October 4, **2006**

Laboratoire de Chimie de Coordination, UMR 7177 CNRS, Institut de Chimie, Université Louis Pasteur, 4 rue Blaise Pascal, F-67070 Strasbourg Cédex, France

for references, see page 39

Nickel Complexes with Functional Zwitterionic *N,O*-Benzoquinonemonoimine-Tpe Ligands: Synthese, Structures and Catalytic Oligomerization of Ethylene.

Introduction

Recent review articles have illustrated the important role played by nickel complexes in the catalytic oligomerization and polymerization of olefins.[1-3] The competition between olefin insertion and chain-transfer processes accounts for the occurrence of oligomerization and polymerization reactions, respectively. Obviously, this is a function of a number of parameters, including of course the nature of the ligands and the structure of the precatalyst. With the exception of SHOP-type systems, which are based on neutral phenyl complexes containing a chelating P,O ligand,[4-7] activation of the nickel precatalyst by a cocatalyst, such as MAO or AlEtCl2, is generally required. The choice of the cocatalyst is crucial to the activity and selectivity of the system.[1-3,8,9] Brookhart *et al.* have reported very active and selective α-diimine nickel complexes for ethylene polymerization and oligomerization.[10] This work has inspired the synthesis of a number of new nickel complexes with N,N-type ligands as precatalysts, using MMAO,[11] MAO,[12] $B(C_6F_5)_3$,[13] and $Al_2Et_3Cl_3$[14] as cocatalysts. Difunctional P,Ntype ligands can also lead to very interesting Ni(II) precatalysts, some of them being very active and highly selective for dimerization and trimerization of ethylene in the presence of MAO or $AlEtCl_2$.[3]

Considerable research effort has been devoted over the past few years to the design of new chelating N,O ligands, and their nickel complexes have shown very high catalytic activity for olefin oligomerization and polymerization.[15-22] Efficient ethylene polymerization catalysts with N,O-type ligands were developed by Grubbs *et al.*[23-25] and Brookhart *et al.*[26-28] which are based on salicylaldimine and anilinotropone ligands, respectively, and do not require the use of a cocatalyst. Other Ni(II) complexes with N,O chelates catalytically oligomerize ethylene only in the presence of a cocatalyst, such as MAO,[29,30] $AlEt_3$,[31] $B(C_6F_5)_3$,[32] or ethylaluminum sesquichloride.[33] We have shown that nickel complexes prepared from oxazoline and pyridine alcohols and activated by MAO or $AlEtCl_2$ are very effective and lead to high selectivities for C_4 and C_6 products.[34] Although N,O-type ligands have recently been applied in coordination chemistry to the synthesis of porphyrin dimers and oligomers connected by metal ions,[35,36] only a few examples of mono- or polynuclear metal complexes based on N,O ligands supported by a quinonoid core have been reported.[37-39] A series of 2,5-disubstituted amino-*p*-benzoquinone ligands of the N,O,N,O type **1** has been

for references, see page 39

used recently by Zhang and co-workers for the preparation of Ni(II) complexes of type **2**, which were active as single-component catalysts in ethylene polymerization.[40]

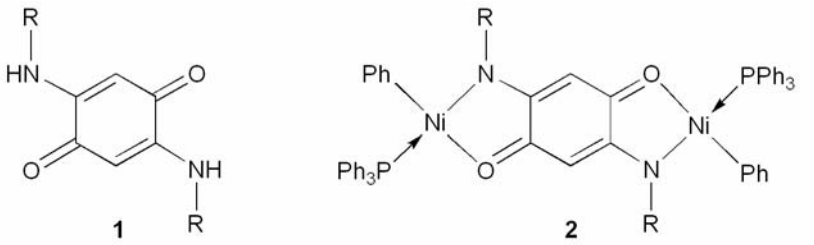

We recently reported the synthesis and electronic structure of the zwitterionic benzoquinonemonoimine ligand **3** from 4,6-diaminoresorcinol dihydrochloride.[41] Assembling of two of these benzoquinonemonoimines around the metal center by a metalation reaction using [M(acac)$_2$] (M = Ni, Zn, Cu) afforded complexes **4**-**6**.[41] Precatalyst **4** was active in ethylene oligomerization and favored the dimerization and trimerization of ethylene when activated with $AlEtCl_2$.[42]

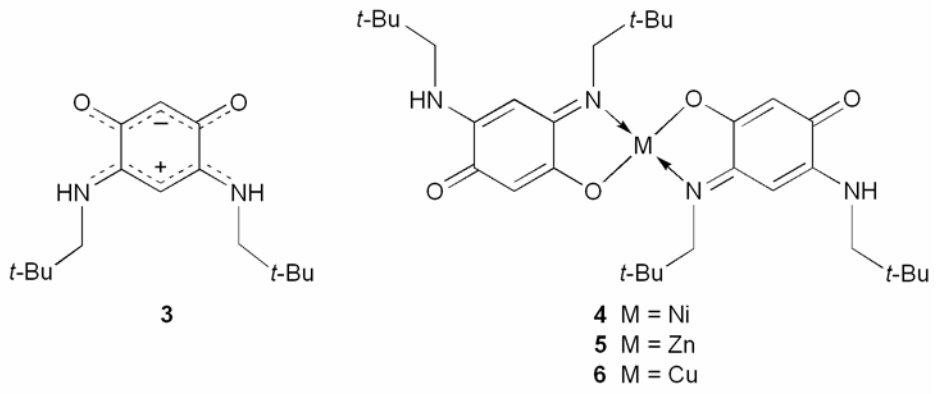

Therefore, the screening of other functional ligands of type **3** with substituents which could lead, for example, to potentially hemilabile behavior[43] should be of particular interest in coordination chemistry and homogeneous catalysis.

The industrial demand for C_4-C_{20} linear α-olefins has triggered research toward their selective synthesis, and the fast growing need for linear α-olefins in the C_4-C_{10} range (a ca. 2.5×10^6 tons/year market) explains why their selective formation from ethylene has become a topic of major fundamental and applied importance.[44] As part of our interest in new ethylene oligomerization Ni(II) catalysts for the production of short-chain oligomers in the presence of only small quantities of $AlEtCl_2$ or MAO, we have extended our preliminary studies on Ni(II) complexes supported by a benzoquinonemonoimine N,O chelate and have now evaluated complexes **13**-**17**.

for references, see page 39

Results and Discussion

Ligands and Complexes

The N-substituted, 6 π + 6 π electron zwitterionic benzoquinonemonoimine ligands **9**-**11** have been previously obtained from 4,6-diaminoresorcinol dihydrochloride (**7**·2HCl) via the parent zwitterion **8**, by using a new and efficient procedure that involved the first transamination reactions in quinonoid chemistry.[45,46] The new ligand **12** has now been prepared in a similar manner (Scheme 1). These ligands react at room temperature with [Ni(acac)$_2$] in a 2:1 molar ratio of ligand to metal to afford the octahedral complexes **13**-**16** in high yields (Scheme 2). Monodeprotonation of the ligand results from the basicity of the acac ligand. Owing to their paramagnetism, compounds **13**-**16** were only characterized by mass spectrometry and elemental analysis. Single crystals of **13**·H_2O·CH_2Cl_2 suitable for X-ray diffraction were obtained by slow diffusion of pentane into a CH_2Cl_2 solution of the complex (which contained adventitious water) (see Figure 1 and Tables 1 and 2). Coordination of the pendant amino (ligands **9**, **10**, and **12**) or ether (ligand **11**) function leads to hexacoordinated nickel centers.

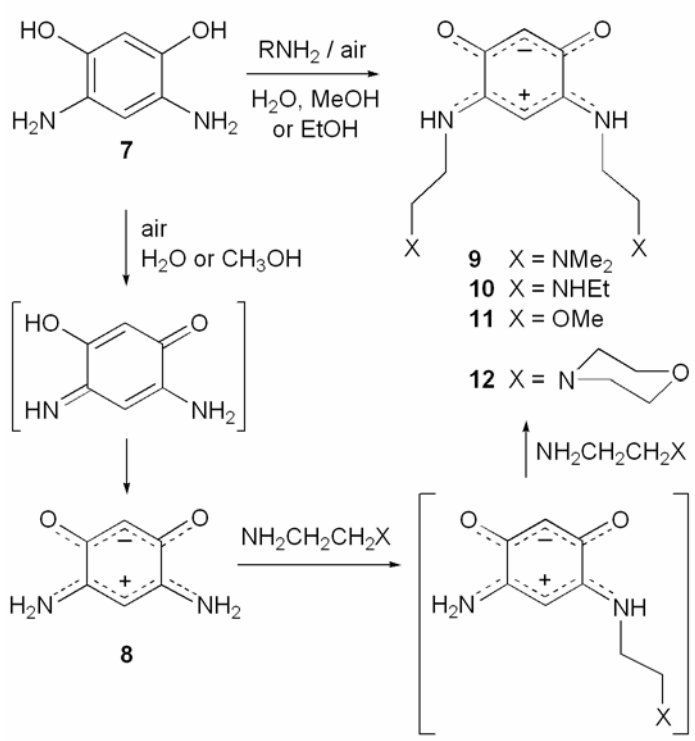

Scheme 1.
Part One-Pot Synthesis of the Functional Zwitterions.

for references, see page 39

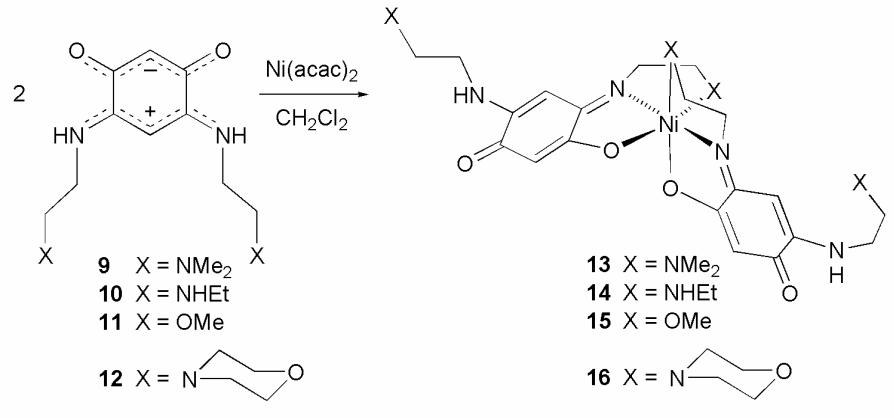

Scheme 2.
Reactions of Ligands **9-12** Affording the Octahedral Ni(II) Complexes **13-16**.

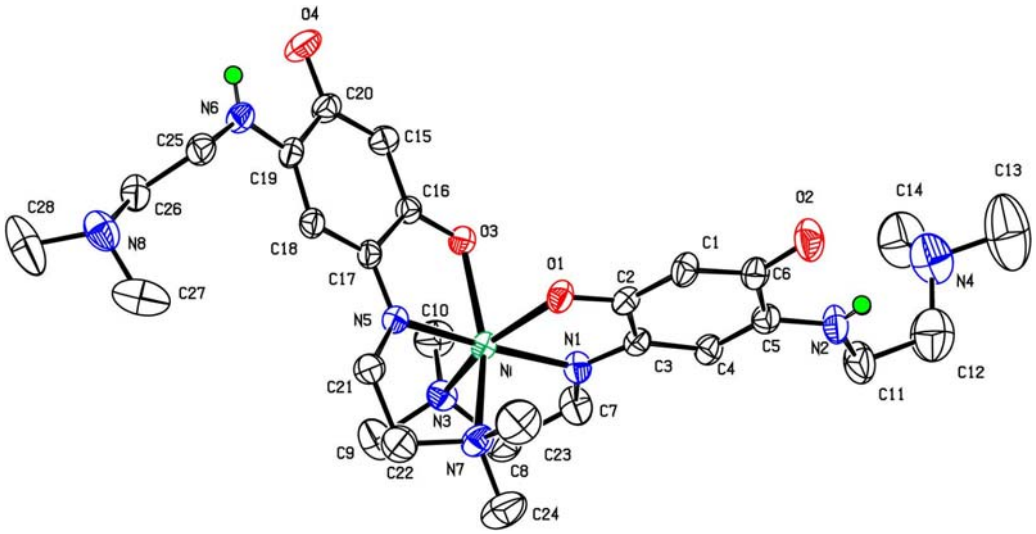

Figure 1.
ORTEP view of the crystal structure of **13** in **13**·H_2O·CH_2Cl_2 (ellipsoids drawn at the 50% probability level).

Table 1.
Selected Bond Distances (Å).

	13·H_2O·CH_2Cl_2	**17**
Ni-N1	2.001(4)	1.975(1)
Ni-N3	2.238(4)	2.138(1)
Ni-N5		
Ni-N7		
Ni-O1	2.105(3)	2.142(1)
Ni-O3		
Ni-Cl1		2.3337(5)
Ni-Cl2		2.3037(5)
O1-C2	1.284(5)	1.289(2)
C2-C1	1.380(6)	1.373(2)
C1-C6	1.407(7)	1.422(2)
C6-O2	1.256(6)	1.240(2)
N1-C3	1.299(6)	1.295(2)
C3-C4	1.422(6)	1.420(2)
C4-C5	1.366(7)	1.371(2)
C5-N2	1.337(6)	1.343(2)
C2-C3	1.506(6)	1.511(2)
C5-C6	1.511(7)	1.514(2)

Table 2.
Selected bond angles (°).

	13·H_2O·CH_2Cl_2	**17**
N5-Ni-N1	175.7(1)	
N5-Ni-O3	78.5(1)	
N1-Ni-O3	100.6(1)	
N5-Ni-O1	97.4(1)	
N1-Ni-O1	78.3(1)	77.96(5)
O1-Ni-O3	86.7(1)	
N5-Ni-N7	79.3(2)	
N1-Ni-N7	101.0(2)	
O3-Ni-N7	156.6(1)	
O1-Ni-N7	89.0(2)	
N5-Ni-N3	104.6(2)	
N1-Ni-N3	79.6(2)	81.58(6)
O1-Ni-N3	156.9(1)	156.73(5)
N3-Ni-N7	101.7(2)	
Cl1-Ni-Cl2		103.43(2)
Cl1-Ni-N1		97.78(4)
Cl2-Ni-N1		157.78(5)
Cl2-Ni-O1		98.28(3)
Cl2-Ni-N3		96.47(4)
Cl1-Ni-N3		95.79(4)
Cl1-Ni-O1		98.15(4)

for references, see page 39

As shown in Figure 1, the octahedral geometry around the metal center in the complex **13**·H_2O·CH_2Cl_2 results from the coordination of two tridentate, monometalated ligands, with their two-electron-donor imine nitrogen atoms N(1) and N(5) in mutually trans positions. The covalently bound oxygens O(1) and O(3) are trans to the X donors N(3) and N(7), respectively. The Ni-O and Ni-N bond distances in complex **13** (Table 1) are only slightly shorter than those of its zinc analogue (corresponding values (Å): Zn-N1 = 2.021(4), Zn-N3 = 2.330(5), Zn-N5 = 2.037(4), Zn-N7 = 2.442(5), Zn-O1 = 2.123(4), Zn-O3 = 2.134(4)),[46] which parallels the differences in metal radii (1.246 and 1.333 Å for Ni and Zn, respectively).[47] Interatomic C-O, C-C, and C-N distances within the quinonemonoimine core of complex **13** indicate an alternation of single and double bonds, which is consistent with a localized π system, as previously observed for the analogous zinc complex,[46] whereas in the free ligand[45] and all related crystallographic structures,[41,42,45,46,48] a highly delocalized π system is present.

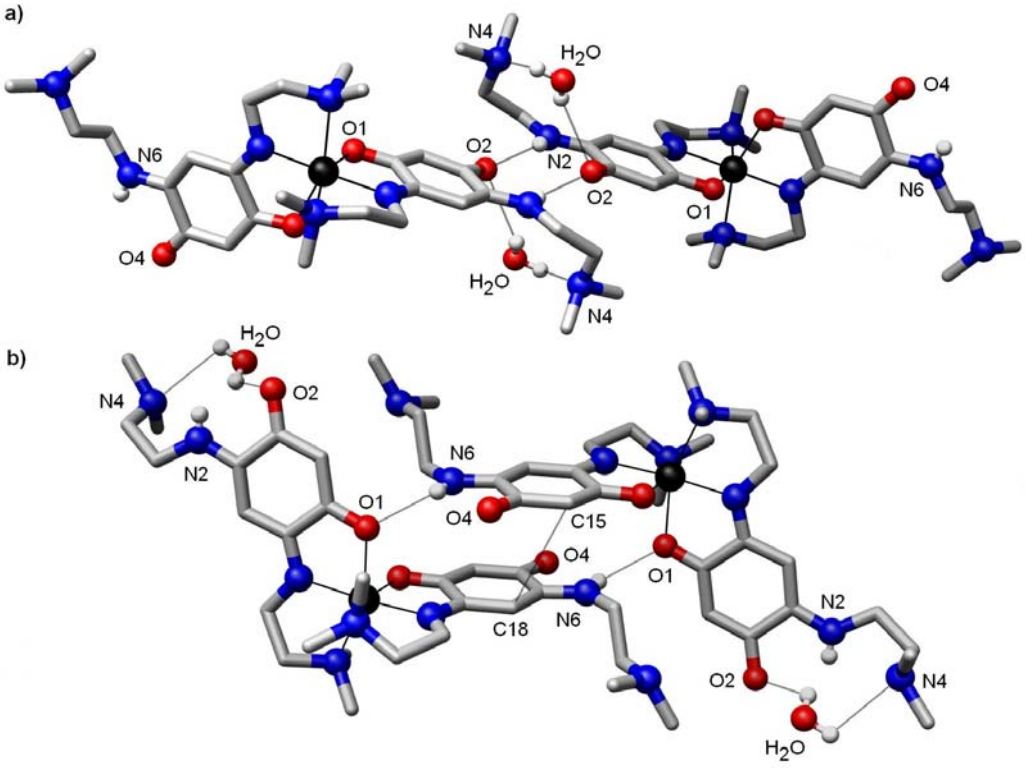

Figure 2.
Hydrogen bonding in the complex **13**·H_2O·CH_2Cl_2 (CH_2Cl_2 solvent molecules omitted for clarity): (a) between N2-H and O2; (b) between N6-H and O1. Color coding: nitrogen, blue; oxygen, red; nickel, black.

Examination of the crystal packing of the complex **13**·H_2O·CH_2Cl_2 reveals intermolecular N2-H···O2 and N6-H···O1 hydrogen-bonding interactions (N2···O2 = 2.971(6) Å, N6···O1 = 2.897(6) Å), which lead to a onedimensional wavelike chain arrangement in the solid-state (Figures 2 and 3). This arrangement also allows stabilizing π-π interactions between quinone rings, with a C15···C18 distance of 3.650(6) Å. A similar arrangement was

for references, see page 39

also observed in its Zn(II) analogue.[45,46] However, in the present case, the complex crystallized with a molecule of water and of dichloromethane. The H_2O molecules interact through hydrogen bonding, with O2···O(H2O) and N4···O(H2O) distances of 2.994(15) and 2.954(12) Å, respectively. The CH_2Cl_2 molecules are placed between the wavelike chains, one of their C-H bonds interacting with O4 (O4···C29(CH_2Cl_2) = 3.23(2) Å, O4-H29A-C29 = 155º).

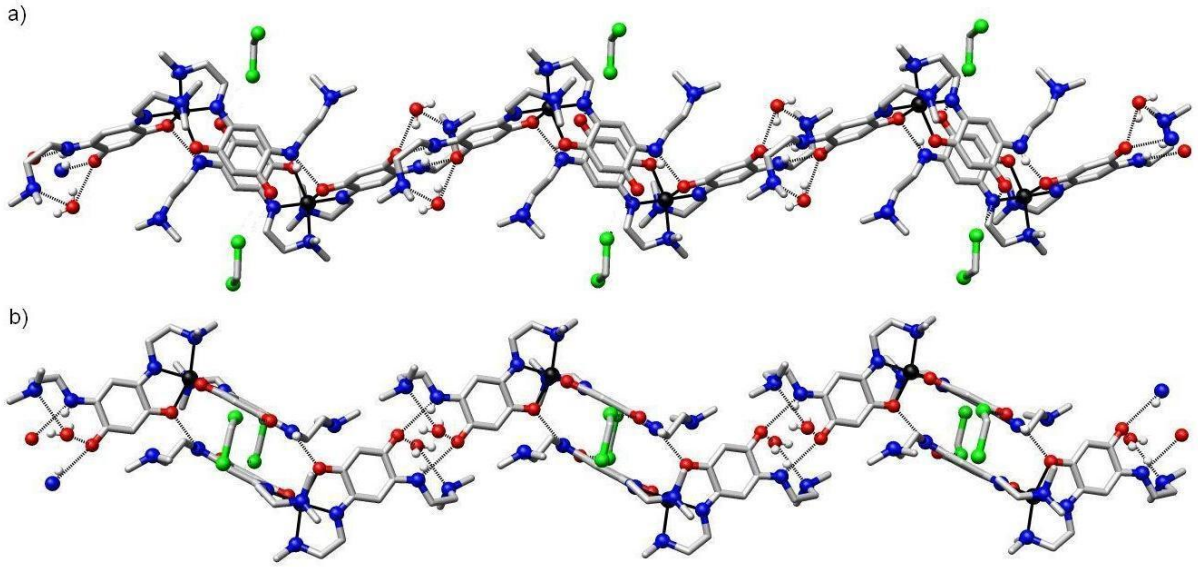

Figure 3.
Views of the supramolecular array generated by **13**·H_2O·CH_2Cl_2 in the solid state: (a) top view; (b) side view. Color coding: nitrogen, blue; oxygen, red; chloride, green; nickel, black.

When ligand **9** was reacted with $NiCl_2·6H_2O$ in a 1:1 molar ratio at room temperature in MeOH, it afforded the mononuclear complex **17** (Scheme 3). In contrast to the fate of the acac ligand in Scheme 2, both chloride ligands remain coordinated to the nickel center in **17**. The molecular structure of this complex was determined by X-ray diffraction (Figure 4 and Tables 1 and 2). Like its Zn(II) analogue,[45] **17** presents a zwitterionic structure, where the negative charge of the metalate moiety is balanced by the ammonium cation resulting from an intramolecular proton shift.

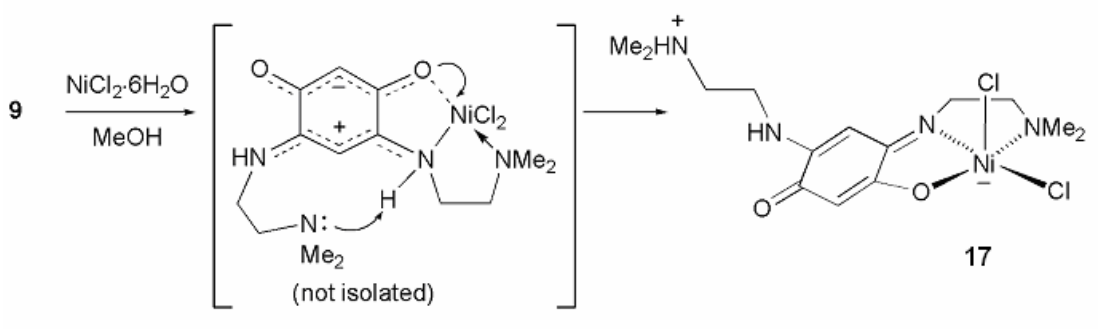

Scheme 3.
Reaction of Ligand **9** with $NiCl_2·6H_2O$ Affording the Pentacoordinated Ni(II) Complex **17.** The negative charge shown for clarity on the Ni(II) center is, of course, partially delocalized on the ligands.

for references, see page 39

This zwitterionic complex contains only one tridentate ligand per nickel center, and the pentacoordination about the metal results in a slightly distorted square-based-pyramidal geometry (Figure 4). The base is formed by the three ligand donor sites (N1, N3, and O1) and Cl2, while Cl1 completes the coordination sphere in the apical position of the pyramid. The nickel is at a distance of 0.3536(3) Å from the mean plane passing through N1, N3, O1, and Cl2.

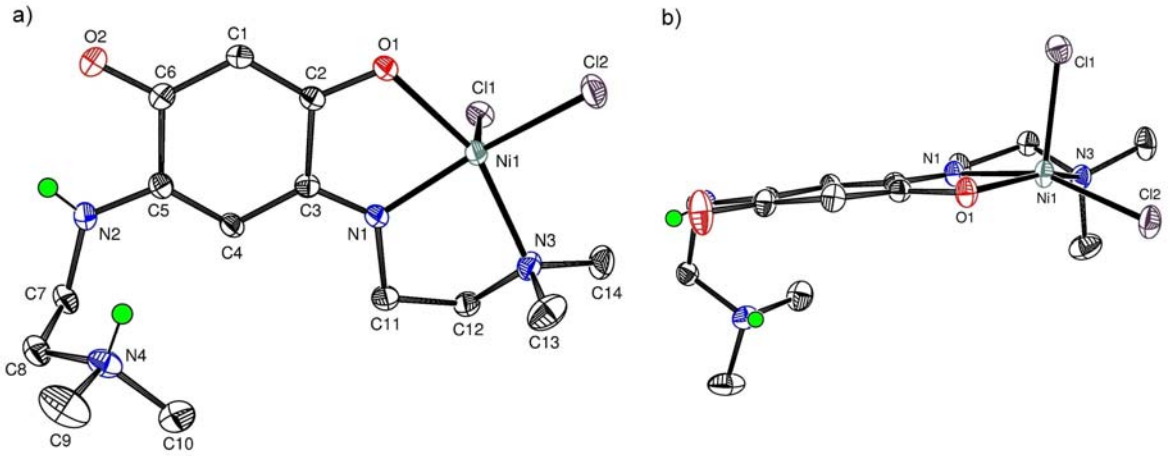

Figure 4.
ORTEP view of the structure of **17** (ellipsoids drawn at the 50% probability level): (a) view from the bottom of the squarebased pyramid; (b) side view. The C-*H* atoms are not shown.

As observed with its Zn(II) analogue,[45] complex **17** forms in the solid state a pseudodimer which is stabilized by the N4-H···O1 interaction (N4···O1 = 2.810(2) Å) and π-π stacking with a C1···C4 distance of 3.542(3) Å (Figure 5). These pseudo-dimers are in turn organized along chains, in an alternate A-A'-A-A' manner, where dimer A is rotated by 88.92(4)º around the chain axis with respect to dimer A' (Figure 6). There are no short contacts between these pseudo-dimers.

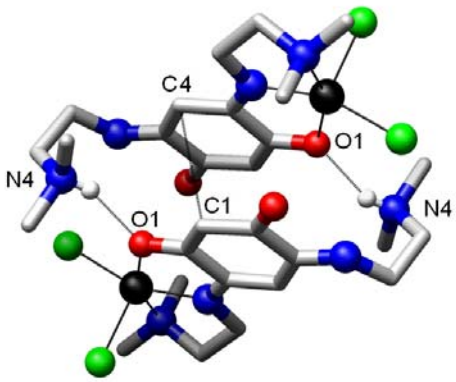

Figure 5.
Hydrogen bonding in the pseudo-dimers formed by the zwitterionic Ni(II) complex **17** in the solid state. Color coding: nitrogen, blue; oxygen, red; chloride, green; nickel, black.

for references, see page 39

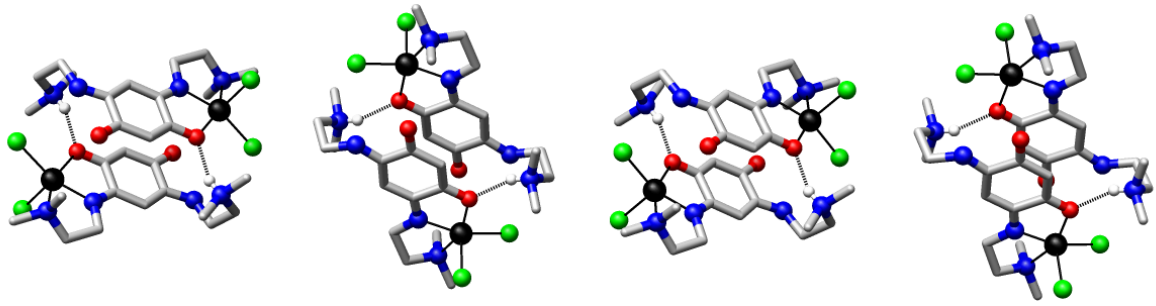

Figure 6.
View of the array generated by the pseudo-dimers formed by the zwitterionic Ni(II) complex **17** in the solid state. Color coding: nitrogen, blue; oxygen, red; chloride, green; nickel, black.

Catalytic Oligomerization of Ethylene

The precatalysts **13-17** have been tested in the presence of variable amounts of $AlEtCl_2$ or MAO as cocatalyst and showed high activities for the dimerization and trimerization of ethylene (Tables 3 and 4). The results were compared with those obtained with $NiCl_2(PCy_3)_2$, a typical α-olefin dimerization catalyst[49,50] (Figures 7-11). We felt it would be interesting to determine the fractions of the different C_6 oligomers formed by chain growth or by reinsertion of 1-butene or 2-butene (Tables 5 and 6). Depending on the nature of their insertion (2,1- or 1,2-insertion) and on which C-H bond undergoes agostic interaction with the metal,[51-54] two schemes can explain the formation of 2-hexene, 3-hexene, and 2-ethylbut-1-ene from 1-butene (Scheme 4) and the formation of 3-methylpent-2-ene and 3-methylpent-1-ene from 2-butene (Scheme 5). 1-Hexene is formed by a chain growth mechanism, and its Ni-catalyzed isomerization leads to 2-hexene and 3-hexene.[55]

Table 3.
Comparative Catalytic Data for Complexes **13-17** in the Oligomerisation of Ethylene with $AlEtCl_2$ as Cocatalyst.[a,b]

	$AlEtCl_2$ (equiv)	Selectivity (mass %)		Productivity (g C_2H_4/(g Ni·h))	TOF (mol C_2H_4/(mol Ni·h))	α-olefin (C_4) (mol %)	k_α[c]
		C_4	C_6				
13	6	88	12	11700	24400	5.8	<0.10
13	10	82	18	17700	37200	5.3	0.15
14	6	90	10	11600	24300	9.4	<0.10
14	10	80	20	17500	36900	6.3	0.16
15	6	89	11	11600	24300	8.3	<0.10
15	10	80	20	17000	35600	4.6	0.16
16	10	83	16	10900	23000	7.1	0.13
17	6	72	28	20600	43300	4.5	0.26
17	10	76	23	23000	48200	5.7	0.20
17[d]	10	76	24	10000	20500	6.2	0.22
4[42]	6	49	45	13500	28500	14.0	0.60
4	10	51	43	21500	45000	7.0	0.57
Ref[e]	6	59	34	27600	57800	11.2	0.38
Ref	10	65	31	24400	51500	9.8	0.32

[a]Conditions: T = 30 °C, 10 bar of C_2H_4, 35 min, $4\cdot\times 10^{-5}$ mol Ni complex, solvent 12 mL of chlorobenzene and 3 ml of cocatalyst solution in toluene, or 10 of mL chlorobenzene and 5 ml of cocatalyst solution in toluene, for 6 or 10 equivalents of $AlEtCl_2$, respectively. [b]No C_8-C_{10} oligomers were detected. [c]k_α = (mol of hexenes/(mol of butenes). [d]Reaction time = 200 min. [e]Reference: $NiCl_2(PCy_3)_2$.

for references, see page 39

Table 4.
Comparative Catalytic Data for Complexes **13-17** in the Oligomerisation of Ethylene with MAO as Cocatalyst.[a,b]

	MAO (equiv)	Selectivity (mass %) C_4	C_8	C_6	Productivity (g C_2H_4/(g Ni·h))	TOF (mol C_2H_4/(mol Ni·h))	α-olefin (C_4) (mol %)	k_α[c]
13	100	92	7	<1	1400	2900	49	<0.10
13	200	87	14	2	3600	7600	47	0.11
13	400	65	29	5	7300	15400	24	0.30
14	100	94	5	<1	600	1300	61	<0.10
14	200	86	12	2	3500	7400	45	0.11
15	100	93	6	<1	1300	2700	68	<0.10
15	200	82	17	1	4800	10300	37	0.14
16	100	86	12	2	2400	5000	50	<0.10
16	200	69	26	5	6100	13000	28	0.25
16	400	63	29	7	8800	18500	22	0.32
17	100	77	21	2	5500	11600	27	0.18
17	200	71	24	5	7400	16100	22	<0.10
17	400	55	35	9	9700	20300	19	0.42
Ref[d]	200	74	18	8	600	1200	76	0.16
Ref	400	70	26	4	3000	6400	72	0.24

[a]Conditions: T = 30 °C, 10 bar of C_2H_4, 35 min, $4\cdot\times 10^{-5}$ mol Ni complex; solvent 12 mL chlorobenzene and 4, 8 or 16 mL of cocatalyst solution in toluene for 100, 200 or 400 equivalents of MAO, respectively. [b]Traces of C_{10} oligomers were detected when using 400 equivalents of MAO. [c]k_α = (mol of hexenes/(mol of butenes). [d]Reference: $NiCl_2(PCy_3)_2$.

A comparison of the various catalytic results should indicate the influence of (i) the nature of the donor function in the complexing ligand arm, (ii) the increase in metal coordination number resulting from the presence of the complexing arm, by comparison with the properties of **4**, (iii) the metal coordination geometry, (iv) the nature of the cocatalyst, and (v) the lifetime of the catalyst.

(i) Influence of the Donor Function in the Arm

Complexes **13-16** display hexacoordinate geometry around the metal center, with the ligand coordinating arm endowed with different donor functions. Precatalysts **13-15** afforded similar results with $AlEtCl_2$, with turnover frequency (TOF) values between 24 300 and 24 400 or between 35 600 and 37 200 mol of C_2H_4/((mol of Ni) h), when 6 or 10 equiv of cocatalyst was used, respectively (Table 3). Complex **16** showed a slightly lower activity (23 000 mol of C_2H_4/((mol of Ni) h) with 10 equiv of $AlEtCl_2$). The selectivities for C_4 olefins observed with **13-16** were very similar and were close to 89% or 82% in the presence of 6 or 10 equiv of $AlEtCl_2$, respectively. However, the selectivities for α-butene were lower than 10%.

With MAO as cocatalyst, the activities and selectivities of **13-15** were of similar orders of magnitude. Their activities were in the range 1300-2900 mol of C_2H_4/((mol of Ni) h) with 100 equiv of MAO and 7400-10 300 mol of C_2H_4/((mol of Ni) h) with 200 equiv, and the activity of **13** was found to be 15 400 mol of C_2H_4/((mol of Ni) h) in the presence of 400 equiv of MAO (Table 4). The selectivities for C_4 olefins were around 93% with 100 equiv and 85% for 200 equiv of MAO. With **13-15,** the selectivity for 1-butene was up to 68% with 100

for references, see page 39

equiv of MAO and 47% with 200 equiv. Under these conditions, precatalyst **16** showed a higher activity but a lower selectivity in C_4 products and 1-butene in comparison to **13-15**.

A comparison between the four different functions available in the complexing arm shows that, with both cocatalysts, the tertiary amine (precatalyst **13**), the secondary amine (precatalyst **14**), and the ether function (precatalyst **15**) led to similar catalytic results in ethylene oligomerization but the morpholine function (precatalyst **16**) led to a less active catalyst with $AlEtCl_2$ but a more active catalyst with MAO.

(ii) Influence of the Ligand Coordinating Arm

In contrast to **4**, complexes **13-17** have a coordinating arm which could display either static chelation or potentialy hemilabile behavior and therefore influence the catalytic results. A comparison of the results obtained with **4** and **13-16**, in which the nickel center is coordinated by two ligands, is provided in Table 3. The activity of **4** (28 500 and 45 000 mol of C_2H_4/((mol of Ni) h) with 6 and 10 equiv of $AlEtCl_2$, respectively) and its selectivity for 1-butene were higher (14%) than those of **13-16**. However, the selectivity for C4 olefins was only 51% with **4** but up to 90% with **13-16**. This suggests that the presence of the coordinating arm in complexes **13-16** disfavors both the insertion of ethylene and the reinsertion mechanism which leads to the C_6 oligomers.

(iii) Influence of the Coordination Geometry of the Metal

One of the objectives of this study was to determine the influence on the catalytic properties of hexacoordination in complexes with two tridentate benzoquinonemonoimine ligands and of pentacoordination in complexes containing only one benzoquinonemonoimine ligand and two chlorides. This can be done by comparing the performances of compounds **13** and **17**. Precatalyst **17** led to higher activities than **13** with $AlEtCl_2$ or MAO as cocatalyst, up to 48 200 mol of C_2H_4/((mol of Ni) h) with $AlEtCl_2$ and 20 300 mol of C_2H_4/((mol of Ni) h) with MAO (Table 4). In the presence of MAO or $AlEtCl_2$, the most active precatalyst in the series was **17**. The difference in activity between **17** and **13** could be due to an easier generation of the active species by nickel alkylation in the former case than with **13**, where it probably requires the loss of a chelating N,O ligand. However, the selectivity of **17** for C_4 products and for 1-butene was lower than with **13**.

The catalyst ability to reinsert the primary C_4 products has a clear impact on product selectivity (Schemes 4 and 5). Data in Table 5 show that the fraction of branched C_6 oligomers formed from 2-butene was ca. 59% for **17** and ca. 53% for **13** with $AlEtCl_2$. A similar observation was made with MAO as cocatalyst. Consequently, precatalyst **17**, which

for references, see page 39

is more active than **13** and reinserts 2-butene more readily than **13** to form C_6 products, leads to a lower selectivity for butenes.

Table 5.
Catalytic Data and Distribution of the C_6 Alkenes for Complexes **13-17** in the Oligomerization of Ethylene with $AlEtCl_2$ as Cocatalyst[a]

	$AlEtCl_2$ (equiv)	Selectivity (mass %)			
		1-hexene	linear C_6[b]	C_6[c] from 1-butene	C_6[d] from 2-butene
13	6	0	40	10	52
13	10	0	39	7	54
14	6	0	42	13	45
14	10	0	43	7	50
15	6	0	46	11	43
15	10	0	43	6	51
16	10	<1[c]	46	3	50
17	6	0	36	6	58
17	10	0	36	4	60

[a]Conditions: T = 30 °C, 10 bar of C_2H_4, 35 min, 4·× 10^{-5} mol Ni complex, solvent 12 mL of chlorobenzene and 3 ml of cocatalyst solution in toluene, or 10 of mL chlorobenzene and 5 ml of cocatalyst solution in toluene, for 6 or 10 equivalents of $AlEtCl_2$, respectively. [b]Sum of 3-*cis*-hexene, 3-*trans*-hexene, 2-*cis*-hexene, and 2-*trans*-hexene. [c]Corresponds to 2-ethyl-1-butene. *d* Sum of 3-methyl-1-pentene, 3-methyl-2-*cis*-pentene, and 3-methyl-
2-*trans*-pentene. [e]Only in this case was 1-hexene detected.

Table 6.
Catalytic Data for Complexes **13-17** and Distribution of the C_6 Alkenes in the Oligomerization of Ethylene with MAO as Cocatalyst[a]

	MAO (equiv)	Selectivity (mass %)			
		1-hexene	linear C_6[b]	C_6[c] from 1-butene	C_6[d] from 2-butene
13	100	18	58	13	11
13	200	9	61	13	20
13	400	5	50	13	32
14	100	20	54	12	14
14	200	9	59	12	20
15	100	20	58	11	9
15	200	7	57	13	23
16	100	10	57	13	20
16	200	6	52	12	30
16	400	4	51	11	34
17	100	5	54	12	29
17	200	4	51	11	36
17	400	4	50	11	35

[a]Conditions: T = 30 °C, 10 bar of C_2H_4, 35 min, 4·× 10^{-5} mol Ni complex; solvent 12 mL chlorobenzene and 4, 8 or 16 mL of cocatalyst solution in toluene for 100, 200 or 400 equivalents of MAO, respectively. [b]Sum of 3-*cis*-hexene, 3-*trans*-hexene, 2-*cis*-hexene, and 2-*trans*-hexene. [c]Corresponds to 2-ethyl-1-butene. [d]Sum of 3-methyl-1-pentene, 3-methyl-2-*cis*-pentene, and 3-methyl-2-*trans*-pentene.

(iv) Influence of the Cocatalyst

The use of $AlEtCl_2$ or MAO as cocatalyst influenced the catalytic results presented in Tables 3 and 4: the activities (up to 48 200 mol of C_2H_4/((mol of Ni) h)) were higher with $AlEtCl_2$ as cocatalyst than with MAO, but MAO generally led to a higher selectivity for C_4 olefins (94% for **14**, with 100 equiv of MAO). The precatalysts activated by $AlEtCl_2$ afforded strongly isomerizing systems so that the fraction of 2-butene is very high (up to 95%). The

for references, see page 39

high selectivity for C_4 olefins is consistent with the more difficult reinsertion of 2-butene to form C_6 oligomers compared to 1-butene. In contrast, MAO associated with **13-17** favored chain growth, as indicated by the percentages of 1-butene (up to 68%) and 1-hexene (up to 21%) within their respective fractions, and of C_8 oligomers (up to 9%).

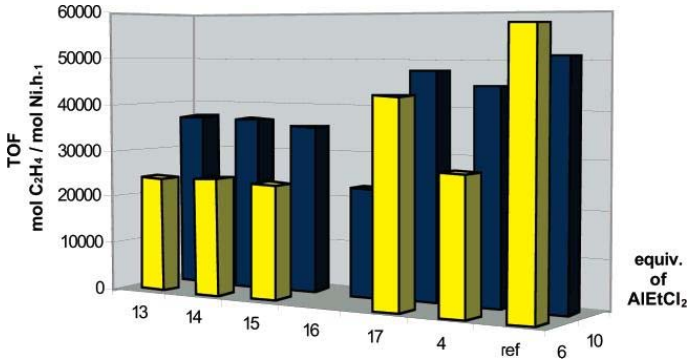

Figure 7.
Catalytic activities of the complexes **13-17** and **4** in the oligomerization of ethylene using $AlEtCl_2$ as cocatalyst, Ref: $NiCl_2(PCy_3)_2$.

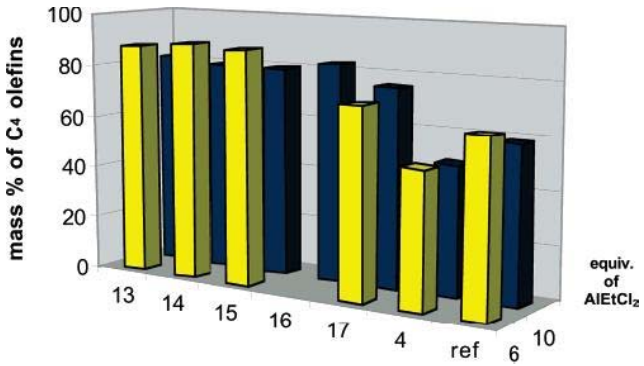

Figure 8.
Selectivity of the complexes **13-17** and **4** for C_4 compounds (1-butene and 2-butene), $NiCl_2(PCy_3)_2$ was used as the reference.

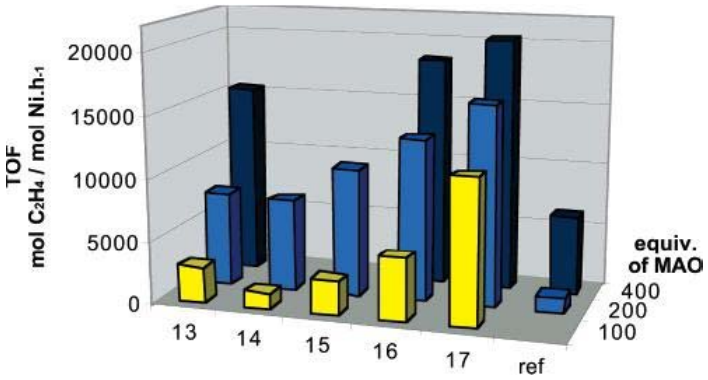

Figure 9.
Catalytic activities of the complexes **13-17** in the oligomerization of ethylene using MAO as cocatalyst. $NiCl_2(PCy_3)_2$ was used as the reference.

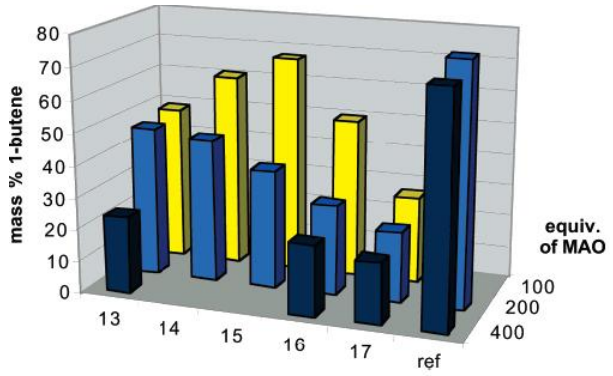

Figure 10.
Selectivity of the complexes **13-17** for 1-butene within the C_4 fraction. $NiCl_2(PCy_3)_2$ was used as the reference.

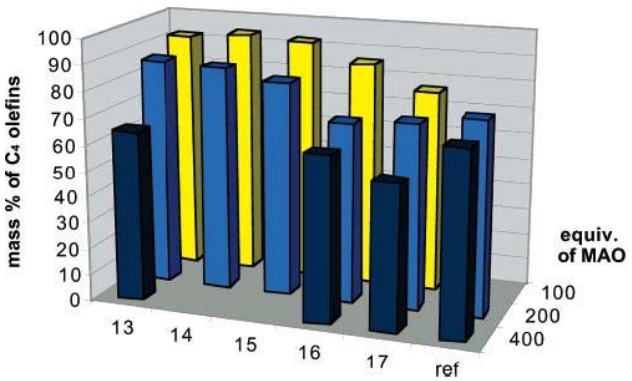

Figure 11.
Selectivity of the complexes **13-17** for C_4 olefins (1-butene and 2-butene). $NiCl_2(PCy_3)_2$ was used as the reference.

The amount of cocatalyst used significantly influences the catalytic results, particularly with MAO. Increasing the amountsof MAO resulted in increased activity for **13-**

for references, see page 39

17 but decreased selectivity in both 1- and 2-butenes (Table 4). Reinsertion of 1-butene results in the formation of higher oligomers (the selectivity for 1-butene decreased from 49% to 24% with **13**, for example). The increased percentage of C_6 oligomers from 2-butene (from 11% with 100 equiv of MAO to 32% with 400 equiv with **13**, for example) shows that the reinsertion of 2-butene is also favored by increasing amounts of MAO.

Scheme 4.
Products Resulting from the Reinsertion of 1-Butene[a]

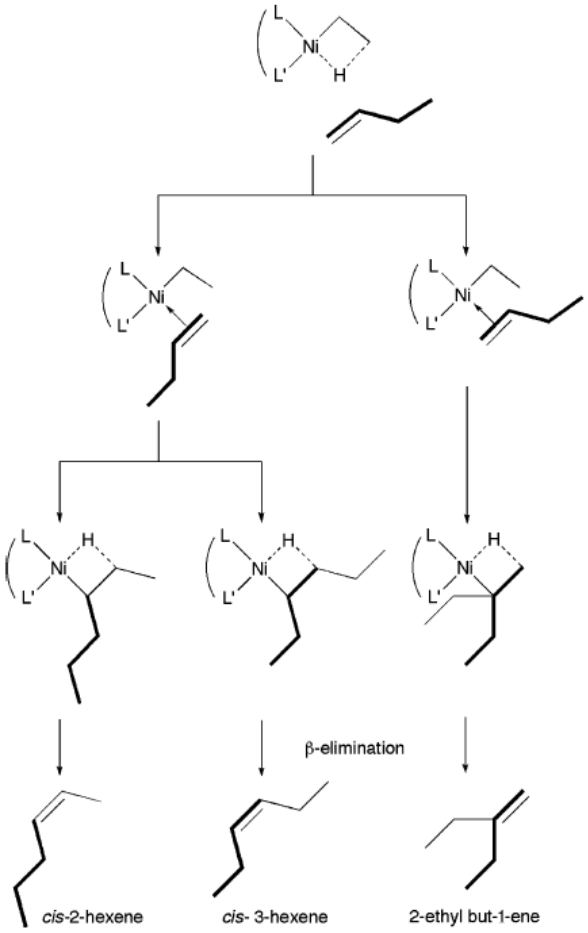

[a]The stereochemical information is not illustrated: agostic interactions with diastereotopic CH_2 protons afford the cis or trans isomers.

Scheme 5.
Pentenes Resulting from the Reinsertion of 2-Butene[b]

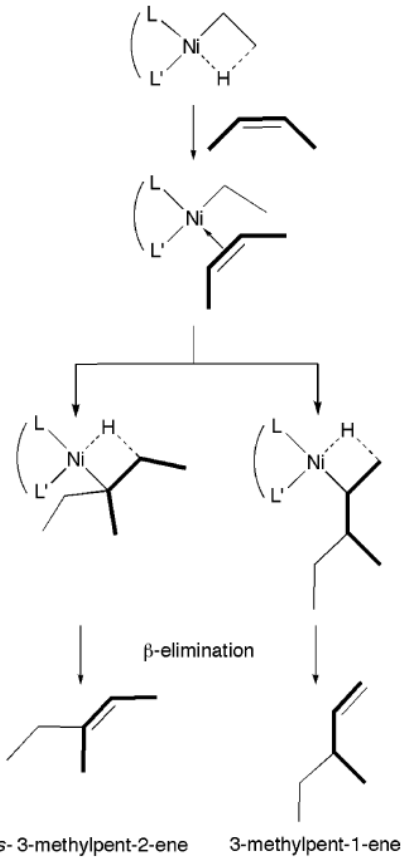

[b]The stereochemical information is not illustrated.

(v) Lifetime of the Catalyst

To study the lifetime of the catalysts, complex **17**, the most active precatalyst, was tested with 10 equiv of $AlEtCl_2$ with a reaction time increased to 200 min. The robustness of the catalyst was indicated by a constant activity during catalysis (the consumption of C_2H_4 was constant, no plateau of activity was observed, and the final activity was 20 500 mol of C_2H_4/((mol of Ni) h)). Selectivities were similar to those observed under standard conditions (Table 3).

for references, see page 39

Conclusion

New Ni(II) complexes have been synthesized with tridentate zwitterionic benzoquinonemonoimine ligands. The reaction of 2 equiv of the ligands **9-12** with $Ni(acac)_2$ led to the formation of **13-16**, respectively, with a hexacoordinated nickel center, whereas the reaction of 1 equiv of **9** with $NiCl_2 \cdot 6H_2O$ afforded the zwitterionic complex **17** with a pentacoordinated nickel center. Obviously, the higher basicity of the acac ligand compared to that of chloride is responsible for the difference observed as a function of the Ni(II) precursor.

The precatalysts **13-17** have been tested in the oligomerization of ethylene with different amounts of $AlEtCl_2$ or MAO as cocatalyst. The results showed that $AlEtCl_2$ led to more active and less selective systems in α-olefins than did MAO. Increasing amounts of MAO or $AlEtCl_2$ as cocatalyst resulted in more active but less selective systems.

The influence of the complexing arm of **9-12** was evaluated by comparing **4** with **13-16**. It was found that its presence led to lower activities but better selectivity in C_4 oligomers because it disfavored butene reinsertion. The comparison of **13-16** showed that the different complexing functions of the arm have no significant consequences on the catalytic results. Only **16** showed higher activities and lower selectivities with MAO as cocatalyst and lower activities with $AlEtCl_2$ as cocatalyst than **13-15**.

The influence of the geometry of the complexes has been determined by the comparison between **13** and **17**, and it was found that pentacoordination favored the insertion of olefins and led to higher activity but lower selectivity.

Experimental section

General Considerations. All solvents were dried and freshly distilled under nitrogen prior to use using common techniques. All manipulations were carried out using Schlenk techniques. ^1H (300 MHz) and ^{13}C NMR (75 MHz) spectra were recorded on a Bruker AC300 instrument. MALDI-TOF mass spectra were recorded on a Biflex III Bruker mass spectrometer. Elemental analyses were performed by the Service de Microanalyse, Université Louis Pasteur (Strasbourg, France). 4,6-Diaminoresorcinol dihydrochloride and the functional amines were commercially available. Ligands **9-11** have been prepared according to the literature.[45,46]

Ligand 12. To a stirred solution of diaminoresorcinol dihydrochloride (2.13 g, 10 mmol) in water (30 mL) was added 4-(2-aminoethyl)morpholine (9.76 g, 75 mmol), and the reaction

for references, see page 39

mixture was extracted with CH_2Cl_2 after 2 h. The organic layer was collected, dried with $MgSO_4$, filtered, and concentrated to ca. 30 mL. Pentane was added to the solution, and the pale gray precipitate was isolated by filtration. Yield: 74%. MS (MALDI-TOF$^+$): *m*/*z* 365.2 [M + 1]$^+$. ^{1}H NMR (300 MHz, $CDCl_3$): δ 2.50 (t, ^3J = 4.5 Hz, 8H, NCH_2CH$_2$O), 2.71 (t, ^3J = 6.1 Hz, 4H, NHCH$_2$CH_2N), 3.42 (t, ^3J = 6.1 Hz, 4H, NHCH_2), 3.73 (t, ^3J = 4.5 Hz, 8H, OCH$_2$), 5.10 (s, 1H, N-C-CH), 5.44 (s, 1H, O-C-CH), 8.48 (br s, 2H, NH). ^{13}C NMR (75 MHz, $CDCl_3$) δ 39.48 (s, NCH$_2$CH$_2$O), 53.29 (s, NHCH$_2$CH$_2$N), 55.42 (s, NHCH$_2$), 66.84 (s, OCH$_2$), 81.27 (s, N-C-*C*), 99.01 (s, O-C-*C*), 156.79 (s, N-C), 172.23 (s, O-C). Anal. Calcd for $C_{18}H_{28}N_4O_4 \cdot 0.5H_2O$: C, 57.89; H, 7.83; N, 15.00. Found: C, 57.75; H, 7.80; N, 15.36.

Complex 13. Ligand **9** (1.12 g, 4.0 mmol) was dissolved in dichloromethane (200 mL), and 0.5 equiv of solid [Ni(acac)$_2$] (0.55 g, 2.0 mmol) was then added to the solution in one portion. After the solution was stirred at room temperature for 3 h, the solvent was concentrated to ca. 20 mL under vacuum and the red crystalline complex **13** was obtained by precipitation from a mixture of dichloromethane and pentane. Yield: 92%. MS (MALDI-TOF$^+$): *m*/*z* 617.3 [M + 1]$^+$. Anal. Calcd for $C_{28}H_{46}N_8NiO_4 \cdot H_2O \cdot CH_2Cl_2$: C, 48.35; H, 7.00; N, 15.56. Found: C, 48.65; H, 7.12; N, 15.78.

Complex 14. The synthetic procedure was similar to that described for complex **13**, but using ligand **10** instead of **9**. Yield: 88%. MS (MALDI-TOF$^+$): *m*/*z* 617.3 [M + 1]$^+$. Anal. Calcd for $C_{28}H_{46}N_8NiO_4 \cdot 0.5H_2O \cdot 0.5CH_2Cl_2$: C, 51.18; H, 7.23; N, 16.75. Found: C, 51.06; H, 7.28; N, 17.04.

Complex 15. The synthetic procedure was similar to that described for complex **13**, but using ligand **11** instead of **9**. Yield: 91%. MS (MALDI-TOF$^+$): *m*/*z* 565.2 [M + 1]$^+$. Anal. Calcd for $C_{24}H_{34}N_4NiO_8$: C, 51.00; H, 6.06; N, 9.91. Found: C, 50.91; H, 6.03; N, 9.85.

Complex 16. The synthetic procedure was similar to that described for complex **13**, but using ligand **12** instead of **9**. Yield: 93%. MS (MALDI-TOF$^+$): *m*/*z* 785.3 [M + 1]$^+$. Anal. Calcd for $C_{36}H_{54}N_8NiO_8 \cdot 0.5H_2O$: C, 54.42; H, 6.98; N, 14.10. Found: C, 54.37; H, 7.03; N, 13.91.

Complex 17. To a solution of ligand **9** (0.28 g, 1.0 mmol) in methanol (30 mL) was added 1 equiv of $NiCl_2 \cdot 6H_2O$ (0.24 g, 1.0 mmol), and the reaction mixture was stirred for 3 h. Complex **17** was obtained as a purple crystalline solid by slow diffusion of ether into the

for references, see page 39

reaction mixture. Yield: 71%. MS (MALDI-TOF$^-$): *m*/*z* 409.1 [*M* - 1]$^-$. Anal. Calcd for $C_{14}H_{24}Cl_2N_4NiO_2$: C, 41.02; H, 5.90; N, 13.67. Found: C, 40.81; H, 6.11; N, 13.33.

Oligomerization of Ethylene. All catalytic reactions were carried out in a magnetically stirred (900 rpm) 145 mL stainless steel autoclave. A 125 mL glass container was used to protect the inner walls of the autoclave from corrosion. All catalytic tests were started at 30 ºC, and no cooling of the reactor was done during the reaction. After injection of the catalytic solution and of the cocatalyst under a constant low flow of ethylene, the reactor was pressurized to 10 bar. A temperature increase was observed which resulted solely from the exothermicity of the reaction. The 10 bar working pressure was maintained during the experiments through a continuous feed of ethylene from a reserve bottle placed on a balance to allow continuous monitoring of the ethylene uptake. In all of the catalytic experiments 4×10^{-2} mmol of Ni complex was used. The oligomerization products and remaining ethylene were only collected from the reactor at the end of the catalytic experiment. At the end of each test (35 min) a dry ice bath, and in the more exothermic cases also liquid N_2, was used to rapidly cool the reactor, thus stopping the reaction. When the inner temperature reached 0 ºC, the ice bath was removed, allowing the temperature to slowly rise to 10 ºC. The gaseous phase was then transferred into a 10 L polyethylene tank filled with water. An aliquot of this gaseous phase was transferred into a Schlenk flask, previously evacuated, for GC analysis. The products in the reactor were hydrolyzed in situ by the addition of ethanol (1 mL), transferred into a Schlenk flask, and separated from the metal complexes by trap-to-trap evaporation (20 ºC, 0.3 mmHg) into a second Schlenk flask previously immersed in liquid nitrogen in order to avoid any loss of product. For GC analyses, 1-heptene was used as an internal reference. When $AlEtCl_2$ was used as cocatalyst, depending on the amount used (6 or 10 equiv), the required quantity of Ni(II) complex was dissolved in 12 or 10 mL of chlorobenzene, respectively, and injected into the reactor. The cocatalyst solution, 3 or 5 mL corresponding to 6 or 10 equiv, respectively, was then added. Therefore, the total volume of the solution inside the reactor, for all the tests performed with $AlEtCl_2$, was 15 mL. In the cases where MAO was used as cocatalyst, the Ni(II) complex was always dissolved in 12 mL of chlorobenzene, and after injection of this solution, the desired amount of cocatalyst was added. The total volume of the solution inside the reactor at the beginning of each test was therefore dependent on the amount of cocatalyst used. Total volumes of 16, 20, and 28 mL correspond to 100, 200, and 400 equiv of MAO, respectively.

for references, see page 39

Crystal Structure Determinations. Diffraction data were collected on a Kappa CCD diffractometer using graphite-monochromated Mo Kα radiation (λ = 0.710 73 Å) (Table 7). Data were collected using Ψ scans, the structures were solved by direct methods using the SHELX97 software,[56,57] and the refinement was by full-matrix least squares on F^2. No absorption correction was used. All non-hydrogen atoms were refined anisotropically, with H atoms introduced as fixed contributors ($d_{C\text{-}H}$ = 0.95 Å, U_{11} = 0.04). Crystallographic data (excluding structure factors) have been deposited in the Cambridge Crystallographic Data Centre as Supplementary Publication Nos. CCDC 618435 and 618436. Copies of the data can be obtained free of charge on application to the CCDC, 12 Union Road, Cambridge CB2 1EZ, U.K. (fax, (+44)-1223-336-033; e-mail, deposit@ccdc.cam.ac.uk).

Acknowledgment. We thank the Centre National de la Recherche Scientifique (CNRS), the Ministère de l'Education Nationale et de la Recherche (Paris), the Institut Français du Pétrole (IFP), Clariant, and the European Commission (Palladium Network HPRN-CT-2002-00196 and COST program) for support. We also thank Dr. A. DeCian and Prof. R. Welter (ULP Strasbourg) for the crystal structure determinations and M. Mermillon-Fournier (LCC Strasbourg) for technical assistance.

Supporting Information Available: CIF files giving crystallographic data for **13** and **17**. This material is available free of charge via the Internet at http://pubs.acs.org. OM060600S

for references, see page 39

References

1. Ittel, S. D.; Johnson, L. K.; Brookhart, M. *Chem. Rev.* **2000**, *100*, 1169-1203.
2. Gibson, V. C.; Spitzmesser, S. K. *Chem. Rev.* **2003**, *103*, 283-315.
3. Speiser, F.; Braunstein, P.; Saussine, L. *Acc. Chem. Res.* **2005**, *38*, 784-793.
4. (a) Keim, W. *Angew. Chem. Int. Ed.* **1990**, *29*, 235-244. (b) Heinicke, J.; He, M.; Dal, A.; Klein, H. F.; Hetche, O.; Keim, W.; Flörke, U.; Haupt, H.-J. *Eur. J. Inorg. Chem.* **2000**, 431-440. (c) Heinicke, J.; Köhler, M.; Peulecke, N.; He, M.; Kindermann, M. K.; Keim, W.; Fink, G. *Chem. Eur. J.* **2003**, *9*, 6093-6107. (d) Heinicke, J.; Peulecke, N.; Köhler, M.; He, M.; Keim, W. *J. Organomet. Chem.* **2005**, *690*, 2449-2457.
5. Braunstein, P.; Chauvin, Y.; Mercier, S.; Saussine, L. *C. R. Chimie* **2005**, *8*, 31-38.
6. Kuhn, P.; Semeril, D.; Jeunesse, C.; Matt, D.; Neuburger, M.; Mota, A. *Chem. Eur. J.* **2006**, *12*, 5210-5219.
7. Komon, Z. J. A.; Bu, X.; Bazan, G. C. *J. Am. Chem. Soc.* **2000**, *122*, 12379-12380.
8. Speiser, F.; Braunstein, P.; Saussine, L.; Welter, R. *Organometallics* **2004**, *23*, 2613-2624.
9. Chen, E. Y.-X.; Marks, T. J. *Chem. Rev.* **2000**, *100*, 1391-1434.
10. Johnson, L. K.; Killian, C. M.; Brookhart, M. *J. Am. Chem. Soc.* **1995**, *117*, 6414-6415.
11. Killian, C. M.; Johnson, L. K.; Brookhart, M. *Organometallics* **1997**, *16*, 2005-2007.
12. Chen, L.; Hou, J.; Sun, W.-H. *Appl. Catal., A* **2003**, *246*, 11-16.
13. Strauch, J. W.; Erker, G.; Kehr, G.; Fröhlich, R. *Angew. Chem., Int. Ed.* **2002**, *41*, 2543-2546.
14. Schareina, T.; Hillebrand, G.; Fuhrmann, H.; Kempe, R. *Eur. J. Inorg. Chem.* **2001**, 2421-2426.
15. Zuideveld, M. A.; Wehrmann, P.; Roehr, C.; Mecking, S. *Angew. Chem., Int. Ed.* **2004**, *43*, 869-873.
16. Held, A.; Mecking, S. *Chem. Eur. J.* **2000**, *6*, 4623-4629.
17. Darensbourg, D. J.; Ortiz, C. G.; Yarbrough, J. C. *Inorg. Chem.* **2003**, *42*, 6915-6922.
18. Carlini, C.; Isola, M.; Liuzzo, V.; Raspolli Galletti, A. M.; Sbrana, G. *Appl. Catal., A* **2002**, *231*, 307-320.
19. Zhang, D.; Jin, G.-X.; Hu, N.-H. *Eur. J. Inorg. Chem.* **2003**, 1570-1576.
20. Li, X.-F.; Li, Y.-S. *J. Polym. Sci., A* **2002**, *40*, 2680-2685.
21. Pickel, M.; Casper, T.; Rahm, A.; Dambouwy, C.; Chen, P. *Helv. Chim. Acta* **2002**, *85*, 4337-4352.
22. Novak, B. M.; Tian, G.; Nodono, M.; Boyle, P. *Polym. Mat. Sci. Eng.* **2002**, *86*, 326-327.
23. Younkin, T. R.; Connor, E. F.; Henderson, J. I.; Friedrich, S. K.; Grubbs, R. H.; Bansleben, D. A. *Science* **2000**, *287*, 460-462.
24. Younkin, T. R.; Connor, E. F.; Henderson, J. I.; Friedrich, S. K.; Grubbs, R. H.; Bansleben, D. A. *Science* **2000**, *288*, 1750-1751.
25. Wang, C.; Friedrich, S.; Younkin, T. R.; Li, R. T.; Grubbs, R. H.; Bansleben, D. A.; Day, M. W. *Organometallics* **1998**, *17*, 3149-3151.
26. Jenkins, J. C.; Brookhart, M. *Organometallics* **2003**, *22*, 250-256.
27. Hicks, F. A.; Jenkins, J. C.; Brookhart, M. *Organometallics* **2003**, *22*, 3533-3545.
28. Brookhart, M.; Jenkins, J. C.; Zhang, L. *Abstracts of Papers*; 227th National Meeting, of the American Chemical Society, Anaheim, CA, March 28-April 1, 2004; American Chemical Society: Washington, D.C., **2004**, POLY-325.
29. Sun, W.-H.; Zhang, W.; Gao, T.; Tang, X.; Chen, L.; Li, Y.; Jin, X. *J. Organomet. Chem.* **2004**, *689*, 917-929.
30. Wang, L.; Sun, W.-H.; Han, L.; Yang, H.; Hu, Y.; Jin, X. *J. Organomet. Chem.* **2002**, *658*, 62-70.
31. Qian, Y.; Zhao, W.; Huang, J. *Inorg. Chem. Commun.* **2004**, *7*, 459-461.

32. Chen, Y.; Wu, G.; Bazan, G. C. *Angew. Chem., Int. Ed.* **2005**, *44*, 1108-1112.
33. Kim, I.; Kwak, C. H.; Kim, J. S.; Ha, C.-S. *Appl. Catal., A* **2005**, *287*, 98-107.
34. Speiser, F.; Braunstein, P.; Saussine, L. *Inorg. Chem.* **2004**, *43*, 4234-4240.
35. Richeter, S.; Jeandon, C.; Ruppert, R.; Callot, H. J. *Chem. Commun.* **2001**, 91-92.
36. Richeter, S.; Jeandon, C.; Gisselbrecht, J.-P.; Ruppert, R.; Callot, H. J. *J. Am. Chem. Soc.* **2002**, *124*, 6168-6179.
37. Moriuchi, T.; Watanabe, T.; Ikeda, I.; Ogawa, A.; Hirao, T. *Eur. J. Inorg. Chem.* **2001**, 277-287.
38. Elduque, A.; Aguilera, F.; Lahoz, F. J.; Lopez, J. A.; Oro, L. A.; Pinillos, M. T. *Inorg. Chim. Acta* **1998**, *274*, 15-23.
39. Kühlwein, F.; Polborn, K.; Beck, W. *Z. Anorg. Allg. Chem.* **1997**, *623*, 1931-1944.
40. Zhang, D.; Jin, G.-X. *Organometallics* **2003**, *22*, 2851-2854.
41. Braunstein, P.; Siri, O.; Taquet, J.-p.; Rohmer, M.-M.; Bénard, M.; Welter, R. *J. Am. Chem. Soc.* **2003**, *125*, 12246-12256.
42. Taquet, J.-p.; Siri, O.; Braunstein, P.; Welter, R. *Inorg. Chem.* **2004**, *43*, 6944-6953.
43. Braunstein, P.; Naud, F. *Angew. Chem. Int. Ed.* **2001**, *40*, 680-699.
44. Rieger, B.; Saunders Baugh, L.; Kacker, S.; Striegler, S., Eds. *Late Transition Metal Polymerization* Catalysis; Wiley -VCH: Weinheim, Germany, 2003.
45. Yang, Q.-Z.; Siri, O.; Braunstein, P. *Chem. Eur. J.* **2005**, *11*, 7237-7246.
46. Yang, Q.-Z.; Siri, O.; Braunstein, P. *Chem.Commun.* **2005**, 2660-2662.
47. Holleman, A. F.; Wiberg, E. *Holleman-Wiberg Lehrbuch der Anorganischen Chemie, 91.-100. Auflage, Walter de Gruyter, Berlin* **1985**, 1152-1156.
48. Siri, O.; Braunstein, P. *Chem. Commun.* **2002**, 208-209.
49. Knudsen, R. D. *Prep.-Am. Chem. Soc., Div. Petrol. Chem.* **1989**, 572-576.
50. Commereuc, D.; Chauvin, Y.; Leger, G.; Gaillard, J. *Rev. Inst. Fr. Pét.* **1982**, *37*, 639-649.
51. Tempel, D. J.; Brookhart, M. *Organometallics* **1998**, *17*, 2290-2296.
52. Svejda, S. A.; Brookhart, M. *Organometallics* **1999**, *18*, 65-74.
53. Gottfried, A. C.; Brookhart, M. *Macromolecules* **2003**, *36*, 3085-3100.
54. Zhao, W.; Qian, Y.; Huang, J.; Duan, J. *J. Organomet. Chem.* **2004**, *689*, 2614-2623.
55. Zhang, J.; Gao, H.; Ke, Z.; Bao, F.; Zhu, F.; Wu, Q. *J. Mol. Catal. A: Chem.* **2005**, *231*, 27-34.
56. *Kappa CCD Operation Manual*; Nonius BV, Delft, The Nederlands, 1997.
57. Sheldrick, G. M.: SHELXL97, Program for the refinement of crystal structures, University of Göttingen, Germany, 1997.

Chapitre II

Complexes de Palladium, études d'insertion de CO/éthylène

Résumé de la Partie A

Trois nouveaux complexes contenant un chélate difonctionnel, les tris(chloro{[1-méthyl-1-(6-méthyl-2-pyridyl)éthoxy]diphénylphosphine-k^2-*N*,*P*}méthylpalladium(II)·chloroforme, 3[Pd(CH_3)Cl($C_{21}H_{22}$NOP)]·$CHCl_3$ (III), dichloro[2-(2,6-dimethylphenyl)-6-(diphénylphosphinométhyl)pyridine-k^2-*N*,*P*]palladium(II), [$PdCl_2$($C_{26}H_{24}$NP)] (IV), et chloro[2-(2,6-diméthylphényl)-6-(diphénylphosphinométhyl)pyridine-k^2-*N*,*P*]methylpalladium(II), [Pd(CH_3)Cl($C_{26}H_{24}$NP)] (V), sont décrits. Les paramètres géométriques et la conformation des ligands autour des centres métalliques, ainsi que les légères distorsions de la coordination autour du Pd par rapport à la géométrie idéale carré plane sont analysés et comparés avec ceux de complexes voisins. Le composé (II) est le premier complexe du type-*P*,*N* chloro-methyl-phosphinite Pd^{II} possédant un chélate à six membres, à être caractérisé structurellement.

Cette partie du chapitre fait l'objet d'une publication dont la référence est donnée ci-dessous. Ce travail a été effectué en collaboration avec le Laboratoire DECOMET de Strasbourg. Ma contribution à cette publication porte sur la synthèse et toutes les caractérisations du complexe (III) et la caractérisation spectroscopique des complexes (IV) et (V).

New palladium complexes with phosphino- and phosphinitopyridine ligands

Magno Agostinho,[a] Andrei Banu,[a] Pierre Braunstein,[a]* Richard Welter[b] and Xavier Morise[a]

Acta Crystallogr., Sect. C: Cryst. Struct. Commun. **2006**, C62, m81.

[a] *Laboratoire de Chimie de Coordination, UMR 7177 CNRS, Institut de Chimie, Université Louis Pasteur, 4 rue Blaise Pascal, F-67070 Strasbourg Cédex, France*

[b] Laboratoire DECOMET, *UMR 7177 CNRS, Institut de Chimie, Université Louis Pasteur, 4 rue Blaise Pascal, F-67070 Strasbourg Cédex, France*

pour les références, voir page 55

Abstract of Part A

Three new palladium complexes containing a difunctional *P*,*N*-chelate, namely tris(chloro{[1-methyl-1-(6-methyl-2-pyridyl)ethoxy]diphenylphosphine-k^2N,*P*} methylpalladium(II) chloroform solvate, 3[Pd(CH_3)Cl($C_{21}H_{22}NOP$)]·$CHCl_3$, (III), dichloro[2-(2,6-dimethylphenyl)-6-(diphenylphosphinomethyl)pyridine-k^2N,*P*] palladium(II), [$PdCl_2$($C_{26}H_{24}NP$)], (IV), and chloro[2-(2,6-dimethylphenyl)-6-(diphenylphosphinomethyl) pyridine-k^2N,*P*] methylpalladium(II), [Pd(CH_3)Cl($C_{26}H_{24}NP$)], (V), are reported. Geometric data and the conformations of the ligands around the metal centers, as well as slight distortions of the Pd coordination environments from idealized square-planar geometry, are discussed and compared with the situations in related compounds. Non-conventional hydrogen-bond interactions (C−H···Cl) have been found in all three complexes. Compound (III) is the first six-membered chloro-methyl-phosphinite *P*,*N*-type Pd^{II} complex to be structurally characterized.

This part of the chapter has been published. This work has been done in collaboration with the Laboratory DECOMET from Strasbourg. My contribution to this publication, whose reference is given below, consists of the synthesis and complete characterisation of (III) and the spectroscopic characterisation of (IV) and (V).

New palladium complexes with phosphino- and phosphinitopyridine ligands

Magno Agostinho,[a] Andrei Banu,[a] Pierre Braunstein,[a]* Richard Welter[b] and Xavier Morise[a]

Acta Crystallogr., Sect. C: Cryst. Struct. Commun. **2006**, C62, m81.

[a] *Laboratoire de Chimie de Coordination, UMR 7177 CNRS, Institut de Chimie, Université Louis Pasteur, 4 rue Blaise Pascal, F-67070 Strasbourg Cédex, France*

[b] Laboratoire DECOMET, *UMR 7177 CNRS, Institut de Chimie, Université Louis Pasteur, 4 rue Blaise Pascal, F-67070 Strasbourg Cédex, France*

for references, see page 55

New palladium complexes with phosphino- and phosphinitopyridine ligands

Comment

Ligands containing at least two chemically different donor functions and able to chelate a metal center are of considerable interest since they provide a way to influence selectively the bonding and/or reactivity of the other ligands, in particular those in trans positions (Braunstein & Naud, 2001). This concept has been successfully applied to ligands containing a *P*,*O*- or a *P*,*N*-donor set (Braunstein & Naud, 2001; Slone *et al*., 1999).

Phosphinito- and phosphinopyridine ligands find widespread applications in the coordination chemistry of transition metals (Newkome, 1993, and references therein; Chen *et al*., 2003a) and in homogeneous catalysis (Agbossou *et al*., 1998, and references therein; Espinet & Soulantica, 1999, and references therein; Bianchini & Meli, 2002, and references therein; Chen *et al*., 2003b; Braunstein, 2004, and references therein; Speiser *et al*., 2004, 2004a,b). We have recently reported the synthesis of the ligands [1-methyl-1-(6-methyl-2-pyridyl)ethoxy]diphenylphospine, (I) (Speiser *et al*., 2004), and 2-(2,6-dimethylphenyl)-6-(diphenylphosphinomethyl)pyridine, (II) (Speiser *et al*., 2004a), and investigated the catalytic properties of their [$NiCl_2$(*P*,*N*)] complexes (*P*,*N* = *P*,*N*-chelating ligand) for ethylene oligomerization. Owing to the paramagnetism of these Ni^{II} compounds, it was felt desirable to prepare analogous Pd^{II} complexes amenable to NMR studies in solution. For comparison, we have selected complexes of the type [$PdCl_2$(*P*,*N*)], for which the Pd−Cl distances should provide direct evidence of the respective *trans* influences of the *P*- and *N*-donor functions, and of the type [$PdCl(CH_3)$(*P*,*N*)], since the stoichiometric or catalytic insertion of small molecules (such as CO or olefins) into the Pd−CH_3 σ bond is very much influenced by the nature of the donor group situated in the *trans* position. The new Pd complexes (III)-(V) have been synthesized, and their structural features are analyzed and, in the case of (III), compared with the Ni analog (Speiser *et al*., 2004).

for references, see page 55

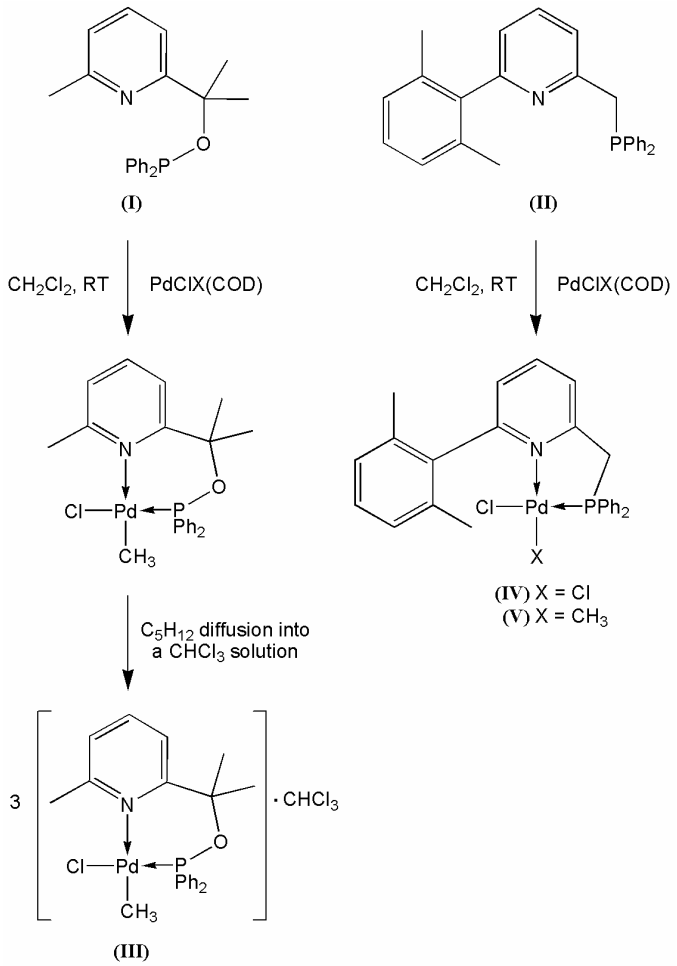

Despite the relevance of Pd complexes featuring these types of *P*,*N*-donor ligands in the catalytic alternating copolymerization of olefins and CO, as well as in other C−C coupling reactions, (III) is the first six-membered chloro-methyl-phosphinite *P*,*N*-type palladium(II) complex to be structurally characterized. Other groups have reported six-membered chloro-methyl-Pd complexes with iminophosphine (van den Beuken *et al*., 1998; Song *et al*., 2002; Reddy *et al*., 2002; Spek, 2003) and 1-(dimethylamino)-8-(diphenylphosphino)-naphthalene ligands (Dekker *et al*., 1992). Recently, Chen *et al*. (2003b) reported the first structurally characterized five-membered chloro-methyl-phosphinopyridine-based Pd^{II} complex. Other five-membered chloro-methyl complexes containing 2-(2-pyridyl)phosphaalkenes (van der Sluis *et al*., 1997), 2-(2-pyridyl)phospholes (Sauthier *et al*., 2002), iminophosphines (Coleman *et al*., 2001; Reddy *et al*., 2001, 2002; Doherty *et al*., 2002; Daugulis & Brookhart, 2002) and phosphinooxazoline (Apfelbacher *et al*., 2003) *P*,*N*-donor ligands have also been reported.

The structure of (III) shows that the asymmetric unit contains three very similar but crystallographically different molecules (*A*-*C*), together with a chloroform solvent molecule. Although the geometric data are as expected for the three molecules (Table 1), examination reveals (Fig. 1) that the *P*,*N*-chelate in molecules *A* and *C* has approximately the same

for references, see page 55

conformation, whereas in *B* the pyridine ring has a different orientation with respect to the Pd−N axis. This is confirmed by the torsion-angle values, which are similar for *A* and *C* [Cl1−Pd1−N1−C9 = -55.9 (3)º and Cl3−Pd3−N3−C53 = -61.6 (3)º, respectively], whereas for *B* the Cl2−Pd2−N2−C31 angle is 51.3 (3)º. The symmetry-equivalent asymmetric units contain enantiomers of molecules *A*, *B* and *C* with opposite torsion angles.

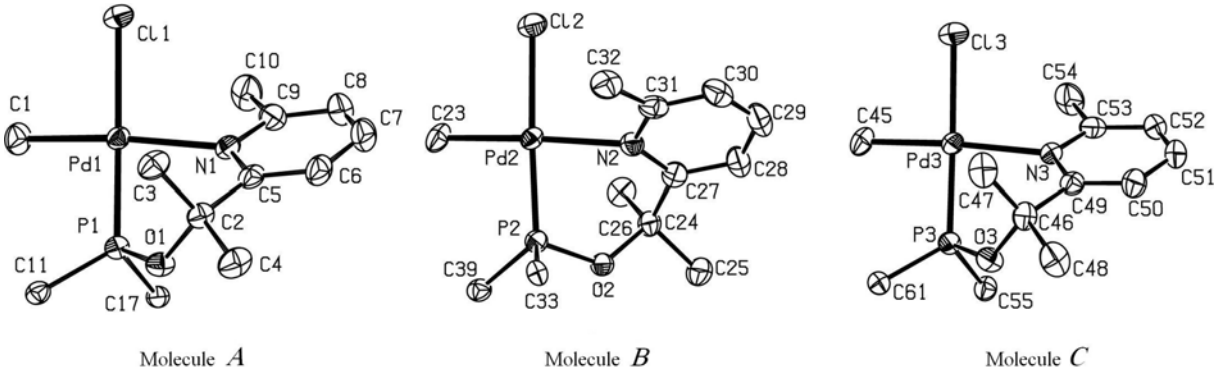

Figure 1
The *P*,*N*-chelate conformations of molecules *A*-*C* in (III), showing the atomic labeling. Displacement ellipsoids are drawn at the 50% probability level. H atoms and CH groups of phenyl rings have been omitted for clarity.

Analysis of molecule *A* shows a folding of the ligand along the Pd1···C2 hinge, creating a roof-like conformation, which generates a niche limited by a phenyl group (Fig. 2). This conformation is similar to the [$NiCl_2$(*P*,*N*)] analog (Speiser *et al*., 2004) for which the Ni coordination geometry was slightly distorted square planar. The Pd atom is almost in the mean plane passing through atoms Cl1, C1, N1 and P1 [the deviation of the Pd atom is 0.0390 (3) Å], and the sum of the bond angles around the Pd atom is 360.56º. Although the distance from the metal atom to the corresponding plane in the analogous Ni complex [0.03 (1) Å] is similar to that for Pd, the sum of the bond angles around the Ni center is larger (365.22º), indicating a slight distortion toward tetrahedral for the Ni coordination (Speiser *et al*., 2004). Molecules *B* and *C* are almost identical to *A* and therefore will not be discussed further.

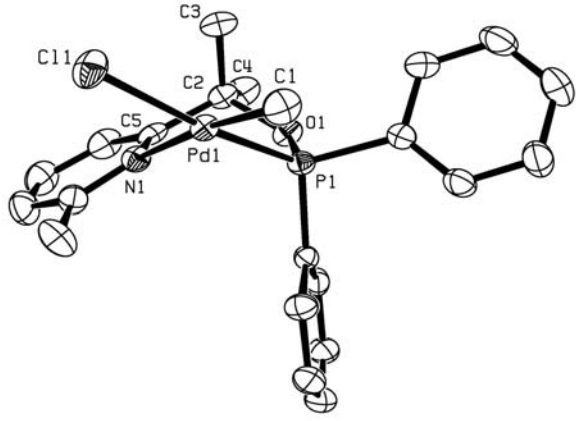

Figure 2
A view of the roof-like conformation formed by the ligand folding along Pd1···C2 hinge in the structure of molecule *A* of (III). Displacement ellipsoids are drawn at the 50% probability level and H atoms have been omitted for clarity.

for references, see page 55

In the ligands of complexes (IV) (Fig. 3) and (V) (Fig. 4), the geometric data (Tables 2 and 3) are similar and in the expected ranges; the only marked difference between these two structures concerns the Pd−N distance, which is larger in (V) [2.286 (3) Å] than in (IV) [2.098 (2) Å]. The aromatic substituent at the 6-position is oriented nearly perpendicular to the pyridine ring, as evidenced by the N1−C6−C7−C12 torsion angles [70.3 (3)º for (IV) and 78.9 (4)º for (V)].

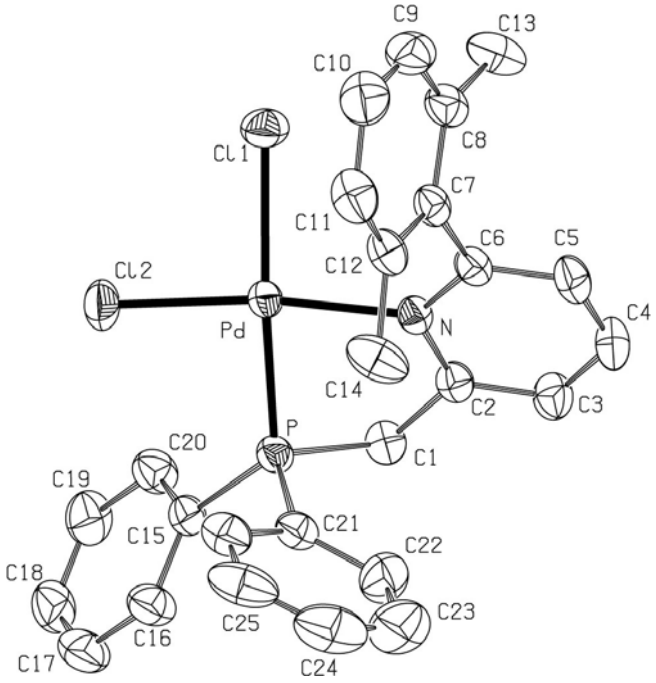

Figure 3
A view of (IV), showing the atomic labeling. Displacement ellipsoids are drawn at the 50% probability level and H atoms have been omitted for clarity.

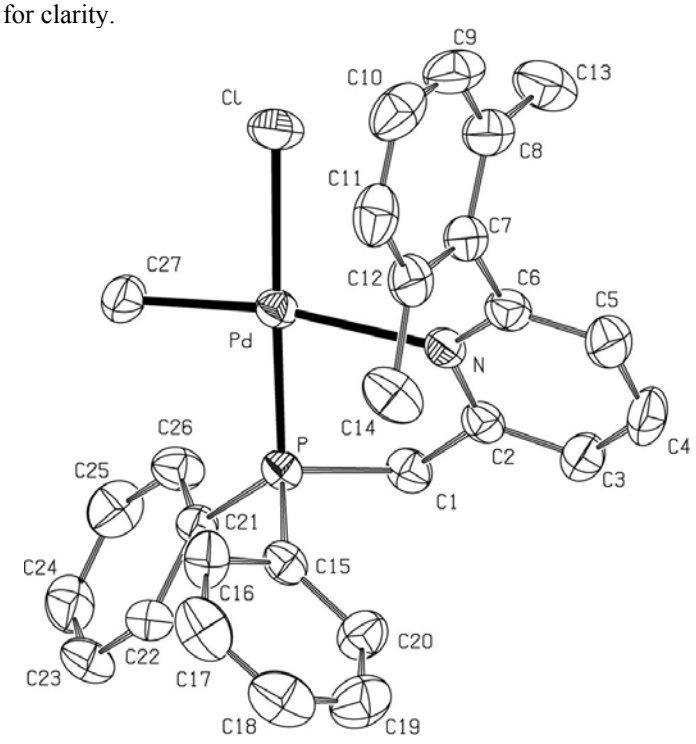

Figure 4
A view of (V), showing the atomic labeling. Displacement ellipsoids are drawn at the 50% probability level and H atoms have been omitted for clarity.

for references, see page 55

In (IV), the Pd−Cl bond distance *trans* to the P atom is longer than that *trans* to the N atom, which is consistent with the respective *trans* influences of the P- and N-donor atoms (Hartley, 1973). The methyl group in (III) and (V) is *cis* to the P atom, which is in agreement with the fact that the donor groups with the largest *trans* influence avoid being mutually *trans* to one another. This is consistent with complexes of the type [Pd(CH_3)Cl(*P*,*N*)] (Apfelbacher *et al*., 2003; Chen *et al*., 2003b; Coleman *et al*., 2001; Daugulis & Brookhart, 2002).

The *P*,*N*-chelate bite angle [81.74 (5)º for (IV) and 78.92 (8) for (V)º] is in accordance with that of other five-membered P,N-chelates [82.5 (2)º; Perera *et al*., 1995]. As expected, on increasing in size from this five-membered chelate ring to a six-membered ring as in (III), the chelate bite angle increases by 4-5º [84.03 (8)º for molecule A in (III)].

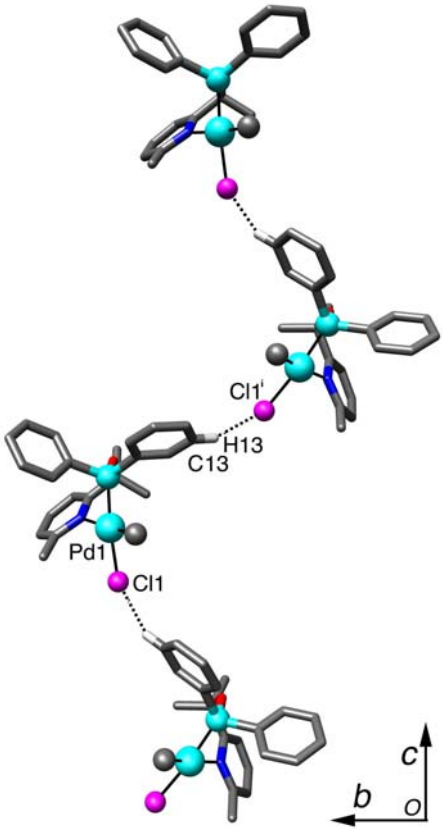

Figure 5
Part of the crystal structure of (III), showing the C−H···Cl interactions (viewed down the *a* axis). (The symmetry code is as in Table 4.)

Although no classical intermolecular hydrogen bonds were detected in (III)-(V), significant non-conventional C−H···Cl hydrogen bonds are present and these constitute structure directing elements. Compound (III) has an interaction involving the Cl atom on the Pd metal center of molecule *A* and a phenyl H atom of a neighboring *A* molecule (C13−H13···Cl1^{i}; all symmetry codes as in Table 4; Fig. 5). Another interaction of this type is observed between the H atom of the chloroform solvent molecule and the Cl atom from the palladium metal center of molecule *B* (C67−H67···Cl2^{ii}). Furthermore, molecules *A* and *C*

for references, see page 55

have an intramolecular interaction between a phenyl H atom and the O atom adjacent to the P atom (C22−H22···O1 and C66−H66···O3), and finally in molecule *B* an interaction involves the H atoms of the pyridine methyl group and the Pd-bound Cl atom (C32−H32···Cl2). In (IV), an interaction exists between a Pd-bound Cl atom and a pyridine H atom (C4−H4···Cl2^{ii}) (Fig. 6). A similar interaction occurs in (V) involving a phenyl H atom (C23−H23···Cl1^{ii}; Fig. 7). In both cases, these interactions result in infinite one-dimensional chains of molecules along (100).

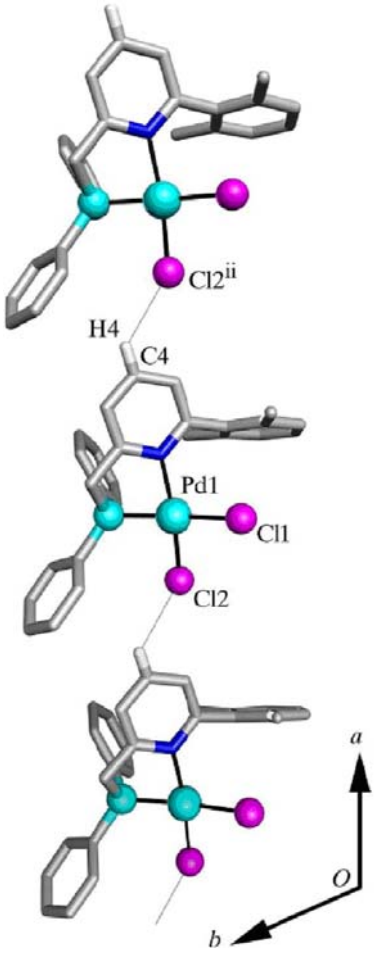

Figure 6
Part of the crystal structure of (IV), showing the C−H···Cl interactions (viewed down the *c* axis). (The symmetry code is as in Table 4.)

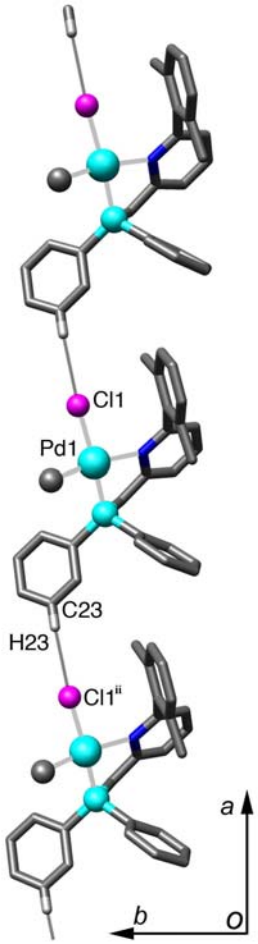

Figure 7
Part of the crystal structure of (V), showing the C−H···Cl interaction (viewed down the *c* axis). (The symmetry code is as in Table 4.)

From a packing viewpoint, the crystal structure of (III) can be described in term of pseudo-slabs stacked along (001). These slabs, interconnected by van der Waals contacts, are constituted by a succession of *A*, *B* and *C* moieties, as defined above (Fig. 1), with chloroform solvent molecules located between these slabs (Fig. 8). For (IV) and (V), the *bc* and *ac* projections show that the molecular moieties are placed along pseudo-slabs, with these slabs connected *via* van der Waals contacts, but specifically through the organic part of the corresponding molecules (Fig. 8).

for references, see page 55

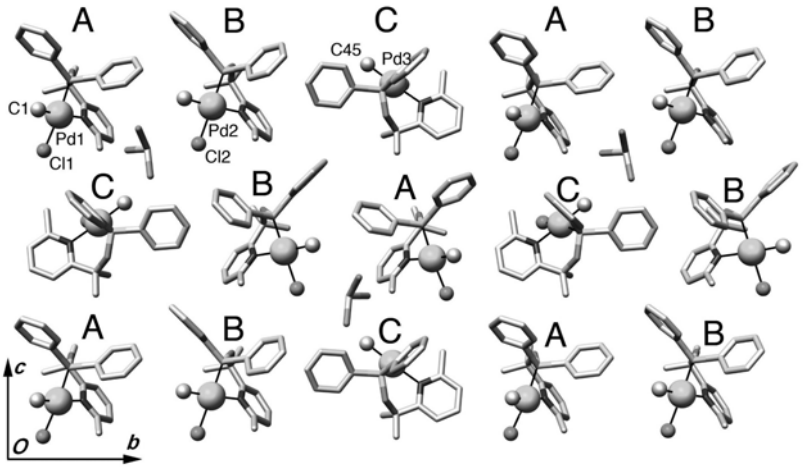

Complex (III)

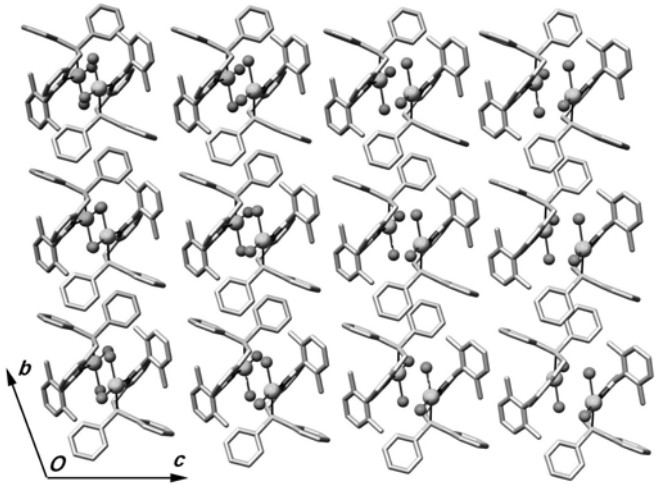

Complex (IV)

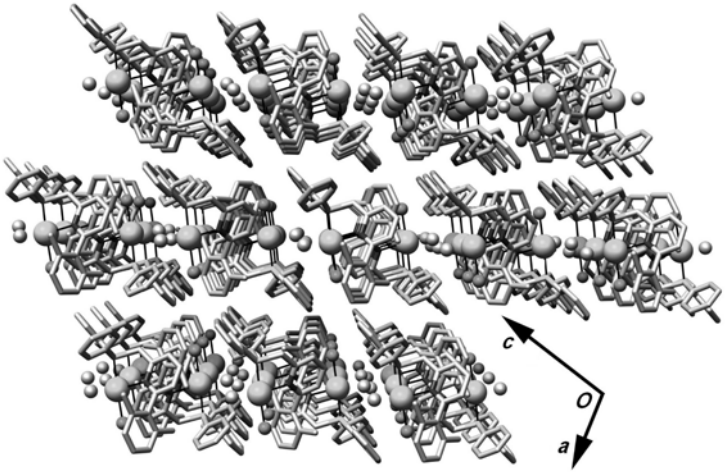

Complex (V)

Figure 8
A view of the packing for complex (III) (viewed down the *a* axis), complex (IV) (viewed down the *a* axis) and (V) (viewed down the *b* axis)

for references, see page 55

Experimental

The ^{1}H and $^{31}P\{^{1}H\}$ NMR spectra were recorded at or 300.13 and 121.5 MHz, respectively, on FT Bruker AC300, Avance 300 instrument. All solvents were dried and distilled under N_2 using common techniques unless otherwise stated. [Pd(CH_3)Cl(COD)] and [$PdCl_2$(COD)] (COD is 1,5-cyclooctadiene, C_8H_{12}) were prepared according to literature methods (Rulke *et al*., 1993; Ladipo & Anderson, 1994; Chatt *et al*., 1957), as were ligands (I) and (II) (Speiser *et al*., 2004, 2004a).

Compound (III) was synthesized by the addition of solid [Pd(CH_3)Cl(COD)] (0.391 g, 1.475 mmol) to a solution of (I) (0.545 g, 1.623 mmol) in CH_2Cl_2 (20 ml); the resulting yellow mixture was stirred for 2 h at room temperature. The solvent was evaporated under reduced pressure and the white residue was washed with diethyl ether (2 × 10 ml) and pentane (1 × 10 ml). The product was dried under vacuum overnight, and (III) was obtained as a white solid. Crystals of (III) suitable for X-ray diffraction were obtained by slow diffusion of pentane into a $CHCl_3$ solution of (III) (yield 0.442 g, 0.897 mmol, 61%). ^{1}H NMR ($CDCl_3$, room temp.): δ 0.88 (s, 3H, Pd-CH_3), 2.35 (s, 6H, C(CH_3)$_2$), 3.15 (s, 3H, py-CH_3), 7.08-7.94 (13H, aromatics); $^{31}P\{1H\}$ NMR ($CDCl_3$, room temp.): δ 115.1 (s).

Compound (IV) was obtained using a procedure similar to that described for (III), using (II) (0.615 g, 1.612 mmol) and [$PdCl_2$(COD)] (0.460 g, 1.612 mmol), and was obtained as a yellow white solid. Crystals of (IV) suitable for X-ray diffraction were obtained by slow diffusion of pentane into a CH_2Cl_2 solution of (IV) (yield 0.595 g, 1.064 mmol, 66%). ^{1}H NMR ($CDCl_3$, room temp.): δ 2.01 (s, 6H, Ph(CH_3)$_2$), 4.27 (d, 2H, PCH_2, $^{2}J_{PH}$ = 13.7 Hz), 7.03-7.88 (16H, aromatics); $^{31}P\{1H\}$ NMR ($CDCl_3$, room temp.): δ 46.1 (s).

Compound (V) was obtained using a procedure similar to that described above for the preparation of (III), using (II) (0.588 g, 1.541 mmol) and [Pd(CH_3)Cl(COD)] (0.408 g, 1.541 mmol), and was obtained as a yellow white solid. Crystals of (V) suitable for X-ray diffraction were obtained by slow diffusion of pentane into a CH_2Cl_2 solution of this complex (yield 0.463 g, 0.859 mmol, 56%). ^{1}H NMR ($CDCl_3$, ροομ τεμπ.): δ 0.80 (s, 3H, Pd-CH_3), 2.01 (s, 6H, Ph(CH_3)$_2$), 4.19 (d, 2H, PCH_2, $^{2}J_{PH}$ = 11.4 Hz), 7.09-7.90 (16H, aromatics); $^{31}P\{1H\}$ NMR ($CDCl_3$, room temp.): δ 42.6 (s).

for references, see page 55

Compound (III)

Crystal data

$3[Pd(CH_3)Cl(C_{21}H_{22}NOP)]\cdot CHCl_3$
$M_r = 1596.12$
Monoclinic, $P2_1/c$
$a = 14.628$ (1) Å
$b = 28.573$ (5) Å
$c = 17.324$ (2) Å
$\beta = 106.39$ (5)º
$V = 4947$ (2) Å^3
$Z = 4$

$D_x = 1.526$ Mg m^{-3}
Mo $K\alpha$ radiation
Cell parameters from 53191 reflections
$\theta = 1.0$-30.0º
$\mu = 1.11$ mm^{-1}
$T = 173$ (2) K
Prism, yellow
0.13 × 0.10 × 0.08 mm

Data collection

Nonius KappaCCD diffractometer
ω scans
58356 measured reflections
20304 independent reflections
13997 reflections with $I > 2\sigma(I)$

$R_{int} = 0.067$
$\theta_{max} = 30.0$º
$h = -20 \rightarrow 20$
$k = -40 \rightarrow 37$
$l = -20 \rightarrow 24$

Refinement

Refinement on F^2
$R[F^2 > 2\sigma(F^2)] = 0.059$
$wR(F^2) = 0.123$
$S = 1.09$
20304 reflections
766 parameters

H-atom parameters constrained
$w = 1/[\sigma^2(F_o^2) + (0.05P)^2]$ where $P = (F_o^2 + 2F_c^2)/3$
$(\Delta/\sigma)_{max} < 0.001$
$\Delta\rho_{max} = 0.069$ e Å^{-3}
$\Delta\rho_{min} = -0.88$ e Å^{-3}

Table 1
Selected geometric parameters (Å, º) for (III)

Pd1−Cl1	2.3838 (10)	Pd3−Cl3	2.3929 (12)
Pd1−P1	2.1650 (9)	Pd3−P3	2.1725 (13)
Pd1−N1	2.205 (3)	Pd3−N3	2.200 (3)
Pd1−C1	2.038 (4)	Pd3−C45	2.034 (4)
Pd2−Cl2	2.4047 (10)	P1−O1	1.611 (2)
Pd2−P2	2.1717 (10)	P2−O2	1.608 (2)
Pd2−N2	2.193 (3)	P3−O3	1.617 (2)
Pd2−C23	2.050 (4)		
C1−Pd1−P1	91.45 (12)	C23−Pd2−Cl2	88.48 (12)
C1−Pd1−N1	173.65 (14)	P2−Pd2−Cl2	175.46 (4)
P1−Pd1−N1	84.03 (8)	N2−Pd2−Cl2	94.50 (8)
C1−Pd1−Cl1	90.20 (12)	C45−Pd3−P3	91.45 (12)
P1−Pd1−Cl1	172.09 (4)	C45−Pd3−N3	174.34 (14)
N1−Pd1−Cl1	94.87 (8)	P2−Pd2−N3	84.71 (8)
C23−Pd2−P2	93.23 (12)	C45−Pd3−Cl3	90.38 (12)
C23−Pd2−N2	176.97 (13)	P3−Pd3−Cl3	168.49 (4)
P2−Pd2−N2	83.76 (8)	N3−Pd3−Cl3	94.21 (9)

Compound (IV)

Crystal data

$[PdCl_2(C_{26}H_{24}NP)]$
$M_r = 558.73$
Triclinic, $P\bar{1}$
$a = 10.151$ (1) Å
$b = 11.461$ (1) Å
$c = 12.106$ (2) Å
$\beta = 109.93$ (5)º
$\gamma = 112.23$ (5)º
$V = 1184.7$ (9) Å^3

$Z = 2$
$D_x = 1.566$ Mg m^{-3}
Mo $K\alpha$ radiation
Cell parameters from 7840 reflections
$\theta = 1.0$-27.9º
$\mu = 1.09$ mm^{-1}
$T = 173$ (2) K
Prism, yellow-orange
0.13 × 0.10 × 0.08 mm

for references, see page 55

Data collection
Nonius KappaCCD diffractometer
ω scans
14956 measured reflections
5587 independent reflections
4878 reflections with $I > 2\sigma(I)$

$R_{int} = 0.033$
$\theta_{max} = 27.8º$
$h = -13 \rightarrow 13$
$k = -14 \rightarrow 15$
$l = -15 \rightarrow 15$

Refinement
Refinement on F^2
$R[F^2 > 2\sigma(F^2)] = 0.031$
$wR(F^2) = 0.078$
$S = 1.00$
5587 reflections
280 parameters

H-atom parameters constrained
$w = 1/[\sigma^2(F_o^2) + (0.0331P)^2 + 0.3488P]$ where $P = (F_o^2 + 2F_c^2)/3$
$(\Delta/\sigma)_{max} = 0.001$
$\Delta\rho_{max} = 0.49$ e Å^{-3}
$\Delta\rho_{min} = -0.80$ e Å^{-3}

Table 2
Selected geometric parameters (Å, º) for (IV)

Pd1−Cl1	2.3747 (12)	P1−C1	1.826 (3)
Pd1−Cl2	2.2749 (13)	N1−C2	1.369 (3)
Pd1−P1	2.2093 (11)	C1−C2	1.506 (3)
Pd1−N1	2.098 (2)		
N1−Pd1−P1	81.74 (5)	N1−Pd1−Cl1	96.05 (5)
N1−Pd1−Cl2	171.99 (5)	P1−Pd1−Cl1	167.92 (2)
P1−Pd1−Cl2	90.52 (3)	Cl2−Pd1−Cl1	91.95 (3)

Compound (V)
Crystal data
$[Pd(CH_3)Cl(C_{26}H_{24}NP)]$
$M_r = 538.32$
Monoclinic, $P2_1/n$
$a = 11.507$ (1) Å
$b = 12.011$ (2) Å
$c = 17.490$ (2) Å
$\beta = 99.92$ (5)º
$V = 2381.2$ (6) Å^3
$Z = 4$

$D_x = 1.502$ Mg m^{-3}
Mo $K\alpha$ radiation
Cell parameters from 23164 reflections
$\theta = 1.0$-$30.0º$
$\mu = 0.97$ mm^{-1}
$T = 173$ (2) K
Prism, yellow
0.10 × 0.08 × 0.06 mm

Data collection
Nonius KappaCCD diffractometer
ω scans
6838 measured reflections
6837 independent reflections
4250 reflections with $I > 2\sigma(I)$

$R_{int} = 0.045$
$\theta_{max} = 30.0º$
$h = -16 \rightarrow 15$
$k = 0 \rightarrow 16$
$l = 0 \rightarrow 24$

Refinement
Refinement on F^2
$R[F^2 > 2\sigma(F^2)] = 0.055$
$wR(F^2) = 0.112$
$S = 0.91$
6837 reflections
280 parameters

H-atom parameters constrained
$w = 1/[\sigma^2(F_o^2)]$ where $P = (F_o^2 + 2F_c^2)/3$
$(\Delta/\sigma)_{max} < 0.001$
$\Delta\rho_{max} = 0.72$ e Å^{-3}
$\Delta\rho_{min} = -0.63$ e Å^{-3}

for references, see page 55

Table 3
Selected geometric parameters (Å, º) for (V)

Pd1−Cl1	2.3681 (14)	P1−C1	1.823 (4)
Pd1−P1	2.189 (2)	N1−C2	1.356 (4)
Pd1−N1	2.286 (3)	C1−C2	1.510 (5)
Pd1−C27	2.042 (4)		
C27−Pd1−P1	91.64 (11)	C27−Pd1−Cl1	88.40 (11)
C27−Pd1−N1	170.52 (11)	P1−Pd1−Cl1	173.30 (4)
P1−Pd1−N1	78.92 (8)	N1−Pd1−Cl1	101.07 (8)

Table 4
Hydrogen-bond parameters (Å, º) for compounds (III)-(V).

Compound	*D*-H...A	*D*-H	H...A	D...A	*D*-H...A
(III)	C13-H13···Cl1^{i}	0.95	2.74	3.630(4)	156
	C22-H22···O1	0.95	2.56	2.975(5)	107
	C32-H32···Cl2	0.98	2.68	3.449(4)	136
	C66-H66···O3	0.95	2.53	2.909(5)	104
	C67-H67···Cl2^{ii}	1.00	2.56	3.523(4)	161
(IV)	C4-H4···Cl2^{ii}	0.95	2.73	3.410(4)	130
(V)	C23-H23···Cl1^{ii}	0.95	2.83	3.750(4)	164

Symmetry codes: (i) *x*, ½ -*y*, -½ +*z*; (ii) 1+*x*, *y*, *z*

The rotational orientations of the methyl groups were refined using the circular Fourier method available in *SHELXL97* (Sheldrick, 1997). All H atoms were treated as riding, with C−H distances ranging from 0.95 to 1.00 Å and U_{iso}(H) values equal to 1.5 (methyl H atoms) or 1.2 (all other H atoms) times U_{eq}(C).

For all compounds, data collection: *COLLECT* (Nonius, 1998); cell refinement: *DENZO* (Otwinowski & Minor, 1997); data reduction: *DENZO*; program(s) used to solve structure: *SHELXS97* (Sheldrick, 1997); program(s) used to refine structure: *SHELXL97* (Sheldrick, 1997); molecular graphics: *PLATON98* (Spek, 1998); software used to prepare material for publication: *SHELXL97*.

The authors thank the CNRS, the Ministère de la Recherche (Paris), the Institut Français du Pétrole (IFP) and the Europeen Commission (Palladium Network HPRN-CT-2002-00196 and COST program) for support.

for references, see page 55

References

Agbossou, F., Carpentier, J.-F., Hapiot, F., Suisse, I. & Mortreux, A. (1998). *Coord. Chem. Rev.* **178-180**, 1615-1645.

Apfelbacher, A., Braunstein, P., Brissieux, L. & Welter, R. (2003). *Dalton Trans*. pp. 1669-1674.

Beuken, E. K. van den, Smeets, W. J. J., Spek, A. L. & Feringa, B. I. (1998). *Chem. Commun.* pp. 223-224.

Bianchini, C. & Meli, A. (2002). *Coord. Chem. Rev.* **225**, 35-66.

Braunstein, P. (2004). *J. Organomet. Chem.* **689**, 3953-3967.

Braunstein, P. & Naud, F. (2001). *Angew. Chem. Int. Ed.* **40**, 680-699.

Chatt, J., Vallarino, L. M. & Venanzi, L. M. (1957). *J. Chem. Soc.* pp. 3413-3416.

Chen, H.-P., Liu, Y.-H., Peng, S.-M. & Liu, S.-T. (2003a). *Dalton Trans.* pp. 1419-1424.

Chen, H.-P., Liu, Y.-H., Peng, S.-M. & Liu, S.-T. (2003b). *Organometallics*, **22**, 4893-4899.

Coleman, K. S., Green, M. L. H., Pascu, S. I., Rees, N. H., Cowley, A. R. & Rees, L. H. (2001). *J. Chem. Soc. Dalton Trans.* pp. 3384-3395.

Daugulis, O. & Brookhart, M. (2002). *Organometallics*, **21**, 5926-5934.

Dekker, G. P. C. M., Buijs, A., Elsevier, C. J., Vrieze, K., van Leeuwen, P. W. N. M., Smeets, W. J. J., Spek, A. L., Wang, Y. F. & Stam, C. H. (1992). *Organometallics*, **11**, 1937-1948.

Doherty, S., Knight, J. G., Scanlan, T. H., Elsegood, M. R. J. & Clegg,W. (2002). *J. Organomet. Chem.* **650**, 231-248.

Espinet, P. & Soulantica, K. (1999). *Coord. Chem. Rev.* **193-195**, 499-556.

Hartley, F. R. (1973). *Chem. Soc. Rev.* **2**, 163-179.

Ladipo, F. T. & Anderson, G. K. (1994). *Organometallics*, **13**, 303-306.

Newkome, G. R. (1993). *Chem. Rev.* **93**, 2067-2089.

Nonius (1998). *COLLECT*. Nonius BV, Delft, The Netherlands.

Otwinowski, Z. & Minor, W. (1997). *Methods in Enzymology*, Vol. 276, *Macromolecular Crystallography*, Part A, edited by C. W. Carter Jr & R. M. Sweet, pp. 307-326. New York: Academic Press.

Perera, S. D., Shaw, B. L. & Thornton-Pett, M. (1995). *Inorg. Chim. Acta*, **236**, 7-12.

Reddy, K. R., Surekha, K., Lee, G.-H., Peng, S.-M., Chen, J.-T. & Liu, S.-T. (2001). *Organometallics*, **20**, 1292-1299.

Reddy, K. R., Tsai, W.-W., Surekha, K., Lee, G.-H., Peng, S.-M., Chen, J.-T. & Liu, S.-T. (2002). *J. Chem. Soc. Dalton Trans.* pp. 1776-1782.

Rulke, R. E., Ernsting, J. M., Spek, A. L., Elsevier, C. J., van Leeuwen, P. W. N. M. & Vrieze, K. (1993). *Inorg. Chem.* **32**, 5769-5778.

Sauthier, M., Leca, F., Toupet, L. & Reau, R. (2002). *Organometallics*, **21**, 1591-1602.

Sheldrick, G. M. (1997). *SHELXL97* and *SHELXS97*. University of Göttingen, Germany.

Slone, C. S., Weinberger, D. A. & Mirkin, C. A. (1999). *Prog. Inorg. Chem*. **48**, 233-350.

Sluis, M. van der, Beverwijk, V., Termaten, A., Gavrilova, E., Bickelhaupt, F., Kooijman, H., Veldman, N. & Spek, A. L. (1997). *Organometallics*, **16**, 1144-1152.

Song, H.-B., Zhang, Z.-Z. & Mak, T. C. W. (2002). *Polyhedron*, **21**, 1043-1050.

Speiser, F., Braunstein, P. & Saussine, L. (2004a). *Organometallics*, **23**, 2633-2640.

Speiser, F., Braunstein, P. & Saussine, L. (2004b). *Organometallics*, **23**, 2625-2632.

Speiser, F., Braunstein, P., Saussine, L. & Welter, R. (2004). *Inorg. Chem.* **43**, 1649-1658.

Spek, A. L. (1998). *PLATON98*. Utrecht University, The Netherlands.

Spek, A. L. (2003). *Acta Cryst.* **E59**, m97-m98.

Résumé de la Partie B

Le ligand phosphinito-oxazoline 4,4-diméthyl-2-[methoxy(diphénylphosphine)]-4,5-dihydrooxazole (**2a**) et le ligand phosphonite-oxazoline 4,4-diméthyl-2-[méthoxy(6H-dibenz[c,e][1,2]oxaphosphorin)]-4,5-dihydrooxazole (**8a**) ont été préparés par déprotonation de (4,5-dihydro-4,4-diméthyloxazol-2-yl)méthanol (**1a**) suivie de la réaction avec la fonction P-Cl correspondante, de façon analogue aux ligands **2b** (4,4-diméthyl-2-[1-oxy(diphénylphosphine)-1-méthyléthyl]-4,5-dihydrooxazole) et **8b** (4,4-diméthyl-2-[1-oxy(6H-dibenz[c,e][1,2]oxaphosphorin)-1-méthyléthyl]-4,5-dihydrooxazole) publiés auparavant. Ces ligands réagissent avec [PdClX(COD)] pour former des complexes de type [PdClX(P,N)] (**3a** P,N = **2a**, X = Cl; **4a** P,N = **2a**, X = Me; **4b** P,N = **2b**, X = Me; **9a** P,N = **8a**, X = Cl; **9b** P,N = **8b**, X = Cl; **10a** P,N = **8a**, X = Me; **10b** P,N = **8b**, X = Me). Les complexes **4a**,**b** and **10a**,**b** ont réagit avec $AgCF_3SO_3$ pour former [Pd(CF_3SO_3)Me(P,N)] **5a**,**b** et **11a**,**b**, respectivement. Par insertion de monoxyde de carbone puis de l'éthylène dans la liaison Pd-C de **5a** and **11a**,**b**, les complexes alkyles [Pd{$CH_2CH_2C(O)$Me}(P,N)]CF_3SO_3 **7a** and **14a**,**b**, respectivement, ont été isolés et caractérisés spectroscopiquement. Les complexes **3a**·CH_2Cl_2, **5a**, **9b**, **10a**,**b**, [PdMe(H_2O)(P,N)]CF_3SO_3 **12b**, (P,N = **8b**) and **14a**,**b** on été complètement caractérisés par diffraction des rayons X et les structures de **14a**,**b** sont de rares exemples de produits d'insertion CO/éthylène ainsi caractérisés.

Cette partie du chapitre fait l'objet d'une publication, à soumettre,
dont la référence est donnée ci-dessous.

Phosphinito- and Phosphonito-oxazoline Pd(II) Complexes as CO/Ethylene Insertion Intermediates: Synthesis and Structural Characterization

Magno Agostinho and Pierre Braunstein*

À soumettre

Laboratoire de Chimie de Coordination, UMR 7177 CNRS, Institut de Chimie, Université Louis Pasteur, 4 rue Blaise Pascal, F-67070 Strasbourg Cédex, France

pour les références, voir page 80

Abstract of Part B

The phosphinito-oxazoline ligand 4,4-dimethyl-2-[methoxy(diphenylphosphine)]-4,5-dihydrooxazole (**2a**) and the phosphonite-oxazoline ligand 4,4-dimethyl-2-[methoxy(6H-dibenz[c,e][1,2]oxaphosphorin)]-4,5-dihydrooxazole (**8a**) were prepared by deprotonation of (4,5-dihydro-4,4-dimethyloxazol-2-yl)methanol (**1a**) and reaction with the corresponding P-Cl function, similarly to the ligands **2b** (4,4-dimethyl-2-[1-oxy(diphenylphosphine)-1-methylethyl]-4,5-dihydrooxazole) and **8b** (4,4-dimethyl-2-[1-oxy(6H-dibenz[c,e][1,2]oxaphosphorin)-1-methylethyl]-4,5-dihydrooxazole) reported previously. These ligands react with [PdClX(COD)] to give complexes of the type [PdClX(P,N)] (**3a** P,N = **2a**, X = Cl; **4a** P,N = **2a**, X = Me; **4b** P,N = **2b**, X = Me; **9a** P,N = **8a**, X = Cl; **9b** P,N = **8b**, X = Cl; **10a** P,N = **8a**, X = Me; **10b** P,N = **8b**, X = Me). Complexes **4a**,**b** and **10a**,**b** reacted with $AgCF_3SO_3$ to yield [Pd(CF_3SO_3)Me(P,N)] **5a**,**b** and **11a**,**b**, respectively. From the stepwise insertion reaction of CO and ethylene into the Pd-C bond of **5a** and **11a**,**b**, the alkyl ketone chelate complexes $[Pd\{CH_2CH_2C(O)Me\}(P,N)]CF_3SO_3$ **7a** and **14a**,**b** respectively, have been isolated and spectroscopically characterized. Complexes **3a**·CH_2Cl_2, **5a**, **9b**, **10a**,**b**, $[PdMe(H_2O)(P,N)]CF_3SO_3$ **12b**, (P,N = **8b**) and **14a**,**b** have been fully characterized by X-ray crystallography and the structures of **14a**,**b** are still rare examples of structurally characterized CO/ethylene coupling products.

This part of the chapter will be submitted for publication; its reference is given below.

Phosphinito- and Phosphonito-oxazoline Pd(II) Complexes as CO/Ethylene Insertion Intermediates: Synthesis and Structural Characterization

Magno Agostinho and Pierre Braunstein*

To be submitted

Laboratoire de Chimie de Coordination, UMR 7177 CNRS, Institut de Chimie, Université Louis Pasteur, 4 rue Blaise Pascal, F-67070 Strasbourg Cédex, France

for references, see page 80

Phosphinito- and Phosphonito-oxazoline Pd(II) Complexes as CO/Ethylene Insertion Intermediates: Synthesis and Structural Characterization

Introduction

The alternating insertion of carbon monoxide and olefins into metal carbon bonds leading to the formation of polyketones is catalysed by various palladium complexes and has attracted much interest from both academic and industrial laboratories (for recent reviews see[1-15]). This interest stems from the easy and cheap access to the starting materials, the possibility of fine-tuning the reaction at the molecular level and the possible subsequent functionalization of the resulting polyketones.[16-21] Previous studies have illustrated that both the steric environment and the coordinating ability of the ancillary ligand(s) are crucial in controlling the efficiency of the catalyst during the polymerization reaction. Palladium-based systems containing phosphorus (P,P) chelating ligands have been found to be effective in CO/ethylene[22-29] and CO/propylene[30,31] copolymerization. On the other hand, aromatic olefins, such as styrene and its derivatives, are efficiently copolymerized when bidentate nitrogen (N,N) ligands chelate the Pd(II) centre.[32-36] There has been a recent increase in interest for catalysts bearing new unsymmetrical bidentate ligands, in particular P,N ligands.[37-50] The simultaneous presence of nitrogen- and phosphorus-based donor groups with different stereoelectronic properties, their different trans-effect and trans-influence due to the different σ donor and π acceptor properties of phosphorus and nitrogen atoms[51] and finally their potential hemilabile character in metal complexes[52] may provide an easier control of such catalytic processes. P,N ligands have recently allowed isolation and characterization of several insertion intermediates, thus providing valuable information on these catalysts reactivity.

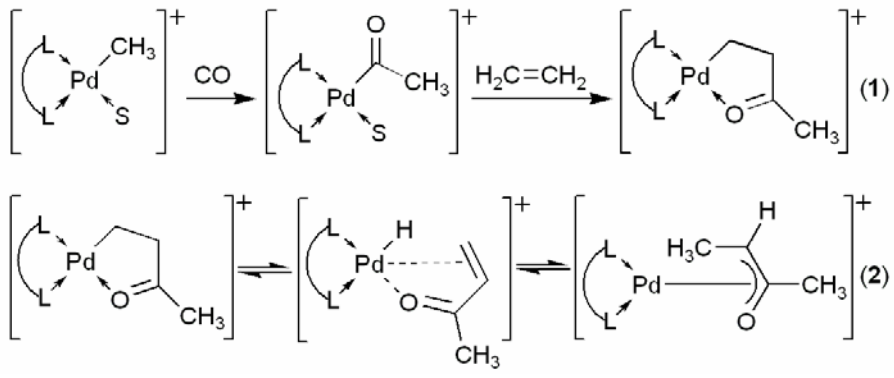

for references, see page 80

It is established that a growing polymer chain may act as a chelating ligand, in which the ketonic oxygen atom coordinates to the electrophilic palladium centre (eq. 1). This is a key step in the copolymerization procedure, the higher binding affinity of Pd(II) for CO relative to ethene inhibits multiple ethene insertions even in the presence of very low concentrations of CO.[26,53,54] It follows that, once a palladium alkyl bond is formed, the ketonic oxygen coordination ensures that the next incorporated monomer will be a CO molecule to generate the acyl complex. In some cases the 5 membered ring complex resulting from ethylene insertion can be unstable, even at room temperature, and rearrange to a palladium enolate (eq. 2).[55]

The first structural reports of an ethylene-CO coupling product by Cavell and co-workers in 1996, using monodentate PPh_3 and a N,O chelating ligand,[56] and our group in 2000 using a unsymmetrical P,O chelating ligand[57] and in 2001 using a diphosphine-bridged heterobimetallic Fe–Pd complex[58] were followed by only few examples with P,N,[47,48,50] N,N[59] and P,P[60] chelating ligands. In a recent study we demonstrated that cationic Pd(II) catalysts stabilised by diphenylphosphino-*P*,*N* type ligands,[37] allow to isolate and fully characterise initial intermediates in the sequential CO/ethylene or CO/methyl acrylate copolymerisation reactions.[50] Therefore investigating the behaviour of other functional ligands with different stereoelectronic properties should be of particular interest for these types of reactions. Here have now prepared and characterized a series of phosphinito- and phosphonitooxazoline P,N-type ligands and their corresponding palladium (II) complexes. CO and ethylene stoichiometric insertion studies and structurally characterized intermediates are also reported.

Results and Discussion

Preparation of the Ligands 2a and 2b.

We recently reported the synthesis of the phosphinite ligand **2b** from the 4,4'-dimethyl-2-(1-hydroxy-1-methylethyl)-4,5-dihydrooxazole (**1b**) by lithiation of the oxazoline alcohol with one equivalent of *n*-BuLi and subsequent reaction with PPh_2Cl.[61] This ligand allowed us to characterize an unusually stable η^1-allyl Pd(II) complex,[62] and afforded Ni(II) complexes active in catalytic ethylene oligomerisation.[63] Since substituent effects were found to be very notable on the structures and properties of the complexes,[64] we now report the synthesis of the unsubstituted analogue **2a**, using a similar procedure (Scheme1).

for references, see page 80

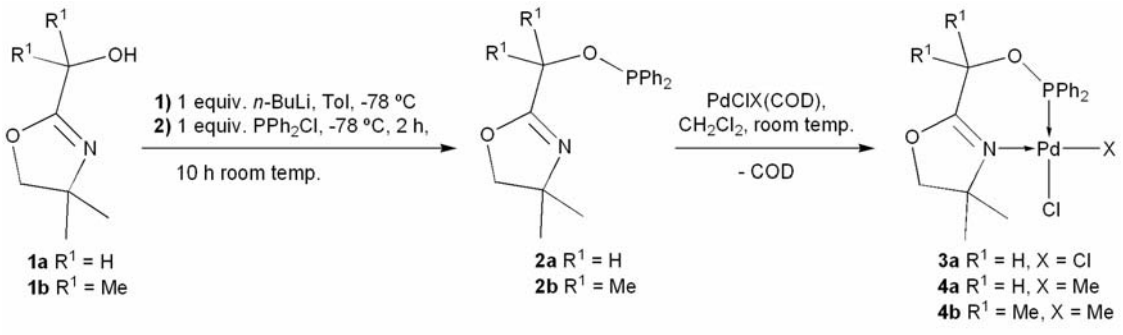

Scheme 1 Synthesis of ligands **2a**,**b** and complexes **3a** and **4a**,**b**.

Preparation of the Complexes [$PdCl_2$(P,N)] (3a) and [PdClMe(P,N)] (4a,b)

Reaction of 1 equiv. of ligand **2a** with [$PdCl_2$(COD)] (COD = cycloocta-1,5-diene) in dichloromethane afforded complex [$PdCl_2$(P,N)] (**3a**) in good yield (Scheme 1). Coordination of the ligand was confirmed spectroscopically by a downfield shift of ca. 5 ppm in the $^{31}P\{^1H\}$ NMR spectrum with respect to the free ligand and by a shift of the $\nu_{C=N}$ absorption to 1631 cm^{-1} (Table 1). Other characterizing data are given in the Experimental Section. For comparative purposes the structure of **3a**·CH_2Cl_2 was determined by X-ray diffraction, its ORTEP diagram is shown in Fig. 1 and selected bond distances and angles are given in Table 2. The Pd-Cl bond distances are in the expected range and that *trans* to the P atom [2.3754(9) Å] is longer than that *trans* to N [2.2932(9) Å], which is consistent with the respective *trans* influences of the P and N donor atoms.[65] The P,N chelate bite angle of 91.54 (8)º is in accordance with that found in other Pd complexes stabilized by the same ligand.[62] As expected on going from this six-membered ring chelate to a five-membered ring as in [$PdCl_2$L] [L = 2-oxazoline-2-ylmethyl-4,4-dimethyl)diphenylphosphine] or [$PdCl_2$L'] [L' = 2-(2,6-dimethylphenyl)-6-(diphenylphosphinomethyl)pyridine], the bite angle decreases by about 7-10º.[37,66]

Table 1
Selected IR and NMR data of the free ligands **2a**,**b** and their complexes.

	IR		NMR[d]	
	$\nu_{C=N}$	$\nu_{C=O}$	^1H	^{31}P
2a	1668[a] (s)			121.8
2b	1661[a] (s)			95.4
3a	1635[b] (s)			116.3
4a	1635[b] (s)		0.61 $PdCH_3$ (d, $^3J_{PH}$ = 4.3)	137.0
4b	1625[b] (s)		0.65 $PdCH_3$ (d, $^3J_{PH}$ = 3.9)	119.8
5a	1652[b] (s)		0.69 $PdCH_3$ (d, $^3J_{PH}$ = 1.7)	139.6
5b	1642[b] (m)		0.70 $PdCH_3$ (d, $^3J_{PH}$ = 1.4)	122.5
6a				124.1
7a	1658[b] (m)	1636[b] (m)	2.50 $C(O)CH_3$ (s)	138.1

[a]In CH_2Cl_2, [b]in KBr, cm^{-1}. [d]In $CDCl_3$, ppm, *J* in Hz.

for references, see page 80

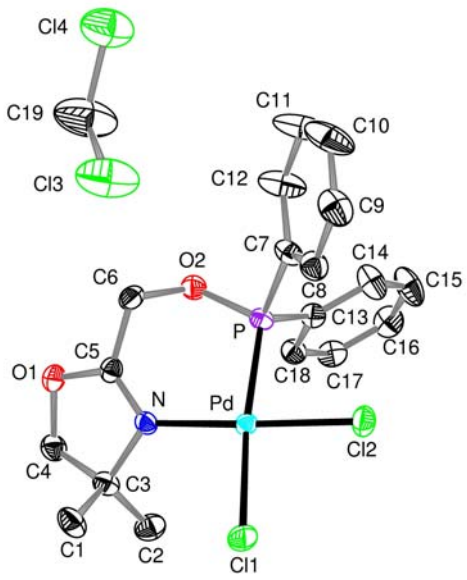

Fig. 1 ORTEP plot of complex **3a**·CH_2Cl_2 (H atoms omitted). Displacement ellipsoids are drawn at 50% probability level.

The complexes [PdMeCl(P,N)] **4a** and **4b** were similarly obtained from [PdMeCl(COD)] and **2a** and **2b** in 79 and 86% yield, respectively (Scheme 1). The presence of a single peak in the $^{31}P\{^1H\}$ NMR spectrum of the complexes suggests the formation of a single isomer. The Pd-Me resonance of **4a** and **4b** appears as a doublet at δ 0.61 and δ 0.65 with $^3J_{PH}$ = 4.3 and 3.9 Hz, respectively. The magnitude of these coupling constants indicates a *cis* relationship between the two groups with the largest *trans* influence, namely the phosphorus atom and the methyl group.

Preparation of the Cationic Complexes [PdMe(P,N) OSO_2CF_3] (5a,b)

Cationic complexes **5a** and **5b** were prepared by treatment of **4a**,**b** with $AgCF_3SO_3$ in a dichloromethane solution (Scheme 2). After removal of AgCl by filtration through Celite, the solvent was evaporated and the desired complexes obtained as solids and washed with diethylether and pentane. Selected IR and NMR data of the complexes are also shown in Table 1. As observed for the neutral complexes, the Pd-Me protons appear in the ^1H NMR spectrum as doublets, however the hydrogen-phosphorus coupling constants observed are slightly smaller ($^3J_{PH}$ = 1.7 and 1.4 Hz for **5a** and **5b**, respectively). $^{31}P\{^1H\}$ NMR again shows only one peak corresponding to the formation of the *cis* isomer with respect to the phosphorus atom and the methyl group. The $^{31}P\{^1H\}$ NMR peaks are slightly shifted downfield (2-3 ppm) compared to those for the P nucleus of the less electrophilic neutral analogues. An X-ray structural analysis of **5a** (Figure 2) also confirms the *cis* arrangement of the phosphinite and methyl groups, as well as the coordination of the CF_3SO_3 ion. Selected bond lengths and angles are given in Table 2.

for references, see page 80

Table 2 Selected bond lengths [Å] and angles [°] in complexes **3a**·CH_2Cl_2, **5a**, **9b**, **10a**,**b**, **12b** and **14a**,**b**.

	3a·CH_2Cl_2	**5a**	**9b**	**10a**	**10b**	**12b**	**14a**	**14b**
Pd-N	2.069 (3)	2.166 (2)	2.075 (2)	2.187 (3)	2.188 (3)	2.158 (3)	2.123 (5)	2.145 (3)
Pd-P	2.2052 (9)	2.1567 (7)	2.1881 (8)	2.1629 (8)	2.1530 (9)	2.1447 (8)	2.1535 (15)	2.143 (1)
Pd-C7		2.033 (3)		2.047 (3)	2.064 (3)	2.045 (3)	2.006 (7)	2.028 (3)
Pd-O4		2.169 (2)				2.128 (2)	2.124 (4)	2.136 (2)
Pd-Cl1	2.3754 (9)		2.3527 (9)	2.3909 (8)	2.3960 (9)			
Pd-Cl2	2.2932 (9)		2.2879 (10)					
N-C5	1.279 (4)	1.269 (4)	1.280 (3)	1.274 (4)	1.276 (4)	1.278 (4)	1.256 (8)	1.275 (4)
C5-C6	1.496 (4)	1.499 (4)	1.515 (3)	1.501 (5)	1.531 (5)	1.516 (4)	1.495 (10)	1.519 (4)
C6-O2	1.448 (4)	1.441 (3)	1.480 (3)	1.444 (4)	1.463 (4)	1.475 (3)	1.413 (8)	1.467 (4)
O2-P	1.624 (3)	1.617 (2)	1.599 (2)	1.618 (2)	1.610 (2)	1.600 (2)	1.584 (4)	1.607 (2)
N-Pd-P	91.54 (8)	94.48 (6)	90.38 (7)	91.56 (7)	90.72 (7)	91.47 (7)	93.12 (14)	91.91 (8)
N-Pd-C7		175.65 (13)		176.92 (12)	174.75 (12)	177.73 (12)	178.3 (3)	175.37 (12)
N-Pd-O4		92.67 (8)				92.76 (10)	97.54 (18)	98.40 (10)
N-Pd-Cl1	96.38 (7)		95.82 (8)	96.25 (7)	98.34 (8)			
N-Pd-Cl2	170.34 (8)		172.52 (6)					
P-Pd-O4		172.68 (6)				175.76 (7)	169.16 (12)	167.90 (7)
P-Pd-C7		84.79 (9)		85.36 (10)	84.03 (10)	86.47 (10)	87.5 (2)	88.29 (11)
P-Pd-Cl1	170.69 (3)		173.70 (3)	172.18 (3)	170.43 (3)			
P-Pd-Cl2	83.30 (3)		84.57 (5)					
C7-Pd-O4		87.97 (11)				89.30 (12)	81.9 (2)	81.94 (13)
C7-Pd-Cl1				86.83 (10)	86.91 (10)			
Cl1-Pd-Cl2	89.53 (3)		89.36 (5)					

for references, see page 80

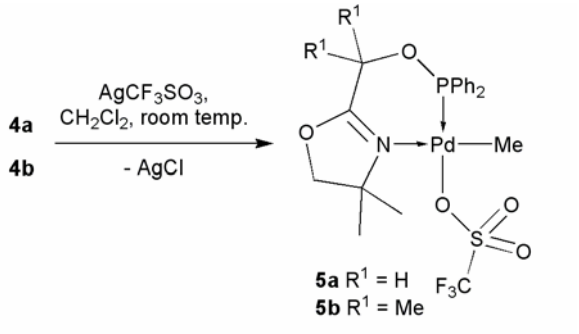

Scheme 2
Preparation of cationic complexes **5a** and **5b**.

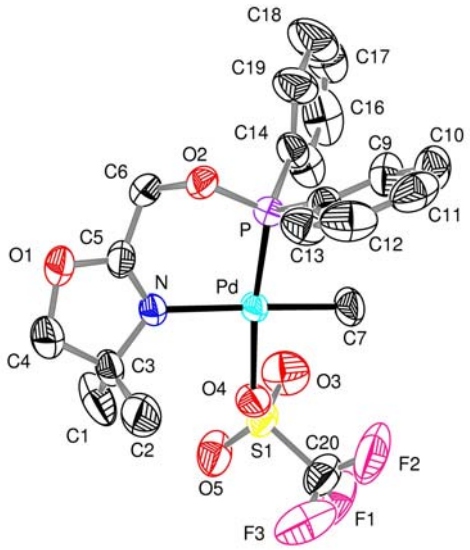

Fig. 2
ORTEP plot of complex **5a** (H atoms omitted). Displacement ellipsoids are drawn at 50% probability level.

CO and Ethylene insertion reactions into Cationic Palladium Complexes 5a and 5b.

Insertion reactions of CO into the Pd-C bond of complexes **5a**,**b** were monitored by $^{31}P\{^{1}H\}$ and ^{1}H NMR. In a typical experiment, a CH_2Cl_2 solution of the respective complex (100-150 mg) was stirred under 1 atmosphere of carbon monoxide, and $^{31}P\{^{1}H\}$ NMR spectra were recorded every hour. The insertion of CO into the Pd methyl bond of **5a** produced the acyl complex [Pd{C(O)Me}(P,N)CF_3SO_3] **6a** (Scheme 3) as evidenced by the large high-field resonance shift in $^{31}P\{^{1}H\}$ NMR ($\Delta\delta$ = -15.4, Table 1). Complete conversion of the complex **5a** into the acyl derivative **6a** was observed after 7 h (Fig. 3), whereas the reaction of **5b** with CO to form **6b** was much slower and after 22 h only one third of the precursor complex was converted into its acyl form. After this reaction time, decomposition of the complex was observed and it has not been possible to isolate **6b**. Despite complete conversion, attempts to isolate pure **6a** were also unsuccessful, the complex was found to be air- and moisture-sensitive, decomposing when exposed to moisture to yield palladium metal. When monitoring the CO insertion reaction by $^{31}P\{^{1}H\}$ and ^{1}H NMR spectroscopy, no signal other than those of the starting material and product was observed, indicating that the isomerisation necessary for the formation of the observed product is too fast to be detected at ambient temperature.[43,45]

Ethylene insertion into the palladium-acyl bond of **6a** occurred at room temperature under atmospheric pressure, the reaction was completed in less than 1 h ($^{31}P\{^{1}H\}$NMR, Fig. 3). It afforded complex **7a** (Scheme 3) in which coordination of the ketonic oxygen atom to the Pd centre (see $\nu_{C=O}$, Table 1) forms a stabilizing chelate which makes β-hydrogen elimination less likely.[67,68] This complex is stable at room temperature for several hours in

for references, see page 80

solution, and several weeks in the solid state, which illustrates the beneficial role of the P,N ligand. The $^{31}P\{^{1}H\}$ NMR signal of **7a** (δ 138.1) is shifted to low field relative to that of **6a** (δ 124.2) (Table 1). In the ^{1}H NMR spectrum of **7a**, the methylene protons Pd-CH_2 give rise to a triplet further coupled with phosphorous(δ 1.43) whereas the $CH_2C{=}O$ protons appear as a broad triplet (δ 3.20), indicating a smaller $^{4+5}J_{HP}$ (see Experimental Section).

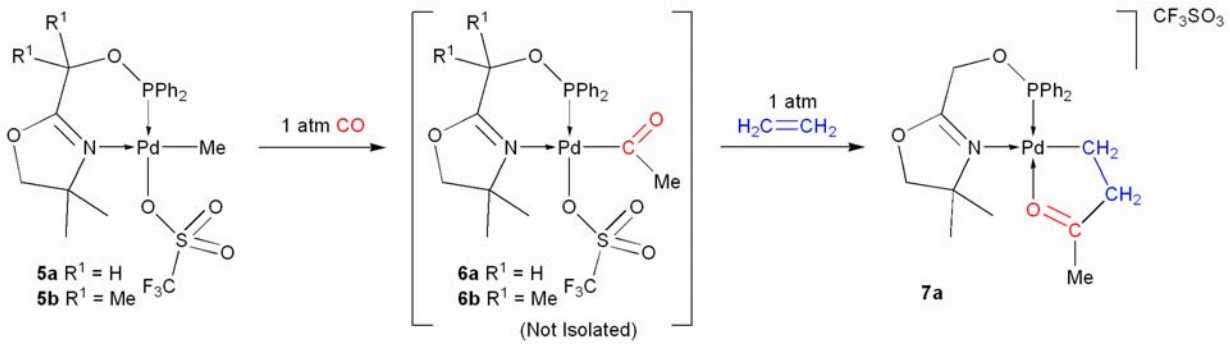

Scheme 3 All reactions performed at room temperature in CH_2Cl_2.

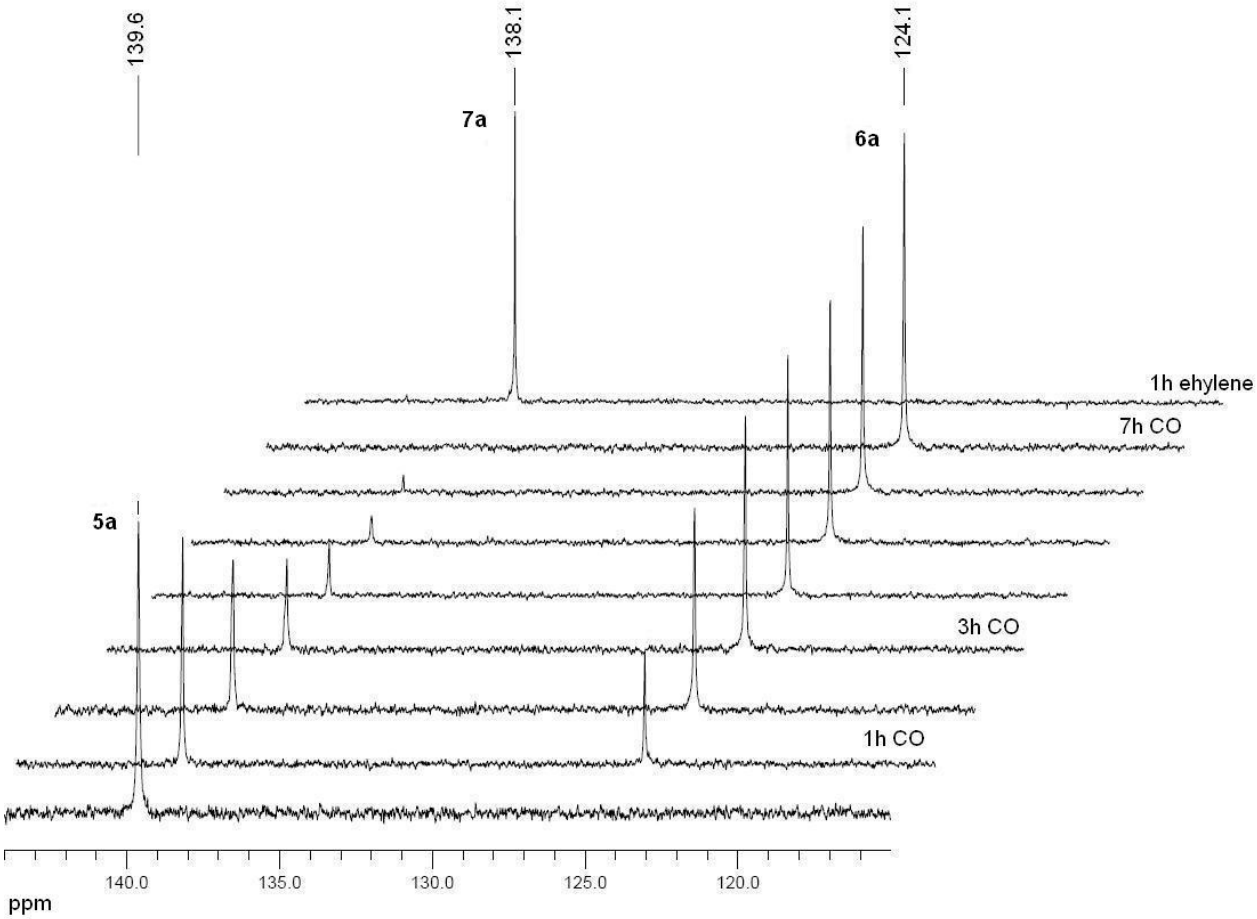

Fig. 3 Stack plot of the $^{31}P\{1H\}$NMR monitoring of the reaction of **5a** with CO to afford **6a** and subsequent reaction with ethylene to afford **7a**.

for references, see page 80

Preparation of the Ligands 8a and 8b.

We recently reported the synthesis of the bidentate, racemic ligand **8b** which allowed us to fully characterize a stable palladium complex featuring an ally ligand in an unusual monohapto-bonding mode.[69] In that report, ligand **8b** was prepared by reaction of 6-chloro-6H-dibenz[c,e]-[1,2]oxaphosphorin with the lithium alcoholate derived from 4,4-dimethyl-2-(1-hydroxy-1-methylethyl)-4,5-dihydrooxazole **1b**. However this procedure was not optimal and it was difficult to completely remove the residual 4,4-dimethyl-2-(1-hydroxy-1-methylethyl)-4,5-dihydrooxazole. Therefore it was felt desirable to develop a more efficient synthesis for this ligand. An improved synthesis of **8b** and of its new unsubstituted analogue **8a** consists in the deprotonation of the corresponding oxazoline alcohol (**1a** or **1b**) with NEt_3 in toluene at low temperature, and subsequent reaction with 6-chloro-6H-dibenz[c,e]-[1,2]oxaphosphorin. After filtration, ligands **8a** and **8b** were obtained in 63 and 75% yield, respectively (Scheme 4). The purity of the ligands synthesized through this procedure was established from satisfactory elemental analyses and spectroscopic data (see Experimental Section).

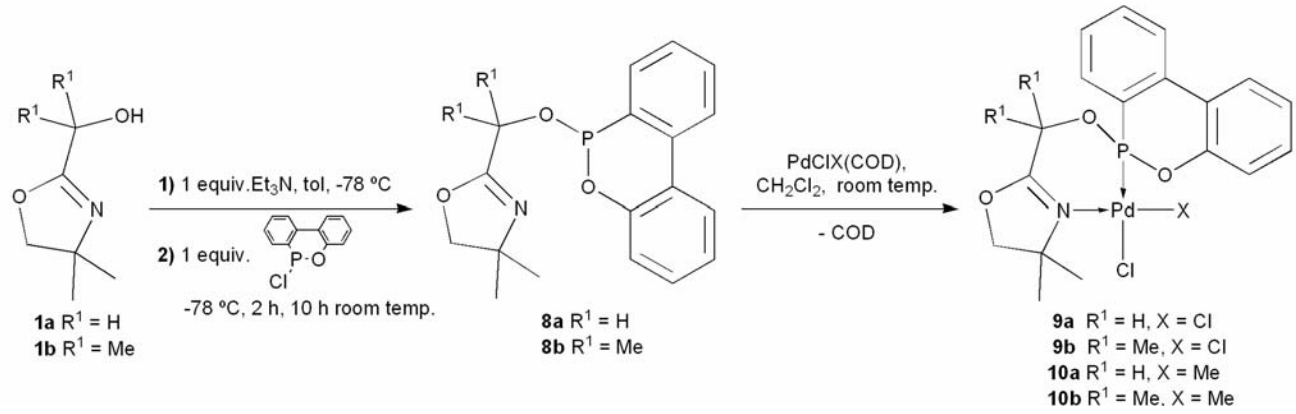

Scheme 4 Synthesis of ligand **8a**,**b**, complexes **9a**,**b** and **10a**,**b**.

Preparation of the Complexes [$PdCl_2$(P,N)] (9a,b) and [PdClMe(P,N)] (10a,b)

Ligands **8a**,**b** were reacted with [$PdCl_2$(COD)] to afford [$PdCl_2$(P,N)] complexes **9a** and **9b** (Scheme 4). Upon coordination of the ligand, the $POCH_2$ protons in **9a** give rise to a ABX spin system (A = B = H, X = P) with different proton-phosphorous coupling constants ($^2J_{HH}$ = 14.2, $^3J_{HP}$ = 28.5 and $^3J_{HP}$ = 14.1 Hz) in the ^{1}H NMR spectrum, whereas in the free ligand (**8a**) the proton-phosphorous coupling constants are very similar, giving rise to an almost symmetrical ABX system ($^2J_{HH}$ = 13.8, $^3J_{HP}$ = 9.2 and $^3J_{HP}$ = 10.0 Hz). In the IR spectrum the $\nu_{C=N}$ absorption shifts to 1653 and 1619 cm^{-1} for **9a** and **9b**, respectively (Table 3). Crystals of **9b** suitable for X-ray diffraction were obtained by slow diffusion of hexane into a CH_2Cl_2 solution of the complex. A view of the molecular structure is show in Fig. 3a

for references, see page 80

and selected bond distances and angles are given in Table 2. As observed for **3a,** there is a clear differentiation between the Pd-Cl bond lengths in **9b**, the Pd-Cl bond *trans* to the P atom being longer than that *trans* to N. The chelate bite angle of 90.38 (7)º is in accordance with other Pd complexes stabilized by the same ligand.[69]

Table 3
Selected IR and NMR data of the free ligands **8a**,**b** and their complexes.

	IR		NMR	
	$\nu_{C=N}$	$\nu_{C=O}$	^{1}H	^{31}P
8a	1669[a] (s)			131.1[d]
8b	1660[a] (w)			123.1[d]
9a	1653[b] (s)			107.4[c]
9b	1619[b] (s)			99.5[c]
10a	1654[b] (s)		0.92 Pd-CH_3 (d, $^3J_{PH}$ = 3.1)[d]	134.2[d]
10b	1628[b] (s)		0.90 Pd-CH_3 (d, $^3J_{PH}$ = 2.6)[d]	124.8[d]
11a	1653[b] (m)		1.00 Pd-CH_3 (s)[d]	134.9[d]
11b	1632[b] (m)		0.97 Pd-CH_3 (s)[d]	125.6[d]
13a				125.5[d]
13b				115.8[d]
14a	1655[b] (m)	1634[b] (m)	2.50 C(O)CH_3[d]	134.7[d]
	$\nu_{C=N/C=O}$			
14b	1635[b] (m)		2.50 C(O)CH_3[d]	125.6[d]

[a]In CH_2Cl_2, [b]in KBr, cm^{-1}. [c]In DMSO, [d]In $CDCl_3$, ppm, *J* in Hz.

Reactions of equimolar amounts of **8a**,**b** with [PdClMe(COD)] in dichloromethane solution afforded the corresponding complexes **10a** and **10b**. The resonances for the Pd-methyl protons are characteristic of the coordination geometries in these complexes, being doublets with $^3J_{PH}$ = 3.1 and 2.6 Hz, respectively. The low $^3J_{PH}$ values indicate a *cis* arrangement of the phosphorous atom and the methyl group. Upon coordination, the $POCH_2$ protons in **10a** give rise to an ABX system (A = B = H, X = P) with different proton-phosphorous coupling constants ($^2J_{HH}$ = 14.3, $^3J_{HP}$ = 27.6 and $^3J_{HP}$ = 13.4 Hz), as observed in **9a**. In the IR spectrum of **10a** and **10b** the $\nu_{C=N}$ absorption shifts to 1654 and 1628 cm^{-1}, respectively (Table 3). The X-ray structures of **10a** and **10b** were also determined, their ORTEP diagrams are shown in Figures 4b and 4c, respectively, and selected bond distances and angles are given in Table 2. As expected, in **10a** and **10b** the Pd-Me group is positioned *cis* to the P atom, which is in agreement with the donor groups with the largest *trans* influence avoiding being mutually *trans* to one another. The coordination geometry is close to square planar with deviations of the Pd atom to the mean plane defined by N, P, Cl and C7 of 0.0040(2) and 0.0290(2) Å for **10a** and **10b**, respectively. When comparing the structures of complexes **9b** and **10b** the only marked difference between them concerns the Pd-N distance, which is larger in **10b** [2.188(3) Å] than in **9b** [2.075(2) Å] owing to the larger trans influence of the methyl ligand compared to chloride.

for references, see page 80

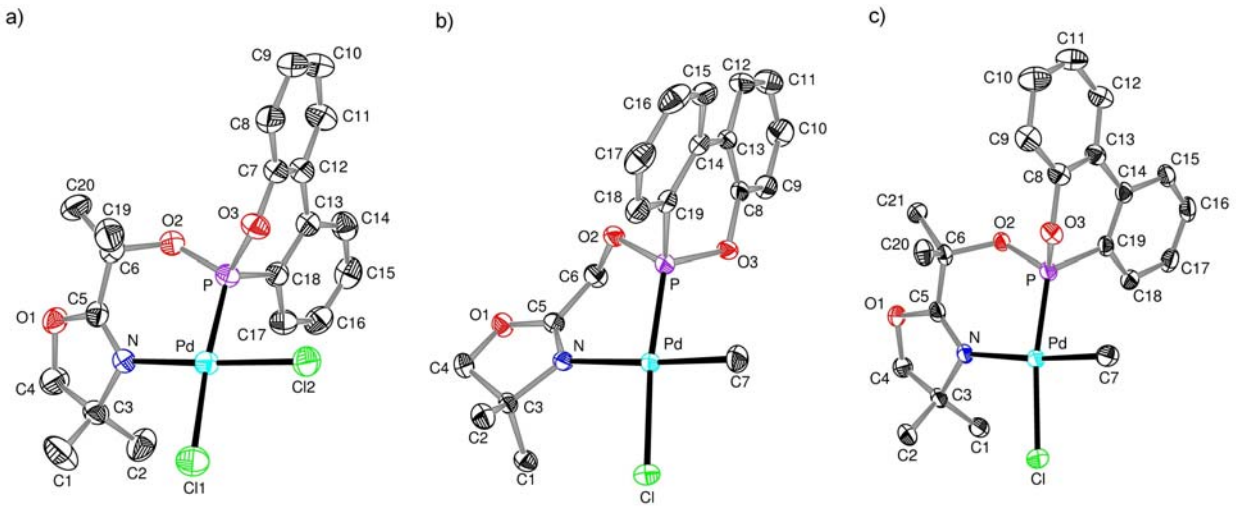

Fig. 4
ORTEP plot of: a) complex **9b**, b) complex **10a**, c) complex **10b** (H atoms omitted). Displacement ellipsoids are drawn at 50% probability level.

Preparation of the Cationic Complexes [PdMe(P,N)OSO$_2$CF$_3$] (11a,b)

Cationic complexes **11a**,**b** were prepared by treatment of **10a**,**b** with $AgCF_3SO_3$ in a dichloromethane solution (Scheme 5). After removal of AgCl by filtration through Celite, the solvent was evaporated and the desired complexes were obtained as solids and washed with diethylether and pentane. Selected IR and NMR data of the complexes are shown in Table 3. In contrast to cationic complexes **5a**,**b** where the Pd-Me resonances appeared in the ^{1}H NMR spectrum as doublets, these resonances were observed as a singlet in **11a** and **11b** at δ 1.00 and δ 0.97, respectively. When compared to the $^{31}P\{^1H\}$NMR data for their less electrophilic neutral analogues (**10a**,**b**) the downfield shift is smaller (0.7-0.8 ppm) than that observed when going from neutral **4a**,**b** to the cationic complexes **5a**,**b**.

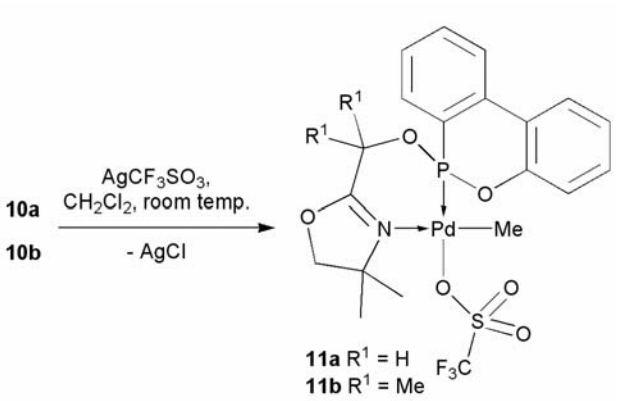

Scheme 5 Preparation of cationic complexes **11a** and **11b**.

In an attempt to crystallize the cationic complex **11b,** by slow diffusion of hexane into a CH_2Cl_2 solution of the complex, the aqua complex **12b** [PdMe(H_2O)(P,N)]CF_3SO_3 (P,N = **8b**) was identified in the solid state, owing presumably to the substitution of triflate in **11b** by adventitious water during the recrystallization process. This phenomenon has been observed

for references, see page 80

before in cationic palladium complexes stabilized by P,N type ligands.[70] An ORTEP plot of the cation in **12b** is shown in Fig. 5 and selected bond distances and angles are given in Table 2. The water molecule interacts through H-bonding with the triflate anion O4-H···O6 [O4-O6 = 2.680(4) Å] and O4-H···O7 [O4-O7 = 2.695(3) Å] thus forming a pseudo-dimer (Fig. 6). The coordination geometry is close to square planar with deviation of the Pd atom from the mean plane defined by N, P, O4 and C7 of 0.0110 (2)Å.

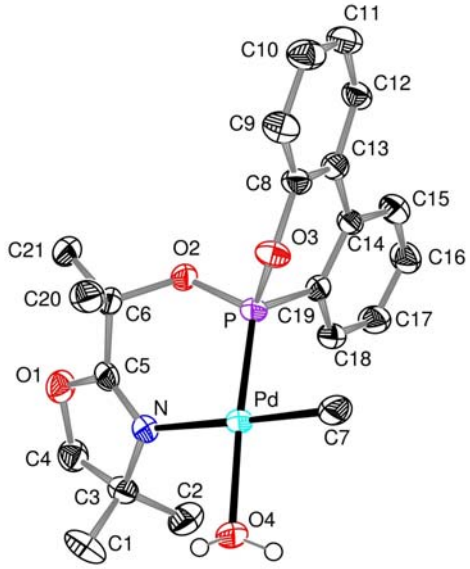

Fig. 5
ORTEP plot of the cation in **12b** (H atoms omitted, except coordinated H_2O). Displacement ellipsoids are drawn at 50% probability level.

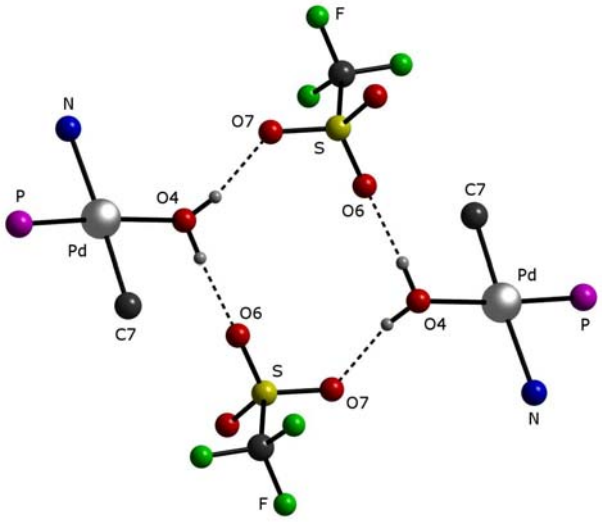

Fig. 6
Hydrogen bonding in complex **12b**.

CO and Ethylene insertion reactions into Cationic Palladium Complexes 11a and 11b.

The insertion reaction of CO into the Pd-C bond of complexes **11a**,**b** was monitored by $^{31}P\{^1H\}$ and ^1H NMR. In a typical experiment, a CH_2Cl_2 solution of the respective complex (0.100-0.150 g) was stirred under 1 atmosphere of carbon monoxide, and $^{31}P\{^1H\}$ NMR spectra were recorded every hour. In contrast to the phosphinite complexes **5a**,**b** insertion of CO into the Pd methyl bond of **11a**,**b** to form the acyl complexes [Pd{C(O)Me}(P,N)CF_3SO_3] **13a,b** (Scheme 6) required only 3 h and 1 h, respectively, to reach completion. A large typical high-field shift of the $^{31}P\{^1H\}$ NMR resonance was also observed when going from **11a**,**b** to the acyl complexes **13a**,**b** ($\Delta\delta$ = -9.4 and $\Delta\delta$ = -9.8, respectively, Table 1). Like **6a**, complexes **13a**,**b** were also found to be air- and moisture-sensitive, decomposing to yield palladium metal, and attempts to isolate them pure were unsuccessful.

for references, see page 80

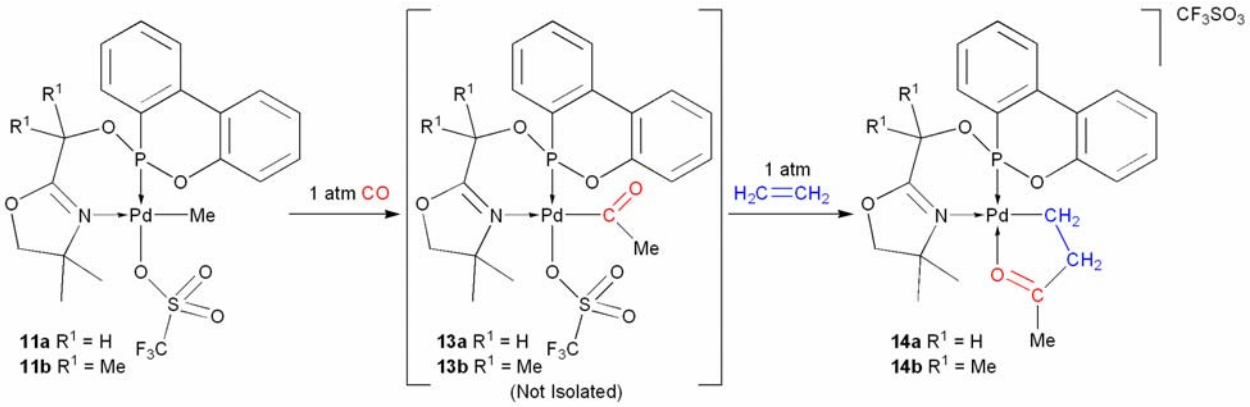

Scheme 6 All reactions performed at room temperature in CH_2Cl_2.

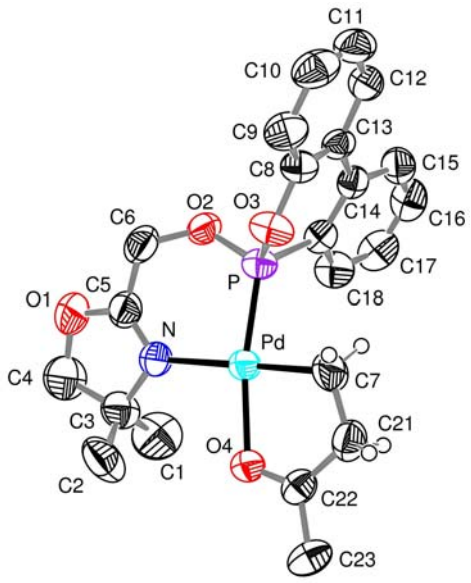

Fig. 7
ORTEP plot of the cation in **14a** (H atoms omitted, except inserted ethylene). Displacement ellipsoids are drawn at 50% probability level.

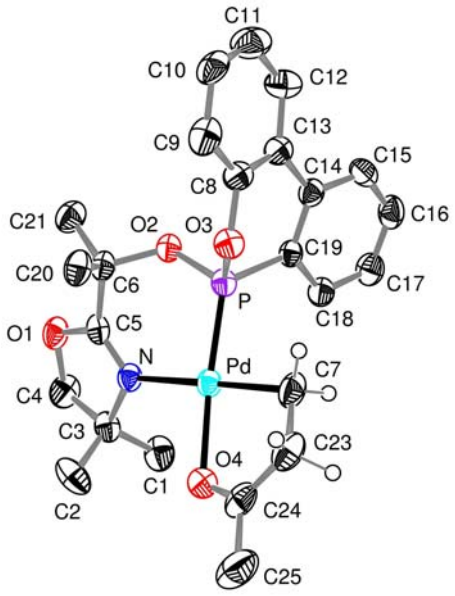

Fig. 8
ORTEP plot of the cation in **14b** (H atoms omitted, except inserted ethylene). Displacement ellipsoids are drawn at 50% probability level.

Ethylene insertion into the palladium-acyl bond of **13a**,**b** occurred at room temperature under atmospheric pressure and afforded complexes **14a**,**b** (Scheme 6). These reactions were faster than the CO insertion reactions, and were completed in less than 1 h. When the conversions of **13a** into **14a** and **13b** into **14b** were monitored by $^{31}P\{^1H\}$NMR spectroscopy, no signal other than those of the starting material and product was observed, which indicated that, as for the CO insertion reactions and conversion of **6a** into **7a**, the isomerisation necessary to generate the observed isomer is too fast to be detected. The ligand arrangement in **14a**,**b** was determined by multinuclear NMR and IR spectroscopy and confirmed by single crystal X-ray diffraction studies. The $^{31}P\{^1H\}$ NMR spectra of **14a**,**b** contains singlets at δ 134.7 and δ 125.6 respectively, which are shifted to low field with respect of **13a**,**b**. In both complexes (**14a** and **14b**) the expected coordination of the ketonic oxygen atom to the Pd center to form a stabilizing 5 membered chelate was observed (see ν_{CO}, Table 3). Further confirmation was obtained from the X-ray crystallographic studies, the

for references, see page 80

structures of **14a** and **14b** are show in Fig. 7 and Fig. 8, and selected bond distances and angles are given in Table 2. The metal center in both complexes exhibits a distorted square planar coordination geometry with the coordinated ketonic oxygen *trans* to phosphorous. The structures of **14a** and **14b** represent rare examples of structurally characterized ethylene-CO coupling products,[47,48,50,56-60] and to the best of our knowledge the first in which the metal center is stabilized by a phosphonite ancillary ligand.

Conclusion

Oxazoline based P,N-donor ligands containing phosphinite and phosphonite functions were prepared in a two step process involving the deprotonation of the oxazoline alcohol followed by reaction with a chlorophosphine. These ligands readily coordinate to palladium (II) and the resulting complexes were characterized in solution by spectroscopic methods and, in some cases, in the solid state by X-ray diffraction.

Controlled stepwise insertion reactions of CO in the palladium methyl complexes **5a**,**b** and **11a**,**b** afforded the acyl complexes **6a**,**b** and **13a**,**b** identified in situ by means of $^{31}P\{^{1}H\}$ NMR. Interesting differences in the conversion rates were observed depending on the ligand. The replacement of the $POCH_2$ protons of the ligands by Me groups produced opposite effects on the rate of conversion of the respective methyl-palladium cationic complexes into their acyl forms: in the phosphinite case, the conversion was faster when R^1 = H (complex **5a**, 7 h) whereas in the phosphonite case, it was faster for R^1 = Me (complex **11b**, 1 h). This is in contrast with results obtained for related complexes stabilized by (2-oxazoline-2-ylmethyl)diphenyl phosphine and (2-oxazoline-2-ylmethyl-4,4-dimethyl)diphenyl phosphine P,N ligands,[50] which inserted CO to produce the acyl forms within minutes.

The acyl intermediates **6a** and **13a**,**b** reacted with ethylene to form the alkyl complexes **7a** and **14a**,**b** which were unambiguously identified and characterized, in the case of **14a** and **14b,** the X-ray structural characterization was also obtained. Attempts to insert methyl acrylate into the Pd-C bond of **6a** and **13a**,**b** were not successful but we have shown very recently that related P,N chelates allow this reaction to take place.[50] This difference in the reactivity of the ethylene and methyl acrylate monomers is consistent with results obtained in related study with a P,O chelating ligand.[57]

for references, see page 80

Experimental Section

The ^{1}H, $^{13}C\{^{1}H\}$, $^{31}P\{^{1}H\}$ and $^{19}F\{^{1}H\}$ NMR spectra were recorded at 500.13 or 300.13, 75.48, 121.49 and 282.38 MHz, respectively, on FT Bruker AC300, Avance 300 and Avance 500 instruments. IR spectra in the range 4000–400 cm^{-1} were recorded on a Bruker IFS66FT and a Perkin Elmer 1600 Series FTIR. Elemental analyses were preformed by the "Service de Microanalyse, Université Louis Pasteur (Strasbourg, France)". All reactions were carried out under purified N_2, using Schlenk techniques, and the solvents were freshly distilled under nitrogen prior to use. [PdMeCl(COD)] and [$PdCl_2$(COD)] (COD is 1,5-cyclooctadiene, C_8H_{12}) were prepared according to literature procedures,[71,72] as were **1a** and **1b**,[73] 6-chloro-6H-dibenz[c,e]-[1,2]oxaphosphorin[74] and ligand **2b**.[61-63]

Selected data: **2a**: The oxazoline alcohol **1a** (0.58 g, 4.5 mmol) was dissolved in toluene (30 mL). To this colourless solution cooled to –78 °C was added BuLi (2.75 mL, 1.6 M in hexane, 4.5 mmol), and after stirring at -78 °C for 1 h, PPh_2Cl (0.99 g, 4.5 mmol) in toluene (5 mL) was added dropwise, and the solution further stirred at -78 ºC for 2 h. The reaction mixture was then allowed to slowly reach room temperature and stirred overnight. The white precipitate was filtered and the filtrate was evaporated under vacuum overnight, affording a colourless oil (1.17 g, 83%). IR (CH_2Cl_2): 1668 (s, $\nu_{C=N}$) cm^{-1}. ^{1}H NMR (300.13 MHz, $CDCl_3$, room temp.): δ 1.22 [s, 6H, $NC(CH_3)_2$], 3.88 (s, 2H, $COCH_2$), 4.49 (d, 2H, $^{3}J_{HP}$ = 11.8 Hz, $POCH_2$), 7.33-7.39 (complex m, 6H, aromatic), 7.49-7.55 (complex m, 4H, aromatic) .$^{13}C\{^{1}H\}$ NMR (75.48 MHz, $CDCl_3$, room temp.): δ 28.2 [s, $NC(CH_3)_2$], 64.4 (d, $^{2}J_{PC}$ = 20.4 Hz, $POCH_2$), 67.2 [s, $NC(CH_3)_2$], 79.3 (s, $COCH_2$), 128.3 (d, $^{3}J_{PC}$ = 6.8 Hz, *meta*-Ph), 129.5 (s, *para*-Ph), 130.7 (d, $^{2}J_{PC}$ = 21.8 Hz, *ortho*-Ph), 141.1 (d, $^{1}J_{PC}$ = 17.9 Hz, *ipso*-Ph), 162.3 (d, $^{3}J_{PC}$ = 6.2 Hz, C=N). $^{31}P\{^{1}H\}$ NMR (121.5 MHz, $CDCl_3$, room temp.): δ 121.8 (s).

3a: To a solution of ligand **2a** (0.79 g, 2.5 mmol) in CH_2Cl_2 (20 mL) was added solid [$PdCl_2$(COD)] (0.58 g, 0.8 equiv.) at room temperature and the resulting mixture was stirred overnight. The solvent was then evaporated under reduced pressure affording a yellow residue. The latter was washed with diethylether (2 × 15 mL) and pentane (15 mL) and dried under vacuum (0.81 g, 82%). IR (KBr): 1635 (s, $\nu_{C=N}$) cm^{-1}. ^{1}H NMR (300.13 MHz, $CDCl_3$, room temp.): δ 1.78 [s, 6H, $NC(CH_3)_2$], 4.30 (s, 2H, $COCH_2$), 4.43 (d, $^{3}J_{HP}$ = 19.8 Hz, 2H, $POCH_2$), 7.45-7.62 (complex m, 6H, aromatic), 7.90-8.00 (complex m, 4H, aromatic). $^{31}P\{^{1}H\}$ NMR

for references, see page 80

(121.49 MHz, $CDCl_3$, room temp.): δ 116.3 (s). Anal. Calcd for $C_{18}H_{20}Cl_2NO_2PPd$: C, 44.06; H, 4.11; N, 2.85. Found: C, 43.82; H, 4.23; N, 2.67.

4a: Complex **4a** was obtained using a similar procedure to that described above for **3a,** from **2a** (1.12 g, 3.6 mmol) and [PdClMe(COD)] (0.76 g, 0.8 equiv.). It was obtained as a pale yellow solid (1.06 g, 79%). IR (KBr): 1635 (s, $\nu_{C=N}$) cm^{-1}. ^1H NMR (300.13 MHz, $CDCl_3$, room temp.): δ 0.61 (d, $^3J_{HP}$ = 4.3 Hz, 3H, $PdCH_3$), 1.72 [s, 6H, $NC(CH_3)_2$], 4.10 (s, 2H, $COCH_2$), 4.30 (d, $^3J_{HP}$ = 19.3 Hz, 2H, $POCH_2$), 7.45-7.59 (complex m, 6H, aromatic), 7.69-7.77 (complex m, 4H, aromatic). $^{31}P\{^1H\}$ NMR (121.49 MHz, $CDCl_3$, room temp.): δ 137.0 (s). Anal. Calcd for $C_{19}H_{23}ClNO_2PPd$: C, 48.53; H, 4.93; N, 2.98. Found: C, 48.22; H, 4.71; N, 2.74.

4b: Complex **4b** was obtained using a similar procedure to that described above for **3a,** from **2b** (1.61 g, 4.72 mmol) and [PdClMe(COD)] (1.00 g, 0.8 equiv.). It was obtained as a orange solid (2.02 g, 86%). IR (KBr): 1625 (s, $\nu_{C=N}$) cm^{-1}. ^1H NMR (300.13 MHz, $CDCl_3$, room temp.): δ 0.65 (d, $^3J_{HP}$ = 3.9 Hz, 3H, $PdCH_3$), 1.57 [s, 6H, $NC(CH_3)_2$], 1.78 [s, 6H, $OC(CH_3)_2$], 3.97 (s, 2H, OCH_2), 7.41-7.51 (complex m, 6H, aromatic), 7.57-7.64 (complex m, 4H, aromatic). $^{31}P\{^1H\}$ NMR (121.49 MHz, $CDCl_3$, room temp.): δ 119.8 (s). Anal. Calcd for $C_{21}H_{27}ClNO_2PPd$: C, 50.62; H, 5.46; N, 2.81. Found: C, 50.58; H, 5.40; N, 2.73.

5a: To a solution of complex **4a** (0.47 g, 1.00 mmol) in CH_2Cl_2 (15 mL) was added $AgSO_3CF_3$ (0.31 g, 1.2 equiv). The reaction mixture was protected from room light with aluminum foil and stirred for 2 h at room temperature. The solution was then filtered through dry Celite and the solvent evaporated under reduced pressure. The residue was washed with diethylether (2 × 10 mL), pentane (10 mL) an dried under vacuum overnight. Complex **5a** was obtained as a light brown solid (0.48 g, 82%). IR (KBr): 1652 (s, $\nu_{C=N}$) cm^{-1}. ^1H NMR (300.13 MHz, $CDCl_3$, room temp.): δ 0.69 (d, $^3J_{HP}$ = 1.7 Hz, 3H, $PdCH_3$), 1.56 [s, 6H, $NC(CH_3)_2$], 4.16 (s, 2H, $COCH_2$), 4.28 (d, $^3J_{HP}$ = 19.0 Hz, 2H, $POCH_2$), 7.50-7.64 (complex m, 6H, aromatic), 7.68-7.77 (complex m, 4H, aromatic). $^{31}P\{^1H\}$ NMR (121.49 MHz, $CDCl_3$, room temp.): δ 139.7 (s). $^{19}F\{^1H\}$ NMR (282.38 MHz, $CDCl_3$): δ -78.2 (s). Anal. Calcd for $C_{20}H_{23}F_3NO_5PPdS$: C, 41.14; H, 3.97; N, 2.40. Found: C, 40.98; H, 3.77; N, 2.21.

5b: Complex **5b** was obtained using a similar procedure to that described above for **5a,** from **4b** (0.67 g, 1.34 mmol) and $AgSO_3CF_3$ (0.41g, 1.2 equiv). It was obtained as a yellow solid

for references, see page 80

(0.75 g, 91%). IR (KBr): 1642 (s, $\nu_{C=N}$) cm^{-1}. ^1H NMR (300.13 MHz, $CDCl_3$, room temp.): δ 0.70 (d, $^3J_{HP}$ = 1.4 Hz, 3H, $PdCH_3$), 1.43 [s, 6H, $NC(CH_3)_2$], 1.74 [s, 6H, $OC(CH_3)_2$], 4.08 (s, 2H, $COCH_2$), 7.44-7.64 (complex m, 10H, aromatic). $^{31}P\{^1H\}$ NMR (121.49 MHz, $CDCl_3$, room temp.): δ 122.5 (s). $^{19}F\{^1H\}$ NMR (282.38 MHz, $CDCl_3$): δ -78.0 (s). Anal. Calcd for $C_{22}H_{27}F_3NO_5PPdS$: C, 43.18; H, 4.45; N, 2.29. Found: C, 43.37; H, 4.58; N, 2.12.

7a: A solution of **5a** (0.31 g, 0.53 mmol) in CH_2Cl_2 (25 mL) was stirred under 1 atm CO at room temperature for 7 h, the CO was then replaced by 1 atm ethylene and the solution further stirred for 1 h. After filtration and removal of the volatiles under vacuum, the residue was washed with diethylether (20 mL) and pentane (2 × 20 mL) and dried under vacuum, to afford **7a** as a pale yellow powder (0.29 g, 87% yield). IR (KBr): 1658 (m, $\nu_{C=N}$), 1636 (m, $\nu_{C=O}$) cm^{-1}. ^1H NMR (300.13 MHz, $CDCl_3$): δ 1.43 (td, $^3J_{HH}$ = 5.7, $^3J_{HP}$ = 3.3 Hz, 2H, $PdCH_2$), 1.57 [s, 6H, $NC(CH_3)_2$], 2.50 [s, 3H, $C(O)CH_3$], 3.20 (brt, $^3J_{HH}$ = 5.7 Hz, 2H, $PdCH_2CH_2$), 4.27 (s, 2H, $COCH_2$), 4.42 (d, $^2J_{HP}$=18.0 Hz, 2H, $POCH_2$), 7.59-7.74 (complex m, 10H, aromatic); $^{31}P\{^1H\}$ NMR (121.49 MHz, $CDCl_3$): δ 138.1 (s); $^{19}F\{^1H\}$ NMR (282.38 MHz, $CDCl_3$): δ -78.6 (s); Anal. Calcd for $C_{23}H_{27}F_3NO_6PPdS$: C, 43.17; H, 4.25; N, 2.19. Found: C, 42.95; H, 4.01; N, 2.07.

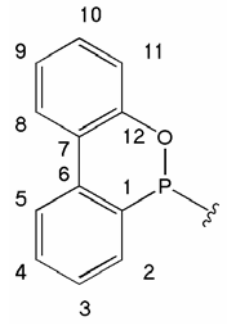

8a: The oxazoline alcohol **1a** (1.3 g, 10 mmol) and NEt_3 (1.4 mL, 10 mmol) were dissolved in toluene (20.0 mL). To this colourless solution cooled to -78 °C was added dropwise 6-chloro-6H-dibenz[c,e][1,2]oxaphosphorin (2.35 g, 10 mmol) in 10 mL of the same solvent. The mixture was stirred for 6 h while the solution was gradually warmed to room temperature. The white precipitate was filtered off and the solution concentrated under reduced pressure to yield a pale yellow oil which was dissolved in Et_2O and washed with degassed water (3 x 10 mL). The organic phase was dried over anhydrous $MgSO_4$, filtered, and the solvent was removed under reduced pressure to yield a beige oil (2.07 g, 63%). IR (CH_2Cl_2): 1669 (m, $\nu_{C=N}$) cm^{-1}. ^1H NMR (500.13 MHz, $CDCl_3$, room temp.): δ 1.19 [s, 3H, $NC(CH_3)(CH_3)$], 1.21 [s, 3H, $NC(CH_3)(CH_3)$], AB spin system (A = B = H, δ_A 3.85, δ_B 3.87, $^2J_{AB}$ = 8.1 Hz, 2H, $COCH_2$), ABX spin system (A = B = H, X = P, δ_A 4.22, δ_B 4.30, $^2J_{AB}$ = 13.8 Hz, $^3J_{AX}$ = 9.2

for references, see page 80

Hz, $^{3}J_{BX}$ = 10.0 Hz, 2H, $POCH_2$), 7.14-7.26 (complex m, 2H, aromatic), 7.30-7.34 (m, 1H, aromatic), 7.44-7.48 (complex m, 1H, aromatic), 7.58-7.63 (m, 1H, aromatic), 7.70-7.75 (m, 1H, aromatic), 7.93-8.00 (m, 2H, aromatic). $^{13}C\{^{1}H\}$ NMR (75.48 MHz, $CDCl_3$, room temp.): δ 28.1 [s, $NC(CH_3)(CH_3)$], 28.2 [s, $NC(CH_3)(CH_3)$], 62.2 (d, $^{2}J_{PC}$ = 9.8 Hz, $POCH_2$), 67.2 [s, $NC(CH_3)_2$], 79.3 (s, $COCH_2$), 120.5 (d, $^{3}J_{PC}$ = 1.2 Hz, C^{11}), 122.2 (d, $^{3}J_{PC}$ = 6.1 Hz, C^{7}), 123.3 (s), 123.5 (s), 124.9 (s), 127.7 (d, J_{PC} = 14.0 Hz), 129.7 (d, J_{PC} = 1.0 Hz), 131.0 (d, J_{PC} = 18.8 Hz), 131.8 (d, J_{PC} = 51.9 Hz), 132.0 (s), 132.2 (d, overlapping), 149.8 (d, $^{2}J_{PC}$ = 9.9 Hz, C^{12}), 161.7 (d, $^{3}J_{PC}$ = 4.3 Hz, C=N). $^{31}P\{^{1}H\}$ NMR (121.49 MHz, $CDCl_3$, room temp.): δ 131.1 (s). Anal. Calcd for $C_{18}H_{18}NO_3P$: C, 66.05; H, 5.54; N, 4.28. Found: C, 65.86; H, 5.76; N, 3.83.

8b: Ligand **8b** was obtained using a similar procedure to that described above for **8a,** from **1b** (1.58 g, 10 mmol) and NEt_3 (1.4 mL, 10 mmol) in toluene (20.0 mL) and 6-chloro-6H-dibenz[c,e][1,2]oxaphosphorin (2.35 g, 10 mmol) in 10 mL of the same solvent. It was obtained as a beige oil (2.70 g, 75%). IR (CH_2Cl_2): 1660 (w, $\nu_{C=N}$) cm^{-1}. ^{1}H NMR (300.13 MHz, $CDCl_3$, room temp.): δ 1.32 [s, 3H, $NC(CH_3)(CH_3)$], 1.35 [s, 3H, $NC(CH_3)(CH_3)$], 1.42 [s, 3H, $OC(CH_3)(CH_3)$], 1.67 [s, 3H, $OC(CH_3)(CH_3)$], AB spin system (A = B = H, δ_A 4.01, δ_B 4.03, $^{1}J_{AB}$ = 8.1 Hz, 2H, OCH_2), 7.13-7.20 (complex m, 2H, aromatic), 7.29-7.37 (complex m, 1H, aromatic), 7.39-7.47 (m, 1H, aromatic), 7.52-7.69 (complex m, 2H, aromatic), 7.90-7.98 (complex m, 2H, aromatic). $^{13}C\{^{1}H\}$ NMR (75.48 MHz, $CDCl_3$, room temp.): δ 27.2 [d, $^{3}J_{PC}$ = 9.3 Hz, $OC(CH_3)(CH_3)$], 28.0 [d, $^{3}J_{PC}$ = 5.6 Hz, $OC(CH_3)(CH_3)$], 28.2 [s, $NC(CH_3)(CH_3)$], 28.3 [s, $NC(CH_3)(CH_3)$], 67.6 [s, $NC(CH_3)_2$], 75.7 [d, $^{2}J_{PC}$ = 11.2 Hz, $POC(CH_3)_2$], 79.4 (s, OCH_2), 120.6 (d, $^{3}J_{PC}$ = 1.2 Hz, C^{11}), 122.9 (d, $^{3}J_{PC}$ = 6.8 Hz, C^{7}), 123.1 (s), 123.6 (s), 124.9 (s), 127.4 (d, J_{PC} = 13.6 Hz), 129.3 (s), 131.2 (d, J_{PC} = 49.0 Hz), 131.4 (s), 132.0 (d, J_{PC} = 2.5 Hz), 132.9 (d, J_{PC} = 12.4 Hz), 149.4 (d, $^{2}J_{PC}$ = 8.1 Hz, C^{12}), 167.2 (d, $^{3}J_{PC}$ = 1.3 Hz, C=N). $^{31}P\{^{1}H\}$ NMR (121.5 MHz, $CDCl_3$, room temp.): δ 123.1 (s). Anal. Calcd for $C_{20}H_{22}NO_3P$: C, 67.60; H, 6.24; N, 3.94. Found: C, 67.35; H, 6.41; N, 3.54.

9a: Complex **9a** was obtained using a similar procedure to that described above for **3a,** from **8a** (0.89 g, 2.7 mmol) and $[PdCl_2(COD)]$ (0.68 g, 0.8 equiv.). It was obtained as a yellow solid (0.81 g, 75%). IR (KBr): 1653 (s, $\nu_{C=N}$) cm^{-1}. ^{1}H NMR (500.13 MHz, DMSO, room temp.): δ 1.71 [s, 3H, $NC(CH_3)(CH_3)$], 1.75 [s, 3H, $NC(CH_3)(CH_3)$], AB spin system (A = B = H, δ_A 4.40, δ_B 4.49, $^{2}J_{AB}$ = 8.6 Hz, 2H, $COCH_2$), ABX spin system (A = B = H, X = P, δ_A 4.88, δ_B 5.16, $^{2}J_{AB}$ = 14.2 Hz, $^{3}J_{AX}$ = 28.5 Hz, $^{3}J_{BX}$ = 14.1 Hz, 2H, $POCH_2$), 7.37-7.42 (m, 2H, aromatic), 7.50-7.55 (m, 1H, aromatic), 7.72-7.77 (complex m, 1H, aromatic), 7.87-7.91 (m,

for references, see page 80

1H, aromatic), 8.10-8.16 (m, 1H, aromatic), 8.26-8.34 (complex m, 2H, aromatic). $^{31}P\{^{1}H\}$ NMR (121.49 MHz, DMSO, room temp.): δ 107.4 (s). Anal. Calcd for $C_{18}H_{18}Cl_2NO_3PPd$: C, 42.84; H, 3.60; N, 2.78. Found: C, 42.68; H, 3.68; N, 2.51.

9b: Complex **9b** was obtained using a similar procedure to that described above for **3a,** from **8b** (1.68 g, 4.7 mmol) and [$PdCl_2$(COD)] (1.19 g, 0.8 equiv.). It was obtained as a yellow solid (1.46 g, 73%). IR (KBr): 1619 (s, $\nu_{C=N}$) cm^{-1}. ^{1}H NMR (300.13 MHz, DMSO, room temp.): δ 1.59 [s, 3H, OC(C*H*$_3$)(CH$_3$)], 1.69 [s, 3H, NC(C*H*$_3$)(CH$_3$)], 1.80 [s, 3H, NC(CH$_3$)(C*H*$_3$)], 2.13 [s, 3H, OC(CH$_3$)(C*H*$_3$)], AB spin system (A = B = H, δ_A 4.49, δ_B 4.57, $^{2}J_{AB}$ = 8.5 Hz, 2H, OCH$_2$), 7.37-7.44 (m, 2H, aromatic), 7.51-7.58 (m, 1H, aromatic), 7.74-7.78 (complex m, 1H, aromatic), 7.87-7.93 (m, 1H, aromatic), 7.99-8.09 (m, 1H, aromatic), 8.26-8.35 (complex m, 2H, aromatic). $^{31}P\ \{^{1}H\}$NMR (121.49 MHz, DMSO, room temp.): δ 99.5 (s). Anal. Calcd for $C_{20}H_{22}Cl_2NO_3PPd$: C, 45.09; H, 4.16; N, 2.63. Found: C, 44.90; H, 4.33; N, 2.41.

10a: Complex **10a** was obtained using a similar procedure to that described above for **3a,** from **8a** (1.03 g, 3.2 mmol) and [PdClMe(COD)] (0.75 g, 0.8 equiv.). It was obtained as a yellow pale solid (0.93 g, 75%). IR (KBr): 1654 (s, $\nu_{C=N}$) cm^{-1}. ^{1}H NMR (300.13 MHz, $CDCl_3$, room temp.): δ 0.92 (d, $^{3}J_{HP}$ = 3.1 Hz, 3H, PdCH$_3$), 1.77 [s, 3H, NC(C*H*$_3$)(CH$_3$)], 1.80 [s, 3H, NC(CH$_3$)(C*H*$_3$)], AB spin system (A = B = H, δ_A 4.10, δ_B 4.19, $^{2}J_{AB}$ = 8.3 Hz, 2H, COCH$_2$), ABX spin system (A = B = H, X = P, δ_A 4.30, δ_B 4.67, $^{2}J_{AB}$ = 14.3 Hz, $^{3}J_{AX}$ = 27.6 Hz, $^{3}J_{BX}$ = 13.4 Hz, 2H, POCH$_2$), 7.25-7.33 (complex m, 2H, aromatic), 7.39-7.45 (m, 1H, aromatic), 7.53-7.60 (complex m, 1H, aromatic), 7.70-7.77 (m, 1H, aromatic), 7.98-8.11 (complex m, 3H, aromatic). $^{31}P\{^{1}H\}$ NMR (121.49 MHz, $CDCl_3$, room temp.): δ 134.2 (s). Anal. Calcd for $C_{19}H_{21}ClNO_3PPd$: C, 47.13; H, 4.37; N, 2.89. Found: C, 47.12; H, 4.41; N, 2.64.

10b: Complex **10b** was obtained using a similar procedure to that described above for **3a,** from **8b** (1.47 g, 4.1 mmol) and [PdClMe(COD)] (0.98 g, 0.8 equiv.). It was obtained has a yellow solid (1.21 g, 72%). IR (KBr): 1628 (s, □$_{C=N}$) cm^{-1}. ^{1}H NMR (300.13 MHz, $CDCl_3$, room temp.): δ 0.90 (d, $^{3}J_{HP}$ = 2.6 Hz, 3H, PdCH$_3$), 1.32 [s, 3H, OC(C*H*$_3$)(CH$_3$)], 1.77 [s, 3H, NC(C*H*$_3$)(CH$_3$)], 1.82 [s, 3H, NC(CH$_3$)(C*H*$_3$)], 2.05 [s, 3H, OC(CH$_3$)(C*H*$_3$)], AB spin system (A = B = H, δ_A 4.03, δ_B 4.18, $^{2}J_{AB}$ = 8.3 Hz, 2H, OCH$_2$), 7.19-7.31 (complex m, 2H, aromatic), 7.37-7.41 (m, 1H, aromatic), 7.52-7.55 (m, 1H, aromatic), 7.66-7.72 (m, 1H, aromatic), 7.96-8.06 (complex m, 3H, aromatic). $^{31}P\{^{1}H\}$ NMR (121.49 MHz, $CDCl_3$, room

for references, see page 80

temp.): δ 124.8 (s). Anal. Calcd for $C_{21}H_{25}ClNO_3PPd$: C, 49.24; H, 4.92; N, 2.73. Found: C, 49.06; H, 4.99; N, 2.36.

11a: Complex **11a** was obtained using a similar procedure to that described above for **5a,** from **10a** (0.427 g, 0.88 mmol) and $AgSO_3CF_3$ (0.27 g, 1.2 equiv). It was obtained has a yellow solid (0.40 g, 70%). IR (KBr): 1653 cm^{-1} (m, $\nu_{C=N}$). ^1H NMR (300.13 MHz, $CDCl_3$, room temp.): δ 1.00 (s, 3H, $PdCH_3$), 1.61 [s, 3H, $NC(CH_3)(CH_3)$], 1.62 [s, 3H, $NC(CH_3)(CH_3)$], AB spin system (A = B = H, δ_A 4.17, δ_B 4.23, $^2J_{AB}$ = 8.5 Hz, 2H, $COCH_2$), ABX spin system (A = B = H, X = P, δ_A 4.33, δ_B 4.67, $^2J_{AB}$ = 14.9 Hz, $^3J_{AX}$ = 27.5 Hz, $^3J_{BX}$ = 12.4 Hz, 2H, $POCH_2$), 7.27-7.36 (complex m, 2H, aromatic), 7.41-7.48 (m, 1H, aromatic), 7.58-7.65 (complex m, 1H, aromatic), 7.74-7.80 (m, 1H, aromatic), 7.99-8.09 (m, 3H, aromatic). $^{31}P\{^1H\}$ NMR (121.49 MHz, $CDCl_3$, room temp.): δ 134.9 (s). $^{19}F\{^1H\}$ NMR (282.38 MHz, $CDCl_3$): δ -78.1 (s). Anal. Calcd for $C_{20}H_{21}F_3NO_6PPdS$: C, 40.18; H, 3.54; N, 2.34. Found: C, 39.84; H, 3.23; N, 2.37.

11b: Complex **14b** was obtained using a similar procedure to that described above for **5a,** from **10b** (1.94 g, 3.79 mmol) and $AgSO_3CF_3$ (1.17 g, 1.2 equiv). It was obtained has a yellow solid (2.01 g, 89%). IR (KBr): 1632 (s, $\nu_{C=N}$) cm^{-1}. ^1H NMR (300.13 MHz, $CDCl_3$, room temp.): δ 0.97 (s, 3H, $PdCH_3$), 1.34 [d, $^4J_{HP}$ = 1.1 Hz, 3H, $OC(CH_3)(CH_3)$], 1.58 [s, 3H, $NC(CH_3)(CH_3)$], 1.66 [s, 3H, $NC(CH_3)(CH_3)$], 2.02 [s, 3H, $OC(CH_3)(CH_3)$], AB spin system (A = B = H, δ_A 4.12, δ_B 4.22, $^2J_{AB}$ = 8.5 Hz, 2H, OCH_2), 7.19-7.24 (m, 1H, aromatic), 7.29-7.36 (m, 1H, aromatic), 7.40-7.47 (m, 1H, aromatic), 7.55-7.63 (m, 1H, aromatic), 7.70-7.78 (m, 1H, aromatic), 7.92-8.03 (complex m, 3H, aromatic). $^{31}P\{^1H\}$ NMR (121.49 MHz, $CDCl_3$, room temp.): δ 125.6 (s). $^{19}F\{^1H\}$ NMR (282.38 MHz, $CDCl_3$): δ -78.1 (s). Anal. Calcd for $C_{22}H_{25}F_3NO_6PPdS$: C, 42.22; H, 4.03; N, 2.24. Found: C, 42.09; H, 3.87; N, 2.21.

14a: A solution of **11a** (0.17 g, 0.28 mmol) in CH_2Cl_2 (25 mL) was stirred under 1 atm CO at room temperature for 3 h, the CO was then replaced by 1 atm ethylene and the solution further stirred for 1 h. Workup was as described for **7a**, and afforded **14a** as a yellow powder (0.17 g, 91% yield). IR (KBr): 1655 (m, $\nu_{C=N}$), 1634 (m, $\nu_{C=O}$) cm^{-1}. ^1H NMR (300.13 MHz, $CDCl_3$): δ 1.63 [s, 3H, $NC(CH_3)(CH_3)$], 1.64 [s, 3H, $NC(CH_3)(CH_3)$], broad ABMNX system (A = B = M = N = H, X = P, δ_A 1.74, δ_B 1.93, 2H, $PdCH_2$), 2.55 [s, 3H, $C(O)CH_3$], broad ABMNX system (A = B = M = N = H, X = P, δ_A 3.15, δ_B 3.27, $^2J_{AB}$ = 20.6 Hz, 2H, $PdCH_2CH_2$), AB spin system (A = B = H, δ_A 4.30, δ_B 4.33, $^2J_{AB}$ = 8.6 Hz, 2H, $COCH_2$), ABX

for references, see page 80

spin system (A = B = H, X = P, δ_A 4.44, δ_B 4.79, $^2J_{AB}$ = 15.5 Hz, $^3J_{AX}$ = 26.3 Hz, $^3J_{BX}$ = 12.5 Hz, 2H, $POCH_2$), 7.31-8.23 (complex m, 8H, aromatic). $^{31}P\{^1H\}$ NMR (121.49 MHz, $CDCl_3$): δ 134.7 (s). $^{19}F\{^1H\}$ NMR (282.38 MHz, $CDCl_3$): δ -78.6 (s). Anal. Calcd for $C_{23}H_{25}F_3NO_7PPdS$: C, 42.25; H, 3.85; N, 2.14. Found: C, 41.95; H, 3.71; N, 2.00.

14b: A solution of **11b** (0.13 g, 0.21 mmol) in CH_2Cl_2 (25 mL) was stirred under 1 atm CO at room temperature for 1 h, the CO was then replaced by 1 atm ethylene and the solution further stirred for 1 h. Workup was as described for **7a**, and afforded **14b** as a yellow solid (0.13 g, 93%). IR (KBr): 1635 (m, $\nu_{C=N}$ and $\nu_{C=O}$) cm^{-1}. ^1H NMR (300.13 MHz, $CDCl_3$): δ 1.38 [s, 3H, $OC(CH_3)(CH_3)$], 1.60 [s, 3H, $NC(CH_3)(CH_3)$], 1.68 [s, 3H, $NC(CH_3)(CH_3)$], broad ABMNX system [A = B = M = N = H, X = P, δ_A 1.71 overlapping with $NC(CH_3)(CH_3)$, δ_B 1.91 overlapping with $OC(CH_3)(CH_3)$, 2H, $PdCH_2$], 1.96 [s, 3H, $OC(CH_3)(CH_3)$], 2.57 [s, 3H, $C(O)CH_3$], broad ABMNX system (A = B = M = N = H, X = P, δ_A 3.15, δ_B 3.31, $^2J_{AB}$ = 21.3 Hz, 2H, $PdCH_2CH_2$), AB spin system (A = B = H, δ_A 4.26, δ_B 4.35, $^2J_{AB}$ = 8.7 Hz, 2H, OCH_2), 7.22-7.26 (m, 1H, aromatic), 7.32-7.38 (m, 1H, aromatic), 7.42-7.48 (m, 1H, aromatic), 7.65-7.80 (complex m, 2H, aromatic), 8.00-8.18 (complex m, 3H, aromatic). $^{31}P\{^1H\}$ NMR (121.5 MHz, $CDCl_3$, room temp.): δ 125.6 (s). $^{19}F\{^1H\}$ NMR (282.4 MHz, $CDCl_3$): δ -78.5 (s). Anal. Calcd for $C_{25}H_{29}F_3NO_7PPdS$: C, 44.03; H, 4.29; N, 2.05. Found: C, 43.78; H, 4.01; N, 1.94.

Crystal Structure Determinations

Crystals suitable for X-ray determination of **3a**, **5a**, **9b**, **10a**, **10b**, **12b**, **14a** and **14b** were obtained by slow diffusion of hexane into a CH_2Cl_2 solution of the respective complex at 5ºC. Diffraction data were collected on a Kappa CCD diffractometer using graphite-monochromated Mo Kα radiation (λ = 0.71073 Å) (Table 4). Data were collected using phi-scans and the structures were solved by direct methods using the SHELX 97 software,[75,76] and the refinement was by full-matrix least squares on F^2. No absorption correction was used. All non-hydrogen atoms were refined anisotropically with H atoms introduced as fixed contributors (d_{C-H} = 0.95 Å, U_{11} =0.04). Crystallographic data (excluding structure factors) have been deposited in the Cambridge Crystallographic Data Centre as Supplementary publication n° CCDC ******. Copies of the data can be obtained free of charge on application to CCDC, 12 Union Road, Cambridge CB2 1EZ, UK (fax: (+44)1223-336-033; e-mail: deposit@ccdc.cam.ac.uk).

for references, see page 80

Table 4 a) Crystal data and details of the structure determination for the complexes **3a**·CH_2Cl_2, **5a**, **9b** and **10a**.

	3a·CH_2Cl_2	**5a**	**9b**	**10a**
Formula	$C_{18}H_{20}Cl_2NO_2PPd{\cdot}CH_2Cl_2$	$C_{19}H_{23}NO_2PPd{\cdot}CF_3SO_3$	$C_{20}H_{22}Cl_2NO_3PPd$	$C_{19}H_{21}ClNO_3PPd$
M_r	575.55	583.82	532.66	484.19
Crystal system	Orthorhombic	Monoclinic	Monoclinic	Orthorhombic
Space group	*P*na2_1	*P*2_1/n	*P*2_1/n	*P*bca
a [Å]	29.65600 (10)	11.5800 (2)	8.7850 (10)	10.79900 (10)
b [Å]	8.96500 (10)	9.1090 (2)	28.238 (3)	16.2160 (2)
c [Å]	8.6870 (4)	22.6660 (4)	9.6720 (10)	21.6790 (3)
α [°]				
β [°]		90.6710 (9)	114.84 (5)	
γ [°]				
V [Å^3]	2309.58 (11)	2390.70 (8)	2177.4 (9)	3796.35 (8)
Z	4	4	4	8
D_x [Mg m^{-3}]	1.655	1.622	1.625	1.694
μ [mm^{-1}]	1.351	0.984	1.192	1.222
T [K]	173 (2)	173 (2)	173 (2)	173 (2)
λ [Å]	0.71073	0.71073	0.71070	0.71069
θ_{max} [°]	30.03	30.01	30.04	30.02
data set [*h*; *k*; *l*]	-41/41; -12/12; -12/12	-16/16; 0/12; 0/31	-12/12; -39/35; -13/13	0/15; 0/22; 0/30
tot., unique data, *R*(int)	6464, 6464	6971, 6970	10357, 6304, 0.0214	5540, 5539, 0.049
observed data [$I > 2\sigma(I)$]	5941	4006	5046	3422
No. reflns, No. params	6465, 253	6970, 289	6304, 253	5539, 235
R_1, wR_2, GOF	0.0323, 0.0887, 1.139	0.0362, 0.0943, 0.898	0.0345, 0.1096, 1.123	0.0300, 0.0978, 0.767

for references, see page 80

Table 4 b) Crystal data and details of the structure determination for the complexes **10**,**b**, **12b** and **14a**,**b**.

	10b	**12b**	**14a**	**14b**
Formula	$C_{21}H_{25}ClNO_3PPd$	$C_{21}H_{25}NO_3PPd{\cdot}H_2O{\cdot}CF_3SO_3$	$C_{22}H_{25}NO_4PPd{\cdot}CF_3SO_3$	$C_{24}H_{29}NO_4PPd{\cdot}CF_3SO_3$
M_r	512.24	643.88	653.87	681.92
Crystal system	Monoclinic	Monoclinic	Monoclinic	Monoclinic
Space group	$P2_1/n$	$C2/c$	$P2_1/c$	$P2_1/n$
a [Å]	12.4150 (3)	27.5110 (5)	18.6170 (5)	12.1860 (10)
b [Å]	10.8760 (2)	10.4110 (2)	12.4040 (6)	14.6170 (10)
c [Å]	15.5810 (4)	20.7470 (5)	11.6760 (13)	16.1040 (10)
α [º]				
β [º]	96.3340 (9)	117.1600 (8)	104.5330 (17)	105.62 (5)
γ [º]				
V [Å^3]	2090.99 (8)	5287.07 (19)	2610.0 (3)	2762.6 (7)
Z	4	8	4	4
D_x [Mg m^{-3}]	1.627	1.618	1.664	1.640
μ [mm^{-1}]	1.114	0.904	0.917	0.870
T [K]	173 (2)	173 (2)	173 (2)	173 (2)
λ [Å]	0.71073	0.71070	0.71073	0.71070
θ_{max} [º]	30.05	30.06	30.49	29.99
data set [h; k; l]	-17/17; 0/15; 0/21	-38/24; -14/12; -17/29	-26/26; -16/17; -16/16	-17/11; -18/20; -17/22
tot., unique data, R(int)	6117, 6116	18463, 7756, 0.0473	13289, 7710, 0.0510	29429, 8030, 0.0734
observed data [$I > 2\sigma(I)$]	4353	5419	3858	4540
No. reflns, No. params	6116, 253	7756, 332	7710, 334	8030, 352
R_1, wR_2, GOF	0.0347, 0.1235, 0.956	0.0434, 0.1441, 0.878	0.0668, 0.1823, 0.964	0.0445, 0.1164, 0.985

for references, see page 80

Acknowledgements

We thank the CNRS, the Ministère de la Recherche (Paris), the Institut Français du Pétrole (IFP) and the Europeen Commission (Palladium Network HPRN-CT-2002-00196 and COST program) for support. We also thank Prof. R. Welter and Dr A. DeCian (ULP Strasbourg) for the crystal structure determinations and Mrs. A. Degrémont (LCC) for technical assistance.

References

1. A. Sen, *Acc. Chem. Res.*, 1993, **26**, 303-310.
2. K. J. Cavell, *Coord. Chem. Rev.*, 1996, **155**, 209-243.
3. E. Drent and P. H. M. Budzelaar, *Chem. Rev.*, 1996, **96**, 663-681.
4. A. Sommazzi and F. Garbassi, *Progr. Polym. Sci.*, 1997, **22**, 1547-1605.
5. K. Nozaki and T. Hiyama, *J. Organomet. Chem.*, 1999, **576**, 248-253.
6. G. J. P. Britovsek, V. C. Gibson and D. F. Wass, *Angew. Chem., Int. Ed.*, 1999, **38**, 428-447.
7. S. D. Ittel, L. K. Johnson and M. Brookhart, *Chem. Rev.*, 2000, **100**, 1169-1203.
8. G. P. Belov, *Russ. Chem. Bull., Int. Ed.*, 2002, **51**, 1605-1615.
9. C. Bianchini and A. Meli, *Coord. Chem. Rev.*, 2002, **225**, 35-66.
10. E. Drent, J. A. M. van Broekhoven and P. H. M. Budzelaar, in *Applied Homogeneous Catalysis with Organometallic Compounds (2nd Edition)*, eds. B. Cornils and W. A. Herrmann, Wiley-VCH, Weinheim, Editon edn., 2002, vol. 1, pp. 344-361.
11. R. A. M. Robertson and D. J. Cole-Hamilton, *Coord. Chem. Rev.*, 2002, **225**, 67-90.
12. C. Bianchini, A. Meli and W. Oberhauser, *Dalton Trans.*, 2003, 2627-2635.
13. G. Consiglio, in *Late Transition Metal Polymerization Catalysis*, eds. B. Rieger, L. S. Baugh, S. Kacker and S. Striegler, Wiley-InterScience, Editon edn., 2003, pp. 279-305.
14. G. P. Belov and E. V. Novikova, *Russ. Chem. Rev.*, 2004, **73**, 267-291.
15. J. Durand and B. Milani, *Coord. Chem. Rev.*, 2006, **250**, 542-560.
16. A. Sen, *Adv. Polym. Sci.*, 1986, **73-74**, 125-144.
17. Z. Jiang, S. Sanganeria and A. Sen, *J. Polym. Sci., Part A: Polym. Chem.*, 1994, **32**, 841-847.
18. M. J. Green, A. R. Lucy, S.-Y. Lu and R. M. Paton, *J. Chem. Soc., Chem. Commun.*, 1994, 2063-2064.
19. M. D. E. Forbes, S. R. Ruberu, D. Nachtigallova, K. D. Jordan and J. C. Barborak, *J. Am. Chem. Soc.*, 1995, **117**, 3946-3951.
20. A. Gray, *Chem. Br.*, 1998, **34**, 44-45.
21. N. Kosaka, T. Oda, T. Hiyama and K. Nozaki, *Macromolecules*, 2004, **37**, 3159-3164.
22. J. Schwarz, E. Herdtweck, W. A. Herrmann and M. G. Gardiner, *Organometallics*, 2000, **19**, 3154-3160.
23. G. Verspui, F. Schanssema and R. A. Sheldon, *Angew. Chem., Int. Ed.*, 2000, **39**, 804-806.
24. C. Bianchini, H. M. Lee, A. Meli, W. Oberhauser, F. Vizza, P. Bruggeller, R. Haid and C. Langes, *Chem. Comm.*, 2000, 777-778.
25. S. Doherty, G. R. Eastham, R. P. Tooze, T. H. Scanlan, D. Williams, M. R. J. Elsegood and W. Clegg, *Organometallics*, 1999, **18**, 3558-3560.
26. E. Drent, J. A. M. Van Broekhoven and M. J. Doyle, *J. Organomet. Chem.*, 1991, **417**, 235-251.

27. C. Bianchini, H. M. Lee, A. Meli, W. Oberhauser, M. Peruzzini and F. Vizza, *Organometallics*, 2002, **21**, 16-33.
28. C. Bianchini, P. Brueggeller, C. Claver, G. Czermak, A. Dumfort, A. Meli, W. Oberhauser and E. J. Garcia Suarez, *Dalton Trans.*, 2006, 2964-2973.
29. M. Caporali, C. Mueller, B. B. P. Staal, D. M. Tooke, A. L. Spek and P. W. N. M. van Leeuwen, *Chem. Commun.*, 2005, 3478-3480.
30. A. S. Abu-Surrah, R. Wursche, B. Rieger, G. Eckert and W. Pechhold, *Macromolecules*, 1996, **29**, 4806-4807.
31. Z. Jiang, S. E. Adams and A. Sen, *Macromolecules*, 1994, **27**, 2694-2700.
32. B. Milani, E. Alessio, G. Mestroni, E. Zangrando, L. Randaccio and G. Consiglio, *J. Chem. Soc., Dalton Trans.*, 1996, 1021-1029.
33. A. Scarel, B. Milani, E. Zangrando, M. Stener, S. Furlan, G. Fronzoni, G. Mestroni, S. Gladiali, C. Carfagna and L. Mosca, *Organometallics*, 2004, **23**, 5593-5605.
34. B. Milani, A. Scarel, G. Mestroni, S. Gladiali, R. Taras, C. Carfagna and L. Mosca, *Organometallics*, 2002, **21**, 1323-1325.
35. A. Sen and Z. Jiang, *Macromolecules*, 1993, **26**, 911-915.
36. M. Brookhart, F. C. Rix, J. M. DeSimone and J. C. Barborak, *J. Am. Chem. Soc.*, 1992, **114**, 5894-5895.
37. P. Braunstein, M. D. Fryzuk, M. L. Dall, F. Naud, S. J. Rettig and F. Speiser, *J. Chem. Soc., Dalton Trans.*, 2000, 1067-1074.
38. E. K. van den Beuken, W. J. J. Smeets, A. L. Spek and B. I. Feringa, *Chem. Commun.*, 1998, 223-224.
39. A. Aeby, A. Gsponer and G. Consiglio, *J. Am. Chem. Soc.*, 1998, **120**, 11000-11001.
40. A. Aeby, F. Bangerter and G. Consiglio, *Helv. Chim. Acta*, 1998, **81**, 764-769.
41. A. Aeby and G. Consiglio, *Helv. Chim. Acta*, 1998, **81**, 35-39.
42. M. Sperrle, A. Aeby, G. Consiglio and A. Pfaltz, *Helv. Chim. Acta*, 1996, **79**, 1387-1392.
43. P. H. P. Brinkmann and G. A. Luinstra, *J. Organomet. Chem.*, 1999, **572**, 193-205.
44. A. Aeby and G. Consiglio, *J. Chem. Soc., Dalton Trans.*, 1999, 655-656.
45. G. A. Luinstra and P. H. P. Brinkmann, *Organometallics*, 1998, **17**, 5160-5165.
46. G. P. C. M. Dekker, A. Buijs, C. J. Elsevier, K. Vrieze, P. W. N. M. van Leeuwen, W. J. J. Smeets, A. L. Spek, Y. F. Wang and C. H. Stam, *Organometallics*, 1992, **11**, 1937-1948.
47. A. D. Burrows, M. F. Mahon and M. Varrone, *Dalton Trans.*, 2003, 4718-4730.
48. K. R. Reddy, K. Surekha, G.-H. Lee, S.-M. Peng, J.-T. Chen and S.-T. Liu, *Organometallics*, 2001, **20**, 1292-1299.
49. M. Sauthier, F. Leca, L. Toupet and R. Réau, *Organometallics*, 2002, **21**, 1591-1602.
50. M. Agostinho and P. Braunstein, *to be published*, 2006.
51. W. Keim, S. Killat, C. F. Nobile, G. P. Suranna, U. Englert, R. Wang, S. Mecking and D. L. Schröder, *J. Organomet. Chem.*, 2002, **662**, 150-171.
52. P. Braunstein and F. Naud, *Angew. Chem. Int. Ed.*, 2001, **40**, 680-699.
53. J. T. Chen and A. Sen, *J. Am. Chem. Soc.*, 1984, **106**, 1506-1507.
54. A. Sen, J. T. Chen, W. M. Vetter and R. R. Whittle, *J. Am. Chem. Soc.*, 1987, **109**, 148-156.
55. M. A. Zuideveld, P. C. J. Kamer, P. W. N. M. van Leeuwen, P. A. A. Klusener, H. A. Stil and C. F. Roobeek, *J. Am. Chem. Soc.*, 1998, **120**, 7977-7978.
56. M. J. Green, G. J. P. Britovsek, K. J. Cavell, B. W. Skelton and A. H. White, *Chem. Commun.*, 1996, 1563-1564.
57. P. Braunstein, C. Frison and X. Morise, *Angew. Chem., Int. Ed.*, 2000, **39**, 2867-2870.
58. P. Braunstein, J. Durand, M. Knorr and C. Strohmann, *Chem. Commun.*, 2001, 211-212.
59. S. Stoccoro, G. Minghetti, M. A. Cinellu, A. Zucca and M. Manassero, *Organometallics*, 2001, **20**, 4111-4113.

60. C. Bianchini, A. Meli, W. Oberhauser, P. W. N. M. van Leeuwen, M. A. Zuideveld, Z. Freixa, P. C. J. Kamer, A. L. Spek, O. V. Gusev and A. M. Kal'sin, *Organometallics*, 2003, **22**, 2409-2421.
61. *Fr Pat.*, 2837725, 2003.
62. P. Braunstein, J. Zhang and R. Welter, *Dalton Trans.*, 2003, 507-509.
63. F. Speiser, P. Braunstein, L. Saussine and R. Welter, *Inorg. Chem.*, 2004, **43**, 1649-1658.
64. F. Speiser, P. Braunstein and L. Saussine, *Acc. Chem. Res.*, 2005, **38**, 784-793.
65. F. R. Hartley, *Chem. Soc. Rev.*, 1973, **2**, 163-179.
66. M. Agostinho, A. Banu, P. Braunstein, R. Welter and X. Morise, *Acta Crystallogr., Sect. C: Cryst. Struct. Commun.*, 2006, **C62**, m81-m86.
67. J. X. McDermott, J. F. White and G. M. Whitesides, *J. Am. Chem. Soc.*, 1973, **95**, 4451-4452.
68. J. X. McDermott, J. F. White and G. M. Whitesides, *J. Am. Chem. Soc.*, 1976, **98**, 6521-6528.
69. J. Zhang, P. Braunstein and R. Welter, *Inorg. Chem.*, 2004, **43**, 4172-4177.
70. H.-P. Chen, Y.-H. Liu, S.-M. Peng and S.-T. Liu, *Organometallics*, 2003, **22**, 4893-4899.
71. R. E. Rulke, J. M. Ernsting, A. L. Spek, C. J. Elsevier, P. W. N. M. van Leeuwen and K. Vrieze, *Inorg. Chem.*, 1993, **32**, 5769-5778.
72. F. T. Ladipo and G. K. Anderson, *Organometallics*, 1994, **13**, 303-306.
73. L. N. Pridgen and G. Miller, *J. Het. Chem.*, 1983, **20**, 1223-1230.
74. S. D. Stephen, J. D. Spivack and L. P. Steinhuebel, *Phosphorus, Sulfur and Silicon*, 1987, **31**, 71-76.
75. *Kappa CCD Operation Manual; Nonius BV*, (1997), Kappa CCD Operation Manual; Nonius BV, Delft, The Nederlands.
76. G. M. Sheldrick, *SHELXL97*, (1997), SHELXL97, Program for the refinement of crystal structures, University of Göttingen, Germany.

Chapitre III

Complexes de Palladium, études d'insertion de CO/éthylène et CO/acrylate de méthyle

Résumé de la Partie A

Les premières étapes d'insertion de CO/éthylène ou CO/acrylate de méthyle dans la liaison Pd-Me des complexes méthylpalladium(II) avec les ligands (2-oxazoline-2-ylméthyl)diphénylphosphine (**1a**) et (2-oxazoline-2-ylméthyl-4,4-diméthyl)diphénylphosphine (**1b**), menant aux complexes métallacycles de type $[Pd\{CHRCH_2C(O)Me\}(P,N)]CF_3SO_3$ (**6a** P,N = **1a**, R = H; **6b** P,N = **1b**, R = H; **7a** P,N = **1a**, R = CO_2Me; **7b** P,N = **1b**, R = CO_2Me) ont été complètement caractérisés, y compris par diffraction des rayons X pour **6b** et **7a**,**b**.

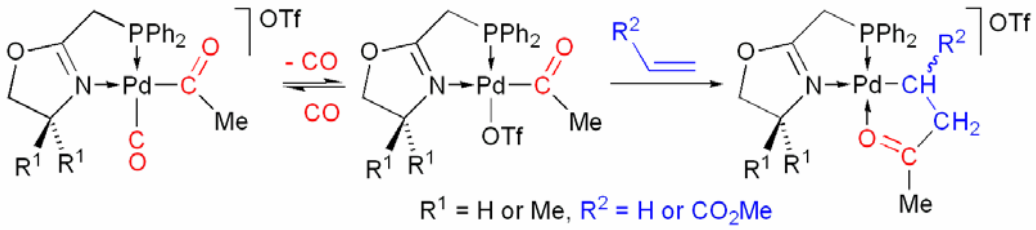

Cette partie du chapitre fait l'objet d'une publication dont la référence est donné ci dessous.

Structurally Characterized Intermediates in the Stepwise Insertion of CO/Ethylene or CO/Methyl Acrylate into the Metal-Carbon Bond of Pd(II) Complexes Stabilized by (Phosphinomethyl)Oxazoline Ligands

Magno Agostinho and Pierre Braunstein.*

Chem. Commun., **2007**, DOI: 10.1039/b613865a.

Laboratoire de Chimie de Coordination, UMR 7177 CNRS, Institut de Chimie, Université Louis Pasteur, 4 rue Blaise Pascal, F-67070 Strasbourg Cédex, France

références, voir page 91; † supporting information, voir page 93

Abstract of Part A

The first CO/ethylene or CO/methyl acrylate insertion steps into the Pd-Me bond of methylpalladium(II) complexes with the ligands (2-oxazoline-2-ylmethyl)diphenylphosphine (**1a**) and (2-oxazoline-2-ylmethyl-4,4-dimethyl)diphenylphosphine (**1b**), leading to the metallacyclic complexes $[Pd\{CHRCH_2C(O)Me\}(P,N)]CF_3SO_3$ (**6a** P,N = **1a**, R = H; **6b** P,N = **1b**, R = H; **7a** P,N = **1a**, R = COOMe; **7b** P,N = **1b**, R = COOMe), have been fully characterized, including by X-ray diffraction for **6b** and **7a**,**b**.

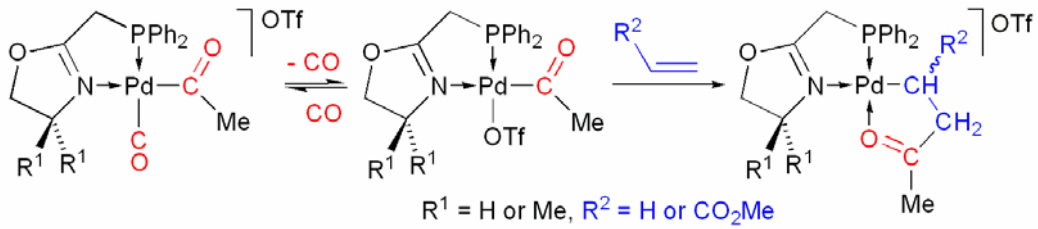

This part of the chapter has been published; its reference is given below.

Structurally Characterized Intermediates in the Stepwise Insertion of CO/Ethylene or CO/Methyl Acrylate into the Metal-Carbon Bond of Pd(II) Complexes Stabilized by (Phosphinomethyl)Oxazoline Ligands

Magno Agostinho and Pierre Braunstein.*

Chem. Commun., **2007**, DOI: 10.1039/b613865a.

Laboratoire de Chimie de Coordination, UMR 7177 CNRS, Institut de Chimie, Université Louis Pasteur, 4 rue Blaise Pascal, F-67070 Strasbourg Cédex, France

references, see page 91; † supporting information, see page 93

Structurally Characterized Intermediates in the Stepwise Insertion of CO/Ethylene or CO/Methyl Acrylate into the Metal-Carbon Bond of Pd(II) Complexes Stabilized by (Phosphinomethyl)Oxazoline Ligands

Introduction

The palladium-catalyzed alternating copolymerisation of olefins and carbon monoxide, which leads to the formation of polyketones, has become a major field of research in both academic and industrial laboratories.[1]

Although the basic reaction mechanism of CO–olefin copolymerisation, which involves mutually *cis* sites of square-planar Pd(II) species, has been established,[1,2] detailed investigations on the early stages of the chain-growth process have mostly been carried out with strained alkenes owing to the difficulties often encountered in the isolation of intermediates. The first structural reports of an ethylene–CO coupling product by Green *et al.*, using monodentate PPh_3 and a N,O ligand,[3a] then by us using a P,O ligand[3b] or a diphosphine-bridged heterodimetallic Fe–Pd complex[3c] were followed by only a few examples with P,N,[3d,e] N,N[3f] and P,P[3g] chelating ligands. Furthermore, despite the considerable interest in the copolymerisation of olefins with polar monomers, such as methyl acrylate,[2e,4] only a few CO–methyl acrylate coupling products have been isolated and characterized.[2c,3b,c,5] Using a bidentate phosphine-imine (P,N) ligand, Reddy *et al.* have reported what appears to be the only structure of a CO–methyl acrylate coupling product.[3e] These authors used a large excess of olefin (33 to 67 equiv.) in CH_2Cl_2, with a reaction time between 1–3 h.

Results and Discussion

Following the synthesis of the ligands **1a,b** and of the Pd(II) methyl complexes **2a,b** (Scheme 1), we investigated the catalytic activity of Ni(II) complexes with **1b** in ethylene oligomerisation,[6] and that of the Pd(II) complexes **3a,b** (Scheme 2) in ethylene–CO copolymerisation.[7] Starting from **3a,b**, we have now isolated the initial intermediates in CO–ethylene or CO–methyl acrylate copolymerisation reactions, without the need to use excess methyl acrylate. The structures of the new insertion products **4b**, **6b** and **7a,b** have been determined by X-ray diffraction as well as those of the known **2a,b** and **3a,b** for comparative purposes.†

references, see page 91; † supporting information, see page 93

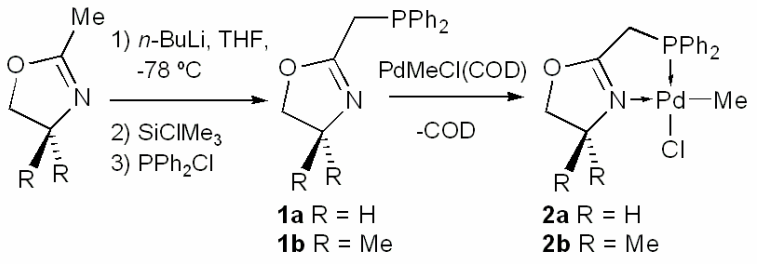

Scheme 1.

Reactions of **2a,b** and **3a,b** with CO in CH_2Cl_2 at room temperature were monitored by $^{31}P\{^1H\}$ and ^1H NMR. CO insertion into their Pd–Me bond produced within a few minutes the acyl complexes **4a,b** and **5a,b**, respectively (Scheme 2), as evidenced by the large high-field shift of the $^{31}P\{^1H\}$ NMR resonance ($\Delta\delta = -14.7$ **4a**, $\Delta\delta = -14.8$ **4b**, $\Delta\delta = -15.4$ **5a**, $\Delta\delta = -15.1$ **5b**, Table 1).

Table 1
Selected IR and NMR data of the ligands and complexes.

	IR		NMR[d]	
	ν_{CN}	ν_{CO}	^1H	^{31}P
1a	1660[a] (s)			-15.8
1b	1660[a] (s)			-15.8
2a	1647[a] (s)		0.55 Pd-CH_3 (d, $^3J_{PH}$ = 2.7)	33.1
2b	1628[a] (s)		0.65 Pd-CH_3 (d, $^3J_{PH}$ = 3.3)	32.8
3a	1633[b] (s)		0.60 Pd-CH_3 (s)	37.4
3b	1632[b] (s)		0.70 Pd-CH_3 (s)	37.4
4a	1642[b] (s)	1684[b] (s)	2.20 PdC(O)CH_3 (d, $^4J_{PH}$ = 1.1)	18.4
4b	1632[b] (s)	1685[b] (s)	2.17 PdC(O)CH_3 (d, $^4J_{PH}$ = 1.6)	18.0
5a	1644[a] (s)	1704[a] (s)		22.0
5b	1655[a] (s)	1707[a] (s)		22.3
	$\nu_{CN/CO}$	$\nu_{C(O)OMe}$		
6a	1634[b] (s)		2.45 C(O)CH_3 (s)	34.4
6b	1629[b] (s)		2.49 C(O)CH_3 (s)	34.7
7a	1633[b] (s)	1683[b] (s)	2.52 C(O)CH_3 (s)	32.8
7b	1629[b] (s)	1684[b] (s)	2.55 C(O)CH_3 (s)	34.3

[a]In CH_2Cl_2, [b]in KBr, cm^{-1}. [d]In $CDCl_3$, ppm, *J* in Hz.

In order to detect the usually elusive palladium acyl, carbonyl complexes of the type [Pd{C(O)Me}(CO)(P,N)]OTf, a CD_2Cl_2 solution of **3b** was exposed to an atmosphere of ^{13}CO, and $^{31}P\{^1H\}$, $^{13}C\{^1H\}$ and ^1H NMR spectra were recorded at different temperatures. At room temperature, the $^{31}P\{^1H\}$ NMR resonance for **5b** is a doublet centred at δ 21.6 ($^2J_{PC}$ = 9.7 Hz). Its acyl carbon appears in the $^{13}C\{^1H\}$ spectrum as an intense doublet at δ 222.7 ($^2J_{PC}$ = 9.7 Hz), and the weak signal observed at δ 179.8 corresponds to the coordinated CO of the acyl, carbonyl derivative. Upon decreasing the temperature to –60 °C, the $^{31}P\{^1H\}$ resonance significantly broadened and shifted to δ 19.1 while the $^{13}C\{^1H\}$ resonances for the acyl carbon and the coordinated CO also became broader and shifted to δ 222.6 and 175.5, respectively. This is indicative of an equilibrium between CO and OTf coordination which, at –100 °C, is completely shifted towards the acyl, carbonyl species and the $^{31}P\{^1H\}$ resonance

references, see page 91; † supporting information, see page 93

becomes a doublet of doublets centred at δ 18.3 ($^2J_{PC(cis)}$ = 4.1, $^2J_{PC(trans)}$ = 83.8 Hz) while the acyl carbon and coordinated CO $^{13}C\{^1H\}$ resonances appear as doublets at δ 223.1 and 175.3, respectively (see ESI for details).† These results are in agreement with those for related complexes stabilized by P,P ligands,[8] but at variance with those with a P,N ligand in which no significant amount of palladium acyl, carbonyl species was detected at –70 °C.[3d]

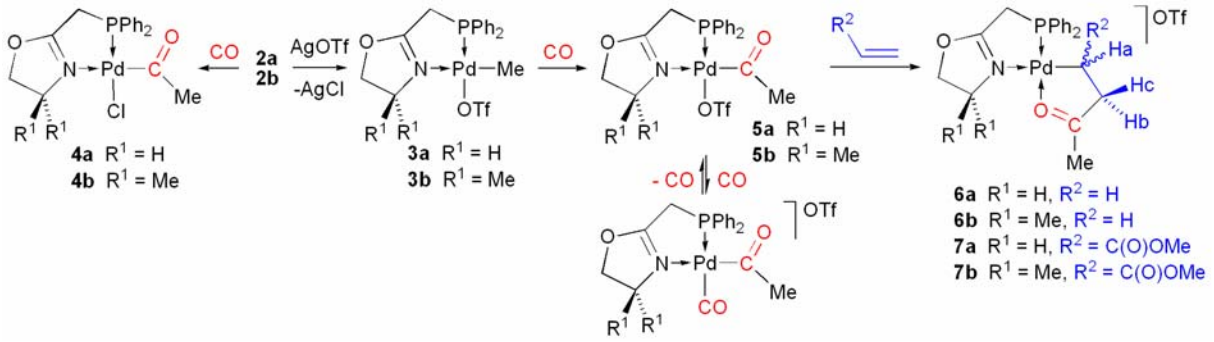

Scheme 2.
All reactions were performed at room temperature in CH_2Cl_2.

Complexes **2a,b**, **3a,b** and **4b** have slightly distorted square planar coordination geometries with the methyl (**2a,b** and **3a,b**) and acyl (**4b**) ligands *cis* to the phosphorus atom (ESI),† in agreement with the donor groups with the largest *trans* influence avoiding a mutually *trans* position, as observed in other complexes of the type [Pd(Me)Cl(P,N)].[3e,9] The Pd–N bond distance in **2a** (Table 2) is longer than that reported for the analogous $PdCl_2$ complex [2.058(2) Å],[7] which reflects the larger *trans* influence of the methyl group compared with chloride. The Pd–C distance of 1.9701(13) Å in **4b**, although slightly shorter than in the analogous Pd–Me complex (**2b**), is normal for an acetyl–palladium bond. The acyl group adopts an orientation approximately perpendicular to the metal coordination plane, as observed in other complexes of the type [Pd{C(O)Me}Cl(P,N)].[3e,10]

Ethylene or methyl acrylate insertion into the Pd–acyl bond of **5a** and **5b** was completed in less than 1 h at room temperature under atmospheric pressure (^{31}P NMR monitoring) and afforded **6a,b** or **7a,b**, respectively (Scheme 2). In all four complexes, coordination of the ketonic oxygen atom to Pd (see ν_{CO}, Table 1) results in a stabilizing chelate which makes β-hydrogen elimination less likely.[11] These complexes are stable at room temperature for several hours in solution and weeks in the solid state, which illustrates the beneficial role of the P–N chelates. The $^{31}P\{^1H\}$ NMR signals of **6a,b** and **7a,b** are shifted to low field relative to those of **5a,b** (Table 1). In the ^1H NMR spectrum of **6a,b** the Pd–CH_2 protons give rise to a triplet of doublets (δ 1.65, **6a** and δ 1.67, **6b**) whereas the $CH_2C{=}O$ protons appear as a broad triplet (δ 3.08, **6a** and δ 3.12, **6b**), indicating a smaller $^{4+5}J_{HP}$ coupling.† The CH and CH_2 protons Ha, Hb and Hc of **7a,b** were unambiguously identified

references, see page 91; † supporting information, see page 93

and resonate at δ 2.46, 2.90 and 3.26 (**7a**) and δ 2.46, 2.87 and 3.27 (**7b**) respectively (vicinal and geminal J_{HH} and J_{HP} coupling constants are given in the ESI).†

The crystal structures of **6b** and **7a,b** (see Fig. 1) were determined by X-ray diffraction and the latter two established the regioselective 2,1 insertion of methyl acrylate, which leads to an α-methoxycarbonyl complex. Deviations from idealized square planar geometries are small (Table 2). The similar Pd–C distances in **6b**, **7a** and **7b** are in agreement with that in the only other reported structure of a CO–methyl acrylate complex.[3e] The Pd–O bond distances in **6b**, **7a** and **7b** are similar and compare with those in related complexes stabilized by P,N ligands.[3d,e,12] At least in the solid state, there is no interaction between the CO_2Me group of **7a,b** and the metal centre, which would have reduced its electrophilicity and increased its steric shielding. It is also interesting to note that related Pd(II) complexes with the P,O chelating ligand $Ph_2PNHC(O)Me$ were generally found to be less reactive than **3a,b** or **5a,b**, longer reaction times being required.[3b]

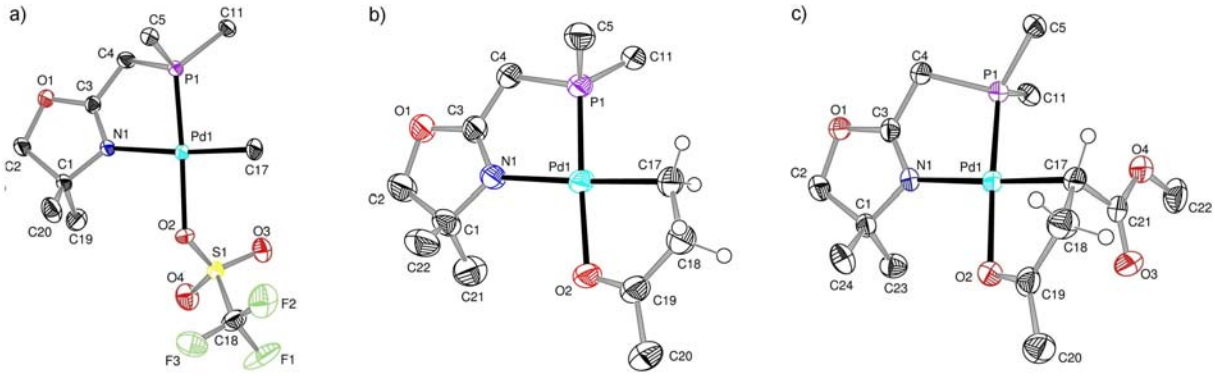

Figure 1.
Molecular structure of: a) complex **3b**, b) the cation in **6b**, c) the cation in **7b** (CH groups of phenyl rings and H atoms omitted, except inserted olefin). Displacement ellipsoids are drawn at the 50% probability level.

In addition to the structural characterization of CO–ethylene and CO–methyl acrylate insertion products, we have spectroscopically observed a temperature-dependent equilibrium between a triflate, acyl complex, **5b**, and a cationic carbonyl, acyl Pd(II) complex. Previous studies have shown that **3a,b** catalyse the CO–ethylene copolymerisation at 60–90 °C.[6] Further investigations are in progress to determine the influence of the ligand bite angle on the reactivity of the chelate ring in **7a,b** towards further insertion of small molecules.

We thank Luc Brissieux for preliminary results and the CNRS, the Ministère de la Recherche (Paris) and the Europeen Commission (Palladium Network HPRN-CT-2002-00196 and COST program) for support. We are grateful to Prof. R. Welter and Dr A. DeCian (ULP Strasbourg) for the crystal structure determinations and to Mrs A. Degrémont (LCC) for assistance.

references, see page 91; † supporting information, see page 93

Table 2 Selected bond lengths [Å] and angles [°] in complexes **2a**,**b**, **3a**,**b**, **4b**, **6b** and **7a**,**b**.

	2a	**2b**	**3a**	**3b**	**4b**	**6b**	**7a**	**7b**
Pd1-N1	2.103 (12)	2.171 (3)	2.131 (4)	2.1550 (18)	2.1896 (11)	2.104 (4)	2.082 (3)	2.114 (3)
Pd1-P1	2.212 (4)	2.1879 (10)	2.1699 (12)	2.1771 (12)	2.2549 (13)	2.1878 (14)	2.2051 (10)	2.2091 (14)
Pd1-C17	2.057 (13)	2.049 (4)	2.026 (5)	2.031 (2)	1.9701 (13)	2.030 (5)	2.046 (4)	2.052 (4)
Pd1-O2			2.156 (3)	2.1631 (17)		2.125 (4)	2.112 (2)	2.138 (3)
Pd1-Cl1	2.383 (4)	2.378 (1)			2.3734 (13)			
N1-C3	1.291 (18)	1.279 (5)	1.281 (6)	1.275 (2)	1.2757 (15)	1.270 (6)	1.285 (5)	1.273 (6)
C3-C4	1.468 (19)	1.485 (5)	1.476 (6)	1.493 (3)	1.4897 (15)	1.480 (7)	1.496 (5)	1.498 (6)
C4-P1	1.847 (13)	1.835 (4)	1.839 (5)	1.837 (2)	1.8468 (12)	1.841 (5)	1.837 (4)	1.835 (4)
C17-C18					1.506 (2)	1.527 (8)	1.545 (6)	1.528 (7)
C18-C19						1.485 (8)	1.472 (6)	1.486 (7)
C19-O2						1.248 (6)	1.220(5)	1.239 (6)
N1-Pd1-P1	82.2 (3)	82.29 (9)	84.85 (11)	83.03 (6)	80.66 (3)	83.91 (12)	82.13 (9)	81.99 (10)
N1-Pd1-C17	176.4 (5)	171.94 (14)	174.97 (17)	174.30 (8)	173.83 (4)	177.1 (2)	174.17 (15)	175.94 (15)
N1-Pd1-O2			95.14 (14)	94.79 (7)		100.03 (14)	96.10 (12)	100.26 (13)
N1-Pd1-Cl1	93.2 (3)	97.94 (9)			97.09 (3)			
P1-Pd1-O2			172.64 (9)	177.32 (4)		174.72 (10)	175.29 (8)	177.54 (9)
P1-Pd1-C17	94.5 (4)	89.70 (13)	90.68 (15)	91.69 (8)	96.35 (4)	93.30 (16)	99.24 (11)	97.25 (14)
P1-Pd1-Cl1	174.66 (15)	179.21 (4)			173.211 (11)			
C17-Pd1-O2			89.00 (18)	90.42 (8)		82.80 (18)	82.10 (14)	80.57 (16)
C17-Pd1-Cl1	90.1 (5)	90.09 (13)			86.48 (4)			

references, see page 91; † supporting information, see page 93

References

1. For recent reviews see: (*a*) A. Sen, *Acc. Chem. Res.*, 1993, **26**, 303; (*b*) K. J. Cavell, *Coord. Chem. Rev.*, 1996, **155**, 209; (*c*) E. Drent and P. H. M. Budzelaar, *Chem. Rev.*, 1996, **96**, 663; (*d*) A. Sommazzi and F. Garbassi, *Progr. Polym. Sci.*, 1997, **22**, 1547; (*e*) K. Nozaki and T. Hiyama, *J. Organomet. Chem.*, 1999, **576**, 248; (*f*) G. J. P. Britovsek, V. C. Gibson and D. F. Wass, *Angew. Chem., Int. Ed.*, 1999, **38**, 428; (*g*) S. D. Ittel, L. K. Johnson and M. Brookhart, *Chem. Rev.*, 2000, **100**, 1169; (*h*) G. P. Belov, *Russ. Chem. Bull., Int. Ed.*, 2002, **51**, 1605; (*i*) C. Bianchini and A. Meli, *Coord. Chem. Rev.*, 2002, **225**, 35; (*j*) E. Drent, J. A. M. van Broekhoven and P. H. M. Budzelaar, in *Applied Homogeneous Catalysis with Organometallic Compounds*, ed. B. Cornils and W. A. Herrmann, Wiley-VCH, Weinheim, 2nd edn, 2002, p. 1; (*k*) R. A. M. Robertson and D. J. Cole-Hamilton, *Coord. Chem. Rev.*, 2002, **225**, 67; (*l*) C. Bianchini, A. Meli and W. Oberhauser, *Dalton Trans.*, 2003, 2627; (*m*) G. Consiglio, in *Late Transition Metal Polymerization Catalysis*, ed. B. Rieger, L. Saunders Baugh, S. Kacker and S. Striegler, Wiley-VCH, Weinheim, 2003, p. 279; (*n*) J. Durand and B. Milani, *Coord. Chem. Rev.*, 2006, **250**, 542.
2. (*a*) J. S. Brumbaugh, R. R. Whittle, M. Parvez and A. Sen, *Organometallics*, 1990, **9**, 1735; (*b*) P. Margl and T. Ziegler, *Organometallics*, 1996, **15**, 5519; (*c*) F. C. Rix, M. Brookhart and P. S. White, *J. Am. Chem. Soc.*, 1996, **118**, 4746; (*d*) M. Svensson, T. Matsubara and K. Morokuma, *Organometallics*, 1996, **15**, 5568; (*e*) S. Mecking, L. K. Johnson, L. Wang and M. Brookhart, *J. Am. Chem. Soc.*, 1998, **120**, 888; (*f*) M. A. Zuideveld, P. C. J. Kamer, P. W. N. M. van Leeuwen, P. A. A. Klusener, H. A. Stil and C. F. Roobeek, *J. Am. Chem. Soc.*, 1998, **120**, 7977.
3. (*a*) M. J. Green, G. J. P. Britovsek, K. J. Cavell, B. W. Skelton and A. H. White, *Chem. Commun.*, 1996, 1563; (*b*) P. Braunstein, C. Frison and X. Morise, *Angew. Chem., Int. Ed.*, 2000, **39**, 2867; (*c*) P. Braunstein, J. Durand, M. Knorr and C. Strohmann, *Chem. Commun.*, 2001, 211; (*d*) A. D. Burrows, M. F. Mahon and M. Varrone, *Dalton Trans.*, 2003, 4718; (*e*) K. R. Reddy, K. Surekha, G.-H. Lee, S.-M. Peng, J.-T. Chen and S.-T. Liu, *Organometallics*, 2001, **20**, 1292; (*f*) S. Stoccoro, G. Minghetti, M. A. Cinellu, A. Zucca and M. Manassero, *Organometallics*, 2001, **20**, 4111; (*g*) C. Bianchini, A. Meli, W. Oberhauser, P. W. N. M. van Leeuwen, M. A. Zuideveld, Z. Freixa, P. C. J. Kamer, A. L. Spek, O. V. Gusev and A. M. Kal'sin, *Organometallics*, 2003, **22**, 2409.

† *supporting information, see page 93*

4. (*a*) L. K. Johnson, S. Mecking and M. Brookhart, *J. Am. Chem. Soc.*, 1996, **118**, 267; (*b*) E. Drent, R. van Dijk, R. van Ginkel, B. van Oort and R. I. Pugh, *Chem. Commun.*, 2002, 744; (*c*) T. Kochi, K. Yoshimura and K. Nozaki, *Dalton Trans.*, 2005, 25.
5. (*a*) F. Ozawa, T. Hayashi, H. Koide and A. Yamamoto, *J. Chem. Soc., Chem. Commun.*, 1991, 1469; (*b*) G. P. C. M. Dekker, C. J. Elsevier, K. Vrieze, P. W. N. M. van Leeuwen and C. F. Roobeek, *J. Organomet. Chem.*, 1992, **430**, 357; (*c*) F. C. Rix and M. Brookhart, *J. Am. Chem. Soc.*, 1995, **117**, 1137.
6. P. Braunstein, M. D. Fryzuk, M. Le Dall, F. Naud, S. J. Rettig and F. Speiser, *J. Chem. Soc., Dalton Trans.*, 2000, 1067.
7. F. Speiser, P. Braunstein, L. Saussine and R. Welter, *Organometallics*, 2004, **23**, 2613.
8. (*a*) J. Ledford, C. S. Shultz, D. P. Gates, P. S. White, J. M. DeSimone and M. Brookhart, *Organometallics*, 2001, **20**, 5266; (*b*) J. Liu, B. T. Heaton, J. A. Iggo, R. Whyman, J. F. Bickley and A. Steiner, *Chem. Eur. J.*, 2006, **12**, 4417.
9. (*a*) M. Agostinho, A. Banu, P. Braunstein, R. Welter and X. Morise, *Acta Cryst.*, 2006, **C62**, m81; (*b*) A. Apfelbacher, P. Braunstein, L. Brissieux and R. Welter, *Dalton Trans.*, 2003, 1669.
10. (*a*) R. E. Ruelke, V. E. Kaasjager, P. Wehman, C. J. Elsevier, P. W. N. M. van Leeuwen, K. Vrieze, J. Fraanje, K. Goubitz and A. L. Spek, *Organometallics*, 1996, **15**, 3022; (*b*) K. R. Reddy, W.-W. Tsai, K. Surekha, G.-H. Lee, S.-M. Peng, J.-T. Chen and S.-T. Liu, *J. Chem. Soc., Dalton Trans.*, 2002, 1776.
11. (*a*) J. X. McDermott, J. F. White and G. M. Whitesides, *J. Am. Chem. Soc.*, 1973, **95**, 4451; (*b*) J. X. McDermott, J. F. White and G. M. Whitesides, *J. Am. Chem. Soc.*, 1976, **98**, 6521.
12. K. R. Reddy, C.-L. Chen, Y.-H. Liu, S.-M. Peng, J.-T. Chen and S.-T. Liu, *Organometallics*, 1999, **18**, 2574.

† *supporting information, see page 93*

† Supporting Information

Experimental

General considerations

All manipulations were carried out under inert dinitrogen atmosphere, using standard Schlenk-line conditions and dried and freshly distilled solvents. The ^{1}H, $^{13}C\{^{1}H\}$, $^{31}P\{^{1}H\}$ and $^{19}F\{^{1}H\}$ NMR spectra were recorded unless otherwise stated on a Bruker Avance 300 instrument at 300.13, 75.48, 121.49 and 282.38 MHz, respectively, using TMS, or H_3PO_4 (85% in D_2O) as external standards with downfield shifts reported as positive. All NMR spectra were measured at 25 ºC, unless otherwise specified. The assignment of the chemical shifts and coupling constants of the complex spin systems formed by the $CHCH_2$ protons in complexes **7a**,**b** was made by $^{1}H,^{1}H$-COSY and $^{1}H,^{13}C$-HMQC, decoupled ^{31}P and dept135 NMR experiments. IR spectra in the range 4000–400 cm^{-1} were recorded on a Bruker IFS66FT and a Perkin Elmer 1600 Series FTIR. Elemental analyses were preformed by the "Service de Microanalyse, Université Louis Pasteur (Strasbourg, France)". [PdMeCl(COD)] and [$PdCl_2$(COD)] (COD is 1,5-cyclooctadiene, C_8H_{12}) were prepared according to literature procedures,[1, 2] as were ligands **1a**,**b**, complexes **2a**,**b** and **3a**,**b**.[3]

Preparation and Spectroscopic Data for 4a

A solution of **2a** (0.31 g, 0.73 mmol) in CH_2Cl_2 (50 mL) was stirred under 1 atm CO at room temperature over 1 h. After removal of the solvent under vacuum, the residue was washed with pentane (20 mL) and dried in vacuum, to afford **4a** as a yellow powder (0.30 g, 91% yield). IR (KBr): ν_{CO} = 1684 s, ν_{CN} = 1642 s cm^{-1}; ^{1}H NMR ($CDCl_3$): δ = 2.20 [d, $^{4}J_{HP}$ = 1.4 Hz, 3H, $C(O)CH_3$], 3.28 (dt, $^{2}J_{HP}$ = 10.1 Hz, $^{5}J_{HH}$ = 1.9 Hz, 2H, PCH_2), 3.94 (tt, $^{3}J_{HH}$ = 9.7 Hz, $^{5}J_{HH}$ = 1.9 Hz, 2H, NCH_2), 4.55 (t, $^{3}J_{HH}$ = 9.7 Hz, 2H, OCH_2), 7.45-7.55 (complex m, 6H), 7.66-7.74 (m, 4H); $^{31}P\{^{1}H\}$ NMR ($CDCl_3$): δ 18.2 (s); Anal. Calcd for $C_{18}H_{19}ClNO_2PPd$: C 47.60, H 4.22, N 3.08, Found: C 47.51; H 4.11; N 2.90.

Preparation and Spectroscopic Data for 4b

Complex **4b** was obtained in a similar manner to **4a** from **2b** (0.25g, 0.55 mmol). Yellow powder (0.25 g, 95% yield). IR (KBr): ν_{CO} = 1685 s, ν_{CN} = 1632 s cm^{-1}; ^{1}H NMR ($CDCl_3$): δ = 1.54 [s, 6H, $NC(CH_3)_2$], 2.17 [d, $^{4}J_{HP}$ = 1.6 Hz, 3H, $C(O)CH_3$], 3.28 (d, $^{2}J_{HP}$ = 10.4 Hz, 2H, CH_2P), 4.12 (s, 2H, OCH_2), 7.45-7.55 (complex m, 6H), 7.67-7.75 (complex m,

4H); $^{31}P\{^{1}H\}$ NMR ($CDCl_3$): δ 18.0 (s); Anal. Calcd for $C_{20}H_{23}ClNO_2PPd$: C 49.81, H 4.81, N 2.90, Found: C 51.10; H 4.90; N 2.60.

Variable temperature NMR measurements with 3b

A solution of **3b** (*ca* 0.020 g, 3.5×10^{-2} mmol) in CD_2Cl_2 (*ca* 0.6 mL) in a NMR tube with Teflon seal was exposed to an atmosphere of ^{13}CO.

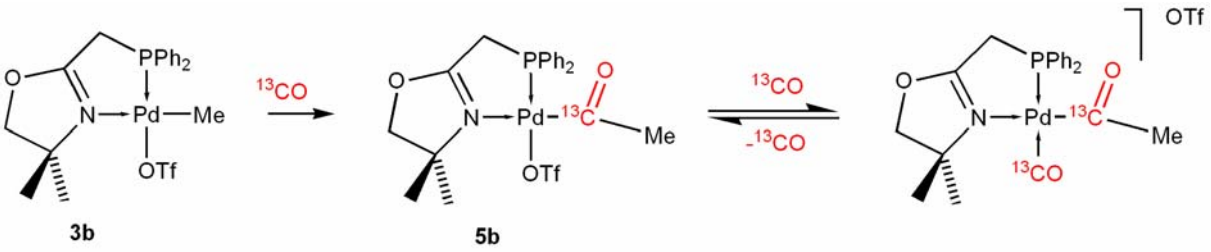

Complex **5b** was identified by its NMR spectra at room temperature. Selected data: ^{1}H NMR (CD_2Cl_2): δ = 1.38 [s, 6H, $NC(CH_3)_2$], 2.09 [dd, $^{4}J_{HP}$ = 2.0 Hz, $^{2}J_{HC}$ = 6.0 Hz, 3H, $C(O)CH_3$], 3.37 (d, $^{2}J_{HP}$ = 11.2 Hz, 2H, CH_2P), 4.18 (s, 2H, OCH_2); $^{31}P\{^{1}H\}$ NMR (CD_2Cl_2): δ 21.6 (d, $^{2}J_{PC}$ = 9.7 Hz); $^{13}C\{^{1}H\}$ NMR (CD_2Cl_2): δ 222.7 [d, $^{2}J_{PC}$ = 9.7 Hz, *C*(O)CH_3].

At -100 ºC, the equilibrium between **5b** and the palladium acyl carbonyl complex [Pd{C(O)Me}(CO)(P,N)]OTf (P,N = **1b**) is completely shifted towards the latter as shown by NMR spectroscopy. Selected data: ^{1}H NMR (CD_2Cl_2, -100 ºC): δ = 1.27 [s, 6H, $NC(CH_3)_2$], 2.00 [d, $^{2}J_{HC}$ = 5.0 Hz, 3H, $C(O)CH_3$], 3.71 (d, $^{2}J_{HP}$ = 9.7 Hz, 2H, CH_2P), 4.29 (s, 2H, OCH_2); $^{31}P\{^{1}H\}$ NMR (CD_2Cl_2, -100 ºC): δ 18.3 (dd, $^{2}J_{PCtrans}$ = 83.8 Hz, $^{2}J_{PCcis}$ = 4.1 Hz); $^{13}C\{^{1}H\}$ NMR (CD_2Cl_2, -100 ºC): δ 223.1 [d, $^{2}J_{PC}$ = 4.1 Hz, *C*(O)CH_3], 175.3 [d, $^{2}J_{PC}$ = 83.8 Hz, PdC(O)].

Figure S-1 $^{31}P\{^{1}H\}$ NMR (CD_2Cl_2, -100 ºC) spectrum of complex [Pd{C(O)Me}(CO)(P,N)]OTf (P,N = **1b**).

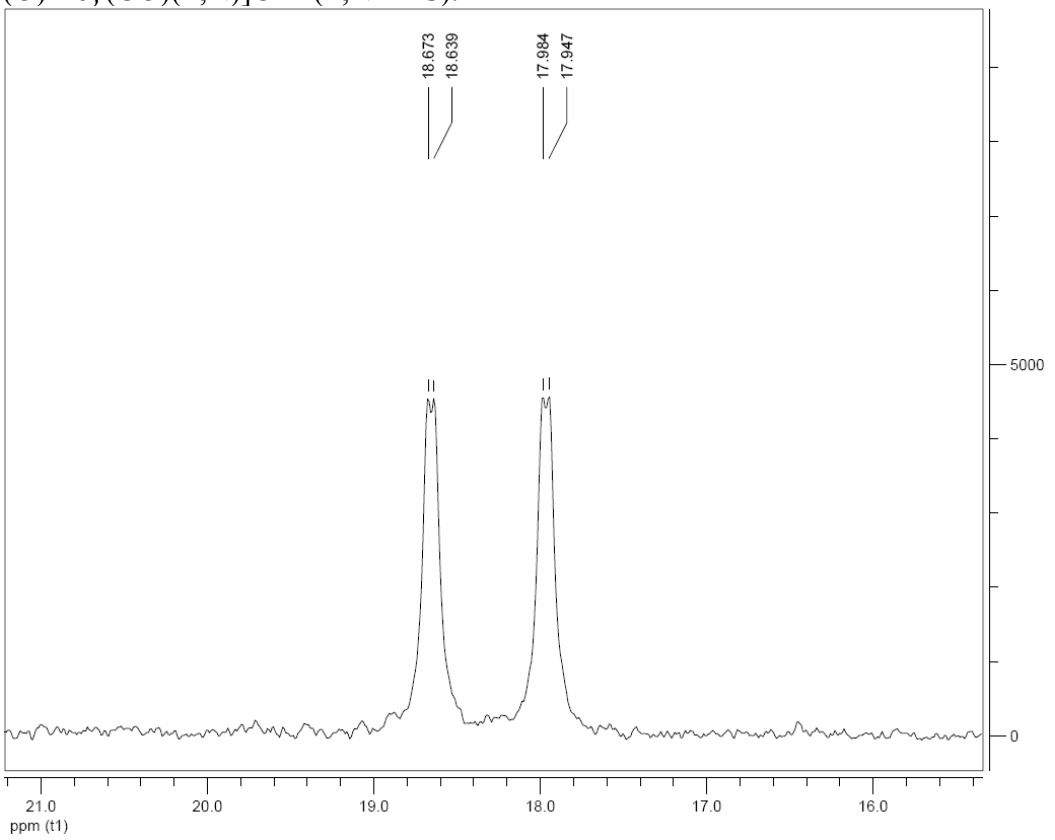

Figure S-2: Portion of the $^{13}C\{^{1}H\}$ NMR (CD_2Cl_2, -100 ºC) spectrum of complex [Pd{C(O)Me}(CO)(P,N)]OTf (P,N = **1b**) showing the peaks corresponding to the acyl carbon (left) and coordinated ^{13}CO (right).

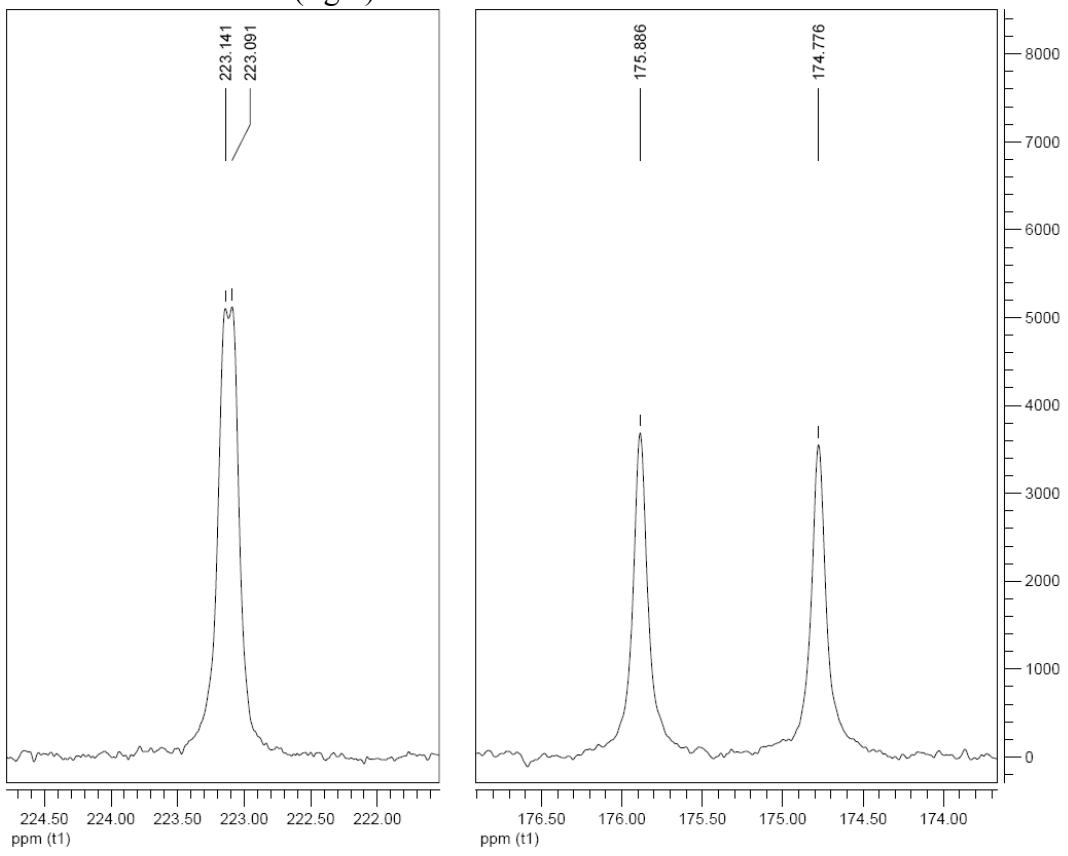

Preparation and Spectroscopic Data for 6a

A solution of **3a** (0.48 g, 0.89 mmol) in CH_2Cl_2 (50 mL) was stirred under 1 atm CO at room temperature for 1 h, which was then replaced by 1 atm ethylene and the solution was further stirred for 1 h. After filtration and removal of the volatiles under vacuum, the residue was washed with diethylether (20 mL) and pentane (2 × 20 mL) and dried under vacuum, to afford **6a** as yellow powder (0.46 g, 87% yield). IR (KBr): $\nu_{CO/CN}$ = 1634 s cm^{-1}; ^1H NMR ($CDCl_3$): δ = 1.65 (td, $^3J_{HH}$ = 6.1, $^3J_{HP}$ = 1.9 Hz, 2H, $PdCH_2$), 2.45 [s, 3H, $C(O)CH_3$], 3.08 (brt, $^3J_{HH}$ = 6.1 Hz, 2H, $PdCH_2CH_2$), 3.55 (dt, $^2J_{HP}$ = 10.8 Hz, $^5J_{HH}$ = 1.8 Hz, 2H, CH_2P), 4.05 (tt, $^3J_{HH}$ = 9.6 Hz, $^5J_{HH}$ = 1.8 Hz, 2H, NCH_2), 4.74 (t, $^3J_{HH}$ = 9.6 Hz, 2H, OCH_2), 7.51-7.59 (complex m, 6H), 7.64-7.73 (m, 4H); $^{31}P\{^1H\}$ NMR ($CDCl_3$): δ 34.4 (s); $^{19}F\{^1H\}$ NMR ($CDCl_3$): δ -78.6 (s); Anal. Calcd for $C_{21}H_{23}F_3NO_5PPdS$: C 42.33, H 3.89, N 2.35, Found: C 42.51; H 4.01; N 2.28.

Preparation and Spectroscopic Data for 6b

Complex **6b** was obtained in a similar manner to **6a** from **3b** (0.37 g, 0.65 mmol). White pale powder (0.37 g, 91% yield). IR (KBr): $\nu_{CO/CN}$ = 1629 s cm^{-1}; ^1H NMR ($CDCl_3$): δ = 1.47 [s, 6H, $NC(CH_3)_2$], 1.67 (td, $^3J_{HH}$ = 6.2, $^3J_{HP}$ = 1.9 Hz, 2H, $PdCH_2$), 2.49 [s, 3H, $C(O)CH_3$], 3.12 (brt, $^3J_{HH}$ = 6.2 Hz, 2H, $PdCH_2CH_2$), 3.58 (d, $^2J_{HP}$ = 11.0 Hz, 2H, CH_2P), 4.36 (s, 2H, OCH_2), 7.52-7.60 (complex m, 6H), 7.65-7.73 (m, 4H); $^{31}P\{^1H\}$ NMR ($CDCl_3$): δ 34.7 (s); $^{19}F\{^1H\}$ NMR ($CDCl_3$): δ -78.5 (s); Anal. Calcd for $C_{23}H_{27}F_3NO_5PPdS$: C 44.28, H 4.36, N 2.24, Found: C 44.45; H 4.40; N 2.05.

Preparation and Spectroscopic Data for 7a

A solution of **3a** (0.96 g, 1.78 mmol) and methyl acrylate (160 μL, 1equiv.) in CH_2Cl_2 (50 mL) was stirred under 1 atm CO at room temperature for 1 h. The workup as described for **6a**, afforded **7a** as a yellow powder (1.09 g, 93.6% yield). IR (KBr): $\nu_{C(O)OMe}$ = 1683 m, $\nu_{CO/CN}$ = 1633 s cm^{-1}; ^1H NMR (500.13 MHz, $CDCl_3$): spin system for $PdCH_aCH_bH_c$: δ = 2.46 (appearance of dt, $^3J_{HaHb}$ = 1.2, $^3J_{HaHc}$ = 6.2, $^3J_{HaP}$ = 1.5 Hz, 1H, H_a), 2.90 (brd, $^2J_{HbHc}$ = 18.7 Hz, 1H, H_b), 3.26 (brdd, $^3J_{HaHc}$ = 6.2, $^2J_{HbHc}$ = 18.7 Hz, 1H, H_c, partial overlap with $C(O)OCH_3$), 2.52 [s, 3H, $C(O)CH_3$], ABMNX spin system (A = B = M = N = H, X = P, δ_A 3.15, δ_B 4.14, $^2J_{AB}$ = 17.6, $^2J_{AX}$ = 12.7, $^2J_{BX}$ = 9.2, $^5J_{AH}$ = 1.0, $^5J_{AH}$ = 1.6, $^5J_{BH}$ = 1.9, $^5J_{BH}$ = 2.2, Hz, 2H, CH_2P, δ_B partial overlap with NCH*H*) 3.24 [s, 3H, $C(O)OCH_3$], 3.90 (m, 1H, NC*H*H), 4.19 (m, 1H, NCH*H*) ABMN spin system (A = B = M = N = H, δ_A 4.62, δ_B 4.81, $^2J_{AB}$ = 10.8, $^3J_{AH}$ = 8.3, $^3J_{BH}$ = 8.6 Hz, 2H, OCH_2), 7.52-7.67 (complex m, 6H), 7.79-7.91 (m, 4H); $^{31}P\{^1H\}$

NMR ($CDCl_3$): δ 32.8 (s); $^{19}F\{^1H\}$ NMR ($CDCl_3$): δ -78.6 (s); Anal. Calcd for $C_{23}H_{25}F_3NO_7PPdS$: C 42.25, H 3.85, N 2.14, Found: C 42.22; H 3.99; N 2.00.

Preparation and Spectroscopic Data for 7b

Complex **7a** was obtained in a similar manner to **7a** from **3b** (0.54 g, 0.95 mmol) and methyl acrylate (85.6 μL, 1 equiv.). Yellow powder (0.53 g, 82% yield). IR (KBr): $\nu_{C(O)OMe}$ = 1684 m, $\nu_{CO/CN}$ = 1629 s cm^{-1}; ^1H NMR (500.13 MHz, $CDCl_3$): δ = 1.45 [s, 3H, NC(C*H*$_3$)(CH$_3$)], 1.51 [s, 3H, NC(CH$_3$)(C*H*$_3$)], spin system for $PdCH_aCH_bH_c$: 2.46 (appearance of dt, $^3J_{HaHb}$ = 1.4, $^3J_{HaHc}$ = 6.3, $^3J_{HaP}$ = 1.8 Hz, 1H, H_a), 2.87 (brd, $^2J_{HbHc}$ = 18.7 Hz, 1H, H_b), 3.27 (brdd, $^3J_{HaHc}$ = 6.3, $^2J_{HbHc}$ = 18.7 Hz, 1H, H_c), 2.55 [s, 3H, C(O)CH$_3$], ABX spin system (A = B = H, X = P, δ_A 3.08, δ_B 4.38, $^2J_{AB}$ = 17.6, $^2J_{AX}$ = 13.6, $^2J_{BX}$ = 9.6 Hz, 2H, CH_2P, δ_B partially overlapping with OCH_2), 3.22 [s, 3H, C(O)OCH$_3$], AB spin system (A = B = H, δ_A 4.2, δ_B 4.4, $^2J_{AB}$ = 8.5 Hz, 2H, OCH_2), 7.54-7.67 (complex m, 6H), 7.81-7.94 (m, 4H); $^{31}P\{^1H\}$ NMR ($CDCl_3$): δ 34.3 (s); $^{19}F\{^1H\}$ NMR ($CDCl_3$): δ -78.6 (s); Anal. Calcd for $C_{25}H_{29}F_3NO_7PPdS$: C 44.03, H 4.29, N 2.05, Found: C 44.28; H 4.44; N 1.80.

Complexes **2a,b**, **4a,b**, and **7a,b** can be stored for several months in a Schlenk flask under N_2 atmosphere, whereas complexes **3a,b** and **6a,b** start to show signs of decomposition into palladium black after 3-4 weeks.

Crystal Structure Determinations

Crystals suitable for X-ray determination were obtained for of **2a** (Figure S-3), **2b** (Figure S-4), **3a** (Figure S-5), **3b** (Figure S-6), **4b** (Figure S-7) and **6b** (Figure S-8) by slow diffusion of hexane into a CH_2Cl_2 solution of the respective complex at 5 ºC, and for **7a** (Figure S-9) and **7b** (Figure S-10) by slow diffusion of pentane into a THF solution of the respective complex also at 5 ºC. Diffraction data were collected on a Kappa CCD diffractometer using graphite-monochromated Mo Kα radiation (λ = 0.71073 Å) (Tables S-1 and S-2). Data were collected using phi-scans and the structures were solved by direct methods using the SHELX 97 software,[4, 5] and the refinement was by full-matrix least squares on F^2. No absorption correction was used. All non-hydrogen atoms were refined anisotropically with H atoms introduced as fixed contributors ($d_{C\text{-}H}$ = 0.95 Å, U_{11} = 0.04). Crystallographic data (excluding structure factors) have been deposited in the Cambridge Crystallographic Data Centre as Supplementary publication n° CCDC ******. Copies of the data can be obtained free of charge on application to CCDC, 12 Union Road, Cambridge CB2 1EZ, UK (fax: (+44)1223-336-033; e-mail: deposit@ccdc.cam.ac.uk).

Complex **2a** crystallized with two independent molecules in the asymmetric unit (Figure S-3). A comparison between the bond lengths and angles (Table S-3) of the independent molecules reveals that they present approximately the same conformation around the metal centre.

Complex **2b** crystallized in a chiral space group ($P2_12_12_1$), however, in solution the complex is not chiral.

The structure of **3a** (Figure S-5) contains three independent molecules in the asymmetric unit with approximately the same conformation around the metal centre (Table S-3).

Insertion products **6b** and **7a** crystallized with two independent cations and two triflate anions in the asymmetric unit (Figures S-8 and S-9 respectively). In the structure of **6b** the two independent cations have very similar bonding parameters (Table S-4), however the comparison between these 2 cations (Figure S-8 b)) reveals that the ellipsoids of the cation containing Pd2 are larger than those of the cation containing Pd1. This is probably due to a less efficient stabilization by the neighbouring triflate anions thus leading to higher thermal parameters in the Pd2 than in the Pd1 cation. In **7a** the two slightly different cations found in the asymmetric unit also have very similar bonding parameters (Table S-4), but present stereogenic centres of opposite chirality. This is confirmed by their opposite torsion-angle values [O2-Pd1-C17-C21 = 87.2 (3)] and [O6-Pd2-C39-C43 = -87.2 (3)]. The symmetryequivalent asymmetric units contain enantiomers of these cations.

Figure S-3 ORTEP view of the molecular structure of compound **2a** (H atoms omitted for clarity). Thermal ellipsoids include 50% of the electron density

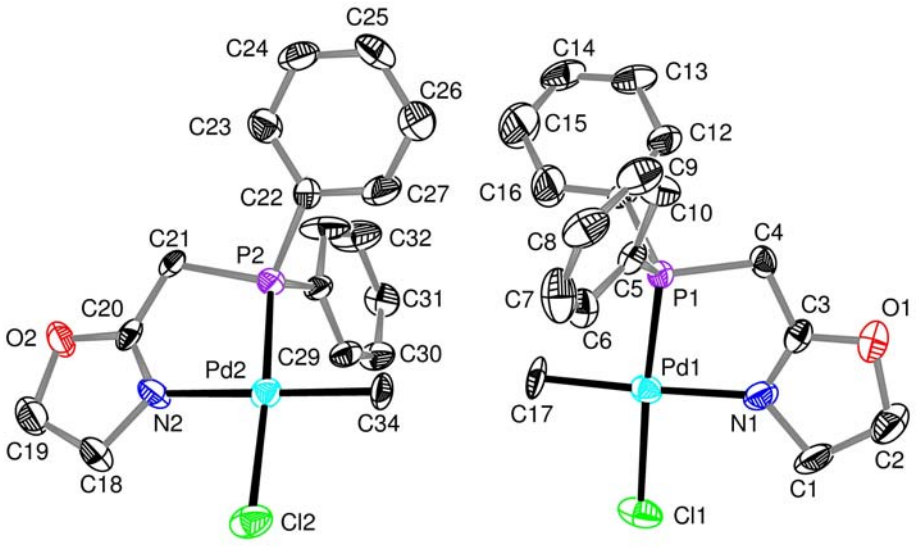

Figure S-4 ORTEP view of the molecular structure of compound **2b** (H atoms omitted for clarity). Thermal ellipsoids include 50% of the electron density

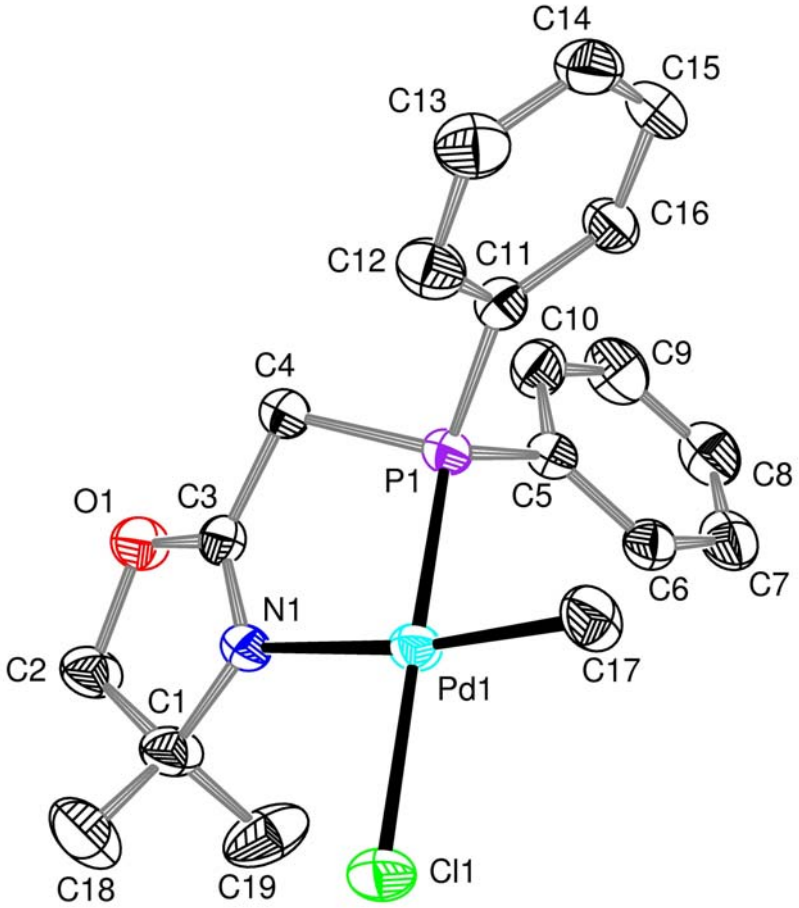

Figure S-5: a) ORTEP view of the molecular structure of compound **3a**; **b)** Comparative views of the three different molecules in **3a** (H atoms omitted for clarity). Thermal ellipsoids include 50% of the electron density.

a)

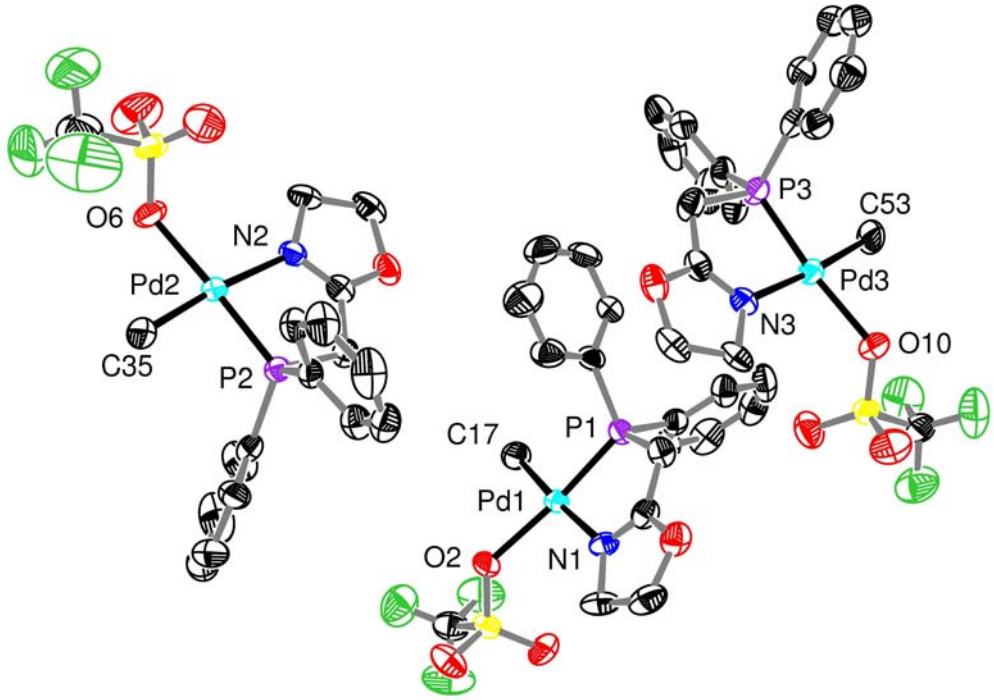

b)

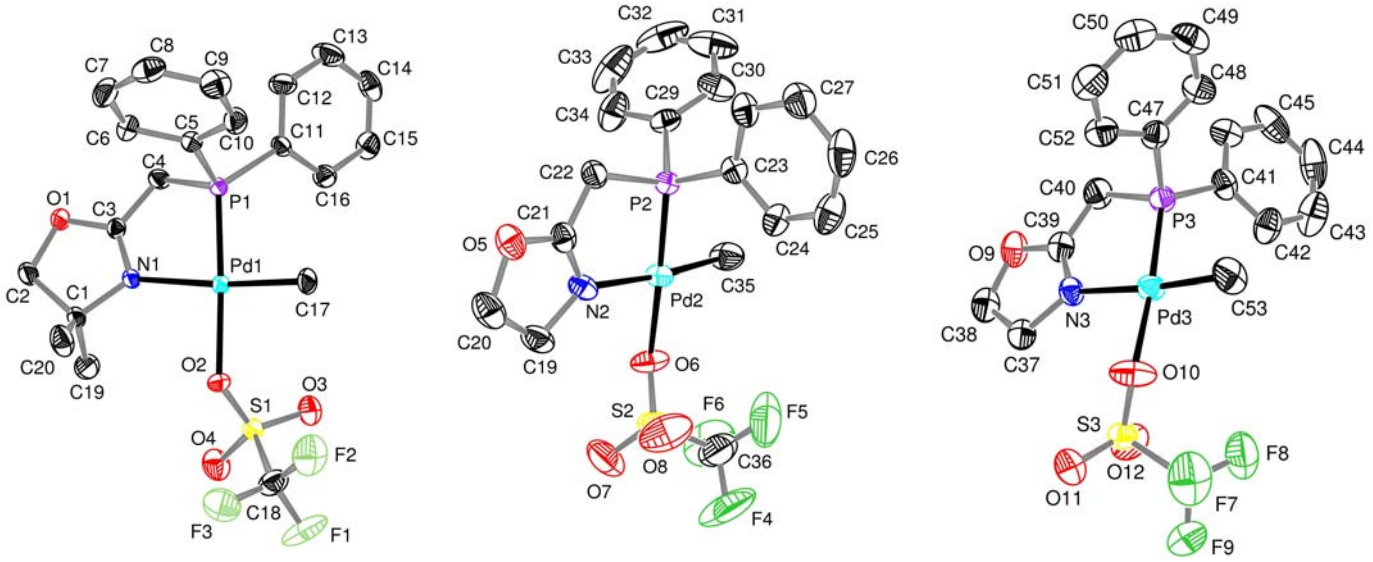

Figure S-6: ORTEP view of the molecular structure of compound **3b** (H atoms omitted for clarity). Thermal ellipsoids include 50% of the electron density

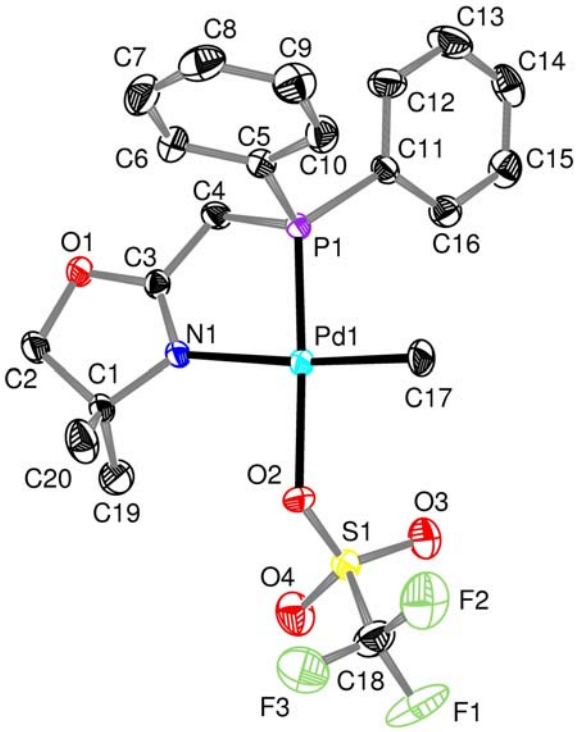

Figure S-7: ORTEP view of the molecular structure of compound **4b** (H atoms omitted for clarity). Thermal ellipsoids include 50% of the electron density

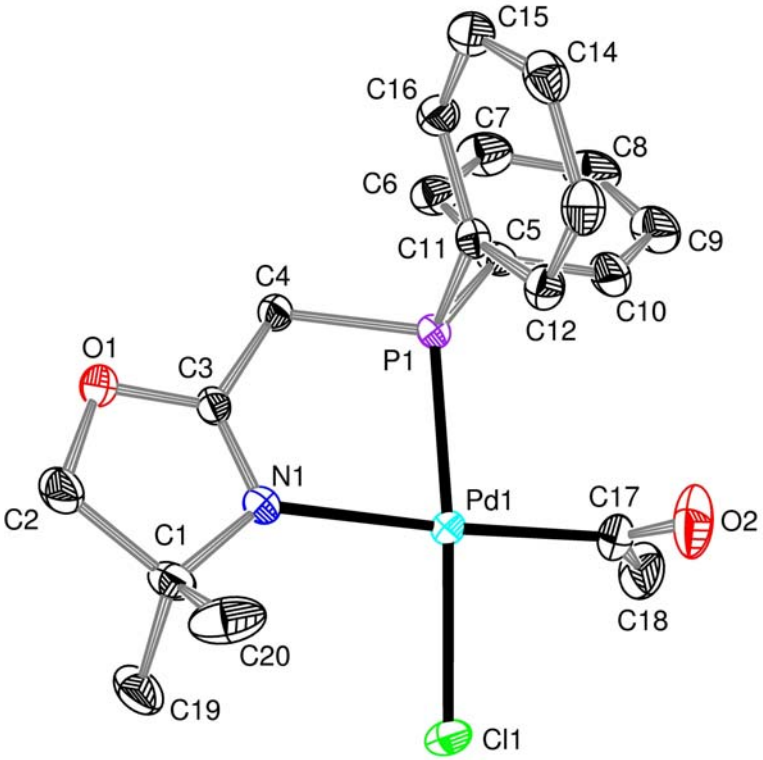

Figure S-8: a) ORTEP view of the molecular structure of compound **6b**; **b)** Comparative view of the two different cations in **6b** (H atoms omitted for clarity). Thermal ellipsoids include 50% of the electron density

a)

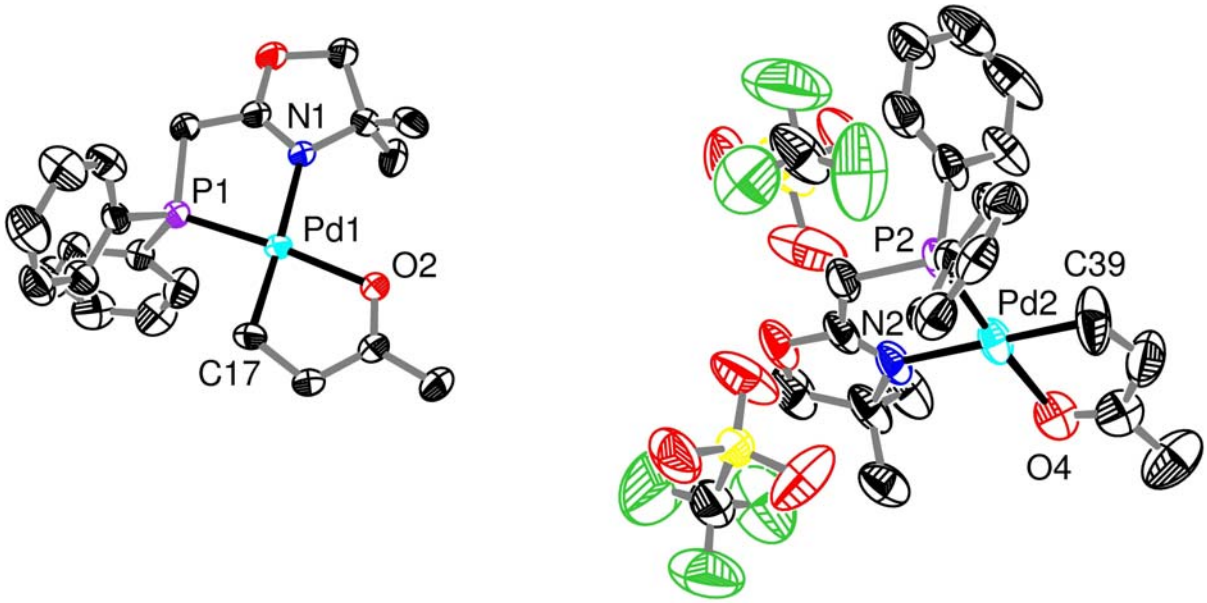

b)

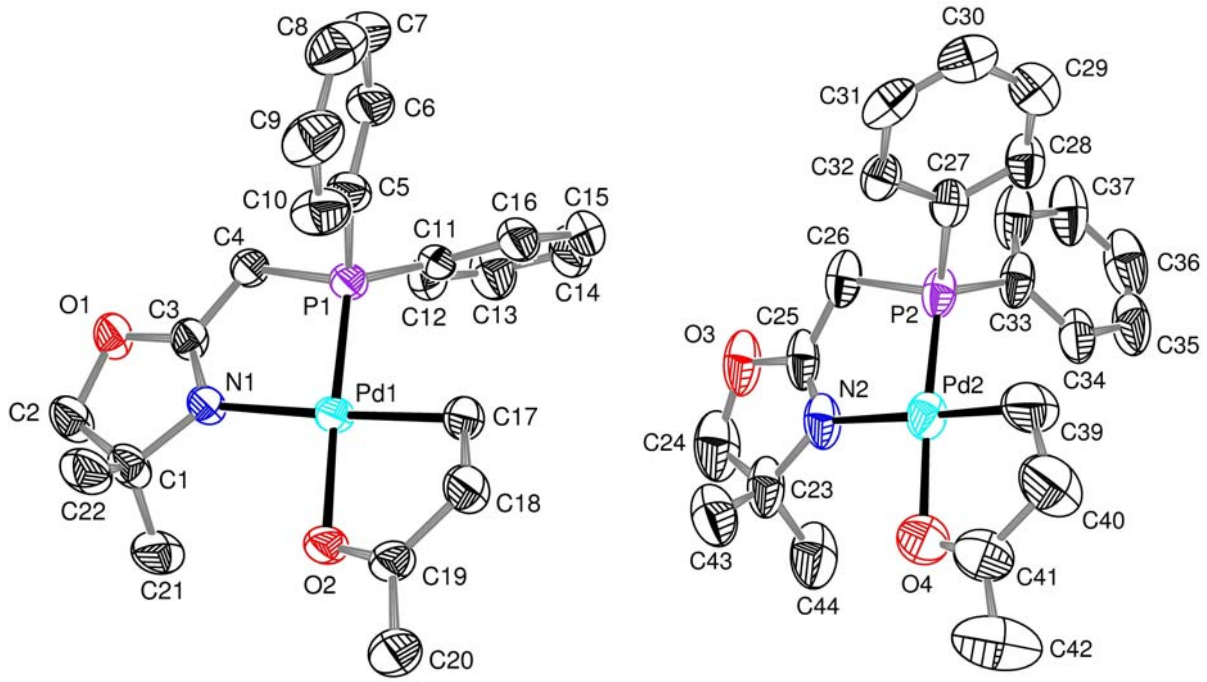

Figure S-9: ORTEP view of the molecular structure of compound **7a**; **b)** Comparative view of the two different cations in **7a** (on the left cation with stereogenic centre of configuration S and on the right of configuration R) (H atoms omitted for clarity). Thermal ellipsoids include 50% of the electron density.

a)

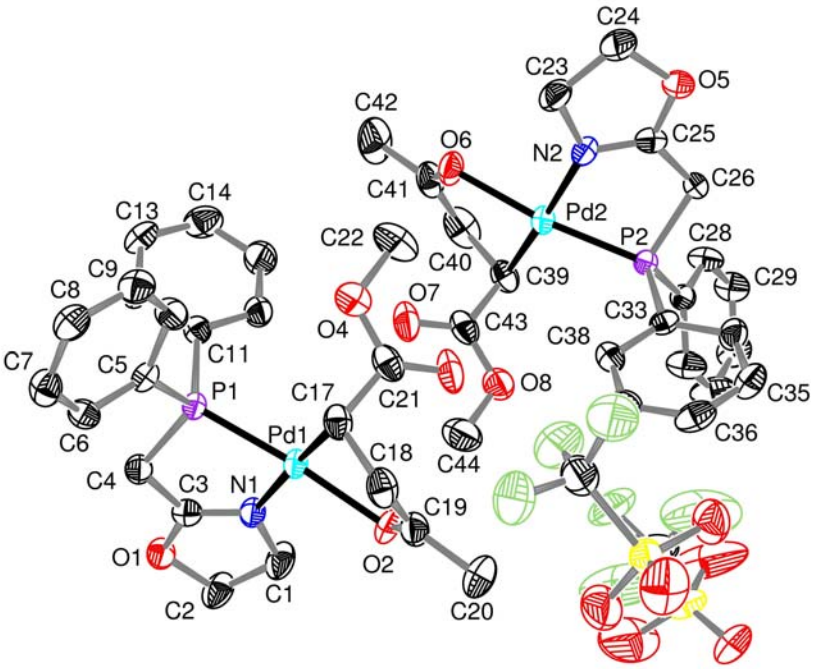

b)

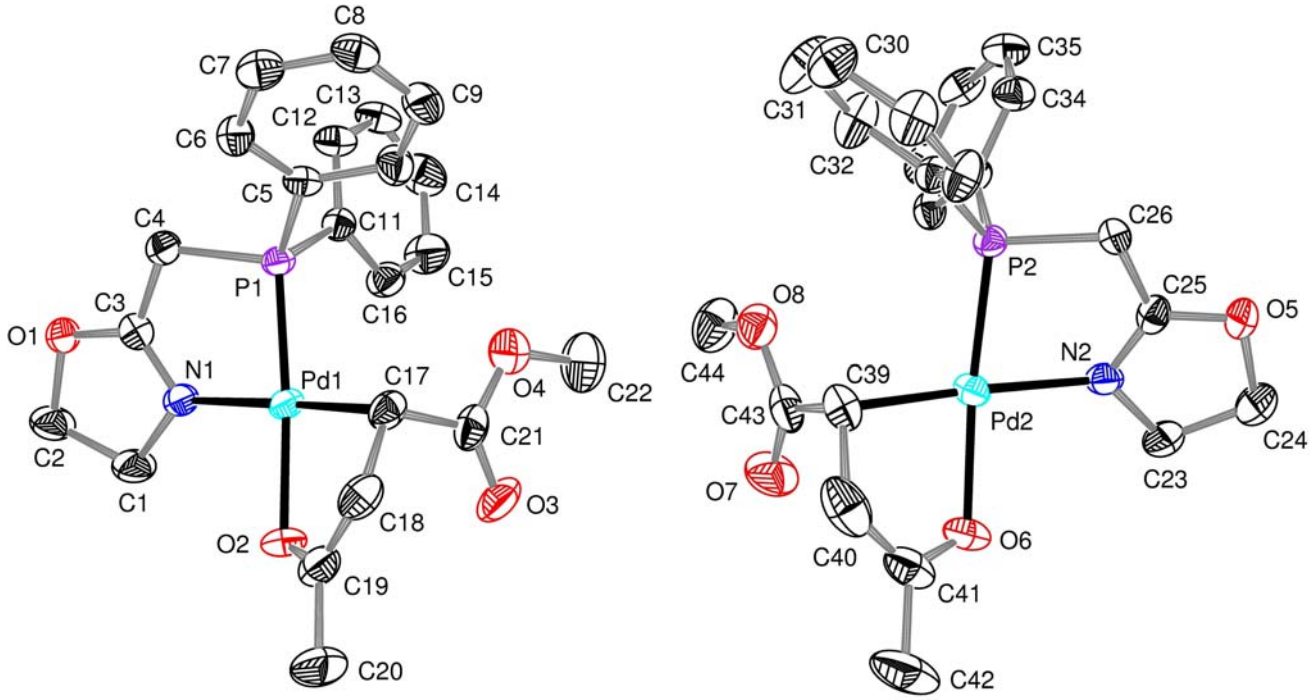

Figure S-10: ORTEP view of the molecular structure of the cation in complex **7b** (H atoms omitted for clarity). Thermal ellipsoids include 50% of the electron density

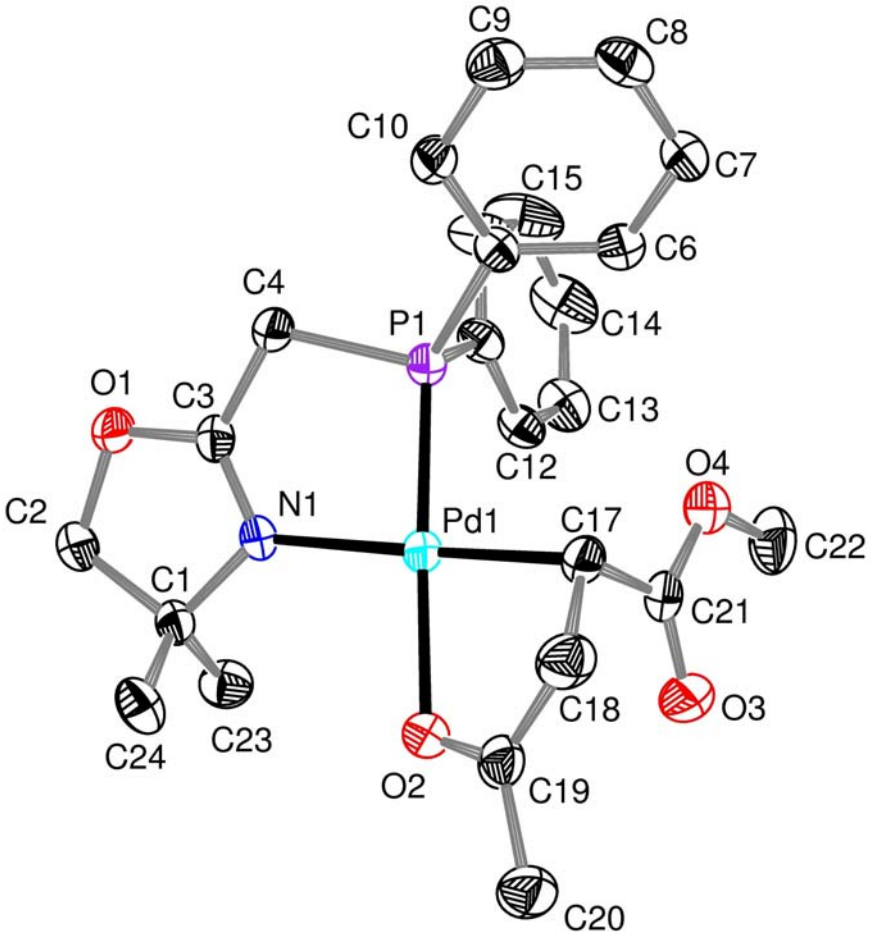

Table S-1 Crystal data and details of the structure determination for the complexes **2a**,**b**, and **3a**,**b**.

	2a	**2b**	**3a**	**3b**
Formula	$2[C_{17}H_{19}ClNOPPd]$	$C_{19}H_{23}ClNOPPd$	$3[C_{17}H_{19}NOPPd{\cdot}CF_3SO_3]$	$C_{19}H_{23}NOPPd{\cdot}CF_3SO_3$
M_r	426.15	454.20	539.77	567.82
Crystal system	Triclinic	Orthorhombic	Monoclinic	Triclinic
Space group	$P\bar{1}$	$P2_12_12_1$	$P2_1/n$	$P\bar{1}$
a [Å]	8.5550 (4)	7.7310 (10)	17.4710 (2)	8.3330 (10)
b [Å]	8.8270 (5)	11.711 (2)	13.1780 (2)	9.827 (2)
c [Å]	22.6280 (9)	21.589 (4)	29.3020 (3)	14.261 (3)
α [º]	82.744 (4)			92.55 (5)
β [º]	83.051 (4)		107.1200 (6)	100.18 (5)
γ [º]	86.4320 (16)			98.93 (5)
V [Å^3]	1680.70 (14)	1954.6 (6)	6447.36 (14)	1132.4 (4)
Z	4	4	12	2
D_x [Mg m^{-3}]	1.684	1.543	1.668	1.665
μ [mm^{-1}]	1.358	1.173	1.084	1.033
T [K]	173 (2)	173 (2)	173 (2)	173 (2)
λ [Å]	0.71073	0.71073	0.71073	0.71073
θ_{max} [º]	27.46	30.04	30.03	30.05
data set [h; k; l]	-7/11; -9/11; -25/25	-10/10; -16/16; -30/30	-24/24; -18/17; -41/41	-11/11; -13/11; -13/20
tot., unique data, R(int)	8059, 6429, 0.0480	5650, 5650	33223, 18821, 0.0835	8568, 6592, 0.0173
observed data [$I > 2\sigma(I)$]	4199	4464	9279	5724
No. reflns, No. params	6429, 397	5650, 217	18821, 784	6592, 280
R_1, wR_2, GOF	0.0956, 0.2694, 1.105	0.0397, 0.1272, 0.863	0.0548, 0.1518, 0.948	0.0303, 0.0714, 1.054
Flack parameter		−0.04 (4)		

Table S-2 Crystal data and details of the structure determination for the complexes **4b**, **6b**, and **7a**,**b**.

	4b	**6b**	**7a**	**7b**
Formula	$C_{20}H_{23}ClNO_2PPd$	$2[C_{22}H_{27}NO_2PPd{\cdot}CF_3SO_3]$	$2[C_{22}H_{25}NO_4PPd{\cdot}CF_3SO_3]$	$C_{24}H_{29}NO_4PPd{\cdot}CF_3SO_3$
M_r	482.21	623.89	1307.74	681.92
Crystal system	Triclinic	Triclinic	Triclinic	Triclinic
Space group	$P\bar{1}$	$P\bar{1}$	$P\bar{1}$	$P\bar{1}$
a [Å]	8.962 (5)	11.4740 (5)	11.2740 (5)	8.927 (5)
b [Å]	10.100 (5)	13.9030 (7)	14.8270 (5)	12.268 (5)
c [Å]	12.534 (5)	18.0810 (10)	17.4450 (9)	13.682 (5)
α [º]	82.414 (5)	92.4860 (15)	73.4310 (16)	76.667 (5)
β [º]	80.486 (5)	96.7650 (15)	85.1550 (15)	87.664 (5)
γ [º]	64.312 (5)	112.951 (3)	73.2490 (14)	75.302 (5)
V [Å^3]	1006.0 (9)	2624.9 (2)	2676.4 (2)	1410.1 (11)
Z	2	4	2	2
D_x [Mg m^{-3}]	1006.0 (9)	1.579	1.623	1.606
μ [mm^{-1}]	1.148	0.902	0.894	0.852
T [K]	173 (2)	173 (2)	173 (2)	173 (2)
λ [Å]	0.71069	0.71073	0.71073	0.71069
θ_{max} [º]	35.00	30.07	29.16	27.46
data set [h; k; l]	-14/14; -16/16; 0/20	-16/14; -18/19; -25/25	-15/15; -20/20; -23/23	-11/11; -15/15; 0/17
tot., unique data, R(int)	8736, 8735, 0.0000	24511, 15294, 0.0395	23205, 14401, 0.0464	6394, 6394,
observed data [$I > 2\sigma(I)$]	8240	8608	8027	5427
No. reflns, No. params	8735, 235	15294, 625	14401, 667	6394, 352
R_1, wR_2, GOF	0.0226, 0.0635, 1.046	0.0724, 0.2146, 1.079	0.0511, 0.1375, 0.961	0.0542, 0.1722, 1.075

Table S-3 Comparison of the bond lengths [Å] and angles [º] for the different molecules in the structures of **2a** and **3a**.

2a		**2a'**		**3a**		**3a'**		**3a''**	
Pd1-N1	2.103 (12)	Pd2-N2	2.098 (11)	Pd1-N1	2.131 (4)	Pd2-N2	2.124 (4)	Pd3-N3	2.139 (4)
Pd1-P1	2.212 (4)	Pd2-P2	2.230 (3)	Pd1-P1	2.1699 (12)	Pd2-P2	2.1716 (12)	Pd3-P3	2.1741 (13)
Pd1-C17	2.057 (13)	Pd2-C34	2.087 (12)	Pd1-C17	2.026 (5)	Pd2-C35	2.017 (5)	Pd3-C53	2.032 (5)
				Pd1-O2	2.156 (3)	Pd2-O6	2.151 (3)	Pd3-O10	2.175 (3)
Pd1-Cl1	2.383 (4)	Pd2-Cl2	2.376 (4)						
N1-C3	1.291 (18)	N2-C20	1.284 (17)	N1-C3	1.281 (6)	N2-C21	1.288 (6)	N3-C39	1.284 (6)
C3-C4	1.468 (19)	C20-C21	1.49 (2)	C3-C4	1.476 (6)	C21-C22	1.483 (6)	C39-C40	1.487 (7)
C4-P1	1.847 (13)	C21-P2	1.851 (13)	C4-P1	1.839 (5)	C22-P2	1.846 (5)	C40-P3	1.858 (5)
N1-Pd1-P1	82.2 (3)	N2-Pd2-P2	82.8 (3)	N1-Pd1-P1	84.85 (11)	N2-Pd2-P2	84.63 (11)	N3-Pd3-P3	84.93 (11)
N1-Pd1-C17	176.4 (5)	N2-Pd2-C34	176.9 (5)	N1-Pd1-C17	174.97 (17)	N2-Pd2-C35	174.38 (17)	N3-Pd3-C53	174.96 (18)
				N1-Pd1-O2	95.14 (14)	N2-Pd2-O6	95.97 (14)	N3-Pd3-O10	95.54 (15)
N1-Pd1-Cl1	93.2 (3)	N2-Pd2-Cl2	92.3 (3)						
				P1-Pd1-O2	172.64 (9)	P2-Pd2-O6	176.65 (9)	P3-Pd3-O10	171.95 (10)
P1-Pd1-C17	94.5 (4)	P2-Pd2-C34	95.3 (4)	P1-Pd1-C17	90.68 (15)	P2-Pd2-C35	90.08 (15)	P3-Pd3-C53	90.44 (16)
P1-Pd1-Cl1	174.66 (15)	P2-Pd2-Cl2	174.38 (14)						
				C17-Pd1-O2	89.00 (18)	C35-Pd2-O6	89.19 (18)	C53-Pd3-O10	88.77 (19)
C17-Pd1-Cl1	90.1 (5)	C34-Pd2-Cl2	89.5 (4)						

Table S-4 Comparison of the bond lengths [Å] and angles [°] for the different cations in the structures of **6a** and **7a**.

6b		**6b'**		**7a**		**7a'**	
Pd1-N1	2.104 (4)	Pd2-N2	2.127 (5)	Pd1-N1	2.082 (3)	Pd2-N2	2.088 (3)
Pd1-P1	2.1878 (14)	Pd2-P2	2.1992 (19)	Pd1-P1	2.2051 (10)	Pd2-P2	2.2022 (10)
Pd1-C17	2.030 (5)	Pd2-C39	2.012 (7)	Pd1-C17	2.046 (4)	Pd2-C39	2.046 (4)
Pd1-O2	2.125 (4)	Pd2-O4	2.145 (5)	Pd1-O2	2.112 (2)	Pd2-O6	2.120 (3)
N1-C3	1.270 (6)	N2-C25	1.249 (9)	N1-C3	1.285 (5)	N2-C25	1.295 (5)
C3-C4	1.480 (7)	C25-C26	1.523 (10)	C3-C4	1.496 (5)	C25-C26	1.487 (5)
C4-P1	1.841 (5)	C26-P2	1.855 (6)	C4-P1	1.837 (4)	C26-P2	1.843 (4)
C17-C18	1.527 (8)	C39-C40	1.383 (12)	C17-C18	1.545 (6)	C39-C40	1.543 (7)
C18-C19	1.485 (8)	C40-C41	1.485 (11)	C18-C19	1.472 (6)	C40-C41	1.472 (7)
C19-O2	1.248 (6)	C41-O4	1.223 (9)	C19-O2	1.220 (5)	C41-O6	1.237 (6)
N1-Pd1-P1	83.91 (12)	N2-Pd2-P2	83.88 (18)	N1-Pd1-P1	82.13 (9)	N2-Pd2-P2	81.72 (9)
N1-Pd1-C17	177.1 (2)	N2-Pd2-C39	178.7 (3)	N1-Pd1-C17	174.17 (15)	N2-Pd2-C39	174.28 (15)
N1-Pd1-O2	100.03 (14)	N2-Pd2-O4	100.6 (2)	N1-Pd1-O2	96.10 (12)	N2-Pd2-O6	95.33 (12)
P1-Pd1-O2	174.72 (10)	P2-Pd2-O4	175.56 (13)	P1-Pd1-O2	175.29 (8)	P2-Pd2-O6	172.10 (8)
P1-Pd1-C17	93.30 (16)	P2-Pd2-C39	95.5 (3)	P1-Pd1-C17	99.24 (11)	P2-Pd2-C39	99.99 (12)
C17-Pd1-O2	82.80 (18)	C39-Pd2-O4	80.1 (3)	C17-Pd1-O2	82.10 (14)	C39-Pd2-O6	82.26 (15)

References

1. R. E. Rulke, J. M. Ernsting, A. L. Spek, C. J. Elsevier, P. W. N. M. van Leeuwen and K. Vrieze, *Inorg. Chem.*, 1993, **32**, 5769-5778.
2. F. T. Ladipo and G. K. Anderson, *Organometallics*, 1994, **13**, 303-306.
3. P. Braunstein, M. D. Fryzuk, M. L. Dall, F. Naud, S. J. Rettig and F. Speiser, *J. Chem. Soc., Dalton Trans.*, 2000, 1067-1074.
4. *Kappa CCD Operation Manual; Nonius BV*, (1997), Kappa CCD Operation Manual; Nonius BV, Delft, The Nederlands.
5. G. M. Sheldrick, *SHELXL97*, (1997), SHELXL97, Program for the refinement of crystal structures, University of Göttingen, Germany.

Résumé de la Partie B

Le nouveau ligand (2-oxazoline-2-ylméthyl)di-isopropylphosphine (**1a**) réagit avec [PdMeCl(COD)] pour former le complexe de palladium plan-carré [PdMeCl(P,N)] (**2a**), à partir duquel le complexe cationique [PdMe(P,N)OSO_2CF_3] (**3a**) a été obtenu par abstraction de chlorure avec $AgCF_3SO_3$. Les complexes alkyles [Pd{$CHRCH_2C(O)$Me}(P,N)]CF_3SO_3 **5a** (R = H) et **6a** (R = COOMe), respectivement, ont été isolés à partir des premières réactions d'insertion de CO/éthylène ou CO/acrylate de méthyle dans la liaison Pd-Me du complexe **3a**. Les complexes **2a**, **3a** et **6a** ont été complètement caractérisés par diffraction des rayons X. Le complexe **6a** est encore un rare exemple d'un produit d'insertion de CO/acrylate de méthyle caractérisé structurellement. Ces complexes sont pertinents pour la copolymérisation alternée d'oléfines avec le monoxyde de carbone, catalysée par des complexes de palladium.

Cette partie du chapitre fait l'objet d'une publication, à soumettre,
dont la référence est donnée ci-dessous.

Palladium(II) intermediate complexes in CO/ethylene or CO/methyl acrylate insertion containing the new P,N-type ligand (2-oxazoline-2-ylmethyl)di-isopropylphosphine

Magno Agostinho and Pierre Braunstein.*

À soumettre

Laboratoire de Chimie de Coordination, UMR 7177 CNRS, Institut de Chimie, Université Louis Pasteur, 4 rue Blaise Pascal, F-67070 Strasbourg Cédex, France

pour les références, voir page 126

Abstract of Part B

The new ligand (2-oxazoline-2-ylmethyl)di-isopropylphosphine (**1a**) was reacted with [PdMeCl(COD)] to yield the square planar methylpalladium(II) complex [PdMeCl(P,N)] (**2a**), from which the cationic complex [PdMe(P,N)OSO_2CF_3] (**3a**) was obtained by $AgCF_3SO_3$-promoted chloride abstraction. The alkyl complexes [$\overline{Pd\{CHRCH_2C(O)\}}$Me}(P,N)]$CF_3SO_3$ **5a** (R = H) and **6a** (R = COOMe), respectively, have been isolated from the initial CO/ethylene or CO/methyl acrylate insertion steps into the Pd-Me bond of **3a**, and spectroscopically characterized. Complexes **2a**, **3a** and **6a** have been fully characterized by single crystal X-ray diffraction. Complex **6a** is a still rare example of a structurally characterized CO/methyl acrylate insertion product. These complexes are relevant to the palladium-catalyzed alternating copolymerization of olefins and carbon monoxide.

This part of the chapter will be submitted for published; its reference is given below.

Palladium(II) intermediate complexes in CO/ethylene or CO/methyl acrylate insertion containing the new P,N-type ligand (2-oxazoline-2-ylmethyl)di-isopropylphosphine

Magno Agostinho and Pierre Braunstein.*

To be submitted

Laboratoire de Chimie de Coordination, UMR 7177 CNRS, Institut de Chimie, Université Louis Pasteur, 4 rue Blaise Pascal, F-67070 Strasbourg Cédex, France

for references, see page 126

Palladium(II) intermediate complexes in CO/ethylene or CO/methyl acrylate insertion containing the new P,N-type ligand (2-oxazoline-2-ylmethyl)di-isopropylphosphine

Introduction

The synthesis of ligands which combine hard and soft donor functionalities is a subject of considerable current interest, in particular with respect to the development of new reactive, hemilabile metal-ligand systems and more selective homogeneous catalysts.[1,2] In particular, numerous metal complexes containing *P*,*N* type ligands are catalytically active in a wide range of reactions of both academic and industrial interest.[3,4]

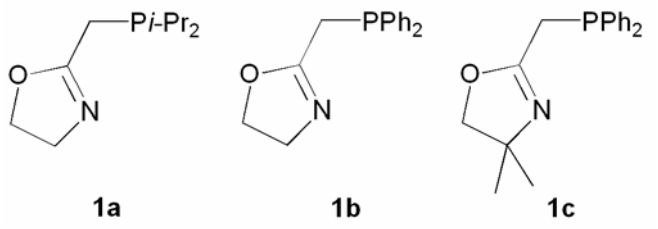

1a **1b** **1c**

We have recently described a series of cationic Pd(II) complexes containing the diphenylphosphino-*P*,*N* type ligands **1b** and **1c**, and investigated their catalytic activity for ethylene oligomerization[5, 6] and ethylene/CO copolymerization.[7] These ligands have allowed us to isolate and fully characterize initial intermediates in the sequential ethylene/CO or methyl acrylate/CO coupling reactions, without the need for using excess methyl acrylate.[8] Despite the considerable interest in the alternating copolymerization of olefins with CO and of olefins with polar monomers, such as methyl acrylate,[8-12] up to date only few metal complexes featuring methyl acrylate/CO coupling have been isolated and characterized.[8, 13-18] Therefore, investigating the behaviour of other functional ligands bearing substituents on the phosphorous donor atom with different stereoelectronic properties, should be of particular interest for these types of reactions. We have now extended our preliminary studies with the diphenylphosphino-*P*,*N* ligands **1b**,**c** to the new isopropyl derivative **1a** and studied the reactivity of its Pd(II) complexes.

for references, see page 126

Results and Discussion

Synthesis of the Ligand

The ligand **1a** was obtained in quantitative yield (95%) by the one-pot procedure previously used to synthesize **1b**,[7] which consists first in the deprotonation of the corresponding 2-methyl-2-oxazoline in THF at -78 ºC, followed by the addition at this temperature of $SiClMe_3$, to form the N-silyl derivative, and reaction with $P(i\text{-}Pr)_2Cl$ (eqn. (1)).

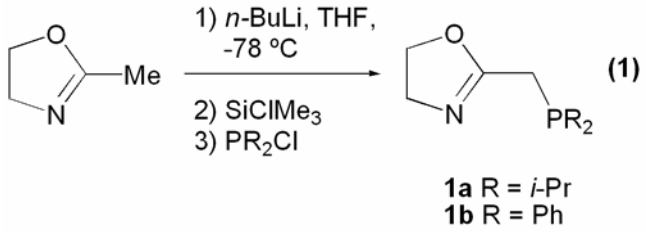

In the ^1H NMR spectrum of ligand **1a**, the PCH_2 (δ = 2.35, $^2J_{PH}$ = 1.0 Hz) and NCH_2 (δ = 3.75, $^3J_{HH}$ = 9.3 Hz) protons appear as a broad singlet and broad triplet, respectively, indicating a small $^5J_{HH}$ coupling while the CH protons of the *i*-Pr substituents on phosphorous appear as a septet of doublets (δ = 1.75, $^2J_{PH}$ = 1.4 Hz, $^3J_{HH}$ = 7.1 Hz). The $^{31}P\{^1H\}$ NMR spectrum contains a singlet at δ 6.4 and the characteristic $\nu_{C=N}$ band for the oxazoline appears in the IR spectrum at 1658 cm^{-1} (Table 1). In contrast to ligand **1b**, which was obtained as a white powder,[7] ligand **1a** is a pale yellow oil that can be exposed to air for short periods of time, but is best kept under an inert atmosphere. Comparative spectroscopic data are presented in Table 1.

Table 1. Selected IR and NMR data for the ligands and complexes.

	IR		NMR[d]	
	ν_{CN}	ν_{CO}	^1H	^{31}P
1a	1658[a] (s)			6.4
1b	1660[a] (s)			-15.8
2a	1639[b] (s)		0.51 Pd-CH_3 (d, $^3J_{PH}$ = 2.3)	57.3
2b	1647[a] (s)		0.55 Pd-CH_3 (d, $^3J_{PH}$ = 2.7)	33.1
3a	1642[b] (m)		0.51 Pd-CH_3 (s)	63.4
3b	1633[b] (s)		0.60 Pd-CH_3 (s)	37.4
4a	1642[a] (m)	1697[a] (m)		54.4
4b	1644[a] (s)	1704[a] (s)		22.0
	$\nu_{CN/CO}$	$\nu_{C(O)OMe}$		
5a	1635[b] (s)		2.45 $C(O)CH_3$ (s)	62.3
5b	1634[b] (s)		2.45 $C(O)CH_3$ (s)	34.4
6a	1639[b] (s)	1679[b] (s)	2.55 $C(O)CH_3$ (s)	59.5
6b	1633[b] (s)	1683[b] (s)	2.52 $C(O)CH_3$ (s)	32.8

[a]In CH_2Cl_2, [b]in KBr, cm^{-1}. [d]In $CDCl_3$, ppm, *J* in Hz.

for references, see page 126

Synthesis of the complex [PdMeCl(P,N)] (2a)

Reaction of one equiv. of **1a** with [PdMeCl(COD)] (COD = cycloocta-1,5-diene) afforded [PdMeCl(P,N)] **2a** in quantitative yield (Scheme 1).

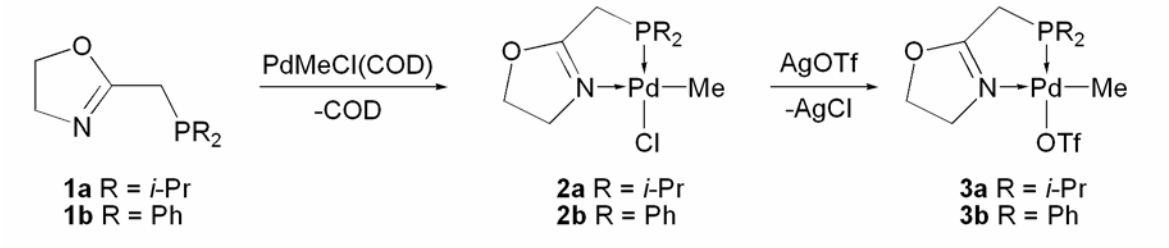

Scheme 1. Synthesis of complexes **2a**,**b** and **2a**,**b**. All reactions were preformed at room temperature in CH_2Cl_2.

Coordination of the ligand resulted in a shift of the $\nu_{C=N}$ absorption to 1639 cm^{-1} (Table 1). In the ^1H NMR spectrum of **2a** the PCH_2 protons appear as a doublet of triplets (δ 2.51, $^2J_{PH}$ = 8.8, $^5J_{HH}$ = 2.0 Hz) owing to a $^5J_{HH}$ coupling between the PCH_2 and NCH_2 protons. A similar $^5J_{HH}$ coupling has been observed for **2b** and related palladium complexes stabilized by ligand **1b**.[7, 8] The CH protons of the *i*-Pr substituents of the phosphorous appear as a doublet of septets (δ = 2.19, $^2J_{PH}$ = 8.6 Hz, $^3J_{HH}$ = 7.1). Other characterizing data are given in the Experimental Section. Single crystals of **2a** suitable for X-ray diffraction were obtained by slow diffusion of hexane into a CH_2Cl_2 solution of the complex. A view of its molecular structure is shown in Fig. 1 and selected distances and angles are given in Table 2.

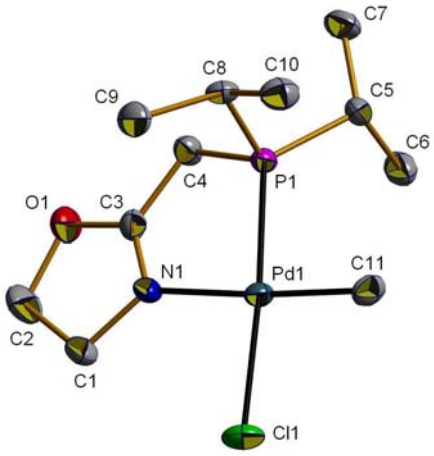

Fig. 1. View of the structure of complex **2a** (H atoms omitted). Displacement ellipsoids are drawn at 50% probability level.

As observed for **2b**[8] the coordination geometry around the palladium centre in **2a** is very close to square planar. As expected, the Me group is positioned *cis* to the phosphorous donor atom, which is consistent with the fact that the groups with the largest *trans* influence avoid being mutually trans to one another.[8,19,20] The P,N-chelate bite angle [82.68(6)°] is close

for references, see page 126

to that reported for **2b** [82.2(3)°],[8] and is consistent with that in other five membered-ring complexes of the type [PdMeCl(P,N)].[20,21]

Table 2. Selected bond lengths [Å] and angles [º] in complexes **2a**, **3a, 6** and **7a**.

	2a	**3a**	**6**	**7a**
Pd1-N1	2.138(2)	2.135(2)	2.008(5)	2.076(6)
Pd1-P1	2.2058(7)	2.1817(7)	2.2140(14)	2.222(2)
Pd1-C11	2.042(3)	2.031(3)		2.049(7)
Pd1-O2		2.177(2)		2.112(5)
Pd1-Cl1	2.3724(7)		2.3220(14)	
Pd1-Cl1^{iv}			2.4357(13)	
N1-C3	1.276(3)	1.274(4)	1.284(7)	1.278(10)
C3-C4	1.488(4)	1.488(4)	1.475(7)	1.480(12)
C4-P1	1.852(3)	1.839(3)	1.833(5)	1.845(8)
O2-C13				1.232(10)
C13-C12				1.506(14)
C12-C11				1.538(13)
N1-Pd1-P1	82.68(6)	83.63(6)	83.18(14)	84.1(2)
N1-Pd1-C11	175.32(10)	174.2(1)		174.7(3)
N1-Pd1-O2		96.73(8)		94.3(2)
N1-Pd1-Cl1	94.19(6)		176.71(14)	
N1-Pd1-Cl1^{iv}			94.09(14)	
P1-Pd1-O2		177.76(6)		174.3(2)
P1-Pd1-C11	92.99(8)	91.55(10)		100.1(2)
P1-Pd1-Cl1	175.80(3)		93.54 (5)	
P1-Pd1-Cl1^{iv}			176.93(5)	
C11-Pd1-O2		88.2(1)		81.8(3)
C11-Pd1-Cl1	90.22(8)			
Cl1-Pd1-Cl1^{iv}			89.19(5)	
Pd1-Cl1-Pd1^{iv}			88.22 (5)	

Symmetry code: (iv) 1 - *x*, *y*, 3/2 - *z*.

Although no classical intermolecular hydrogen bonds were detected in **2a**, a non conventional C-H···Cl hydrogen interaction is present, which involves the Cl atom on the palladium metal center and the unique PC-*H* atom of an isopropyl group of a neighbouring molecule (C8-H···Cl1, Table 3). This results in an infinite one dimensional wavelike chain (Fig. 2). Interactions of this type have been recently reported for related complexes [PdMeCl(P,N)] and [$PdCl_2$(P,N)] (P,N = 2-(2,6-dimethylphenyl)-6-(diphenylphosphinomethyl)pyridine).[20]

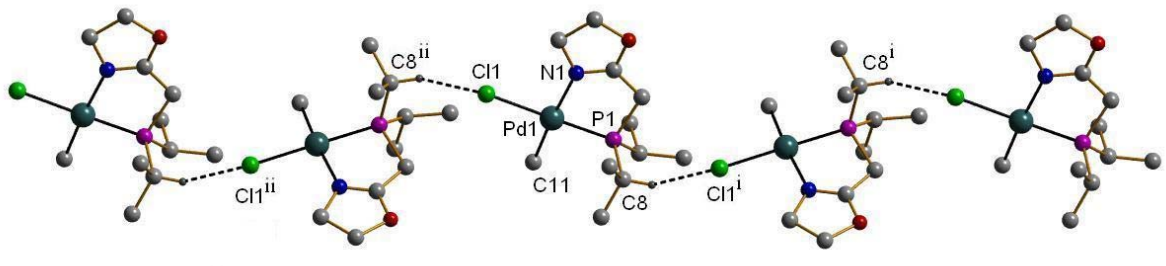

Fig. 2. View of the crystal structure of complex **2a** showing the PC-H···Cl interactions. Symmetry codes: (i) *x*, 0.5 - *y*, 0.5 + *z*; (ii) *x*, 0.5 - *y*, - 0.5 + *z*.

for references, see page 126

Table 3. Hydrogen-bonding parameters (Å, deg) for compounds **2a** and **3a**.

Complex	*D*-H···A	*D*-H	H···A	*D*···A	*D*-H···A
2a	C8-H···Cl1^{i}	1.00	2.77	3.610(3)	142
3a	C4^{iii}-H···O4	0.99	2.26	3.215(4)	160

Symmetry codes: (i) *x*, 0.5 - *y*, 0.5 + *z*; (ii) *x*, 0.5 - *y*, - 0.5 + *z*; (iii) *x*, 1 + *y*, *z*.

Synthesis of the complex [PdMe(P,N)OSO$_2$CF$_3$] (3a)

Complex **3a** was prepared by treatment of a dichloromethane solution of **2a** with $AgCF_3SO_3$, similarly to **3b**[8] (Scheme 1). After removal of AgCl by filtration through Celite, the solvent was evaporated under reduced pressure and the desired complex was obtained as a solid and washed with diethylether and pentane. Selected IR and NMR data are shown in Table 1. There was no spectroscopic indication of a coordinated solvent molecule, consistent with the triflate anion being a better donor than CH_2Cl_2. This contrasts with the formation of cationic Pd(II) complexes in solvents such as MeCN.[7] When compared to the $^{31}P\{^{1}H\}$ NMR data of its less electrophilic but also neutral analogue **2a**, the downfield shift observed ($\Delta\delta$ = 6.1 ppm) is larger than when going from **2b** to **3b** ($\Delta\delta$ = 4.3 ppm) (Table 1).

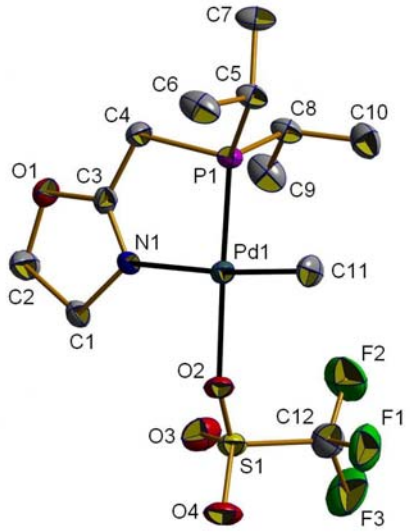

Fig. 3. ORTEP view of the structure of complex **3a** (H atoms omitted). Displacement ellipsoids are drawn at the 50% probability level.

X-ray quality single crystals of **3a** were grown by slow diffusion of hexane into a dichloromethane solution of the complex; its molecular structure is represented in Fig. 3 and selected bond lengths and angles are given in Table 2. It confirmed that the triflate anion is directly bonded to Pd, with a Pd-O2 distance of 2.177(2) Å. The geometry around Pd is square planar, as shown by the values of the P1-Pd1-O2 and N1-Pd1-C11 angles of 177.76(6) and 174.20(11)°, respectively. The bond lengths and angles involving the P,N chelate are similar to those found in **3b**.[8]

for references, see page 126

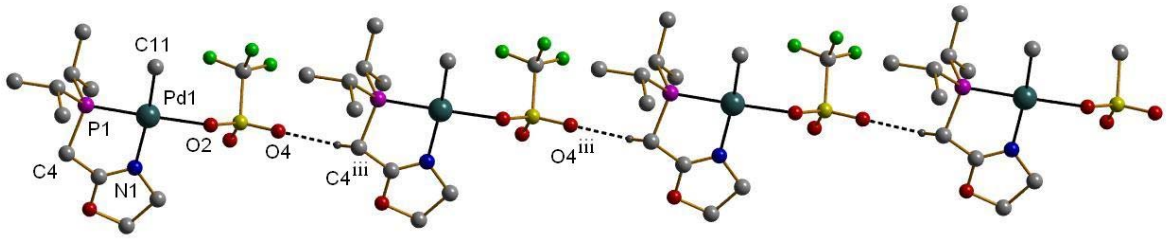

Fig. 4. View of the crystal structure of complex **3a** showing the $C4^{iii}$-H···O4 interaction. Only one of the H atoms at C4 is shown. Symmetry code: (iii) *x*, 1 + *y*, *z*.

Examination of the crystal packing of complex **3a** reveals an intermolecular C4-H···O4 hydrogen-bonding interaction involving a triflate oxygen and a PC4-H hydrogen atom of an adjacent molecule [C4···O4 = 3.215 (4) Å, Table 3], which leads to a one-dimensional chain arrangement in the solid-state (Fig. 4).

CO/Ethylene or CO/Methyl Acrylate Insertion Reactions.

The reaction of complex **3a** with CO in CH_2Cl_2 at room temperature was monitored by $^{31}P\{^1H\}$ NMR spectroscopy. CO insertion into its palladium methyl bond produced in less than 1 h the acyl derivative **4a** (Scheme 2), as evidenced by the large high-field shift of the $^{31}P\{^1H\}$ NMR resonance ($\Delta\delta$ = -9.0, Table 1). The infrared absorption band due to the CO stretching mode of **4a** appears at 1697 cm^{-1}, which is typical for such acyl complexes.[8,21]

As previously observed for **4b**,[8] ethylene insertion into the palladium-acyl bond of **4a**, to the five membered C,O chelate complex **5a,** was completed in less than 1 h ($^{31}P\{^1H\}$ monitoring). The IR spectrum shows only one absorption band at 1635 cm^{-1} corresponding to the CN and CO stretchings ($\nu_{CN/CO}$, Table 1), which represents a shift in the CO stretching band of 62 cm^{-1} to lower wavenumber with respect to that of **4a**. The $^{31}P\{^1H\}$ NMR spectrum of **5a** contains a singlet at δ 62.3 which is shifted to low field relative to that of **4a** (δ 54.4, Table 1). In the ^1H NMR spectrum of **5a**, the Pd-CH_2 protons give rise to a well defined triplet of doublets (δ 1.65, $^3J_{HH}$ = 6.2, $^3J_{PH}$ = 1.6 Hz) whereas the CH_2CO protons appear as a broad triplet (δ 3.09, $^3J_{HH}$ = 6.2 Hz) indicating a smaller J_{PH} coupling constant.

for references, see page 126

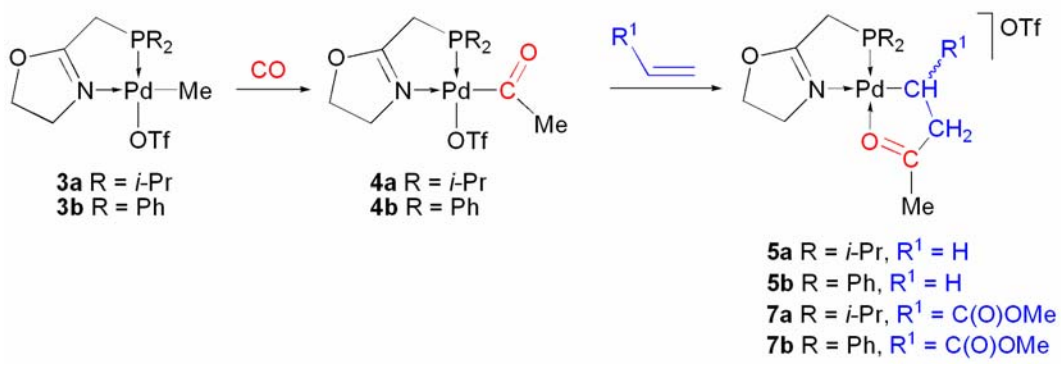

Scheme 2. All reactions were preformed at room temperature in CH_2Cl_2.

Attempts to crystallize **5a** by layering a CH_2Cl_2 solution with hexane were unsuccessful. Nevertheless, this procedure afforded a crystalline material suitable for X-ray crystallography, which subsequently revealed to be the dinuclear palladium complex **6** containing a di-μ-chlorobridge and two equivalent five-membered chelate rings. A view of the centrosymmetric dinuclear complex **6** is shown in Figure 5, and selected bond distances and angles are given in Table 2. According to the Cambridge Structure Database, **6** appears to be the first dinuclear complex of the type $[Pd(\mu\text{-}Cl)(P,N)]_2$ featuring a P,N type ligand, to be characterized by X-ray crystallography. The coordination geometry around the palladium in **6** is close to square planar with the nitrogen donor atoms in *trans* arrangement with respect to the Pd-Pd axis, which is essentially similar to those of the cyclopalladated species with a five-member chelate ring.[22,23] The coordination planes (mean planes passing through Cl1, $Cl1^{iv}$, N1, P1 and through Cl1, $Cl1^{iv}$, $N1^{iv}$, $P1^{iv}$) form an angle of 25.47(1) º and the distance between two palladium atoms is 3.3126(5) Å, which excludes the presence of metal–metal bonding. The length of the Pd-Cl bond *trans* to P [2.4357(13) Å] is longer than that *trans* to N [2.3220(14) Å], which parallels the different trans influences exerted by the phosphorus and the nitrogen atoms.[19,20,24,25]

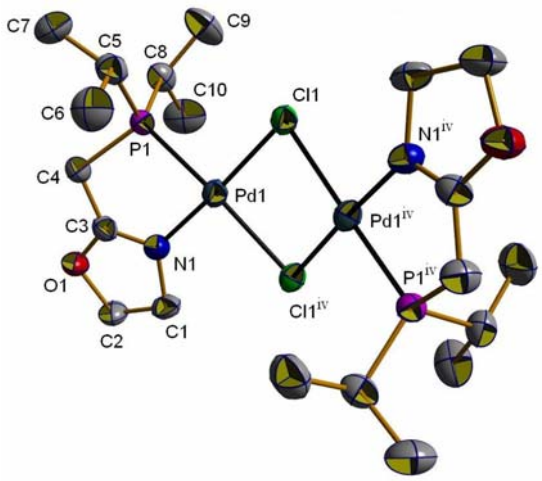

Fig. 5. View of the structure of **6** (H atoms and triflate anions omitted). Displacement ellipsoids are drawn at 50% probability level. Symmetry code: (iv) 1 - *x*, *y*, 3/2 - *z*.

for references, see page 126

In order to determine the fate of the growing polymer chain upon formation of **6**, the ^{13}CO-labeled isotopomer of **5a** was prepared by bubbling ^{13}CO into a solution of [PdMe(P,N)OSO$_2$CF$_3$] (**3a**) wich was subsequently treated with ethylene according to the described procedure. In the ^{1}H NMR spectrum of the ^{13}CO-labeled isotopomer of **5a** the methyl group [^{13}C(O)CH$_3$] appears as a doublet due to the coupling of the protons with the ^{13}C of the labelled ^{13}CO, with a coupling constant ($^2J_{HC}$ = 5.8 Hz) which is in agreement with values reported in a related study with ^{13}CO and propene.[26] The ^{13}C{^{1}H} NMR spectrum displays $^1J_{CC}$ of 40.3 and 40.1 Hz for the [^{13}C(O)*C*H$_3$] and [*C*H$_2$^{13}C(O)CH$_3$], respectively, in agreement with values reported for a ^{13}CO-labeled isotopomer of a CO/methyl acrylate insertion product.[13]

Complex **5a** is stable in the solid state for several weeks; however it decomposes progressively in solution by β-hydrogen elimination. In fact, keeping a CDCl$_3$ solution of the ^{13}CO-labeled isotopomer of **5a** in an NMR tube over a period of 10 days at room temperature affords a few crystals of complex **6**, which deposit along with some palladium metal. The ^{31}P{^{1}H} NMR spectrum of the remaining solution shows only one singlet at δ 56.4, indicating that the only phosphorilated species in solution is the dinuclear complex **6.** In the ^{13}C{^{1}H} NMR spectrum the disappearance of the signal for the ^{13}CO-labeled **5a** is accompanied by the appearance of a new singlet at δ 199.0 corresponding to methyl vinyl ketone resulting from β-hydrogen elimination from complex **5a** (Scheme 3).

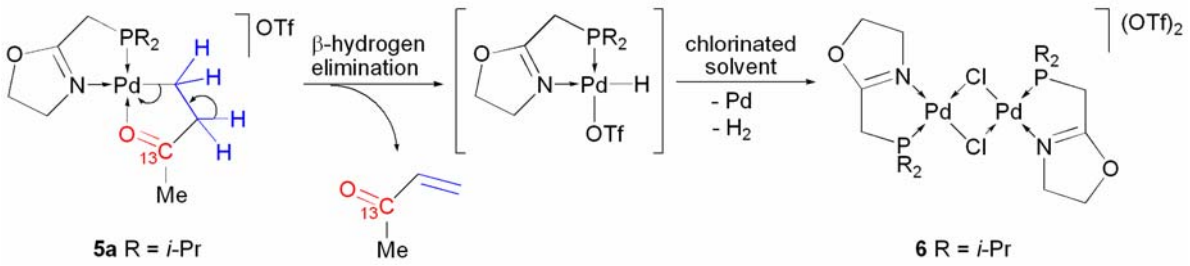

Scheme 3. β-hydrogen elimination from complex **5a** to afford the dinuclear complex **6**.

Further confirmation came from GC-MS analysis of the solution after trap to trap distillation. The fragmentation pattern found for ^{13}C(O)CH=CH$_2$ corresponds perfectly, plus one unit, to that for C(O)CH=CH$_2$.

Palladium hydride complexes resulting from CO-ethylene copolymerization termination reactions usually decompose into dicationic complexes of the type [Pd(L)$_2$] (L = bidentate ligand),[27,28] however Consiglio recently reported the structure of a dinuclear complex of the type [Pd(μ-Cl)(L)]$_2$(OTf)$_2$ (L = diphosphine ligand) obtained by replacement of a CH$_3$ group with a chloride from CHCl$_3$.[29]

for references, see page 126

The insertion of methyl acrylate into the palladium acyl bond of **4a** is regioselective (2,1-insertion) and produces **7a** within 1 h ($^{31}P\{^{1}H\}$ monitoring). The low field shift in the $^{31}P\{^{1}H\}$ resonance of **7a** relative to that of **4a** ($\Delta\delta$ = 5.1, Table 1) is smaller than when considering **7b** and **4b** ($\Delta\delta$ = 10.8, Table 1).[8] The ^{1}H NMR spectrum of **7a** contains methyl signals for the inserted methyl acrylate at δ = 2.55 [$C(O)CH_3$] and 3.63 [$C(O)OCH_3$], the CH and CH_2 protons were identified by means of 2D (COSY and HSQC) NMR experiments and resonate at δ = 2.55 and 3.07, respectively (see Experimental Section). The latter resonance appears, surprisingly, as a slightly broadened singlet. Complex **7a** is stable in the solid state for several weeks, and in contrast to **5a**, no significant decomposition is observed in a $CDCl_3$ solution over a period of 10 days.

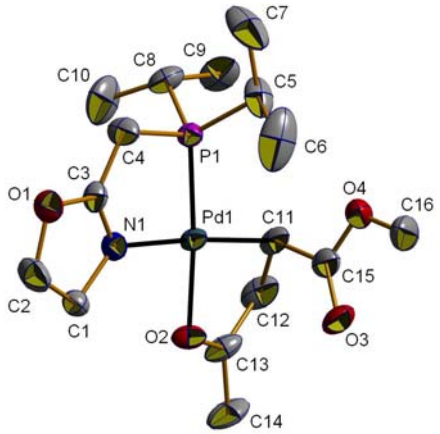

Fig. 6. View of the structure of the cation in **7a** (H atoms omitted). Displacement ellipsoids are drawn at 50% probability level.

The solid state structure of **7a** was unambiguously established by single crystal X-ray diffraction (Figure 6) and it represents, to the best of our knowledge, only the fourth methyl acrylate-acyl coupling product to be structurally characterized.[8,21] This structural determination confirms the formation of a five-membered (C,O) chelated product, which makes β-hydrogen elimination less likely.[30,31] The Pd-C distance in **7a** of 2.049(7) Å (Table 2) is close that in **7b** [2.046(4) Å],[8] the most significant difference between these two structures being the value of the Pd1-P1 bond length, which is longer in **7a** than in **7b** by about 0.02 Å. Although it has no yet been possible to insert a CO molecule into the Pd-C11 bond of **7a** or **7b** (1 atm, 25 °C), our results provide further insight into the comparative reactivity of ethylene and methylacrylate into a Pd-carbon bond, and stability of the corresponding insertion products. Triflate coordination to Pd(II), although resulting in a neutral, less electrophilic and therefore less reactive complex, does not prevent ethylene or methylacrylate insertion into the Pd-Me bond. The increased basicity of the P(*i*-Pr)$_2$ group compared to PPh_2 did not translate into significant reactivity differences.

for references, see page 126

Experimental Section

The ^{1}H, $^{13}C\{^{1}H\}$, $^{31}P\{^{1}H\}$ and $^{19}F\{^{1}H\}$ NMR spectra were recorded at 300.13, 75.48, 121.49 and 282.38 MHz, respectively, on FT Bruker AC300, Avance 300, unless otherwise stated. IR spectra in the range 4000–400 cm^{-1} were recorded on a Bruker IFS66FT and a Perkin Elmer 1600 Series FTIR. Elemental analyses were preformed by the "Service de Microanalyse, Université Louis Pasteur (Strasbourg, France)". All reactions were carried out under purified N_2, using Schlenk techniques, and the solvents were freshly distilled under nitrogen prior to use. [PdMeCl(COD)] (COD is 1,5-cyclooctadiene, C_8H_{12}) was prepared according to literature procedures.[32]

Preparation and spectroscopic data for 1a

To a THF solution (75 mL) of 2-methyl-2-oxazoline (0.5 mL, 5.87 mmol) in a 250 mL flask at -78 ºC, was added dropwise a solution of *n*-butyllithium in hexane (3.67 mL, 1.6 M, 5.87 mmol). The mixture was stirred for 1 h and degassed $SiClMe_3$ (0.75 mL, 5.87 mmol) was added. The mixture was further stirred for 1 h at -78 ºC and $P(i\text{-}Pr)_2Cl$ (0.95 mL, 5.87 mmol) was added. The solution was stirred until it reached room temperature. After evaporation of the solvent under reduced pressure, the oily residue was dissolved in toluene (60 mL) and the solution was filtered through Celite. After evaporation of the toluene under vacuum, **1a** was obtained as a pale yellow oil (1.12 g, 95%). IR (CH_2Cl_2): 1658 (s, ν_{CN}) cm^{-1}. ^{1}H NMR (300.13 MHz, $CDCl_3$, room temp.): δ 1.02 [d, $^{3}J_{HH}$ = 7.1 Hz, 6H, $(CH(CH_3)(CH_3))_2$], 1.06 [dd, $^{3}J_{PH}$ = 2.3 Hz, $^{3}J_{HH}$ = 7.1 Hz, 6H, $(CH(CH_3)(CH_3))_2$], 1.75 [septd, $^{2}J_{PH}$ = 1.4 Hz, $^{3}J_{HH}$ = 7.1 Hz, 2H, $(CH(CH_3)_2)_2$], 2.35 (brd, $^{2}J_{PH}$ = 1.0 Hz, 2H, PCH_2), 3.75 (brt, $^{3}J_{HH}$ = 9.3 Hz, 2H, NCH_2), 4.18 (t, $^{3}J_{HH}$ = 9.3 Hz, 2H, OCH_2). $^{13}C\{^{1}H\}$ (75.48 MHz, $CDCl_3$, room temp.): δ 18.6 [d, $^{2}J_{PC}$ = 10.1 Hz, $(CH(CH_3)(CH_3))_2$], 19.6 [d, $^{2}J_{PC}$ = 15.8 Hz, $(CH(CH_3)(CH_3))_2$], 21.4 (d, $^{1}J_{PC}$ = 25.6 Hz, PCH_2), 23.6 [d, $^{1}J_{PC}$ = 13.9 Hz, $(CH(CH_3)_2)_2$], 54.5 (s, NCH_2), 67.5 (s, OCH_2), 167.3 (d, $^{2}J_{PC}$ = 7.5 Hz, CN). $^{31}P\{^{1}H\}$ NMR (121.49 MHz, $CDCl_3$, room temp.): δ 6.4 (s).

Preparation and spectroscopic data for [PdMeCl(P,N)] (2a)

To a solution of ligand **1a** (0.48 g, 2.37 mmol) in CH_2Cl_2 (20 mL) was added solid [PdMeCl(COD)] (0.49 g, 1.90 mmol, 0.8 equiv.) at room temperature and the resulting mixture was stirred overnight. The solvent was then evaporated under reduced pressure affording a white residue. The latter was washed with diethylether (2x15 mL) and pentane (15 mL) and dried under vacuum (white powder, 0.61 g, 90%). IR (KBr): 1639 (s, ν_{CN}) cm^{-1}. ^{1}H

for references, see page 126

NMR (300.13 MHz, $CDCl_3$, room temp.): δ 0.51 (d, $^3J_{PH}$ = 2.3 Hz, 3H, $PdCH_3$), 1.20 [dd, $^3J_{PH}$ = 16.2 Hz, $^3J_{HH}$ = 7.1 Hz, 6H, $(CH(CH_3)(CH_3))_2$], 1.26 [dd, $^3J_{PH}$ = 19.0 Hz, $^3J_{HH}$ = 7.1 Hz, 6H, $(CH(CH_3)(CH_3))_2$], 2.19 [dsept, $^2J_{PH}$ = 8.6 Hz, $^3J_{HH}$ = 7.1 Hz, 2H, $(CH(CH_3)_2)_2$], 2.51 (dt, $^2J_{PH}$ = 8.8 Hz, $^5J_{HH}$ = 2.0 Hz, 2H, PCH_2), 3.96 (tt, $^3J_{HH}$ = 9.7 Hz, $^5J_{HH}$ = 2.0 Hz, 2H, NCH_2), 4.54 (t, $^3J_{HH}$ = 9.7 Hz, 2H, OCH_2). $^{13}C\{^1H\}$ (75.48 MHz, $CDCl_3$, room temp.): δ -10.9 (d, $^2J_{PC}$ = 2.9 Hz, $PdCH_3$), 17.6 [s, $(CH(CH_3)(CH_3))_2$], 18.3 [d, $^2J_{PC}$ = 4.6 Hz, $(CH(CH_3)(CH_3))_2$], 21.5 (d, $^1J_{PC}$ = 23.6 Hz, PCH_2), 23.9 [d, $^1J_{PC}$ = 26.0 Hz, $(CH(CH_3)_2)_2$], 52.0 (s, NCH_2), 72.0 (s, OCH_2), 171.8 (d, $^2J_{PC}$ = 15.4 Hz, CN). $^{31}P\{^1H\}$ NMR (121.49 MHz, $CDCl_3$, room temp.): δ 57.3 (s). Anal. Calcd for $C_{11}H_{23}ClNOPPd$: C, 36.89; H, 6.47; N, 3.91. Found: C, 36.84; H, 6.30; N, 3.72.

Preparation and spectroscopic data for $[PdMe(P,N)OSO_2CF_3]$ (3a)

To a solution of complex **2a** (0.51 g, 1.42 mmol) in CH_2Cl_2 (20 mL) was added $AgSO_3CF_3$ (0.44 g, 1.71 mmol, 1.2 equiv.). The reaction mixture was protected from room light with an aluminum foil and stirred for 2 h at room temperature. The solution was then filtered through dry Celite and the solvent was evaporated under reduced pressure. The residue was washed with diethylether (2x10 mL), pentane (10 mL) and dried under vacuum overnight. Complex **3a** was obtained as a light beige powder (0.65 g, 97%). IR (KBr): 1642 (m, ν_{CN}) cm^{-1}. ^1H NMR (300.13 MHz, $CDCl_3$, room temp.): δ 0.51 (s, 3H, $PdCH_3$), 1.23 [dd, $^3J_{PH}$ = 16.2 Hz, $^3J_{HH}$ = 7.0 Hz, 6H, $(CH(CH_3)(CH_3))_2$], 1.29 [dd, $^3J_{PH}$ = 18.6 Hz, $^3J_{HH}$ = 7.0 Hz, 6H, $(CH(CH_3)(CH_3))_2$], 2.20 [dsept, $^2J_{PH}$ = 8.8 Hz, $^3J_{HH}$ = 7.0 Hz, 4H, $(CH(CH_3)_2)_2$], 2.58 (dt, $^2J_{PH}$ = 9.1 Hz, $^5J_{HH}$ = 2.0 Hz, 2H, PCH_2), 4.00 (tt, $^3J_{HH}$ = 9.7 Hz, $^5J_{HH}$ = 2.0 Hz, 2H, NCH_2), 4.57 (t, $^3J_{HH}$ = 9.7 Hz, 2H, OCH_2). $^{13}C\{^1H\}$ (75.48 MHz, $CDCl_3$, room temp.): δ -7.4 (d, $^2J_{PC}$ = 3.0 Hz, $PdCH_3$), 17.6 [s, $(CH(CH_3)(CH_3))_2$], 18.3 [d, $^2J_{PC}$ = 3.4 Hz, $(CH(CH_3)(CH_3))_2$], 21.8 (d, $^1J_{PC}$ = 27.0 Hz, PCH_2), 24.4 [d, $^1J_{PC}$ = 29.3 Hz, $(CH(CH_3)_2)_2$], 52.3 (s, NCH_2), 72.1 (s, OCH_2), 171.5 (d, $^2J_{PC}$ = 12.8 Hz, CN). $^{31}P\{^1H\}$ NMR (121.49 MHz, $CDCl_3$, room temp.): δ 63.4 (s). $^{19}F\{^1H\}$ NMR (282.4 MHz, $CDCl_3$): δ -78.1 (s). Anal. Calcd for $C_{12}H_{23}F_3NO_4PPdS$: C, 30.55; H, 4.91; N, 2.97. Found: C, 30.30; H, 4.67; N, 2.74.

Preparation and spectroscopic data for $[Pd\{CH_2CH_2C(O)Me\}(P,N)]CF_3SO_3$ (5a)

A solution of **3a** (0.17 g, 0.35 mmol) in CH_2Cl_2 (25 mL) was stirred under 1 atm CO at room temperature for 1 h, the CO was then replaced by 1 atm ethylene and the solution was further stirred for 1 h. The workup was as described for **2a**, and afforded **5a** as a orange powder (0.13 g, 68% yield). IR (KBr): 1635 (m, ν_{CN} and ν_{CO}) cm^{-1}. ^1H NMR (300.13 MHz,

for references, see page 126

$CDCl_3$, room temp.): δ 1.25 [dd, $^3J_{PH}$ = 16.6 Hz, $^3J_{HH}$ = 7.0 Hz, 6H, $(CH(CH_3)(CH_3))_2$], 1.27 [dd, $^3J_{PH}$ = 18.9 Hz, $^3J_{HH}$ = 7.0 Hz, 6H, $(CH(CH_3)(CH_3))_2$], 1.65 (td, $^3J_{HH}$ = 6.2, $^3J_{PH}$ = 1.6 Hz, 2H, $PdCH_2$), 2.23 [dsept, $^2J_{PH}$ = 8.8 Hz, $^3J_{HH}$ = 7.0 Hz, 2H, $(CH(CH_3)_2)_2$], 2.45 [s, 3H, $C(O)CH_3$], 2.85 (dt, $^2J_{PH}$ = 9.4 Hz, $^5J_{HH}$ = 1.9 Hz, 2H, PCH_2), 3.09 (brt, $^3J_{HH}$ = 6.2 Hz, 2H, $PdCH_2CH_2$), 3.98 (tt, $^3J_{HH}$ = 9.7 Hz, $^5J_{HH}$ = 1.9 Hz, 2H, NCH_2), 4.72 (t, $^3J_{HH}$ = 9.7 Hz, 2H, OCH_2). $^{13}C\{^1H\}$ (75.48 MHz, $CDCl_3$, room temp.): δ 11.9 (s, $PdCH_2$), 17.7 [s, $(CH(CH_3)(CH_3))_2$], 18.3 [d, $^2J_{PC}$ = 3.1 Hz, $(CH(CH_3)(CH_3))_2$], 21.3 (d, $^1J_{PC}$ = 28.3 Hz, PCH_2), 24.5 [d, $^1J_{PC}$ = 28.7 Hz, $(CH(CH_3)_2)_2$], 27.9 [d, $^{4+5}J_{PC}$ = 1.4 Hz, $CH_2C(O)CH_3$], 50.7 (s, $PdCH_2CH_2$), 52.3 (s, NCH_2), 72.2 (s, OCH_2), 173.9 (d, $^2J_{PC}$ = 13.1 Hz, CN), 233.7 [d, $^{3+4}J_{PC}$ = 0.7 Hz, $CH_2C(O)CH_3$]. $^{31}P\{^1H\}$ NMR (121.49 MHz, $CDCl_3$, room temp.): δ 62.3 (s). $^{19}F\{^1H\}$ NMR (282.4 MHz, $CDCl_3$): δ -78.6 (s). Anal. Calcd for $C_{15}H_{27}F_3NO_5PPdS$: C, 34.13; H, 5.16; N, 2.65. Found: C, 34.04; H, 4.93; N, 2.41.

Preparation and spectroscopic data for $[Pd\{CHC(O)OMeCH_2C(O)Me\}(P,N)]CF_3SO_3$ (7a)

A solution of **3b** (0.15 g, 0.32 mmol) in CH_2Cl_2 (20 mL) was stirred under 1 atm CO at room temperature for 1 h, after this period the CO atmosphere was replaced with nitrogen and methyl acrylate (29 μL, 1 equiv.) was added and the solution was further stirred for 1 h. The workup was as described for **2a**, and afforded **7a** as a beige powder (0.16 g, 86% yield). IR (KBr): 1639 (m, ν_{CN} and ν_{CO}), 1679 (m, ν_{CO}) cm^{-1}. ^1H NMR (400.13 MHz, $CDCl_3$, room temp.): 2D (COSY and HSQC) and ^{31}P decoupled NMR experiments were used to determine chemical shifts and coupling constants; δ 1.18-1.47 [complex m, 12H, $(CH(CH_3)_2)_2$], 2.36 [dsept, $^2J_{PH}$ = 1.8 Hz, $^3J_{HH}$ = 7.0 Hz, $(CH(CH_3)_2)(CH(CH_3)_2)$], 2.55 [s, 3H, $C(O)CH_3$], 2.57 [sept, $^3J_{HH}$ = 7.1 Hz, 1H, $(CH(CH_3)_2)(CH(CH_3)_2)$, overlapping with the $C(O)CH_3$ signal], ABMNX spin system (A = B = M = N = H, X = P, δ_A 2.88, δ_B 3.07, $^2J_{AB}$ = 18.8, $^2J_{AX}$ = 9.5, $^2J_{BX}$ = 9.4, $^5J_{AH}$ = 1.6, $^5J_{BH}$ = 1.9 Hz, 2H, PCH_2), 3.07 [appearance of brs, 2H, $CH_2C(O)CH_3$, overlapping with PCH_2 signal], 3.63 [s, 3H, $C(O)OCH_3$], 3.92 (m, 1H, NCHH), 4.05 (m, 1H, NCHH), ABMN spin system (A = B = M = N = H, δ_A 4.70, δ_B 4.81, $^2J_{AB}$ = 10.7, $^3J_{AH}$ = 8.4, $^3J_{BH}$ = 8.7 Hz, 2H, OCH_2), although it was not possible to clearly observe the signal of the PdCH proton, COSY and HSQC experiments indicate that it resonates at 2.55 ppm, thus overlapping with the signals for the $C(O)CH_3$ and $(CH(CH_3)_2)(CH(CH_3)_2$ protons. $^{13}C\{^1H\}$ (75.48 MHz, $CDCl_3$, room temp.): δ 16.2 [d, $^2J_{PC}$ = 5.6 Hz, $CH(CH_3)$], 17.7 [d, $^2J_{PC}$ = 1.0 Hz, $CH(CH_3)$], 18.8 [d, $^2J_{PC}$ = 2.3 Hz, $CH(CH_3)$], 18.9 [s, $CH(CH_3)$], 21.2 (d, $^1J_{PC}$ = 29.9 Hz, PCH_2), 23.1 [d, $^1J_{PC}$ = 26.4 Hz, $(CH(CH_3)_2)(CH(CH_3)_2)$], 25.5 [d, $^1J_{PC}$ = 29.2 Hz, $(CH(CH_3)_2)(CH(CH_3)_2)$], 27.0 (d, $^2J_{PC}$ = 2.3 Hz, PdCH), 28.2 [d, $^{4+5}J_{PC}$ = 2.4 Hz,

for references, see page 126

$CH_2C(O)CH_3$], 50.7 [s, $CH_2C(O)CH_3$], 51.6 [s, $C(O)OCH_3$], 51.9 (s, NCH_2), 72.6 (s, OCH_2), 174.8 (d, $^2J_{PC}$ = 13.8 Hz, CN), 177.7 [s, $C(O)OCH_3$], 233.2 [d, $^{3+4}J_{PC}$ = 2.2 Hz, $CH_2C(O)CH_3$]. $^{31}P\{^1H\}$ NMR (121.49 MHz, $CDCl_3$, room temp.): δ 59.5 (s). $^{19}F\{^1H\}$ NMR (282.4 MHz, $CDCl_3$): δ -78.6 (s). Anal. Calcd for $C_{17}H_{29}F_3NO_7PPdS$: C, 34.85; H, 4.99; N, 2.39. Found: C, 34.59; H, 4.83; N, 2.14.

Crystal Structure Determinations

Crystals of **2a**, **3a, 6** and **7a** suitable for an X-ray diffraction study were obtained by slow diffusion of hexane into a CH_2Cl_2 solution of the respective complex at 5 ºC. Diffraction data were collected on a Kappa CCD diffractometer using graphite-monochromated MoKα radiation (λ = 0.71073 Å) (Table 4). Data were collected using phi-scans and the structures were solved by direct methods using the SHELX 97 software,[33,34] and the refinement was performed by full-matrix least squares on F^2. No absorption correction was used. All non-hydrogen atoms were refined anisotropically with H atoms introduced as fixed contributors ($d_{C\text{-}H}$ = 0.95 Å, U_{11} =0.04).

Supplementary material

The crystallographic material has been sent to the Cambridge Crystallographic Data Centre, 12 Union Road, Cambridge CB2 1EZ, UK, as supplementary material CCDC XXXX and can be obtained by contacting the CCDC (quoting the article details and the corresponding SUP number). See http://www.rsc.org/suppdata/XXX for crystallographic files in .cif format.

Acknowledgements. We are grateful to Prof. R. Welter and Dr A. DeCian (ULP Strasbourg) for the crystal structure determinations. This work was supported by the European Commission (Palladium Network HPRN-CT-2002-00196, PhD grant to MA), the Centre National de la Recherche Scientifique (France) and the French 'Ministère de la Recherche'.

for references, see page 126

Table 4. X-ray diffraction data for the structural determination of complexes **2a**, **3a, 6** and **7a**.

	2a	**3a**	**6**	**7a**
Formula	$C_{11}H_{23}ClNOPPd$	$C_{12}H_{23}NOPPd{\cdot}CF_3SO_3$	$C_{20}H_{40}Cl_2N_2O_2P_2Pd_2{\cdot}2(CF_3SO_3)$	$C_{16}H_{29}NO_4PPd{\cdot}CF_3SO_3$
M_r	358.12	471.74	984.32	585.84
Crystal system	Monoclinic	Triclinic	Monoclinic	Monoclinic
Space group	$P2_1/c$	$P\bar{1}$	C_2/c	$P2_1/a$
a [Å]	8.3170(2)	8.3800(2)	24.6530(7)	9.4210(2)
b [Å]	10.6290(3)	10.2020(3)	8.6270(3)	25.2850(4)
c [Å]	16.6060(4)	11.3650(4)	18.9330(7)	9.9140(2)
α [º]		86.1340(8)		
β [º]	95.509(2)	80.6550(8)	116.4510(14)	96.68(5)
γ [º]		73.1650(17)		
V [Å^3]	1461.21	917.43(5)	3605.2(2)	2345.6(3)
Z	4	2	4	4
D_x [Mg m^{-3}]	1.628	1.708	1.814	1.659
μ [mm^{-1}]	1.544	1.255	1.425	1.009
T [K]	173(2)	173(2)	173(2)	173(2)
λ [Å]	0.71073	0.71073	0.71073	0.71073
θ_{max} [º]	30.03	30.06	29.14	30.01
data set [h; k; l]	-11/11; -14/14; -23/23	-11/11; -11/14; -14/16	-33/33; -10/11; -25/25	-11/13; -35/32; -13/13
tot., unique data, R(int)	7268, 4255, 0.0305	7018, 5346, 0.0218	7943, 4829, 0.0374	19315, 6815, 0.0672
observed data [$I > 2\sigma(I)$]	3151	4298	3192	5607
No. reflns, No. params	4255, 145	5346, 208	4829, 202	6815, 250
R_1, wR_2, GOF	0.0373, 0.0921, 1.058	0.0382, 0.0918, 1.076	0.0609, 0.1671, 1.068	0.0992, 0.2525, 1.128

for references, see page 126

References

1. C. S. Slone, D. A. Weinberger and C. A. Mirkin, *Prog. Inorg. Chem.*, 1999, **48**, 233-350.
2. A. Bader and E. Lindner, *Coord. Chem. Rev.*, 1991, **108**, 27-110.
3. P. Braunstein and F. Naud, *Angew. Chem. Int. Ed.*, 2001, **40**, 680-699.
4. G. Helmchen and A. Pfaltz, *Acc. Chem. Res.*, 2000, **33**, 336-345.
5. F. Speiser, P. Braunstein, L. Saussine and R. Welter, *Organometallics*, 2004, **23**, 2613-2624.
6. F. Speiser, P. Braunstein and L. Saussine, *Acc. Chem. Res.*, 2005, **38**, 784-793.
7. P. Braunstein, M. D. Fryzuk, M. L. Dall, F. Naud, S. J. Rettig and F. Speiser, *J. Chem. Soc., Dalton Trans.*, 2000, 1067-1074.
8. M. Agostinho and P. Braunstein, *Chem. Commun.*, 2007, DOI: 10.1039/b613865a.
9. S. Mecking, L. K. Johnson, L. Wang and M. Brookhart, *J. Am. Chem. Soc.*, 1998, **120**, 888-899.
10. L. K. Johnson, S. Mecking and M. Brookhart, *J. Am. Chem. Soc.*, 1996, **118**, 267-268.
11. E. Drent, R. van Dijk, R. van Ginkel, B. van Oort and R. I. Pugh, *Chem. Commun.*, 2002, 744-745.
12. T. Kochi, K. Yoshimura and K. Nozaki, *Dalton Trans.*, 2005, 25-27.
13. F. C. Rix, M. Brookhart and P. S. White, *J. Am. Chem. Soc.*, 1996, **118**, 4746-4764.
14. P. Braunstein, C. Frison and X. Morise, *Angew. Chem., Int. Ed.*, 2000, **39**, 2867-2870.
15. P. Braunstein, J. Durand, M. Knorr and C. Strohmann, *Chem. Commun.*, 2001, 211-212.
16. F. Ozawa, T. Hayashi, H. Koide and A. Yamamoto, *J. Chem. Soc., Chem. Commun.*, 1991, 1469-1470.
17. G. P. C. M. Dekker, C. J. Elsevier, K. Vrieze, P. W. N. M. van Leeuwen and C. F. Roobeek, *J. Organomet. Chem.*, 1992, **430**, 357-372.
18. F. C. Rix and M. Brookhart, *J. Am. Chem. Soc.*, 1995, **117**, 1137-1138.
19. F. R. Hartley, *Chem. Soc. Rev.*, 1973, **2**, 163-179.
20. M. Agostinho, A. Banu, P. Braunstein, R. Welter and X. Morise, *Acta Crystallogr., Sect. C: Cryst. Struct. Commun.*, 2006, **C62**, m81-m86.
21. K. R. Reddy, K. Surekha, G.-H. Lee, S.-M. Peng, J.-T. Chen and S.-T. Liu, *Organometallics*, 2001, **20**, 1292-1299.
22. C.-L. Chen, Y.-H. Liu, S.-M. Peng and S.-T. Liu, *J. Organomet. Chem.*, 2004, **689**, 1806-1815.
23. A. Mentes, R. D. W. Kemmitt, J. Fawcett and D. R. Russell, *J. Mol. Struct.*, 2004, **693**, 241-246.
24. C. J. Richards, D. E. Hibbs and M. B. Hursthouse, *Tetrahedron Lett.*, 1995, **36**, 3745-3748.
25. S. D. Perera, B. L. Shaw and M. Thornton-Pett, *Inorg. Chim. Acta*, 1995, **236**, 7-12.
26. A. Leone and G. Consiglio, *J. Organomet. Chem.*, 2006, **691**, 4204-4214.
27. F. J. Parlevliet, M. A. Zuideveld, C. Kiener, H. Kooijman, A. L. Spek, P. C. J. Kamer and P. W. N. M. van Leeuwen, *Organometallics*, 1999, **18**, 3394-3405.
28. A. D. Burrows, M. F. Mahon and M. Varrone, *Dalton Trans.*, 2003, 4718-4730.
29. A. Leone, S. Gischig and G. Consiglio, *J. Organomet. Chem.*, 2006, **691**, 4816-4828.
30. J. X. McDermott, J. F. White and G. M. Whitesides, *J. Am. Chem. Soc.*, 1976, **98**, 6521-6528.
31. J. X. McDermott, J. F. White and G. M. Whitesides, *J. Am. Chem. Soc.*, 1973, **95**, 4451-4452.
32. R. E. Rülke, J. M. Ernsting, A. L. Spek, C. J. Elsevier, P. W. N. M. van Leeuwen and K. Vrieze, *Inorg. Chem.*, 1993, **32**, 5769-5778.
33. *Kappa CCD Operation Manual; Nonius BV*, (1997), Kappa CCD Operation Manual; Nonius BV, Delft, The Nederlands.
34. G. M. Sheldrick, *SHELXL97*, (1997), SHELXL97, Program for the refinement of crystal structures, University of Göttingen, Germany.

Conclusion Générale

Conclusion Générale

La formation de nouvelles liaisons chimiques, en particulier des liaisons carbone-carbone, est l'un des enjeux de la recherche actuelle en chimie organique, en chimie organométallique et en catalyse. Pour cela, l'utilisation de métaux de transition pour des réactions d'insertion ou de couplage est un outil très puissant. En effet, l'activation d'un substrat dans la sphère de coordination d'un complexe métallique permet d'effectuer un certain nombre de réactions dans des conditions douces, que l'on peut optimiser en particulier grâce à la l'utilisation de ligands appropriés. Une grande variété de métaux a ainsi été étudiée et parmi eux les éléments de la colonne 10 de la classification periodique (Ni, Pd, Pt) occupent une place importante.

Dans le premier chapitre de ce mémoire, nous avons étudié la chimie de coordination des ligands zwitterioniques de type benzoquinonemonoimine **1-4** vis-à-vis du nickel. Ces ligands sont des molécules planes potentiellement antiaromatiques caractérisées par un système à 6π + 6π électrons délocalisés et qui ont pu être obtenus par une nouvelle procédure, très efficace, basée sur les premières réactions de transamination en chimie des quinones.

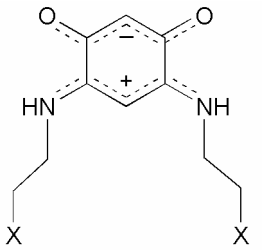

1 X = NMe_2
2 X = NHEt
3 X = OMe
4 X = N⟨ ⟩O

La réaction de ces ligands avec 0.5 équivalent de $Ni(acac)_2$ a mené à la formation des complexes **5-8**, avec un centre de nickel hexacoordiné, alors que la réaction de 1 équivalent de **1** avec $NiCl_2{\cdot}6H_2O$ à conduit à la formation du complexe zwitterionique **9** avec un centre de nickel pentacoordiné. Évidemment la plus forte basicité du ligand acac comparée à celle du chlore est responsable de la nature différente des produits en fonction du précurseur de nickel choisi.

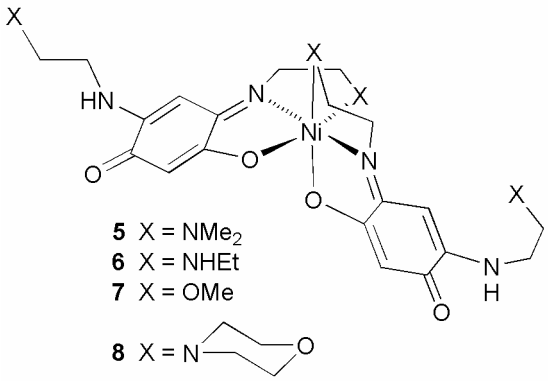

5 X = NMe_2
6 X = NHEt
7 X = OMe
8 X = N⟨ ⟩O

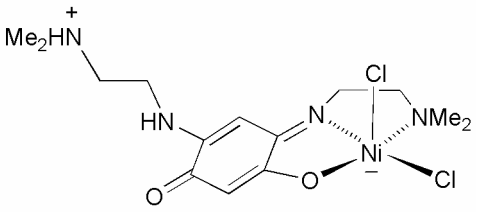

9

Les complexes **5-9** ont été utilisés comme précatalyseurs en oligomérisation de l'éthylène avec différentes quantités de cocatalyseur (MAO ou $AlEtCl_2$). Les résultats ont montré que le cocatalyseur $AlEtCl_2$ mène à des systèmes plus actifs, mais moins sélectifs en α-oléfines, que MAO. L'augmentation de la quantité de cocatalyseur (MAO ou $AlEtCl_2$) utilisé a produit des systèmes plus actifs, mais moins sélectifs.

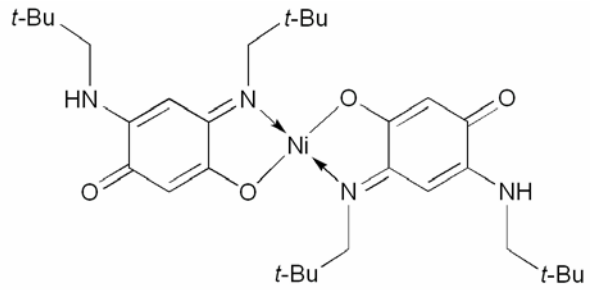

10

En comparant les résultats catalytiques obtenus avec le complexe **10,** publiés auparavant, avec ceux obtenus pour **5-8**, nous avons constaté que la présence d'atomes donneurs sur la chaîne liée à l'azote du fragment benzoquinonemonoimine mène à una diminution de l'activité, mais à une augmentation de la sélectivité en oléfines C_4. La comparaison entre les complexes **5-8** montre que les différentes fonctions présentes sur le bras coordinant n'ont pas d'influence significative sur les résultats catalytiques. La seule différence notable est que le complexe **8** est plus actif et moins sélectif en utilisant MAO comme cocatalyseur, et moins actif avec $AlEtCl_2$, que les complexes **5-7**. L'influence de la géométrie autour du métal a pu être déterminée en comparant les résultats obtenus avec les complexes **5** et **9**, en effet la pentacoordination favorise l'insertion d'oléfines et mène à des activités plus élevées mais les sélectivités sont inférieures.

Il serait intéressant de trouver une stratégie efficace permettant d'obtenir des ligands du type de **1-4** ou le substituent **X** serait une phosphine.

Dans les deuxième et troisième chapitres de ce mémoire, nous nous sommes intéressés à la chimie de coordination de ligands bidentes du type P,N vis-à-vis du palladium, et à l'utilisation de leurs complexes pour des réactions d'insertion. Nous nous sommes attachés à mettre en évidence l'influence de la phosphine sur l'activité et la sélectivité du catalyseur de palladium.

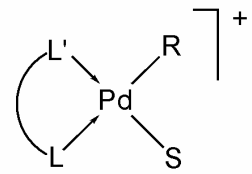

A

Des études préliminaires menées au laboratoire avaient en effet montré que des systèmes de type **A**, stabilisés par des ligands hétérodifonctionnels de type P,O pouvaient, toujours dans des conditions douces, insérer du monoxyde de carbone puis de l'éthylène ou de l'acrylate de méthyle. Nous avons donc poursuivi ces études avec des ligands de type P,N sur lesquelles l'atome donneur de phosphore est représenté par des fonctions phosphinite (**11** et **12**), phosphonite (**13** et **14**) et phosphine (**15-17**).

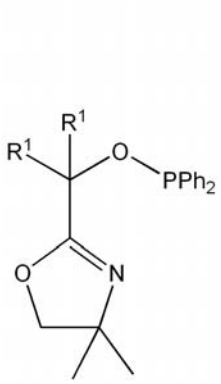

11 R^1 = H
12 R^1 = Me

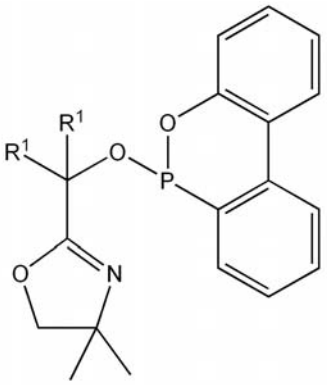

13 R^1 = H
14 R^1 = Me

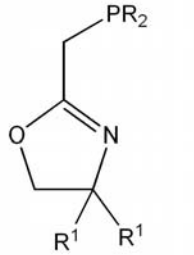

15 R = Ph, R^1 = H
16 R = Ph, R^1 = Me
17 R = *i*-Pr, R^1 = H

Nous avons montré que l'insertion de monoxyde de carbone dans la liaison Pd-C des complexes méthyl-palladium stabilisés par les ligands phosphinite (**11**, **12**) et phosphonite (**13**, **14**) conduit à la formation des intermédiaires acylés **20**, **21**, **25** et **26**, respectivement. Il est intéressant de noter l'influence des substituents R^1 sur les taux de conversion, et que l'effet de ces substituents est opposé pour les ligands phosphinite et phosphonite. Dans le cas des ligands phosphinite, la conversion a été plus élevé quand R^1 = H (complexe **18**, 7 h) alors que pour les ligands phosphonite elle a été plus rapide pour R^1 = Me (complexe **24**, 1 h).

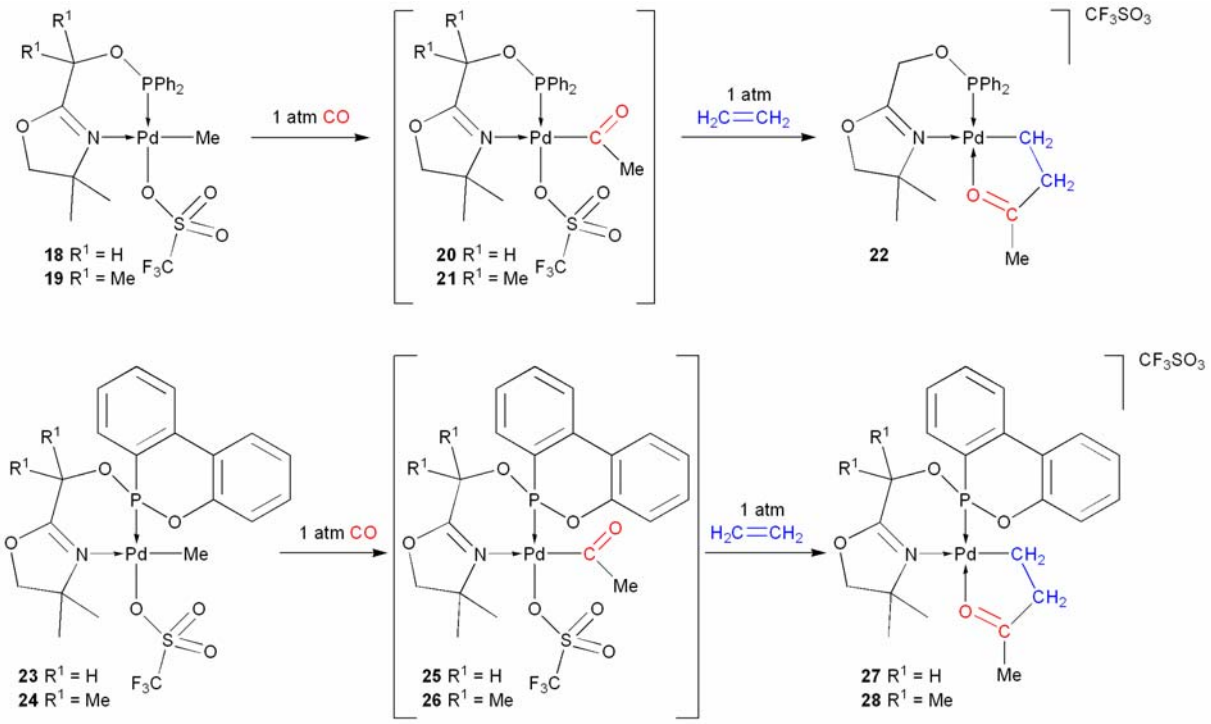

Premières étapes dans la formation de copolymères alternés CO/éthylène, les intermédiaires à ligand acyle **20**, **25** et **26** réagissent avec l'éthylène pour former les complexes alkyles **22**, **27** et **28**, qui ont été complètement caractérisés. Les complexes **27** et **28** ont aussi été caractérisés à l'état solide, par diffraction des rayons X, et leurs structures sont des rares exemples de produits de couplage CO/éthylène.

L'insertion contrôlée de monomères fonctionnels, tels que l'acrylate de méthyle, dans une chaîne polyoléfinique reste un enjeu majeur, aussi bien sur le plan fondamental qu'appliqué. La réaction des dérivés acylés **20**, **25** et **26** avec l'acrylate de méthyle ne conduit pas à la formation d'un produit d'insertion. Nous nous sommes donc tournés vers des systèmes stabilisés par les ligands phosphine **15-17** avec un cycle chélatant à 5 chaînons, plus semblables au système P,O étudié auparavant, et qui nous avait permis d'isoler un produit de couplage CO/acrylate de méthyle. Comme dans le cas des ligands phosphinite et phosphonite, nous avons montré que l'insertion de monoxyde de carbone dans la liaison Pd-C des complexes méthyl-palladium stabilisés par les ligands phosphinés **15-17** conduit à la formation des intermédiaires acylés **32-34**. Il est intéressant de noter que la conversion est plus rapide avec ces derniers qu'avec les ligands phosphinite et phosphonite (1 h).

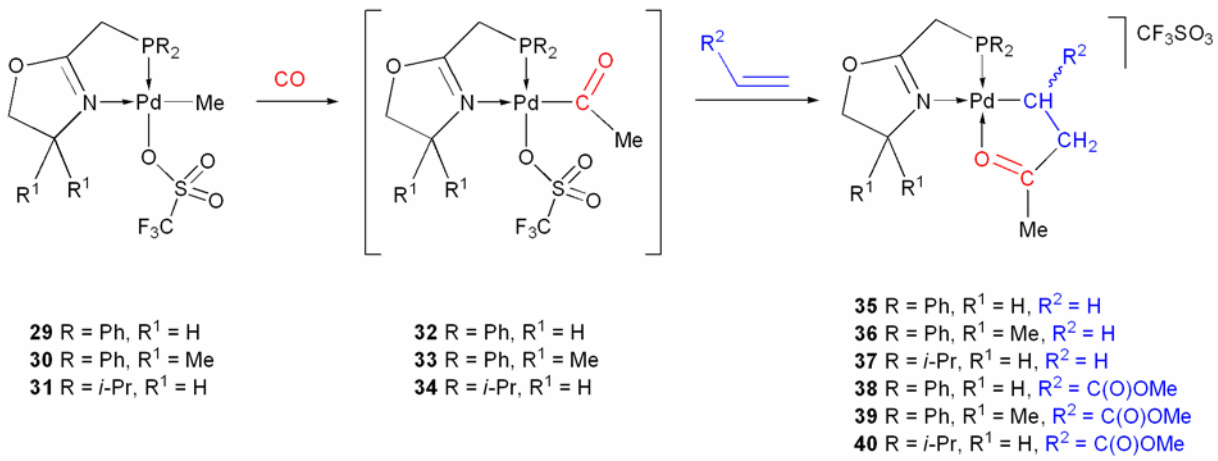

Les intermédiaires acyle **32-34** réagissent avec l'éthylène ou l'acrylate de méthyle pour former les complexes alkyles **35-37** et **38-40**, respectivement, qui ont été complètement caractérises. Les complexes **36** et **38-40** ont aussi été caractérisés à l'état solide, par diffraction des rayons X. Les complexes **38**, **39** et **40** sont parmi les rares exemples de produits de couplage CO/acrylate de méthyle caractérisés structurellement. En effet, il n'existe, à notre connaissance, q'une telle structure publiée à ce jour.

Dans la continuité de ces travaux, des développements futurs pourraient inclure la préparation de nouveaux ligands phosphinés avec un cycle 6 chaînons. Ceci permettrait dans un premier temps d'évaluer l'influence de l'angle de chélation, et dans un second temps de mesurer l'influence de la basicité de l'atome donneur de phosphore.

Les études d'insertion stoechiométriques menées ici pourront aussi être étendues à d'autres monomères fonctionnels et permettre des transformations élémentaires de substrats organiques autour du palladium.

Formulaire du Chapitre I

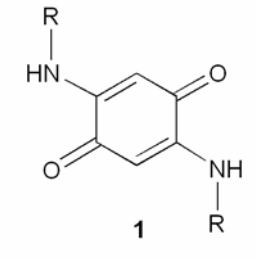

1

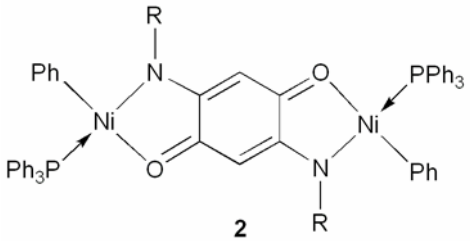

2

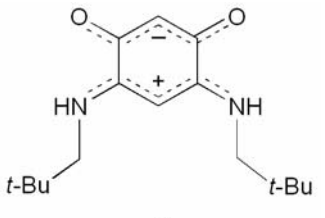

3

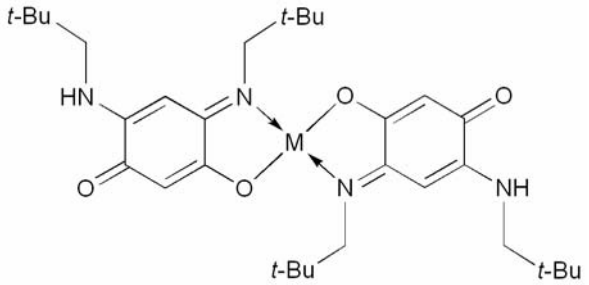

4 M = Ni
5 M = Zn
6 M = Cu

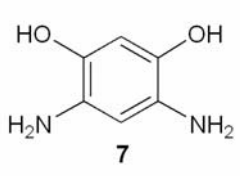

7

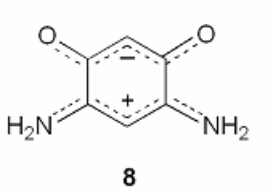

8

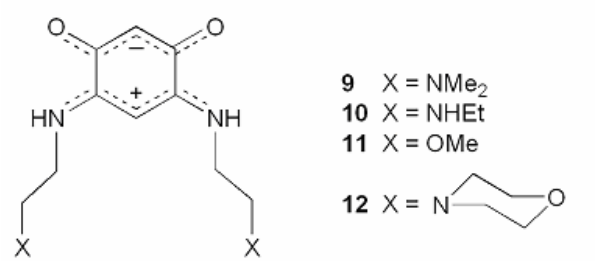

9 X = NMe_2
10 X = NHEt
11 X = OMe
12 X =

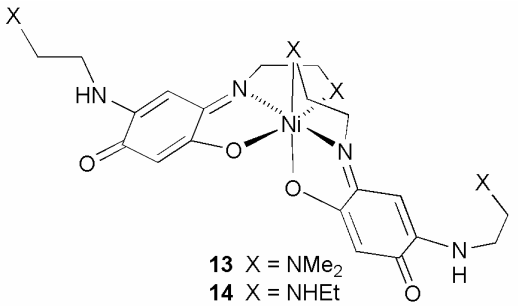

13 X = NMe_2
14 X = NHEt
15 X = OMe
16 X =

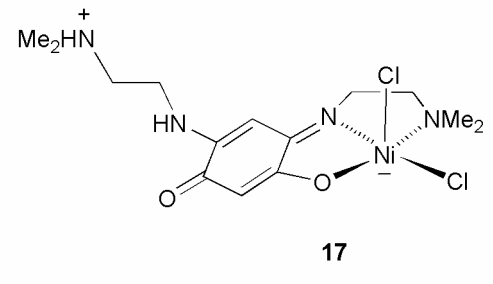

17

Formulaire du Chapitre II

Partie A

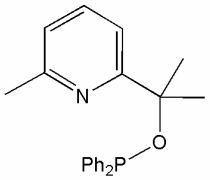

(I)

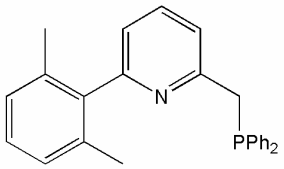

(II)

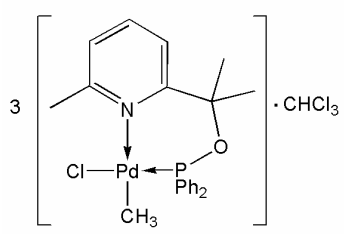

(III)

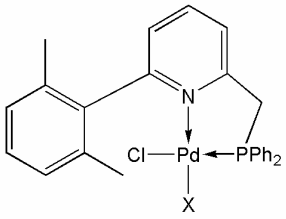

(IV) X = Cl
(V) X = CH_3

Formulaire du Chapitre II

Partie B

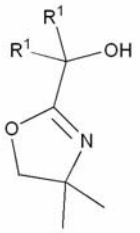

1a R^1 = H
1b R^1 = Me

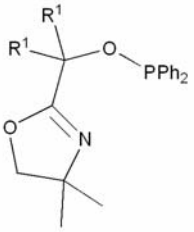

2a R^1 = H
2b R^1 = Me

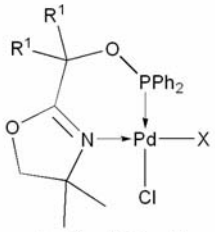

3a R^1 = H, X = Cl
4a R^1 = H, X = Me
4b R^1 = Me, X = Me

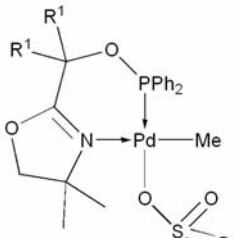

5a R^1 = H
5b R^1 = Me

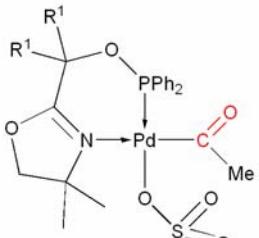

6a R^1 = H
6b R^1 = Me

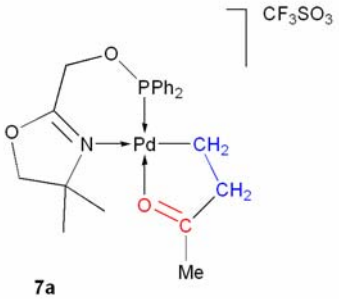

7a

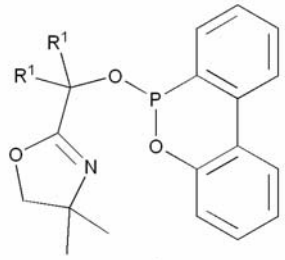

8a R^1 = H
8b R^1 = Me

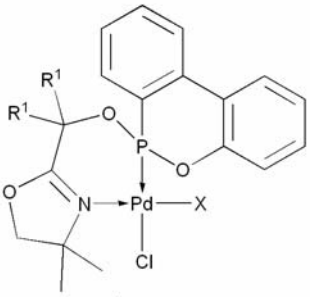

9a R^1 = H, X = Cl
9b R^1 = Me, X = Cl
10a R^1 = H, X = Me
10b R^1 = Me, X = Me

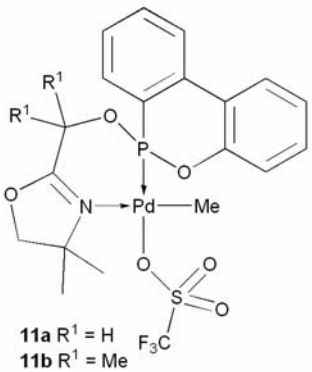

11a R^1 = H
11b R^1 = Me

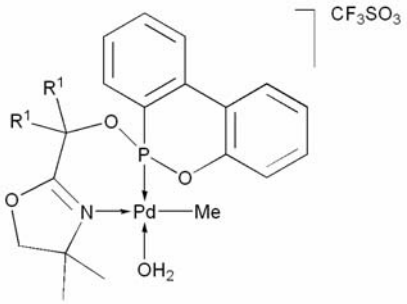

12b

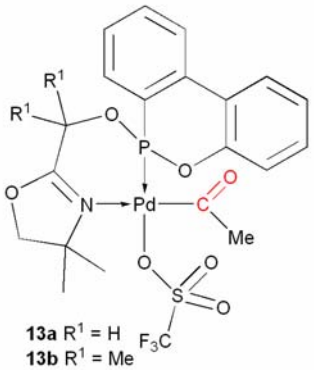

13a R^1 = H
13b R^1 = Me

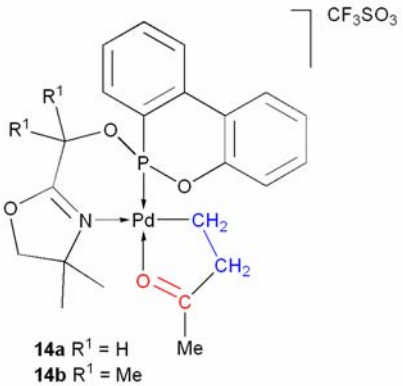

14a R^1 = H
14b R^1 = Me

Formulaire du Chapitre III

Partie A

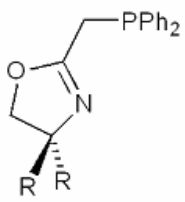

1a R = H
1b R = Me

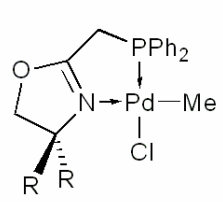

2a R = H
2b R = Me

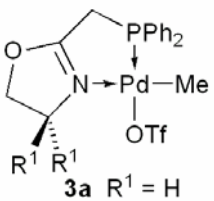

3a R^1 = H
3b R^1 = Me

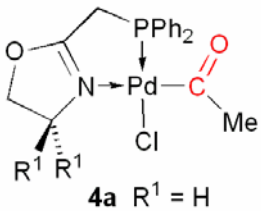

4a R^1 = H
4b R^1 = Me

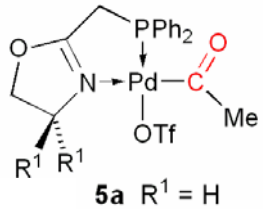

5a R^1 = H
5b R^1 = Me

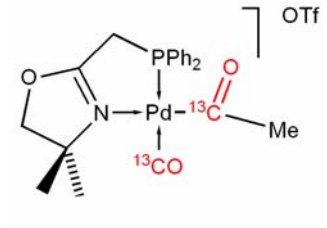

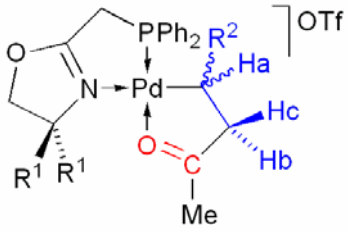

6a R^1 = H, R^2 = H
6b R^1 = Me, R^2 = H
7a R^1 = H, R^2 = C(O)OMe
7b R^1 = Me, R^2 = C(O)OMe

Formulaire du Chapitre III

Partie B

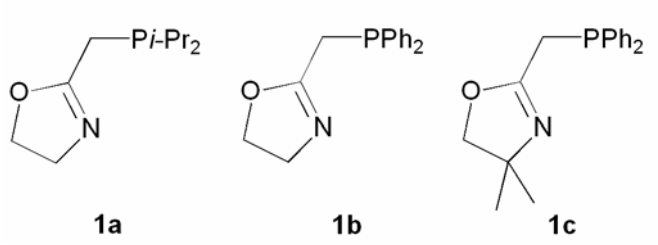

1a **1b** **1c**

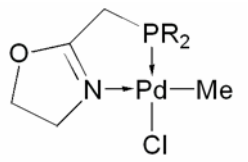

2a R = *i*-Pr
2b R = Ph

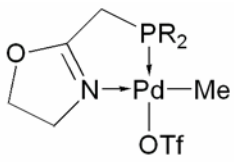

3a R = *i*-Pr
3b R = Ph

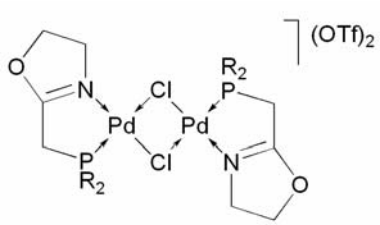

6 R = *i*-Pr

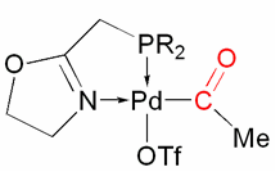

4a R = *i*-Pr
4b R = Ph

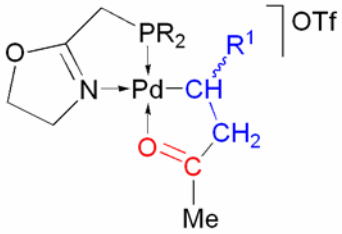

5a R = *i*-Pr, R^1 = H
5b R = Ph, R^1 = H
7a R = *i*-Pr, R^1 = C(O)OMe
7b R = Ph, R^1 = C(O)OMe